Characterisation of nongrowing *Salmonella* during macrophage infection

Robert Andrew Fisher

2017

Imperial College London
Department of Medicine

Submitted to Imperial College London for
the degree of Doctor of Philosophy

Abstract

Persisters are antibiotic tolerant cells thought to be responsible for the recalcitrance and the recurrence of many bacterial infections. *Salmonella* has been shown to form persisters during macrophage infection, the source of which is a reservoir of nongrowing bacteria. This thesis describes the use of dual RNA-seq, combined with fluorescence dilution and FACS, to analyse the transcriptomes of nongrowing and growing *Salmonella* as well as the transcriptomes of their respective host macrophages during infection. Interestingly, nongrowing *Salmonella* were found to express the SPI-2 type three secretion system (T3SS) and infected macrophages were found to be polarised towards an M2 phenotype compared to uninfected bystander cells. Further activity in nongrowing *Salmonella* was uncovered using fluorescence dilution combined with DAPI-staining, which provided evidence of DNA synthesis during infection. In addition, the toxin-antitoxin module *yhfG-fic* was investigated in *Salmonella* after a deletion mutant in this module was found to have a defect during infection, however this was discovered to be due to a polar effect of the deletion on the expression of the downstream gene *pabA*. Heterogeneity in the lag distributions of growing and nongrowing *Salmonella* post-infection was also investigated in this study, using the ScanLag technique. Deletion of TA modules, which have previously been linked to persister formation, had a minimal effect of the lag distributions of nongrowing *Salmonella*, however the lag times of growing bacteria were increased. The SOS response was found to affect lag times and is important for *Salmonella* recovery post-infection, regardless of growth state.

Acknowledgements

First and foremost I would like to thank Dr. Sophie Helaine for all of her help and advice over the years. I really do not think I could have had a better supervisor, you were both kind and caring whilst also focused and incredibly hard-working. You are an incredible scientist and I feel lucky to have worked with you while you started your own research group and I know you will continue to enjoy great success in your work!

I would like to thank the people that helped with the work in this study: Dr. Sophie Helaine for cell sorting for the dual RNA-seq experiments; Dr. Alex Westermann and Dr. Konrad Förstner for carrying out sequencing and analysis on the dual RNA-seq project; Dr. Daphne Stapels for sharing cell culture lab duties (and for answering so many of my questions!); Dr. Peter Hill for cell sorting *Salmonella* for ScanLag and carrying out further analysis on the dual RNA-seq data set; Dr. Luciano Rigano for cell sorting stationary phase *E. coli* for ScanLag; Dr. Rita Figueira for starving *E. coli* strains of nitrogen for ScanLag and Miles Priestman for modifying some of the Matlab scripts to make my ScanLag analysis easier!

Thank you to everyone in the (exponentially growing) Helaine group and the Holden group and the Mostowy group for always being willing to give help and advice on any issue.

Angie, Bridget, Alex, Regina, Carrie, Sina, Julian, baby David, Daphne, Peter, Chris, Elliott, Alan, GG, Alex 2.0, Matt and Miles - you guys made my time

here so much fun, and I will always appreciate the moral support that was available when needed. I would also like to thank my friends and family outside of the CMBI who have been a huge support to me while I have been working on this project. Finally, a very big thank you to Megan Winterbotham who does an amazing job managing the lab, you keep the place from descending into chaos!

Declaration of originality

I declare that the work described here is my own unless otherwise stated or referenced.

Copyright declaration

The copyright of this thesis rests with the author and is made available under a Creative Commons Attribution Non-Commercial No Derivatives licence. Researchers are free to copy, distribute or transmit the thesis on the condition that they attribute it, that they do not use it for commercial purposes and that they do not alter, transform or build upon it. For any reuse or redistribution, researchers must make clear to others the licence terms of this work

Contents

TITLE PAGE 1

ABSTRACT 2

ACKNOWLEDGEMENTS 3

DECLARATION OF ORIGINALITY 5

COPYRIGHT DECLARATION 5

CONTENTS 6

FIGURES AND TABLES 9

ABBREVIATIONS 17

INTRODUCTION 20

1.1 HISTORY AND TAXONOMY OF *SALMONELLA* 20
1.2 *SALMONELLA* PATHOGENESIS IN HUMANS 22
1.2.1 GASTROENTERITIS 22
1.2.2 INVASIVE NONTYPHOIDAL BACTERAEMIA 23
1.2.3 ENTERIC FEVER 24
1.2.4 ANTIBIOTIC RESISTANCE IN *SALMONELLA* 26
1.3 MODELS OF *SALMONELLA* INFECTION 27
1.3.1 ANIMAL MODELS OF GASTROENTERITIS 28
1.3.2 ANIMAL MODELS OF TYPHOID FEVER 29
1.3.3 *IN VITRO* MODELS 32
1.4 BACTERIAL PERSISTENCE IN THE HOST (ADAPTED FROM FISHER *ET AL.,* 2017) 33
1.4.1 PERSISTENT INFECTIONS 33
1.4.2 INEFFECTIVE CLEARANCE BY THE HOST 35
1.4.3 INEFFECTIVE CLEARANCE BY ANTIBIOTICS 36
1.5 PERSISTER CELLS (ADAPTED FROM FISHER *ET AL.,* 2017) 41
1.5.1 LINKS TO PERSISTENT INFECTIONS 41
1.5.2 PERSISTER CELL FORMATION 43
1.5.3 TOXIN-ANTITOXIN MODULES AND PERSISTER FORMATION 45
1.5.5 REGROWTH OF PERSISTERS 53
1.5.5.1 MOLECULAR MECHANISMS OF REGROWTH RESEARCH 53
1.5.5.1 ENVIRONMENTAL RESTRICTION OF GROWTH 56
1.5.5.2 STATE OF REGROWERS 57
1.6 METHODS OF STUDYING PERSISTERS (ADAPTED FROM FISHER *ET AL.,* 2017) 58
1.6 DUAL RNA-SEQ OF PATHOGEN AND HOST DURING INFECTION 59
1.6.1 TRADITIONAL METHODS OF TRANSCRIPTOMICS 59
1.6.2 RNA-SEQ 61
1.6.3 DUAL RNA-SEQ 64
1.7 THE BACTERIAL CELL CYCLE DURING INFECTION 65
1.8 AIMS AND OBJECTIVES 71

MATERIALS AND METHODS 73

2.1 BACTERIAL STRAINS, PLASMIDS AND PRIMERS 73

2.2 BACTERIAL GROWTH CONDITIONS 75
2.3 TISSUE CULTURE CONDITIONS 75
2.4 PLASMID EXTRACTION AND POLYMERASE CHAIN REACTION (PCR) 76
2.5 DELETION OF *YHFG-FIC* IN *S.* TYPHIMURIUM 77
2.6 CONSTRUCTION OF TOXIN AND ANTITOXIN OVEREXPRESSION PLASMIDS 79
2.7 PREPARATION AND TRANSFORMATION OF ELECTRO-COMPETENT BACTERIAL CELLS 79
2.8 TOXIN AND ANTITOXIN OVEREXPRESSION ASSAYS 80
2.9 BACTERIAL GROWTH CURVES 81
2.10 MACROPHAGE INFECTION WITH *S.* TYPHIMURIUM 81
2.11 DIFFERENTIATION OF GROWING AND NONGROWING *SALMONELLA* USING FLUORESCENCE DILUTION (FD) 82
2.12 DNA QUANTIFICATION OF *S.* TYPHIMURIUM 83
2.13 *S.* TYPHIMURIUM DNA REPLICATION RUN-OUT 83
2.14 RNA EXTRACTION AND DUAL RNA-SEQ ANALYSIS 84
2.15 P_{SSAG}-*GFPLVA* TRANSCRIPTIONAL FUSION EXPRESSION ASSAY 85
2.16 SCANLAG ANALYSIS 85
2.17 STATISTICS 86

TRANSCRIPTOMIC ANALYSIS OF BOTH HOST AND PATHOGEN: CELL SORTING AND DUAL RNA-SEQ OF MACROPHAGES INFECTED WITH EITHER GROWING OR NONGROWING *SALMONELLA* 88

3.1 INTRODUCTION 88
3.2.1.1 PRELIMINARY RUN OF DUAL RNA-SEQ AND CELL SORTING 91
3.2.1.2 PROPORTIONS OF RNA IN SEQUENCING 93
3.2.2.1 DIFFERENCES IN GENE EXPRESSION BETWEEN GROWING AND NG *SALMONELLA* DURING MACROPHAGE INFECTION 97
3.2.2.2 DIFFERENCES IN MACROPHAGE GENE EXPRESSION 100
3.3.1 REPEAT OF OPTIMISED DUAL RNA-SEQ EXPERIMENT TO PRODUCE A LARGER DATA SET 104
3.3.2.1 DIFFERENCES IN GENE EXPRESSION BETWEEN GROWING AND NG *SALMONELLA* DURING MACROPHAGE INFECTION 110
3.3.2.2 DIFFERENCES IN MACROPHAGE GENE EXPRESSION 114
3.4 NG *SALMONELLA* EXPRESS SPI-2 DURING MACROPHAGE INFECTION 119
3.5 CONCLUSION 122

DNA SYNTHESIS OCCURS IN NONGROWING *SALMONELLA* DURING MACROPHAGE INFECTION 125

4.1 INTRODUCTION 125
4.2 *IN VITRO* DETECTION OF DIFFERENTIAL LEVELS OF DNA CONTENT IN *SALMONELLA* 126
4.3.1 DNA REPLICATION OCCURS IN *SALMONELLA* DURING INFECTIONS OF RAW 264.7 MACROPHAGES 129
4.3.2 DNA REPLICATION OCCURS IN *SALMONELLA* DURING INFECTIONS OF IBMM MACROPHAGES 134
4.3.3 DNA REPLICATION OCCURS IN *SALMONELLA* DURING INFECTIONS OF PRIMARY BMMS 138
4.4 DNA SYNTHESIS IN NONGROWING *SALMONELLA* CAN BE MORE EFFECTIVELY MONITORED BY USING CEFOTAXIME ISOLATION TO KILL GROWING *SALMONELLA* 142
4.5 NONGROWING *SALMONELLA* THAT UNDERGO DNA SYNTHESIS DURING MACROPHAGE INFECTION ARE METABOLICALLY ACTIVE 149
4.6 RECOVERY OF NONGROWING *SALMONELLA* 154
4.9 CONCLUSION 156

CHARACTERISING THE *YHFG-FIC* TOXIN-ANTITOXIN MODULE 157

5.1 INTRODUCTION 157

5.2 DELETION OF BOTH *parDE* AND *yhfG-fic* IN *SALMONELLA* LEADS TO A GROWTH DEFECT IN RAW 267.4 MACROPHAGES 160
5.3.1 OVEREXPRESSION OF *fic* INHIBITS GROWTH IN *E. coli* DH5A BUT NOT IN *S.* TYPHIMURIUM 162
5.3.2 TOXICITY OF FIC AND YHFG OBSERVED IN *E. coli* IS LIKELY A NON-SPECIFIC EFFECT OF OVEREXPRESSION 167
5.4.1 *S.* TYPHIMURIUM Δ*parDE*Δ*yhfG-fic* HAS A GROWTH DEFECT IN MINIMAL MEDIUM 170
5.4.2 DELETION OF BOTH *parDE* AND *yhfG-fic* LEADS TO A GREATER VARIABILITY IN SURVIVAL DURING LONG-TERM GROWTH IN NUTRIENT LIMITING AND ACIDIC CONDITIONS 174
5.4.3 THE GROWTH DEFECT IN *S.* TYPHIMURIUM Δ*parDE*Δ*yhfG-fic* IS THE RESULT OF A POLAR EFFECT ON THE EXPRESSION OF THE *pabA* GENE 176
5.5 CONCLUSION 181

PHENOTYPIC HETEROGENEITY IN THE LAG TIMES OF STRESSED *E. COLI* AND MACROPHAGE-INDUCED *SALMONELLA* PERSISTERS 183

6.1 INTRODUCTION 183
6.2.1 HETEROGENEITY IN METABOLIC ACTIVITY OF STATIONARY PHASE *E. coli* CAN BE LINKED TO HETEROGENEITY IN LAG TIME DISTRIBUTION 184
6.2.2 SCANLAG CAN REVEAL A DECREASE IN HETEROGENEITY OF LAG IN *E. coli* Δ*yeaG* COMPARED TO WILD-TYPE 189
6.3.1 SCANLAG ANALYSIS REVEALS NO DIFFERENCE IN REGROWTH DEPENDING ON DNA CONTENT OF NG *SALMONELLA* 192
6.3.2 SCANLAG ANALYSIS REVEALS NO DIFFERENCE IN REGROWTH OF NG ΔTA *SALMONELLA* BUT DOES IN GROWING ΔTA *SALMONELLA* 196
6.3.3 THE SOS RESPONSE IS IMPORTANT FOR RECOVERY OF *SALMONELLA* POST-INFECTION 202
6.4 CONCLUSION 207

DISCUSSION 209

7.1 DUAL RNA-SEQ REVEALS SPI-2 ACTIVITY IN NG *SALMONELLA* AND POLARISATION TOWARDS AN M2 PHENOTYPE IN MACROPHAGES INFECTED WITH VIABLE *SALMONELLA* 209
7.2 NG *SALMONELLA* ARE CAPABLE OF DNA REPLICATION DURING INFECTION 214
7.3 THE TOXIN-ANTITOXIN MODULES *yhfG-fic* AND *parDE* 217
7.4 THE SCANLAG TECHNIQUE IS USEFUL FOR STUDYING BACTERIAL HETEROGENEITY THROUGH LAG TIME DISTRIBUTIONS 219

BIBLIOGRAPHY 223

APPENDIX 240

Figures and tables

Introduction

Figure 1.1: Phylogenetic tree of *Salmonella* genus. **20**

Figure 1.2: Killing kinetics of persisters and homogeneous populations of bacteria (adapted from Fisher *et al.,* 2017). **37**

Figure 1.3: Killing kinetics of *Salmonella* after addition of cefotaxime during *in vitro, ex*-macrophage and intra-macrophage conditions (adapted from Fisher *et al.,* 2017). **38**

Figure 1.4: Regulation of type II toxin-antitoxin module (adapted from Yamaguchi and Inouye 2011). **44**

Figure 1.5: Mechanisms of persister formation (adapted from Fisher *et al.,* 2017). **46**

Figure 1.6: Mechanisms of persister regrowth (adapted from Fisher *et al.,* 2017). **52**

Materials and Methods

Figure 2.1: λRed recombinase-mediated site-directed mutagenesis of *yhfG-fic*. **77**

Table 2.1: *S.* Typhimurium strains. **68**

Table 2.2: *E. coli* strains. **68**

Table 2.3 Plasmids. **68**

Table 2.4: Primers. **69**

Results:

Transcriptomic analysis of both host and pathogen: Cell sorting and dual RNA-seq of macrophages infected with either growing or nongrowing *Salmonella*

Figure 3.1: Schematic of dual RNA-seq experimental set up. **88**

Figure 3.2: Different subpopulations of BMMs can be identified based on *Salmonella* fluorescence during infection (Preliminary test). **90**

Figure 3.3: Proportions of RNA present in *Salmonella* and BMM transcriptomes (Preliminary test). **92-93**

Figure 3.4: Comparison of growing and NG *Salmonella* transcriptomic profiles during BMM infection (Preliminary test). **96**

Figure 3.5: Comparison of macrophage BMM+G and BMM+NG transcriptomic profiles during infection with *Salmonella* (Preliminary test). **99**

Figure 3.6: Subpopulations of BMMs can be identified based on *Salmonella* fluorescence during infection (Repeated experiment). **103-104**

Figure 3.7: Proportions of RNA present in *Salmonella* and BMM transcriptomes (repeated experiment). **106-107**

Figure 3.8: Principal component analysis of transcriptomes belonging to growing and NG *Salmonella* during infection and the inoculum. **108**

Figure 3.9: Direct comparison of growing and NG *Salmonella* transcriptomic profiles during BMM infection (repeated experiment). **110**

Figure 3.10: Principal component analysis of transcriptomes belonging to BMM+G, BMM+NG, bystanders and uninfected control BMMs infected with *Salmonella*. **113**

Figure 3.11: Comparison of BMM+G and BMM+NG transcriptomic profiles during infection with *Salmonella* (repeated experiment). **115**

Figure 3.12: NG and growing *Salmonella* express SPI-2 through infection of BMMs. **118-119**

Table 3.1: Gene enrichment lists (abridged) for comparison of growing v NG *Salmonella* transcriptomes. **97**

Table 3.2: Gene enrichment lists (abridged) for comparison of BMM+G v BMM+NG transcriptomes. **100**

Table 3.3: Gene enrichment lists (abridged) for direct comparison of growing v NG *Salmonella* transcriptomes. **111**

Table 3.4: Gene enrichment lists (abridged) for direct comparison of BMM+NG v BMM+G *Salmonella* transcriptomes. **116**

DNA synthesis occurs in nongrowing *Salmonella* during macrophage infection

Figure 4.1: Flow cytometry analysis of DAPI-stained run-out *Salmonella* grown to exponential phase and stationary phase in minimal medium. **126**

Figure 4.2: Experimental design for quantifying *Salmonella* proliferation and DNA content during macrophage infection. **129**

Figure 4.3: Infection of RAW 264.7 macrophages with *Salmonella* for fluorescence dilution and DNA quantification. **130-131**

Figure 4.4: Infection of immortalised bone marrow-derived macrophages (iBMMs) with *Salmonella* for fluorescence dilution and DNA quantification. **134-135**

Figure 4.5: Infection of primary bone marrow-derived macrophages (BMMs) with *Salmonella* for fluorescence dilution and DNA quantification. **138-139**

Figure 4.6: Comparison of the quantification of DNA in nongrowing bacteria during infection in the presence of either gentamicin or cefotaxime. **143-144**

Figure 4.7: EdU incorporation into DNA of NG *Salmonella* during infection. **146**

Figure 4.8: Experimental design for measuring metabolic responsiveness and DNA content of nongrowing *Salmonella* during macrophage infection. **148**

Figure 4.9: Metabolic response and DNA content of nongrowing *Salmonella* during BMM infection. **150-151**

Figure 4.10: Recovery of NG *Salmonella* post-infection in LB broth. **153**

Characterising the *yhfG-fic* toxin-antitoxin module

Figure 5.1: Genomic arrangement of *parDE* and *yhfG-fic* operons and amino acid sequence alignments of toxin and antitoxin proteins. **157**

Figure 5.2: *S.* Typhimurium Δ*parDE*Δ*yhfG-fic* has a growth defect during infection of RAW 267.4 macrophages but not during infection of BMMs. **159**

Figure 5.3: Maps of toxin and antitoxin overexpression plasmids. **160**

Figure 5.4: Overexpression of *fic* inhibits growth in *E. coli* DH5α. **161**

Figure 5.5: Fic is not toxic in *S.* Typhimurium Δ*yhfG-fic*. **163**

Figure 5.6: Fic is not toxic in *S.* Typhimurium Δ*parDE*Δ*yhfG-fic*. **164**

Figure 5.7: Fic is not toxic in *E. coli* DH5α when expressed from pNDM220. **166**

Figure 5.8: Fic is toxic in *E. coli* K-12 MG1655 when expressed from pNDM220. **166**

Figure 5.9: Fic is not toxic in *S.* Typhimurium when expressed from pNDM220. **167**

Figure 5.10: Deletion of *parDE* and *yhfG* leads to a growth defect in MgMES pH5 medium when monitored by OD_{600nm} but not by CFU. **170**

Figure 5.11: Growth of *S.* Typhimurium Δ*parDE*Δ*yhfG-fic* ultimately reaches same level as wild-type in stationary phase in MgMES pH5 medium. **171**

Figure 5.12: Long-term survival of *S.* Typhimurium Δ*parDE* and Δ*yhfG-fic* is reduced and is more variable for Δ*parDE*Δ*yhfG-fic* compared the wild-type. **173**

Figure 5.13: Growth defect upon deletion of *parDE* and *yhfG-fic* is dependent on nutrient limitation rather than low pH5 and is accentuated if grown overnight in minimal medium. **175**

Figure 5.14: Growth defect of *S.* Typhimurium Δ*parDE*Δ*yhfG-fic* is complemented by *para*-aminobenzoate suggesting that a polar effect is taking place in the mutant strain. **177**

Figure 5.15: Arrangement of antibiotic resistance cassettes in *S.* Typhimurium wild-type, Δ*parDE*, Δ*yhfG-fic* and Δ*parDE*Δ*yhfG-fic* strains. **178**

Phenotypic heterogeneity in the lag times of stressed *E. coli* and macrophage-induced *Salmonella* persisters

Figure 6.1. ScanLag analysis shows stationary phase *E. coli* has increased heterogeneity lag. **183**

Figure 6.2. ScanLag analysis of stationary phase *E. coli* after FACS based on metabolic activity. **186**

Figure 6.3. *E. coli* ∆*yeaG* is more homogeneous in lag time than wild-type. **189**

Figure 6.4. DNA content of NG *Salmonella* does not affect lag post-infection. **192-193**

Figure 6.5. Deleting single TA modules affects lag in growing but not NG *Salmonella.* **196-198**

Figure 6.6. The SOS response is important for reducing lag times in growing and NG *Salmonella* post-infection **202-203**

Appendix

Appendix figure 1: Comparisons of BMM transcriptomic profiles during infection with *Salmonella* (Preliminary test). **241**

Appendix figure 2: Direct comparisons of *Salmonella* transcriptomic profiles during BMM infection (repeated experiment). **245**

Appendix figure 3: Direct comparisons of BMM transcriptomic profiles during infection with *Salmonella* (repeated experiment). **249**

Appendix figure 4: Example plate from ScanLag experiment. **256**

Appendix figure 5: Growth rates of colonies detected by ScanLag are highly variable. **257**

Appendix table 1: Read statistics for preliminary dual RNA-seq run. **238**

Appendix table 2: Read statistics for repeated dual RNA-seq runs. **239**

Appendix table 3: Genes differentially upregulated in growing and NG *Salmonella* comparison (preliminary run). **240**

Appendix table 4: Genes differentially upregulated in BMM+G v BMM+NG comparison (preliminary run). **242**

Appendix table 5: Genes differentially upregulated in BMM+NG v bystanders comparison (preliminary run). **243**

Appendix table 6: Genes differentially upregulated in BMM+G v bystanders comparison (preliminary run). **244**

Appendix table 7: Genes differentially upregulated in growing v NG *Salmonella* comparison (repeated experiment). **246**

Appendix table 8: Genes differentially upregulated in growing v inoculum *Salmonella* comparison (repeated experiment). **247**

Appendix table 9: Genes differentially upregulated in NGs v inoculum *Salmonella* comparison (repeated experiment). **248**

Appendix table 10: Genes differentially upregulated in BMM+G v BMM+NG comparison (repeated experiment). **250**

Appendix table 11: Genes differentially upregulated in BMM+G v uninfected BMMs comparison (repeated experiment). **251**

Appendix table 12: Genes differentially upregulated in BMM+NG v uninfected BMMs comparison (repeated experiment). **252**

Appendix table 13: Genes differentially upregulated in BMM+G v bystanders comparison (repeated experiment). **253**

Appendix table 14: Genes differentially upregulated in BMM+NG v bystanders comparison (repeated experiment). **254**

Appendix table 15: Genes differentially upregulated in bystanders v uninfected BMMs comparison (repeated experiment). **255**

Abbreviations

(p)ppGpp	Guanosine pentaphosphate
ATP	Adenosine triphosphate
BMM+Deg	BMMs infected with degraded *Salmonella*
BMM+G	BMMs infected with growing *Salmonella*
BMM+NG	BMMs infected with nongrowing *Salmonella*
BMMs	Primary bone marrow-derived macrophages
CAGE	Cap analysis of gene expression
cDNA	Complementary DNA
Cef	Cefalexin
Cefo	Cefotaxime
CFU	Colony forming units
DAPI	4',6-diamidino-2-phenylindole
DMEM	Dulbecco's modified Eagle medium
DNA	Deoxyribonucleic acid
dNTPs	Deoxynucleoside triphosphates
EdU	Ethynyl deoxyuridine
EHF	Expand high fidelity
FACS	Fluorescence-activated cell sorting
FD	Fluorescence dilution
FIC	Filamentation by cAMP
Gent	Gentamicin
GFP	Green fluorescent protein
Hip	High persistence
HSCs	Haematopoeitic stem cells
iBMMs	Immortalised bone marrow-derived macrophages
IFN-**γ**	Interferon-gamma
IGR	Intergenic region
IL-10	Interleukin 10
IL-1b	Interleukin 1 beta
IL-4	Interleukin 4
IL-4R	Interleukin 4 receptor
iNTS	Invasive nontyphoidal salmonellosis / *Salmonella*

IPTG	Isopropyl β-D-1-thiogalactopyranoside
LB	Lennox brother
lncRNA	Long noncoding RNA
LPS	Lipopolysaccharide
m.o.i.	Multiplicity of infection
MHC	Major histocompatibility complex
miRNA	MicroRNA
miscRNA	Miscellaneous RNA
MLEE	Multi-locus enzyme electrophoresis
MLNs	Mesenteric lymph nodes
mRNA	Messanger RNA
MSC	Microbiological safety cabinet
NG	Nongrowing
NGS	Next-generation sequencing
NTS	nontyphoidal salmonellosis / *Salmonella*
OD	Optical Density
p.i.	Post-infection
PABA	*Para*-aminobenzoate
PBS	Phosphate buffered saline
PCR	Polymerase chain reaction
PFA	Paraformaldehyde
PMNs	Polymorphonuclearcytes (PMNs)
qPCR	Quantitative PCR
RAWs	RAW 264.7 macrophages
Rif	Rifampicin
RNA	Ribonucleic acid
RNA-seq	RNA sequencing
RNase	Ribonuclease
RPKM	Reads per kilobase per million
rRNA	Ribosomal RNA
SAGE	Serial analysis of gene expression
SCV	*Salmonella*-containing vacuole
SEM	Standard error of the mean
snoRNA	Small nucleolar RNA

SNPs	Single nucleotide polymorphisms
snRNA	Small nuclear RNA
SPI-1	*Salmonella* pathogenicity island-1
sRNA	Bacterial small RNA
T:A	Toxin : Antitoxin
T3SS	Type three secretion system
TA module	Toxin-antitoxin module
TAE	Tris-acetate EDTA buffer
T_h2	T-helper cell type 2
TLR	Toll-like receptor
TopoIV	Topoisomerase IV
tRNA	Transfer RNA
UPEC	Uropathogenic *E. coli*
UTI	Urinary tract infection

Chapter One

Introduction

1.1 History and taxonomy of *Salmonella*

Bacteria belonging to the genus *Salmonella* are Gram-negative, motile, rod-shaped, facultative anaerobes. The genus lies within the family Enterobacteriaceae, which itself lies within the family γ-proteobacteria. *Salmonella* was first observed by microscopy in the Peyer's patches and spleens of typhoid patients (Eberth 1880), and was successfully isolated and grown in culture soon afterwards (Gaffky 1884). In the same year, *Salmonella enterica* serovar Choleraesuis was discovered by Theobald Smith in the laboratory of Daniel Salmon, whom the genus was subsequently named after (Schultz 2008). *Salmonella* was initially classified into 'serovars' (serum-variants) using the Kauffman-White system based on surface O- and H-antigens, reflecting variations in the lipopolysaccharide and the flagellum respectively (Kauffmann 1972). Using this system, *Salmonella* can be divided into ~2400 serovars, which reflects the huge level of diversity found within the genus of *Salmonella*. Multi-locus enzyme electrophoresis (MLEE) determined that the *Salmonella genus* contained two species, *Salmonella enterica* and *Salmonella bongori* (Reeves et al. 1989). DNA-DNA hybridisation, biotyping and more recently DNA sequencing has further divided *S. enterica* into seven subspecies: *enterica* (I), *salamae* (II), *arizonae* (IIIa), *diarizonae* (IIIb), *houtanae* (IV), *indica* (VI) and subspecies VII, which is unnamed (Crosa et al. 1973; Le Minor et al. 1986; Lan et al. 2009). *S. bongori* was previously considered group V. Based on 16S sequencing and the timings of known

ecological events, *Salmonella* is thought to have diverged from *Escherichia coli* around 120-160 million years ago (Ochman & Wilson 1987). This occurred through the sequential acquisition of several sets of virulence genes including the *fim* and *lpf* operons and the *Salmonella* pathogenicity island-1 (SPI-1) type three secretion system (T3SS). These genes allowed the invasion of host intestinal epithelia, opening up a new niche for the bacteria. The ancestor of *Salmonella enterica,* but not *Salmonella bongori*, acquired a second T3SS encoded by the SPI-2 (Figure 1.1) (Galán & Curtiss 1989; Hensel et al. 1995; Bäumler 1997; Bäumler et al. 1998). This secretion system aids proliferation inside host cells (Helaine et al. 2010; Figueira & Holden 2012), and may be involved in exit from these cells, allowing the pathogen to disseminate throughout the host (Grant et al. 2012). Recently, next-generation sequencing techniques have allowed the analysis of whole genomes of *Salmonella* isolates, providing more accurate phylogenies to be determined (Okoro et al. 2012; Desai et al. 2013).

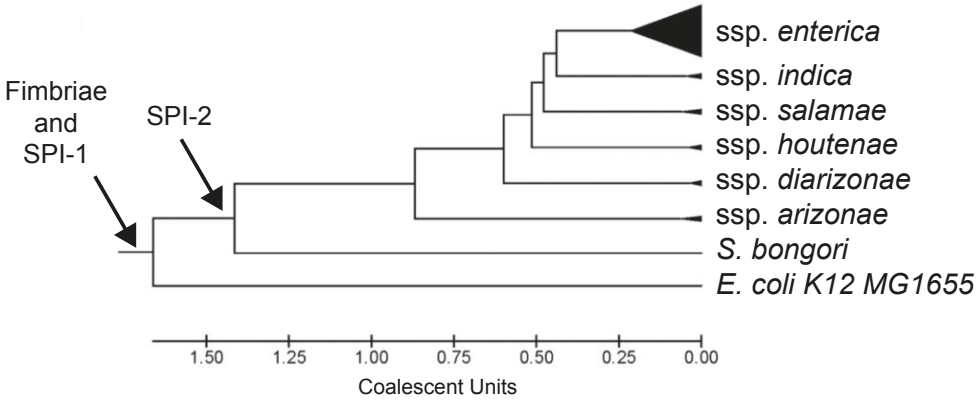


Figure 1.1: Phylogenetic tree of *Salmonella* genus. Arrows indicate the times at which different virulence factors were acquired. SPI-2 was acquired by *Salmonella* after divergence from *E. coli.* Adapted from Desai *et al.*, 2013.

Most of all known *Salmonella* serovars (60%) belong to *Salmonella enterica* subsp. *enterica* (henceforth referred to as *S. enterica* or *Salmonella*). *S. enterica* also contains almost all serovars known to cause disease in birds and mammals. Some of these serovars, such as the human pathogen *Salmonella* Typhi and the poultry pathogen *Salmonella* Gallinarum are host-restricted, meaning that their ability to persist and cause disease within a different host is severely limited. Other serovars such as *Salmonella* Dublin and *Salmonella* Choleraesuis are host-adapted, meaning that they prefer one host, namely cattle and swine respectively, but they have the ability to infect other hosts such as humans. *Salmonella* Typhimurium is a more promiscuous example, able to infect many different warm-blooded hosts (Lan et al. 2009; Kingsley & Bäumler 2000).

1.2 *Salmonella* pathogenesis in humans

Salmonellosis can be divided into three major categories: gastroenteritis, invasive nontyphoidal salmonellosis and enteric (typhoid or paratyphoid) fever. Enteric fever is caused by the typhoidal *Salmonella* serovars Typhi and Paratyphi while gastroenteritis and invasive nontyphoidal salmonellosis are caused by nontyphoidal serovars, most commonly *S.* Typhimurium and *Salmonella* Enteriditis.

1.2.1 Gastroenteritis

Salmonella gastroenteritis presents between 8 to 72 hours post-infection (p.i.) and is generally self-limiting, resolving in 3 to 7 days. The pathology is not systemic, being limited to enterocolitis (inflammation of the

gastro-intestinal tract) with symptoms including abdominal pain, vomiting, diarrhoea and fever, however some patients may develop more severe haemorrhagic enterocolitis characterised by blood and puruloid stool (Coburn et al. 2006; Ina et al. 2003). The disease is transmitted via the faecal-oral route through the consumption of contaminated food and water. The Salmonellae initially colonise the ileum, followed by the Peyer's patches and mesenteric lymph nodes (MLNs). This leads to the recruitment of large numbers of polymorphonuclearcytes (PMNs), which along with complement-mediated killing, effectively helps contain the infection to the intestine. However this PMN-recruitment leads to a high level of exudate into the intestinal lumen resulting in diarrhoea. The most significant risk to health is therefore dehydration, which can be treated with fluids and electrolyte therapy (Coburn et al. 2006). With an incidence of 93 million cases and 155,000 deaths per year gastroenteritis as a result of *Salmonella* infection is a major concern to global public health (Majowicz et al. 2010). As the disease is generally self-limiting, the most effective methods in combatting the illness are preventative in nature; improving hygienic standards in food and water management.

1.2.2 Invasive nontyphoidal bacteraemia

In locations where the epidemiology of the *Salmonella* serovars responsible for gastroenteritis in otherwise healthy individuals (mostly *S.* Enteritidis and *S.* Typhimurium) overlap with immunosuppressive factors such as child-malnourishment, and infection of adults with HIV and malaria, the disease can be invasive and systemic, becoming far more life threatening

(Gordon 2008; Gordon et al. 2010; Kingsley et al. 2009; Park et al. 2016). This is particularly prevalent in Africa, which has an incidence of around 3 cases of invasive nontyphoidal salmonellosis [or *Salmonella*] (iNTS) for every 1000 individuals per year (Gordon 2011). The mortality rate if left untreated is 20-25%, but can be as high as 50% if the meninges are reached. The clinical manifestations of the disease vary from patient to patient, with commonly observed symptoms often similar to those of enteric fever (see below) (Feasey et al. 2012). If the immune system of an individual infected with nontyphoidal *Salmonella* is compromised, the bacteria are no longer contained within the GI tract and are able to invade through the intestinal epithelium and gain access to the bloodstream (Gordon 2008). Complement-mediated killing can be obstructed if adaptive immunity is suppressed, significantly increasing *Salmonella* survival in the blood (MacLennan et al. 2010). This is particularly significant, as complement has also been shown to be important for an optimal oxidative burst upon phagocytosis of nontyphoidal *Salmonella* by immune cells (Gondwe et al. 2010). The main treatment currently used to fight iNTS is antibiotic therapy, therefore factors leading to antibiotic resistance and tolerance of the pathogen are of great concern.

1.2.3 Enteric fever

S. Typhi and *S.* Paratyphi are the causative agents of typhoid fever and paratyphoid fever respectively, which are collectively referred to as enteric fever. It is most prevalent in Asia and North Africa where in poorer regions, hygiene in the management of food and water can be low. There were as many as 26.9 million cases of typhoid fever in 2010 (Buckle et al. 2012).

Symptoms of enteric fever include high fever, abdominal pain, swelling of the MLNs, spleen and liver with the perforation of the intestine in some cases. The incubation period before the onset of symptoms is 8 to 14 days (Parry et al. 2002). Around 2-5% of individuals infected can develop an asymptomatic, chronic carrier state, which is associated with shedding of the bacteria despite the lack of any clinical manifestations of disease (Levine et al. 1982). This carrier state is thought to greatly aid the spread of the pathogen and is notoriously difficult to treat with antibiotics (Caygill et al. 1994; Bhan et al. 2005). It is also associated with a greatly increased chance of developing gallbladder carcinoma (Caygill et al. 1994; Shukla et al. 2000). The transmission route is faecal-oral, as with all forms of salmonellosis. However, unlike the nontyphoidal strains of *Salmonella, S.* Typhi and *S.* Paratyphi are host-restricted to humans and higher primates, meaning that there is thought to be little to no animal reservoir for the pathogen (Lan et al. 2009). This attribute makes the disease a very good target for vaccination. Most of the knowledge of typhoid pathogenesis comes from infecting susceptible mouse strains with *S*. Typhimurium (described below). Upon infection, the Salmonellae first colonise the ileum and invade the intestinal epithelium through microfold (M) cells. They are then taken up by macrophages and dendritic cells in the submucosa within which the bacteria are able to proliferate and be disseminated to distant sites throughout the body via the lymph and blood such as the MLNs, liver and spleen (Watson & Holden 2010). The Salmonellae may then progress through bile-secretions from the liver into the gallbladder (de Jong et al. 2012). In the gallbladder the bacteria can then proliferate in epithelial cells as well as extracellularly, forming

biofilms on gallstones (Crawford et al. 2010; Prouty et al. 2002). The gallbladder is the main reservoir for chronic infection, and is associated with the asymptomatic, chronic carrier state of enteric fever. The Salmonellae can re-seed the gut from the gallbladder, allowing for the effective shedding of bacterial cells into the environment for re-infection (Gonzalez-Escobedo et al. 2011).

1.2.4 Antibiotic resistance in *Salmonella*

Multi-drug resistant nontyphoidal serovars of *Salmonella* such as *S.* Enteritidis and *S.* Typhimurium are now considered to be widespread, greatly reducing the effectiveness of traditional treatments of iNTS such as chloramphenicol, ampicillin and co-trimoxazole. More expensive drugs such as fluoroquinolones and third-generation cephalosporins are being used to manage bacteraemia, poorer countries will struggle to afford this, and even if these more expensive drugs are used, it will contribute to the further development of resistance (Gordon 2008; Feasey et al. 2012). *S.* Typhi and *S.* Paratyphi isolates have been found to be resistant to traditional treatments and fluoroquinolones. Again, third generation cephalosporins including ceftriaxone are now commonly being used, although azithromycin has been suggested as a cheaper alternative for the management of bacteraemia (Crump and Mintz 2010). Unfortunately resistance to all drugs described above has already been detected (Wong et al. 2014). A recent report by the World Health Organisation (WHO) declared fluoroquinolone-resistant *Salmonella* a high priority for the development of novel drugs to the combat disease caused by this pathogen (World Health Organisation 2017).

Several vaccine candidates are in early development for NTS serovars, which could prove promising. Efforts must also be made to combat extreme poverty, improve hygiene standards and to improve the treatment of diseases such as HIV and malaria to reduce the incidence of iNTS. Owing to their monomorphic and host-restricted nature, *S.* Typhi and *S.* Paratyphi are considered to be ideal targets for vaccination and eradication, however this requires increased funding and international coordination (Crump & Mintz 2010). While prevention methods are a long-term goal for fighting these diseases, antimicrobials are currently the only available treatments. Antibiotic tolerance is increasingly recognised as being important in the recalcitrance and recurrence of bacterial disease, likely contributing to the spread of antibiotic resistance (see below). Further understanding of the mechanisms behind antibiotic tolerance in *Salmonella* and how to counteract them, could help us reduce the emergence of antibiotic resistance.

1.3 Models of *Salmonella* infection

It is important to study the behavior of a pathogen in physiologically relevant conditions in order to gain knowledge about the disease in humans and allow more efficient translation of any research into treatments in the clinic. However, physiological relevance must also be balanced with labour, financial cost and reproducibility of experimental results. Importantly there are also ethical considerations when using animals for experimentation; research should always be conducted with the 3R's (replacement, reduction and refinement) in mind. The current models of *Salmonella* infection used for studying gastroenteritis, iNTS and enteric fever are described below.

1.3.1 Animal models of gastroenteritis

Mice have been widely used for studying gastroenteritis caused by *S.* Typhimurium (Hapfelmeier et al. 2004; Coburn et al. 2005). However due to the intrinsic resistance of mice to intestinal colonization by *Salmonella,* streptomycin pre-treatment is required before inoculation with the Salmonellae. This allows colonization of the intestinal mucosa followed by PMN-recruitment, resembling the disease pathology in humans (Barthel et al. 2003). However, the model does not have a normal microbiota present, affecting the relevance of experiments to the human disease. Additionally, the infection is also systemic in the mouse, although with little proliferation (see below), this may affect results. There are also ethical concerns over the use of mice, as with any whole animal model, but especially when the infection model allows them to become sickly, increasing the chance of suffering.

Cattle are natural hosts to *S.* Typhimurium, it being the most commonly isolated serovar from cattle in the US, and also have a similar disease to that observed in humans. This has made calf and ligated bovine ileal loops an ideal model of human *Salmonella*-mediated gastroenteritis (Zhang et al. 2003). However, due the size of the animals, both the labour and financial costs involved are large. Additionally, as the animals are outbred, there is large genetic variation and therefore reduced reproducibility in results (Valdez et al. 2009). Again, there are ethical concerns over the use of large animals such as cattle for experimentation.

1.3.2 Animal models of typhoid fever

Typhoid fever is a difficult disease to model due to the host-restriction of the pathogen to humans and higher primates (Lan et al. 2009). There has a limited amount of research performed on chimpanzees in the past (Metchnikoff & Besredka 1911; Edsall et al. 1960; Gaines et al. 1968), however this is now widely seen as unethical due to the current availability of alternative models. Mouse strains have been developed that are *Nramp*$^{-/-}$, such as BALB/c and C57BL/6, and as a result are susceptible to systemic infection by *S.* Typhimurium. These mice can act as a model for enteric fever and iNTS. The gene *Nramp-1* or *slc11a1* encodes a divalent metal ion transporter present in the membrane of phagosomes (Forbes & Gros 2003). This transporter is thought to reduce the availability of iron inside the *Salmonella*-containing vacuole (the membrane-bound compartment resembling a modified late endosome in which *Salmonella* chiefly resides upon intracellular infection). This in turn limits the ability of the bacteria to proliferate intracellularly (Nairz et al. 2010). The disease in *Nramp*$^{-/-}$ mice is similar to that of enteric fever, with enlarged Peyer's patches, low levels of inflammation in the ileal mucosa and diffuse enterocolitis throughout the GI tract. Importantly, there is proliferation of Salmonellae within macrophages as well as at distant sites such as the liver, spleen and gallbladder (Carter & Collins 1974; Valdez et al. 2009). There are, however, significant differences between *S.* Typhi infection of humans and *S.* Typhimurium infection of mice, which are important to remember when using murine infection to model human typhoid fever. Firstly, there is little evidence to suggest that *S.* Typhimurium can re-seed the intestine from the gallbladder in mice, which is a

notable pathology of typhoid fever in humans as it can incur large amounts of inflammation and necrosis of the gut mucosa (Menendez et al. 2009). Additionally, there are virulence genes that are unique to both serovars. The Vi capsular antigen of *S.* Typhi is not present in *S.* Typhimurium and is known to down-regulate host TLR-mediated signaling and confer resistance to complement (Wilson et al. 2008). The recently discovered typhoid toxin, shown to cause cell cycle arrest in host cells, is also present in *S.* Typhi and but not in *S.* Typhimurium (Spanò et al. 2008). Likewise, the pSLT virulence plasmid of *S.* Typhimurium is not present in *S*. Typhi. The *spv* operon, which encodes four T3SS effectors that are secreted by the SPI-2 secretion apparatus, is found on this plasmid among several other genes not present in *S.* Typhi (McClelland et al. 2001; Sabbagh et al. 2010). Each of these virulence genes may have unique phenotypes that contribute to the overall disease.

The chronic form of typhoid can be studied by infection of the 129sv mouse strain, which is Nramp-1-positive, with *S.* Typhimurium. Upon infection of a 129sv mouse with *S*. Typhimurium, dissemination to distal sites such as the liver, spleen and gallbladder still occurs, where the Salmonellae can persist for long periods. However the bacteria are unable to proliferate intracellularly (Monack et al. 2004). Additionally, humanised mouse strains have also been used to study *S.* Typhi infection. These immunodeficient mouse strains, lacking the IL-2 receptor gamma chain, are able to support grafts of human haematopoeitic stem cells (HSCs). These humanised mice have been shown to be susceptible to infection with *S.* Typhi (Libby et al. 2010; Song et al. 2010). However the high financial and labour costs involved

in using these strains discount regular laboratory use as an option, nevertheless they could be potentially useful for vaccine development.

1.3.3 Alternative animal models of typhoid fever

Salmonella infection has also been studied using *Drosophila* (the fruit fly). Studies using this model have described the importance of P38 MAPK-dependent phagosomes to resisting infection (Shinzawa et al. 2009) and the role of bone morphogenic protein signaling to innate immune responses (Frandsen et al. 2008). In addition, the secretion of bacterial effectors and the TNF-homologue Eiger were both found to contribute to death post-infection with *Salmonella* (Brandt et al. 2004; Schneider et al. 2007). The nematode *Caenorhabditis elegans* has also been used to study *Salmonella* infection *in vivo* (Aballay et al. 2000; Labrousse et al. 2000). The major advantage of studying *Salmonella* in these small invertebrates is the ability to observe infection in real-time using fluorescence microscopy. It could be argued however, that significant differences in immunity between *Drosophila* and *C. elegans* will reduce the relevance of the results gained from using these models. It is for this reason that the Zebrafish (*Danio rerio)* embryo has been recently used to model *Salmonella* infection (Van Der Sar et al. 2003): being a vertebrate, it is more closely related to humans while also transparent, allowing real-time tracking of infection with fluorescence. The ability to monitor infection within the whole host in real time is an incredible advantage to using these small animal models. However due to the reduced physiological relevance of the infection when compared to that in humans, the results are

mostly likely to reflect on general aspects of innate immunity or *Salmonella* pathogenesis rather than elements specific to human disease.

1.3.3 *In vitro* models

Salmonella is able to infect and proliferate inside various types of host cells (Figueira & Holden 2012). As the intracellular lifestyle is essential to the progression of systemic salmonelloses (Ibarra & Steele-Mortimer 2009), studying the infection of cells cultured *in vitro* is invaluable. Owing to the changes to cells that occur when outside of the host and the mutations that tend to accumulate in immortalized cell lines, *in vitro* cell culture is not as physiologically relevant as whole animal models. Nevertheless, the relatively low labour and financial costs, along with increased reproducibility of experiments makes these *in vitro* models a common choice for routine laboratory work on *Salmonella*. Immortal cell lines can either be natural cancerous tissue cells such as HeLa cells (epithelial-like) and RAW 264.7 cells (macrophage-like), or immortalised through the introduction of viral genes such as with HEK293 cells. Primary cell culture from the animal is often considered to be more physiologically relevant as the cells spend less time *ex vivo* before infection. Primary cells can also be freshly immortalised in the laboratory using viral vectors. This can produce high quality immortal cell lines and reduce the number of animals required for primary cell culture alone.

Overall, the use of various different models for *Salmonella* infection is recommended to avoid false conclusions resulting from different biases that may arise in each. *In vitro* models are particularly useful for exploring new

hypotheses and routine laboratory work due to low costs and the ease of work. Results can then be confirmed using animal models if an increased physiological relevance to disease is required. Of course, the physiological relevance of a model matters more or less depending on what is being studied. For example, if the systemic effects of a specific virulence factor during infection are to be investigated, then it will be difficult to carry out the necessary experiments with *in vitro* cell culture infection models. However, if we wish to understand the state of *Salmonella* physiology during intracellular infection, *in vitro* models are ideal for an initial investigation.

1.4 Bacterial persistence in the host (adapted from Fisher *et al.,* 2017)

1.4.1 Persistent infections

Many pathogenic bacteria are able to persist in their host for long periods of time. These persistent infections can be asymptomatic (subclinical) or symptomatic, can take place in various tissues in the host and are associated with antibiotic treatment failure (Rhen et al. 2003; Grant & Hung 2013). Asymptomatic persistent infections regularly escape diagnosis and can be caused by growing or growth arrested bacteria. Subclinical persistent infections with actively growing bacteria are not only a burden on the host, but also have the potential to spread to others and cause persistent infections and disease. For example, typhoid fever can lead to an asymptomatic carrier state in 2-5% of patients, with large amounts of bacteria being shed from the gallbladder (Levine et al. 1982). This condition can take four times longer to treat than acute typhoid fever and substantially increases the risk of gallbladder cancer (Caygill et al. 1994); treatment may still fail, even after this

long course of antibiotics, requiring the removal of the gallbladder followed by additional antibiotic therapy (Bhan et al. 2005). *H. pylori* infection, which is associated with an increased chance of stomach ulcers (Nomura et al. 1994) and gastric cancers (Wotherspoon et al. 1991; Eslick et al. 1999), also leads to the shedding of bacteria. Additionally, asymptomatic persistent infections with latent, nongrowing bacteria may be associated with a chance of relapse of acute symptomatic infections. Typhoid fever recurs in 15% of patients after antibiotic treatment (Gotuzzo et al. 1987) and following a urinary tract infection (UTI) caused by uropathogenic *E. coli* (UPEC), 27% of women will suffer a relapse (Foxman 1990). Several other bacterial infections including streptococcal tonsillitis (Österlund et al. 1997) tend to recur after antibiotic treatment and are likely to have a period of latency within the host.

In contrast to asymptomatic persistent infections, symptomatic persistent infections are characterised by a long period of clinical manifestations, often despite antibiotic treatment (Grant & Hung 2013). They can be life threatening and often follow the use of indwelling medical devices or the suppression of immunity during chemotherapy or HIV infection. Persistent infections associated with indwelling medical devices account for around half of all nosocomial infections and are notoriously recalcitrant to drugs (Bryers 2008). Acute *M. tuberculosis* infection can take several months to treat with antibiotics (Gomez & McKinney 2004), and lung infections in patients with cystic fibrosis, often caused by *P. aeruginosa, Burkholderia cepacia, S. aureus* and *H. pylori* become increasingly difficult to treat with time despite remaining apparently susceptible to antibiotics in laboratory tests (Lyczak et al. 2002). The long courses or repetitive use of antibiotics due to

recalcitrant or relapsing infections will not only have negative impacts on patient health, through side effects and the depletion of the resident microbiota (Jernberg et al. 2010), but it also increases the spread of antibiotic resistance through the selection of antibiotic resistant strains. Therefore, there is a need for more effective strategies to treat persistent infections.

1.4.2 Ineffective clearance by the host

In the absence of antibiotic treatment, a persistent infection is the result of a failure of the host immune system to clear the infection. This may be due to an inability of the immune system to detect the pathogen. In addition, some bacteria have evolved strategies to avoid detection by the host, for example, *Borreliae spp*. vary the expression of surface antigens during infection (Norris 2006). Pathogens can also modulate host immune responses triggering an inappropriate anti-inflammatory response, thus decreasing the chance of pathogen clearance. For example, *M. tuberculosis* and *Listeria monocytogenes* induce IL-10 production in macrophages to suppress the IFN-**γ** response that can restrict growth (Redpath et al. 2001). Moreover, many pathogens, including *M. tuberculosis*, *Legionella* and *Salmonella,* avoid degradation following phagocytosis by host immune cells by inhibiting phagosome maturation (Scott et al. 2003). Pathogens can also interfere with the adaptive immune response, for example, the *S.* Typhimurium SPI-2 type three secretion system effector SteD was recently shown to inhibit MHC class II antigen presentation in dendritic cells (Bayer-Santos et al. 2016), likely influencing the host T cell response in favour of the pathogen. These are only a few choice examples of the diverse strategies used by bacteria to evade

host immunity that are known (Reddick & Alto 2014; Stewart 2002).

Even if the pathogen is detected and an antibacterial response is mounted by the immune system, successful clearance is not guaranteed. For example, *H. pylori* escapes clearance despite inducing large amounts of inflammation in the stomach epithelium (Monack et al. 2004). This is dependent on many factors, including adherence, cell motility, reactive oxygen species (ROS) detoxification and toxin secretion (Salama et al. 2013). Biofilm formation, the secretion of polysaccharides and DNA by bacteria to form a protective extracellular matrix, has also been linked to the persistence of many infections (Costerton et al. 1999). Biofilms can block complement-mediated and cell-mediated killing in many persistent infections, such as those associated with indwelling devices (Bryers 2008; Jesaitis et al. 2003; Domenech et al. 2013). Furthermore, *M. tuberculosis* cells can be effectively 'walled off' by macrophages within the lung tissue, forming granulomas. This restricts the growth of the bacteria, but the pathogen is not cleared. If host immunity is subsequently suppressed, bacterial growth may resume and result in a relapse of acute tuberculosis (Lawn et al. 2002).

1.4.3 Ineffective clearance by antibiotics

Failure of antibiotic treatment can be due to several factors. Low patient compliance and poor pharmacokinetics of drugs in infected tissues can promote treatment failure (Kardas 2002; Gonçalves-Pereira & Póvoa 2011). Additionally, antibiotic resistance that is acquired through genetic adaptation or horizontal gene transfer may allow survival and growth in the presence of antibiotics, even at concentrations that are toxic for the host (Blair

et al. 2015). In the absence of resistance, bacteria may survive drug treatment through antibiotic tolerance (Figure 1.2). Tolerance is a reduction in the susceptibility of a population of bacteria to killing by *bactericidal* antibiotics. Tolerance can also be described as an increase in the time it takes for an entire population to be killed at a given antibiotic concentration (Brauner et al. 2016). Slow growth may increase the duration of antibiotic exposure that is needed to kill the population, due to a reduction in the activity of metabolic targets or decreased uptake of the drug. Antibiotic resistance and tolerance can either occur on the level of a whole population of bacteria, or within a subpopulation through phenotypic heterogeneity as phenotypic resistance or persister formation respectively. Persisters can be multi-drug tolerant but differ in their sensitivity to different antibiotics (Helaine & Kugelberg 2014). They are slow-growing or nongrowing bacteria that are able to re-establish growth once cellular stress pathways have become deactivated, but they regain sensitivity to antibiotics once growth has resumed (Lewis 2010; Helaine & Kugelberg 2014; Harms, Maisonneuve, et al. 2016; Michiels et al. 2017). Homogenous populations of resistant, tolerant or susceptible bacteria theoretically exhibit differential killing kinetics during antibiotic treatment *in vitro* (Figure 1.2), however, clonal populations of bacteria will respond to antibiotic treatment in a heterogeneous manner. For example, *S.* Typhimurium cells that are cultured in nutrient rich media display classic biphasic killing kinetics after the addition of the antibiotic cefotaxime (Figure 1.3). Susceptible bacteria die rapidly after cefotaxime addition, resulting in a large initial drop in colony forming units (CFU), whereas a small proportion of persister cells remain viable, which is represented by a plateau in the kill

kinetics. Heterogeneity tends to increase during infection compared to *in vitro* culture. *Salmonella* cells that are released from macrophages after 30 min of phagocytosis and then cultured in nutrient rich media in the presence of cefotaxime display similar biphasic killing kinetics to *in vitro* culture. However, the persister fraction is much larger owing to the activation of cellular stress responses that are induced by the acidic and nutrient-limiting conditions inside the *Salmonella*-containing vacuole (SCV)(Helaine et al. 2014). A clonal population of *Salmonella* that is treated with antibiotics while inside macrophages is even more heterogeneous in response to antibiotic treatment. This is the result of the total population dividing at a slower rate compared to in a rich medium; it is therefore more tolerant to antibiotic treatment. This is in addition to the nongrowing persister cells that are even less susceptible to the drug. In this case, a more gradual drop in the number of viable cells is observed until only the persister fraction remains (Helaine et al. 2014). During infection of host tissues, antibiotic tolerant slow-growing bacteria and nongrowing persisters are likely to exist simultaneously. Variable sensitivity to antibiotics as a consequence of differential growth kinetics has been described during antibiotic treatment of murine *Salmonella* infection (Claudi et al. 2014). Nongrowing *Salmonella* cells were found to be the least susceptible to killing by fluoroquinolones. Interestingly, the largest surviving fraction of cells had an intermediate rate of growth, which was able to grow at a moderate rate without being killed rapidly by the antibiotic. One could speculate that a slow-growing, tolerant population of bacteria is of greater concern in a chronic infection associated with treatment failure while nongrowing persisters can provide a source of bacterial regrowth after an

apparently successful course of treatment with antibiotics, resulting in the recurrence of clinical symptoms. It is important to consider that the reasons for antibiotic treatment failure in the host are complex and may be the result of the combination of all of the factors mentioned above including interactions between the pathogen and host immunity as well as antibiotic resistance and tolerance occurring on both the population and subpopulation level.

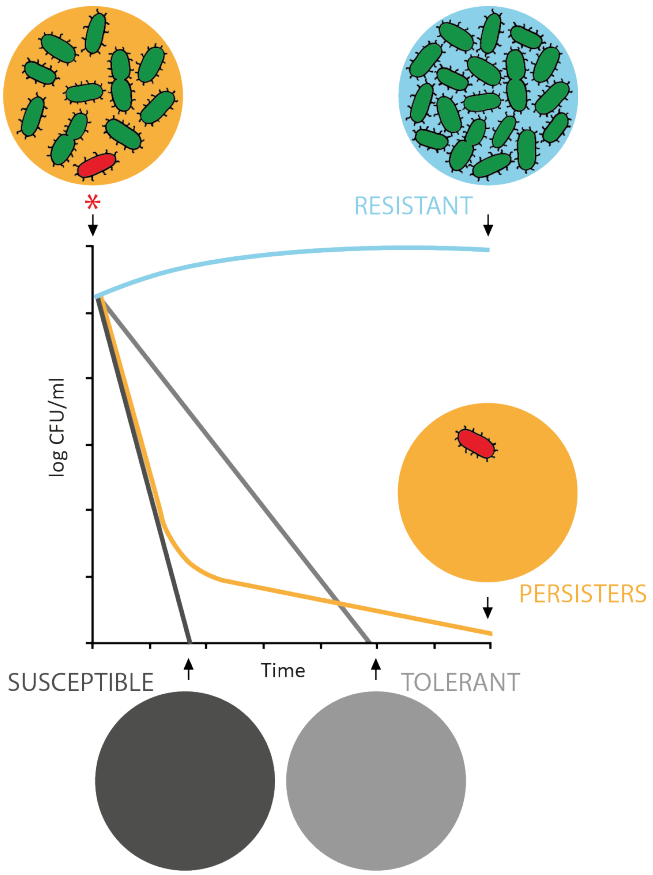


Figure 1.2: Killing kinetics of persisters and homogeneous populations of bacteria. Growth continues when a bactericidal antibiotic is added (red asterisk) to a homogeneous population of resistant bacteria (blue). A homogeneous bacterial population that is susceptible to the drug (dark grey) is killed rapidly, while a tolerant population (light grey) is killed more slowly. Bacterial populations found in nature are usually heterogeneous in the response to antibiotics, tolerant persisters can be revealed by biphasic kill curves (orange) after the addition of a drug, most cells are susceptible and rapidly die while the persister fraction is represented by a slow decrease in colony forming units (CFU). Adapted from Fisher *et al.*, 2017.

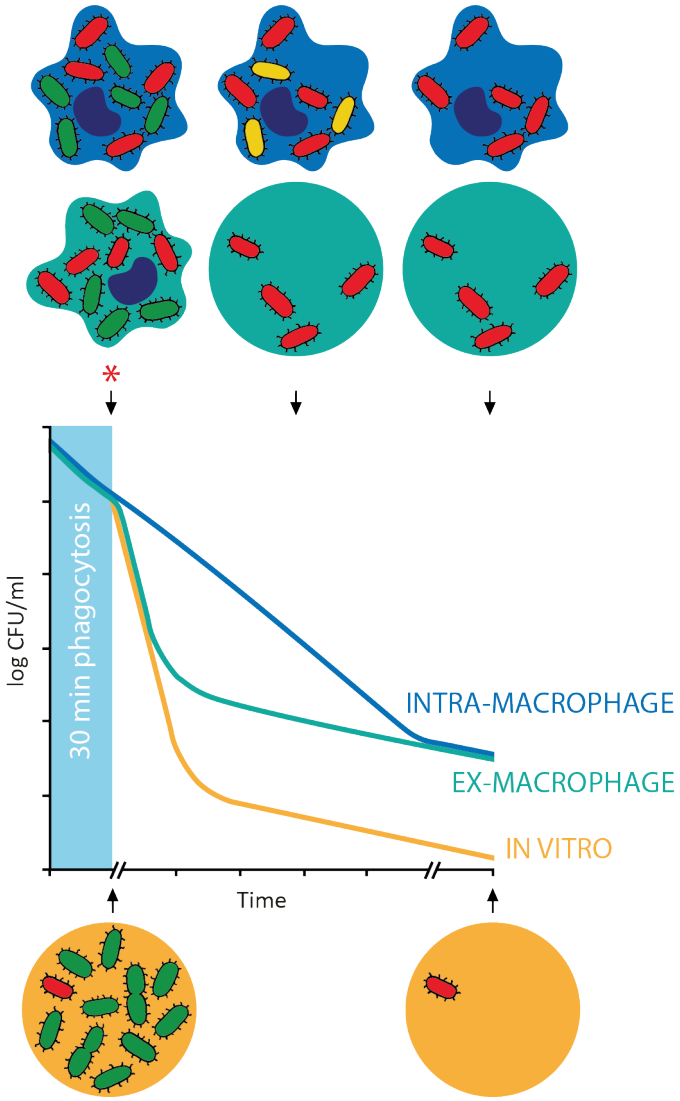


Figure 1.3: Killing kinetics of *Salmonella* after addition of cefotaxime during *in vitro, ex-macrophage* and intra-macrophage conditions. Upon addition of cefotaxime (red asterisk), *Salmonella* growing in LB displays a biphasic kill curve with a low level of persisters ('IN VITRO'; yellow). This level of persisters increases after 30 min phagocytosis by macrophages followed by release and *in vitro* antibiotic treatment ('EX-MACROPHAGE'; green). *Salmonella* treated inside of macrophages displays whole population tolerance and high levels of persisters (INTRA-MACROPHAGE; blue). Diagrams depicting presence and growth state (red – nongrowing; yellow – slow-growing; green – fast-growing) bacteria in macrophages or *in vitro* are shown at various timepoints (indicated by arrows), colour-coded to the appropriate condition described above. Adapted from Fisher *et al.*, 2017.

1.5 Persister cells (adapted from Fisher *et al.,* 2017)

1.5.1 Links to persistent infections

Persisters were first described soon after the discovery of antibiotics (Hobby et al. 1942; Bigger 1944). Joseph Bigger first used the term over 70 years ago after he discovered a culture of *S. aureus* that could not be sterilised with penicillin, regardless of the dose. He hypothesised that a small proportion of the bacteria survived due to their lack of growth rather than a heritable resistance mechanism (Bigger 1944). This hypothesis was corroborated 60 years later, when a study using microfluidics and live imaging showed that the bacterial cells that survived antibiotic treatment were not growing before the addition of the drug (Balaban et al. 2004). Several studies have now correlated a lack of growth with persister formation (Helaine & Kugelberg 2014b). A reduction in metabolic activity is also often associated with the persister phenotype (Amato et al. 2014). However, this does not mean that persisters are metabolically inactive (Helaine et al. 2014).

In recent years, evidence that bacterial persisters play a role in the relapse and recalcitrance of infection has been accumulating. Monitoring single nucleotide polymorphisms (SNPs) in iNTS isolates showed that in cases of recurrent fever, 78% were due to the same genovar as the original infection (Okoro et al. 2012). Similar observations have been made by sequencing UPEC strains from patients with UTIs (Russo et al. 1995) and *Streptococcus pyogenes* strains from patients with streptococcal tonsillitis (Bingen et al. 1992). These findings indicate that the bacteria causing these infections were likely never cleared from the host during antibiotic treatment.

Antibiotic tolerance is generally considered to be the result of nonheritable

phenotypic changes in bacteria, however, genetic mutations may also increase tolerance indirectly by slowing growth, metabolism or the uptake of drugs. For example, mutations that led to an increase in the lag time of bacterial populations were found to increase antibiotic tolerance (Fridman et al. 2014). Similarly, mutations can increase the probability of persister formation within a clonal population. These are called high persistence (hip) mutations and were first described in *E. coli* in reference to the *hipA7* mutation (Moyed & Bertrand 1983). Clinical isolates of *P. aeruginosa* from lung infections in cystic fibrosis patients are more likely to be hip mutants late in infection compared to if they are isolated earlier in infection (Mulcahy et al. 2010). *E. coli* hip mutants have also been isolated from patients with recurrent UTIs (Schumacher et al. 2015). Similarly, periodic treatment of *Candida albicans* with amphotericin B was found to select for hip mutants (LaFleur et al. 2010), indicating that the presence of persisters may also be important in the recalcitrance of fungal infections. Persisters have even been reported outside the field of microbiology, potentially playing a role in the tolerance of tumour cells to chemotherapy (Pearl Mizrahi et al. 2016). Hip mutants have also been observed *in vitro*, after periodic antibiotic treatment of *E. coli* and *S. aureus* cells (Moyed & Bertrand 1983; Mechler et al. 2015; Van den Bergh et al. 2016). These findings suggest that the persister phenotype may be an important first line of defence against drugs before resistance can be acquired.

The intracellular lifestyle of certain bacterial pathogens has been linked to an increase in the relative number of persister cells in a population. For example, *Salmonella* and *M. tuberculosis* both increase persister formation

inside macrophages (Helaine et al. 2014; Mouton et al. 2016). Concurrently, evidence is also building that biofilm formation and the ability of bacteria to persist intracellularly are also associated with persistent infections (Grant & Hung 2013; Costerton et al. 1999; Burmølle et al. 2010; Hunstad & Justice 2010; Helaine et al. 2014). Several studies have described a link between persister formation and biofilms (LaFleur et al. 2010; Brooun et al. 2000; Spoering & Lewis 2001; Keren, Kaldalu, et al. 2004; Maisonneuve et al. 2013; Conlon et al. 2013). *P. aeruginosa* forms biofilms during lung infections in cystic fibrosis patients (Davies 2002) whereas *H. pylori* forms biofilms and adopts an intracellular lifestyle during infection (Oh et al. 2005; Cammarota et al. 2012). UPEC can form biofilms on the bladder epithelium as well as quiescent intracellular reservoirs that could contribute to relapsing infections (Hunstad & Justice 2010). *Salmonella* can form biofilms on gallstones (Prouty et al. 2002) and *Salmonella* persisters have been found residing within macrophages in the spleens of infected mice days after the initial infection (Helaine et al. 2014). Considering the *in vitro* evidence that there are high levels of persister formation in biofilms and inside host cells combined with the prevalence of biofilm formation and the intracellular lifestyles of bacteria during persistent infections, persister formation is likely a significant factor in the relapse and recalcitrance of these infections.

1.5.2 Persister cell formation

There are several environmental and physiological stresses that enhance the formation of persisters in bacterial populations, including nutrient limitation (Maisonneuve et al. 2013), diauxic shifts (Amato et al. 2013),

extreme pH (Helaine et al. 2014) and DNA damage (Dörr et al. 2010). Environments that are physiologically relevant to bacterial infection such as within biofilms and inside host cells such as macrophages have also been shown to be associated with persister formation (Spoering & Lewis 2001; Helaine et al. 2014). These complex environments likely induce persister formation by conferring some or all of the stresses described to induce it *in vitro*. The intriguing nature of this phenomenon is that it only occurs in part of a clonal population. If an environmental stress is placed on the whole population, how is it that only a subpopulation become persister cells? One explanation is that stochastic gene expression across the population could contribute to phenotypic heterogeneity (Fasani & Savageau 2013). Another is that the environmental stress is not evenly spread across the whole population; the formation of microenvironments with greater levels of stress around some bacterial cells and not others, such as those low in nutrients or high in toxic compounds, could also contribute to heterogeneity (Maisonneuve et al. 2013). Differences in stress levels within environments relevant to infection are easy to imagine. The centre of a biofilm is thought to be severely limited for nutrients, which could explain why only part of the bacterial population forms persisters. This is supported by the requirement for an active starvation response for antibiotic tolerance of biofilms (Nguyen et al. 2011). Macrophages may restrict nutrient availability and lower the pH to different extents in different cells or within different phagosomes inducing persister formation in some cells and not in others. However, the exact mechanisms of how these environmental signals induce the formation of persisters are still a matter of debate.

1.5.3 Toxin-antitoxin modules and persister formation

The first link between persister formation and toxin-antitoxin (TA) modules was made over 30 years ago. A chemical mutagenesis screen using ethyl methanesulfonate and repetitive antibiotic treatments found a *hip* mutant of *E. coli* that formed far greater proportions of persisters than the wild type strain was discovered (Moyed & Bertrand 1983). The mutation responsible for the increase in persister levels was mapped to the gene *hipA*, which belongs to a TA module. Around the same time, TA modules on plasmids were being studied for their role in plasmid stability and postsegregational killing in bacteria (Ogura & Hiraga 1983; Gerdes et al. 1986). It was later realised that many of these toxin-antitoxin modules are also encoded on bacterial chromosomes and may be involved in inhibiting metabolic processes and reducing growth in response to stress (Pandey & Gerdes 2005; Gerdes et al. 2005). Toxin-antitoxin modules encode a stable toxin, which may inhibit any one of a diverse set of metabolic processes, and an antitoxin that neutralises the activity of the toxin under unstressed conditions. Stress signals are thought to lead to the degradation of the antitoxin, freeing the toxin to inhibit the activity of its target (Figure 1.4) (Yamaguchi & Inouye 2011). Mathematical modelling of the regulation of a toxin-antitoxin module suggests that a bistable state of expression is possible within a clonal population of cells – one resulting in the production of many free toxin proteins and another that results in the few toxin proteins present being tightly bound by antitoxins (Rotem et al. 2010; Cataudella et al. 2012). This means that there is either strong repression, or strong derepression of the module with intermediate levels of expression only existing when in transition from one extreme to the other. This

goes part of the way to explaining how a clonal population can contain two very disparate phenotypes, growth and growth arrest, possibly depending on the activation of these modules. There are currently six different types of TA module described so far, categorised by the various mechanisms of neutralisation by the antitoxin (Page & Peti 2016). The best described types, I and II, are implicated in persister formation (Helaine et al. 2014; Keren, Shah, et al. 2004; Shah et al. 2006; Maisonneuve et al. 2011; Verstraeten et al. 2015; Dörr et al. 2010), although this does not exclude the possibility of the other types also being involved. In *E. coli*, the SOS response was found to induce the expression of the type I pore-forming toxin gene *tisB*, increasing persister formation (Dörr et al. 2010). The alarmone (p)ppGpp has been

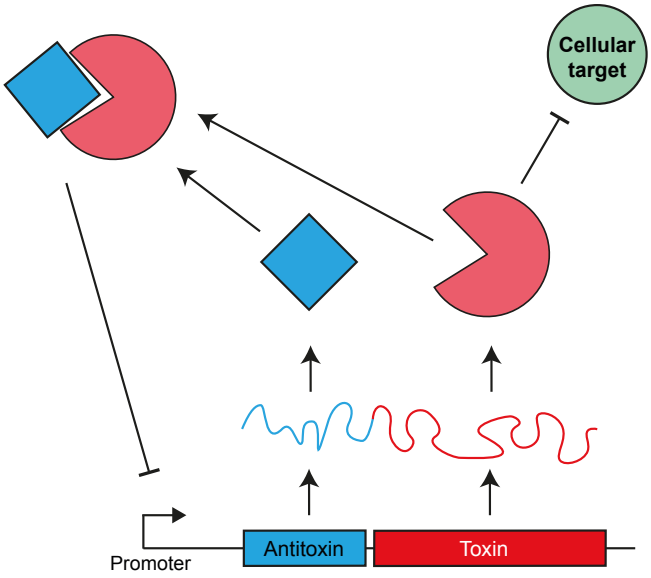


Figure 1.4: Regulation of type II toxin-antitoxin module. Type II TA modules are defined by a protein antitoxin which can bind and block the activity of a protein toxin. This toxin-antitoxin complex can then bind and repress the promoter of the TA operon. Adapted from Yamaguchi and Inouye 2011.

linked to the activation of type II and type I toxin-antitoxin modules through signalling cascades involving Lon protease and the Obg respectively, leading to an increase in persister formation (Maisonneuve et al. 2013; Verstraeten et al. 2015). Both of these proteins have central roles in bacterial metabolism, Lon protease is involved in the degradation of many cellular proteins (Maurizi 1992) while Obg is a GTPase that regulates translation and DNA metabolism (Kint et al. 2014). This fascinating discovery suggests an overlap in the regulation of both types of toxin-antitoxin module with central metabolism in bacteria. The role of Lon protease in persister formation in *E. coli* has been questioned however. The deletion of *lon* in *E. coli* has been shown to have no effect on persister levels isolated through treatment with β-lactams or aminoglycosides (Theodore et al. 2013; Shan et al. 2015). It did not reduce the number of persisters isolated by fluoroquinolones, however the additional deletion of *sulA*, which encodes a cell division inhibitor induced by the SOS response, restored persister formation to wild type levels (Theodore et al. 2013). As SulA is a substrate of Lon protease (Mizusawa & Gottesman 1983), the apparent reduction in persisters could be due to unchecked SulA activity inhibiting regrowth after DNA damage rather than a lack of antitoxin degradation.

There is a diverse range of activities amongst the toxins currently characterised (Figure 1.5). These include inhibiting cellular processes such as translation (Germain et al. 2013; Pedersen et al. 2003; Christensen & Gerdes 2003; Christensen-Dalsgaard et al. 2010; Winther & Gerdes 2011; Winther et al. 2016; Castro-Roa et al. 2013), DNA metabolism (Bernard et al. 1993; Jiang et al. 2002; Harms et al. 2015), and decreasing the proton motive force

(Dörr et al. 2010; Verstraeten et al. 2015). Toxins that inhibit protein synthesis appear to be the most abundant with many targeting RNA, including mRNases such as RelE (Pedersen et al. 2003; Christensen & Gerdes 2003; Christensen-Dalsgaard et al. 2010), tRNases such as VapC (Winther & Gerdes 2011; Winther et al. 2016) and tRNA-acetylating toxins such as TacT (Cheverton et al. 2016). There are also kinases such as HipA and Doc that

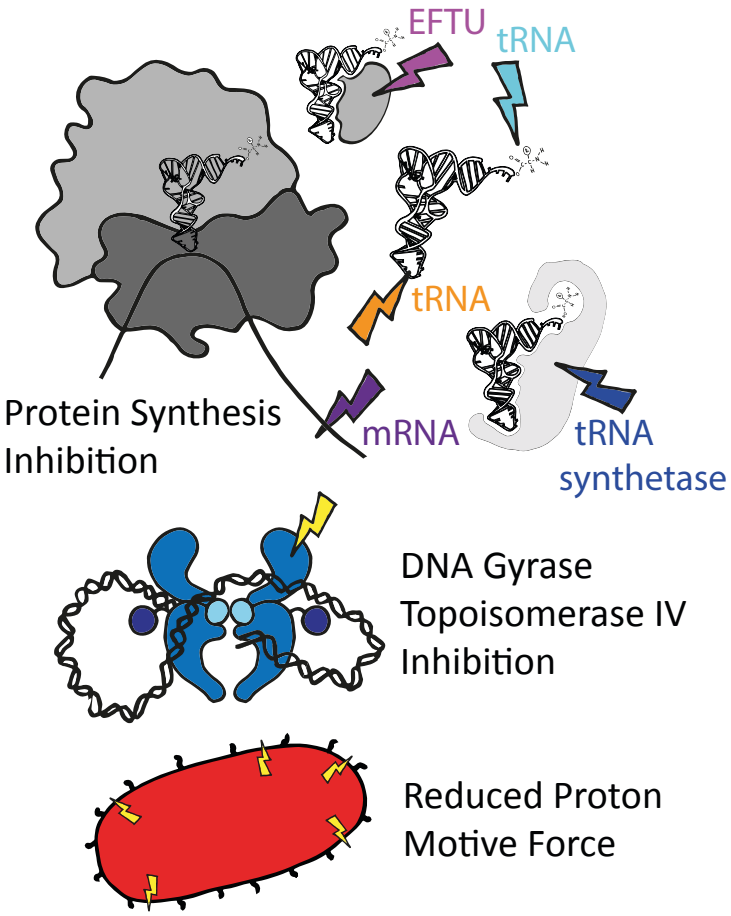


Figure 1.5: Mechanisms of persister formation. Toxin-antitoxin systems can contribute to persister formation by inhibiting protein synthesis through various mechanisms shown: phosphorylation of EF-Tu by Doc (Castro-Roa et al. 2013) (pink lightning bolt); acetylation of tRNA by TacT (Cheverton et al. 2016) (turquoise lightning bolt); phosphorylation of tRNA synthase by HipBA (Germain et al. 2013) (blue lightning bolt); cleavage of tRNA by VapC (Winther & Gerdes 2011) (orange lightning bolt); cleavage of mRNA by RelE (purple lightning bolt). DNA metabolism is also be inhibited by toxins. FicT has been shown to inhibit DNA gyrase and TopoIV activity (Harms et al. 2015). The proton motive force of a bacterial cell has also been reported to be reduced by TisB activity, resulting in the inhibition of growth (Dörr et al. 2010). Adapted from Fisher *et al.*, 2017.

phosphorylate GltX and EF-Tu respectively to inhibit their activity (Germain et al. 2013; Castro-Roa et al. 2013). Pore-forming toxins such as TisB and HokB are known to reduce the proton motive force across the bacterial membrane and consequently lower the ATP synthesis of the cell (Dörr et al. 2010; Verstraeten et al. 2015).

An interesting and little-understood group of TA modules are those whose toxins inhibit aspects of DNA metabolism. ParDE was one of the first toxin-antitoxin modules described (Pecota et al. 1997). The ParE encoded on the RK2 plasmid in *E. coli* was found to bind to and inhibit the activity of DNA gyrase and induce post-segregational killing (Jiang et al. 2002). FicT toxins from *Bartonella*, *Yersinia* and *Pseudomonas* were recently described to block TopoIV and DNA gyrase activity through adenylylation, leading to growth arrest of the cell through the knotting and concatenation of the bacterial chromosome (Harms et al. 2015). Interestingly, the Fic homologue in *E. coli* was the first protein described with a FIC domain capable of adenylylation, in addition to other similar activities, which is now known to be ubiquitous through both prokaryotes and eukaryotes. However, a functional characterisation of the *E. coli* protein was never successful (Harms, Stanger, et al. 2016).

There have been seven type I and 20 type II TA modules identified in *S.* Typhimurium to date, although not all were found to have a toxin that inhibited growth with an antitoxin that could counteract the toxicity. 17 of the type II TA modules are chromosomally encoded (Lobato-Márquez et al. 2015). The RNase toxin-antitoxin homologues present include two VapBC, seven RelBE and three HigBA homologues with one DinJ-YafQ homologue.

Three TacT homologues are present as well as a PasTI, a Phd-Doc, a ParDE and a CcdAB homologue, although the CcdB toxin has a mutation that renders it non-toxic. Two of these TA modules have been fully characterised, VapBC (Winther & Gerdes 2011) and TacT (Cheverton et al. 2016). Our lab has previously shown that if any one of 14 of these chromosomally encoded type II TA modules are deleted, it results in a decrease in macrophage-induced persister levels (Helaine et al. 2014).

There are several landmark studies that have linked toxin-antitoxin modules to persister formation. Firstly, transcriptomics carried out on *E. coli* fractions enriched for persister cells showed that toxin-antitoxin modules are upregulated in these subpopulations of bacteria when compared to growing bacteria (Keren, Shah, et al. 2004; Shah et al. 2006). Furthermore, it was shown that the deletion of five or more type II toxin-antitoxin modules from *E. coli* leads to a decrease in the formation of persisters during exponential growth in rich media (Maisonneuve et al. 2011). Correspondingly, the overexpression of toxins in bacterial cells has been shown to inhibit growth and promote an antibiotic tolerant state that can be countered by overexpression of cognate antitoxins (Keren, Shah, et al. 2004; Cheverton et al. 2016; Pedersen et al. 2002; Harrison et al. 2009; Lobato-Márquez et al. 2015). In *E. coli*, the toxin HipA is a serine-threonine kinase capable of phosphorylating and inhibiting the activity of GltX, the glutamyl-tRNA synthetase (Germain et al. 2013; Kaspy et al. 2013). The shortage of glutamyl-tRNA in the cell triggers an increase in (p)ppGpp that leads to the activation of further toxin-antitoxin modules. This further activation of toxin-antitoxin modules is required for the HipA-induced persister phenotype

(Germain et al. 2015). Type II toxin-antitoxin modules were also shown to be upregulated during macrophage infection by *Salmonella* (Helaine et al. 2014). In this system, deletion of single toxin-antitoxin systems was shown to lead to a significant decrease in the levels of macrophage-induced persister formation. The reason why a defect in persister formation is noticeable during macrophage infection with *Salmonella* upon the deletion of single TA modules, but a decrease in persister formation is not observed *in vitro* (in *E. coli* and *Salmonella*), may be because the macrophage is a more physiologically relevant (and stressful) environment and likely provides a greater trigger of derepression in toxin-antitoxin module expression than that of exponential growth in rich media.

While most of the studies into the mechanisms of persister formation have been carried out in *E. coli*, a Gram-negative bacterium, much less is known about how Gram-positive bacterial persisters are formed. There is currently little evidence of toxin-antitoxin modules being involved in persister formation in Gram-positives. Deletion of the toxin-antitoxin modules did not affect persister levels in *S. aureus* (Conlon et al. 2016). However, overexpression of the toxin $mazF_{SA}$ does induce stasis in *S. aureus*, while coexpression of the entire $mazEF_{SA}$ module does not affect growth (Fu et al. 2009). This suggests that toxin-antitoxin modules likely function in a similar fashion to those in Gram-negative bacteria and are likely still involved in the response to stress (Donegan & Cheung 2009), but they are perhaps not required for antibiotic tolerance.

The model describing how TA module activation through (p)ppGpp signalling leads to persister formation is an attractive one, however there is

evidence that toxin-antitoxin modules are not the only factors involved in persister formation (Figure 1.5). While the deletion of multiple toxin-antitoxin modules or the absence of (p)ppGpp leads to much lower persister formation, it does not fully abrogate the phenotype (Maisonneuve et al. 2013; Maisonneuve et al. 2011; Chowdhury et al. 2016). It is possible that there is heterogeneity within the persister population, with different cells arriving at the antibiotic-tolerant phenotype through different pathways. A screen of *E. coli* single gene deletion mutants from the KEIO collection (Baba et al. 2006) did not find mutants completely lacking persisters, however it did identify several global regulators that are important for the phenotype (Hansen et al. 2008). An alternative model proposes that metabolic regulation is the main driver of persister formation and toxin-antitoxin modules are accessory to this control (Amato et al. 2014). One study recently proposed this was the case for ampicillin-tolerant bacteria formed through a diauxic shift between the carbon sources glucose and fumarate (Radzikowski et al. 2016). Two different pathways, both involving trans-translation – a quality control mechanism utilising transfer-messenger RNA during protein synthesis - and the stringent response have been described as important for diauxic shift-induced persisters isolated by either β-lactams or fluoroquinolones (Amato & Brynildsen 2015). The understanding exactly how these pathways lead to tolerance is currently incomplete however. Two studies recently described, using β-lactams or fluoroquinolones, how persister formation in *E. coli* and *S. aureus* is associated with a drop in ATP levels (Conlon et al. 2016; Shan et al. 2017), without an obvious dependency on toxin-antitoxin modules. Further investigation is needed to determine the exact role and interaction of central

metabolism and toxin-antitoxin modules in persister formation.

1.5.5 Regrowth of persisters

1.5.5.1 Molecular mechanisms of regrowth research

One area of persister biology of which little is currently known is how nongrowing persisters are able to switch back to a growing state. Understanding the mechanisms behind this process is of great importance, as reinitiating growth in persisters – and thereby increasing drug susceptibility – may be an effective method of killing these cells when combined with antibiotics. Persisters have been observed regrowing en masse immediately after an external stress is removed (Radzikowski et al. 2016), but they have also been observed to wake up spontaneously over time (Fridman et al. 2014). This may be due to the type of persister being studied in a particular experimental set up, and the heterogeneity of cellular states that exists within the persister subpopulation itself.

It is known that activation of toxin-antitoxin modules can lead to persister formation in Gram-negative bacteria, however very little has been reported on how this activation can be reversed (Figure 1.6). Several type II toxin-antitoxin modules have been shown to autoregulate their expression as a consequence of conditional cooperativity (Page & Peti 2016), which allows repression of the operon at equal or low T:A ratios and derepression with higher levels of free toxin (Overgaard et al. 2008). Presumably, if antitoxin degradation stops – perhaps when a stress signal is alleviated - then the T:A ratio may be able to return to a level that once more allows repression of the operon. Proteolytic degradation of the toxin could also occur, and as the

antitoxin gene is typically found upstream of the toxin gene, a certain amount of RNA polymerase drop-off during transcription may also be involved in resetting T:A ratios. It is difficult to imagine how the cellular pool of antitoxin can be replenished given that the toxin may have inhibited translation, however mathematical modelling of conditional cooperativity has predicted this to be possible, given that a low level of translation is still active

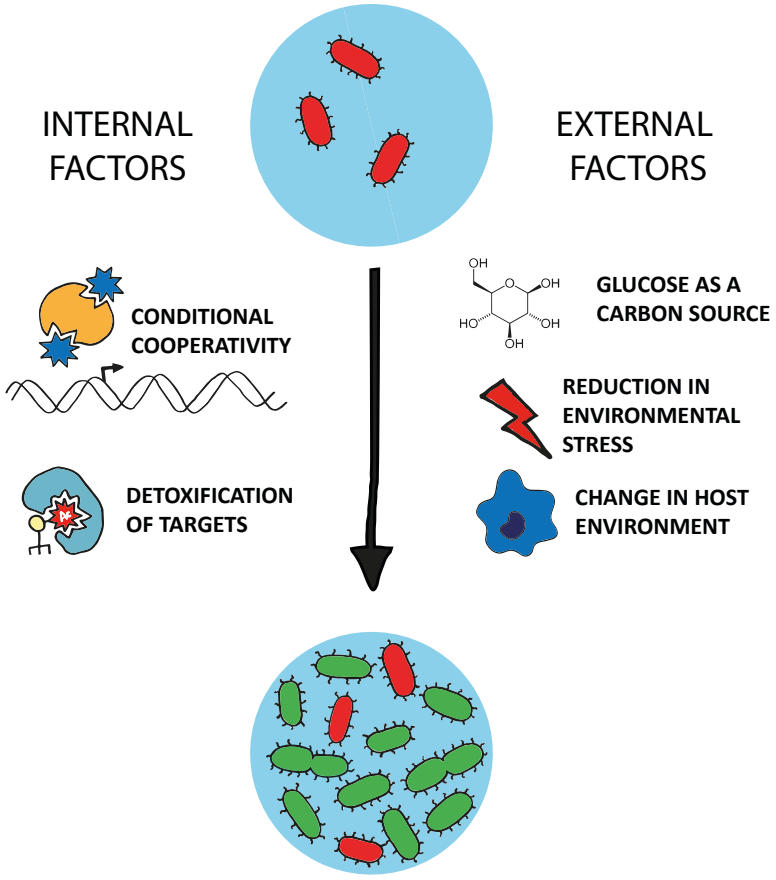


Figure 1.6: Mechanisms of persister regrowth. The ability of bacteria to grow (red – nongrowing; green - growing) is determined by both internal (left; conditional cooperativity of TA module regulation (Cataudella et al. 2012) and detoxification of toxin targets (Cheverton et al. 2016)) and external factors (right; availability of nutrients such as glucose (Radzikowski et al. 2016), reduction of environmental stress and switching host cells (Helaine et al. 2014)). Adapted from Fisher *et al.*, 2017.

(Cataudella et al. 2012). Experimental evidence showing this transition from TA derepression to repression is currently lacking however. It is important to consider that not all toxin-antitoxin modules are regulated in this fashion and so other mechanisms must be involved in repressing toxin expression in these cases (Page & Peti 2016).

Repression of toxin expression is not enough by itself to allow the bacteria to return to a growing state as active toxin must be removed and the effects of the toxin must be counteracted (Hall et al. 2017; Fisher et al. 2017). Plasmid CcdB and ParE toxins preferentially bind to their cognate antitoxins over their target DNA gyrase (Bernard et al. 1993; Jiang et al. 2002). A similar mechanism of detoxification may occur with their chromosomal homologues. The toxicity induced by RelE and MazF was found to be reversed by tmRNA, which rescued ribosomes after stalling on mRNA cleaved by the toxins (Christensen & Gerdes 2003; Christensen et al. 2003). However many toxins inhibit their targets through the addition of post-translational modifications, in these cases these modifications may need to be removed in order to reverse toxicity. It was recently shown that TacT (tRNA-acetylating toxin) in *Salmonella* blocks translation through the acetylation of aminoacylated tRNA molecules (Cheverton et al. 2016). The ability of the toxin to inhibit growth was reduced however, when overexpressing *pth*, which encodes a peptidyl tRNA hydrolase previously reported to cleave peptide chains off tRNA molecules after ribosome stalling (Cheverton et al. 2016; Giudice & Gillet 2013). Pth is able to recognise and cleave acetylated aminoacids from tRNA molecules targeted by TacT, allowing the aminoacyl-tRNA to be recycled. Experimental evidence is currently lacking on other remediation mechanisms,

nevertheless it is possible to speculate as to what these might involve based on the activity of the toxin in question. Toxins that add post-translational modifications to their targets like TacT, may have their modifications removed by other cellular enzymes. Dephosphorylation of EF-Tu and GltX could reverse the toxicity of Doc and HipA respectively and deampylation (the removal of an adenylyl group) of TopoIV and DNA gyrase could relieve Fic toxicity (Fisher et al. 2017).

1.5.5.1 Environmental restriction of growth

The possible mechanisms behind how persisters switch back to a growing state described above are internal factors, but bacteria also require an unrestrictive environment in order to grow. External factors determining the ability to regrow could include chemical cues, physical stresses or the limitation of an essential nutrient (Figure 1.6). Small compounds have been shown to stimulate metabolism in *E. coli* and *Pseudomonas* persisters (Allison et al. 2011; Pan et al. 2012), however as they do not fully reinitiate growth there is clearly still some block to replication in these cells. Determining the mechanism of action of these compounds and the cellular components responsible for this block to growth will be extremely informative. In the case of host immune restriction, it has been known for a long time that immune suppression can lead to relapse of previously latent infections, for example anti-TNF drugs have been linked to the reactivation of latent TB infection (Harris & Keane 2010). If IFN-**γ**-mediated immune responses are suppressed, *Chlamydia* resumes intracellular growth (Belland et al. 2003). This is possibly owing to the relief of the growth restriction imposed on bacterial growth

through innate defence mechanisms and nutrient limitation when residing inside activated cells. This is especially important in respect to patients that are HIV-positive, undergoing chemotherapy or taking immunosuppressant drugs following a transplant. Additionally, persisters can regrow after changing host cell (Helaine et al. 2014). Theoretically, cells harbouring persisters *in vivo* will eventually die and release their contents or cell death may be induced (Grant et al. 2012). A newly acquired host cell may then be far more permissive for bacterial growth.

1.5.5.2 State of regrowers

Not much is known about the physiological state of persister cells after resuming growth. It has previously been suggested that as the stress response is strongly linked to the persister state, regrowing persisters may be primed for mutation and adaptation (Cohen et al. 2013). It is possible that regrowing persisters express higher levels of DNA repair mechanisms such as error-prone polymerases as these are associated with the stress and SOS responses (Layton & Foster 2003; Goodman 2002). These mechanisms could increase the mutation rate during replication, theoretically increasing the probability of antibiotic resistance emerging during persistent infections; especially if low levels of the drug are still present in the host. The SOS response, which has previously been shown to induce persister formation (Dörr et al. 2009; Dörr et al. 2010), is also known to upregulate several mechanisms of horizontal gene transfer (Beaber et al. 2004). This could promote the spread of antimicrobial resistance factors upon recovery from a persister state. One recent study showed that DNA repair mechanisms and

the SOS response are important during the recovery of persisters after ofloxacin treatment (Völzing & Brynildsen 2015). It would be interesting to know if this is a general feature of persister regrowth and is also the case for the recovery of persisters treated with other classes of antibiotics that do not target DNA specifically. Combining evolution experiments with the ScanLag technique developed by the Balaban group, mutations conferring resistance to ampicillin upon repetitive exposure were found to follow those conferring increased tolerance through an increased lag time. This suggests that tolerant bacteria and persister cells are an important bacterial reservoir for the emergence of antibiotic resistance (Levin-Reisman et al. 2017).

1.6 Methods of studying persisters (adapted from Fisher *et al.,* 2017)

The first methods used to study persisters relied on antibiotics selecting for the antibiotic-tolerant cells (Moyed & Bertrand 1983). However in recent years, fluorescent reporters have allowed a much larger repertoire of techniques (Michiels & Fauvart 2016) to be applied to persister studies without the interference of drugs. Fluorescent reporters have been used as a read-out of the metabolic activity or proliferation of bacteria in order to study persisters. A fluorescence dilution reporter plasmid was used to distinguish between growing and nongrowing *Salmonella* within macrophages (Helaine et al. 2014; Helaine et al. 2010). The Lewis group used a GFP reporter and fluorescence-activated cell sorting (FACS) to isolate persister cells for transcriptomic analysis[81] and metabolically active *M. tuberculosis* persisters were monitored *in vitro* and during murine infection using an unstable GFP rRNA gene fusion (Manina et al. 2015). Microfluidics have been used in combination with

fluorescent reporters for example fusions with TA promoters (Maisonneuve et al. 2013) or metabolic reporters (Manina et al. 2015) to study persisters *in vitro.* Transcriptomic analysis has been carried out on enriched persister fractions utilising fluorescent reporters and microarrays (Shah et al. 2006). The ScanLag technique developed by the Balaban group (Levin-Reisman et al. 2010) will likely prove valuable in monitoring the regrowth of persisters. The ScanLag method uses time-lapse imaging to monitor the appearance and growth of bacterial colonies on agar plates over time (Levin-Reisman et al. 2010) and has been used to study the emergence of tolerance and resistance in evolutions experiments (Fridman et al. 2014; Levin-Reisman et al. 2017).

1.6 Dual RNA-seq of pathogen and host during infection

1.6.1 Traditional methods of transcriptomics

The methods first used to monitor changes in gene expression by quantifying RNA were northern blots and quantitative PCR (qPCR). However these techniques utilised only a select few target transcripts for quantification. The development of microarrays allowed quantification of thousands of targeted transcripts simultaneously by hybridising fluorescently labelled RNA (or cDNA) to immobilised specific DNA probes on a chip. The fluorescence intensity corresponding to each probe can then be quantified after hybridisation in order to calculate the abundance of the cognate transcripts (Fodor et al. 1993; Schena et al. 1995). However, similar to qPCR and northern blotting, microarrays could only detect what it was specifically targeting, dependent on the probes that were present on the chip. They also suffered from a low sensitivity coupled with a low point of saturation, giving

them a narrow dynamic range of detection. The use of microarrays for the analysis of pathogen transcriptomics has been widespread, with examples including *Borrelia burgdorferi* (Revel et al. 2002), *Vibrio cholerae* (Merrell et al. 2002), *Chlamydophila pneumonia* (Mäurer et al. 2007), *Chlamydia trachomatis* (Belland et al. 2003) and *S.* Typhimurium (Eriksson et al. 2003). Microarrays have also been used to analysis the changes in gene expression in mammalian cells during bacterial infection (Rappuoli 2000; Bruno et al. 2009; Hannemann et al. 2013).

High-resolution tiling arrays were developed in an attempt to allow the detection of transcripts potentially missed by microarrays. Probes were designed (either overlapping, or contiguous in sequence) to cover entire genomes for the detection of transcripts (Berton 2004; Selingwe 2003). However tiling arrays were extremely costly, limiting their use in routine laboratory research. Additionally, as with microarrays, tiling arrays have a narrow dynamic range, making detection of low abundant transcripts difficult. Tiling arrays have been used to describe the global transcriptional changes of *Listeria monocytogenes* during murine infection (Toledo-Arana et al. 2009).

Tag-based techniques are also used to measure differential gene expression. These involve tagging transcripts upon reverse transcription and enumerating them through Sanger sequencing. Serial analysis of gene expression (SAGE) and cap analysis of gene expression (CAGE) detect the 3'- and 5'-ends of transcripts respectively (Velculescu et al. 1995; Kodzius et al. 2006). These have been followed by improved techniques such as SuperSage, which uses longer tags, allowing greater precision in identifying transcripts (Matsumura et al. 2012). The benefit of tag-based methods is that

no prior knowledge of a transcript is required in order to detect it, making it useful for the detection of novel transcripts. The sensitivity of these tag-based techniques is low however, making them not ideal for whole transcriptome analysis. Additionally, as these techniques detect only the ends of transcripts, it is not suitable for identifying splice-isoforms or bacterial operon structures. Tag-based approaches have been less frequently used for the transcriptomic analysis of pathogenesis, although it has been used for eukaryotic parasites (Kronstad 2006) and, in combination with microarrays, on epithelial cells infected with *Streptococcus pyogenes* (Nakagawa et al. 2004).

1.6.2 RNA-seq

The advent of next-generation sequencing (NGS) technologies such as Illumina (Solexa) or Roches/454 (pyrosequencing) has revolutionised modern biology. The sequencing of entire genomes can now be carried out in a matter of hours, vastly increasing the amount of data we are able to collect (Metzker 2010). These technologies were first used for genomics studies, but are increasingly used for transcriptomics in the form of massively parallel cDNA sequencing, otherwise known as RNA-seq. Generally, RNA-seq is carried out by extracting RNA and converting to cDNA through reverse transcription, amplifying the cDNA and sequencing using NGS. The number of sequencing reads generated that align to a sequence on a reference genome can be used to quantify the relative changes in the levels of specific transcripts between samples. The digital nature of RNA-seq allows for a high sensitivity and a wide dynamic range, making it ideal for the high-throughput profiling of entire transcriptomes. Although the technique benefits from using an annotated

reference genome, it is not required, and sequences can still be detected without alignment. Along with the quantitative information that can be acquired on gene expression using RNA-seq, many forms of qualitative information on the transcriptome can also be acquired. These include the identification of transcript boundaries including untranslated regions (UTRs) of genes, processing sites and splice isoforms in eukaryotes and bacterial operon structures, transcription start sites (TSSs) and novel (noncoding) genes. These attributes make RNA-seq the current method of choice for transcriptomic analysis (Wang et al. 2009). It has been used to analyse the transcriptomes of many pathogens including *S.* Typhi (Perkins et al. 2009), *Helicobacter pylori* (Sharma et al. 2010), *Burkholderia cepacia* (Yoder-Himes et al. 2009), *Chlamydia trachomatis* (Albrecht et al. 2010) and *Bacillus* spp. (Passalacqua et al. 2009). Transcriptomic profiling of mammalian cells during infection has so far been less common, the studies that have been carried out have taken a focus on the miRNA response to infection (Schulte et al. 2011; Maudet et al. 2014).

Despite the huge reduction in the cost of using NGS technologies in recent years, the limiting factor in using RNA-seq is often the cost. However, this can be lowered however, if the sequencing depth is reduced. The general protocol of RNA-seq can be modified to enrich or deplete certain RNA classes. This may reduce the depth of sequencing required in order to effectively analyse a sample. As ribosomal RNA is often constitutively expressed and the most abundant class of RNA found in bacterial and eukaryotic cells, rRNA can fill the sequencing with useless reads. The degradation of rRNA using specific enzymes (Sharma et al. 2010) or

extraction of rRNA with magnetic beads coated in rRNA-specific DNA probes (Sultan et al. 2014) can deplete the rRNA levels in a sample. 'Not-so-random' primer mixes, with sequences complementary to rRNA sequences absent, can be used during reverse transcription to reduce the levels of rRNA sequences present in the cDNA before sequencing (Armour et al. 2009). Small species of RNA molecule such as bacterial sRNAs and eukaryotic miRNAs can also be enriched in a sample using size exclusion of large RNA species. It is sometimes unclear however, what technical biases are introduced during such enrichments and depletions.

Owing to the cDNA amplification step carried out before the sequencing, it is necessary to use tags or specific degradation of one strand of the cDNA produced, in order to maintain the knowledge of the orientation of the transcript sequence in the reference genome (Levin et al. 2010). An alternative would be to carry out direct RNA sequencing, an emerging technology, which has no reverse transcription or amplification steps, removing potential biases and maintaining strand-specificity without a need for tags or targeted degradation of one strand. Currently, this method can only be carried out by directly selecting polyadenylated RNAs for sequencing (Ozsolak et al. 2009). While non-poly(A) RNA species could theoretically be polyadenylated prior to sequencing, this may introduce technical bias to the results.

Another emerging technology in this first is single-cell RNA-seq, which can be used to sequence the entire transcriptome of one cell as opposed to a mixed population of cells (Saliba et al. 2014). The potential for using this technology to explore transcriptomic heterogeneity within a clonal population

of cells is enormous. Recently, single-cell RNA-seq was combined with fluorescence dilution and FACS to quantify the transcriptomic differences between macrophages infected with *Salmonella* that were proliferating intracellularly and macrophages infected with growth-arrested *Salmonella*. Host cells infected with growing *Salmonella* tended to a M2 activation state (anti-inflammatory), whereas a lack of bacterial growth was associated with an M1 activation state (anti-bacterial) (Saliba et al. 2016).

1.6.3 Dual RNA-seq

During infection, the bacteria and host are in intimate contact; this is particularly the case for intracellular pathogens. Disruption of this contact may incur unwanted alterations in the gene expression of either bacterium or host cell before the extraction of RNA can take place. The simultaneous analysis of host and bacterial RNA is therefore the ideal way to analyse the transcriptomics of pathogenesis as it allows a snapshot of gene expression at the time of host-pathogen interaction. Simultaneous analysis of host and pathogen has been attempted by a few microarray studies (Rappuoli 2000). However these studies required the removal of any DNA probes on the chip that had a high risk or cross-hybridisation with the RNA or cDNA from both host and pathogen. This is particularly a problem for analysing the pathogen transcriptome as the amount of host RNA is likely to be an order of magnitude higher than that of the pathogen, potentially overwhelming any measurement of pathogen gene expression. Physical separation of bacteria and host cells, or enrichment of their respective RNA has generally been carried out in microarray studies as a result (Hinton et al. 2004). This is labour-intensive and

a potential source of bias. However, as RNA-seq has a high sensitivity and a wide dynamic range, it has the potential to detect pathogen sequences in amongst the high background of host RNA, provided that the depth of sequencing is at an appropriate level (Westermann et al. 2012). A study recently used dual RNA-seq to analyse the transcriptome of *S.* Typhimurium during infection of mammalian cells (Westermann et al. 2016). The expression of a bacterial sRNA, PinT, was linked to virulence and correlated with host JAK-STAT signalling and an increase in the expression of several long noncoding RNAs (lncRNAs) (Westermann et al. 2016).

1.7 The bacterial cell cycle during infection

The bacterial cell cycle has been well characterised *in vitro*, although most studies have been carried out on the Gram-positive bacterium *Bacillus subtilis* and the Gram-negative bacterium *E. coli*. While early studies described the bacterial cell cycle as one coherent mechanism, current research is painting the picture of a cell cycle that is actually composed of the separate but coordinated processes of cellular growth; chromosome replication, decatenation and segregation; septum formation and cytokinesis (Nordstrom et al. 1991; Boye & Nordström 2003). However, some bacteria such as *Caulobacter crescentus* do appear to have a more segmented and ordered cell cycle, which interestingly also does not include the multifork replication found in *E. coli* and *B. subtilis* (Laub et al. 2007).

1.7.1 Initiation of DNA replication

A landmark study in the 1960s described that, upon an increase in nutrients, the rates at which an *E. coli* cell replicates its chromosome and divides effectively stay the same, while the doubling time of the bacteria gets shorter. These seemingly paradoxical observations were reconciled with the hypothesis of multifork replication; the replication of the chromosome must be initiated multiple times within one cycle (Helmstetter & Cooper 1968). DNA replication in bacteria is initiated through the oligomerisation of DnaA at a sequence of DNA called the origin (*ori*) to form a large nucleoprotein complex (Funnell et al. 1987; Mott & Berger 2007). This complex then unwinds the DNA, forming single strands to which the replisome can be loaded (Katayama et al. 1998). Initiation of DNA replication is regulated in several different ways (Mott & Berger 2007). One example of such regulation is the prevention of the premature initiation of replication by SeqA immediately after replication has already been initiated (Brendler et al. 1995; Slater et al. 1995). GATC sequences within the origin are usually fully methylated by Dam, however upon replication they transiently exist in a hemi-methylated state (Zyskind & Smith 1986). SeqA binds to these hemi-methylated sequences and prevents DnaA oligomerisation (Brendler et al. 1995; Slater et al. 1995). Many mechanisms of regulating DNA replication initiation involve blocking DnaA activity, either through titration of DnaA by DnaA-binding sequences (Kitagawa et al. 1998) or inhibition of DnaA activity by proteins such as Hda in *E. coli* (Kato & Katayama 2001) or YabA in *B. subtilis* (Hayashi et al. 2005). DnaA has also been found to autoregulate its own expression by binding to and suppressing the activity of its own promoter (Atlung et al. 1985; Braun et al. 1985). Organisation of the DNA by nucleoid-associated proteins such as

Fis and IHF have also been found to contribute to the regulation of the initiation of DNA replication (Ryan et al. 2004).

One of the major signals regulating initation is the availability of carbon, potentially regulated through ppGpp levels via the action of SpoT (Chiaramello & Zyskind 1989). Activation of the stringent response has been found to allow the completion of DNA replication, but not the initiation of new rounds of replication upon completion in *E. coli* (Ferullo & Lovett 2008)**.** It was once thought that the rate of origin-firing (initiating DNA replication) was directly proportional to cell mass, however initiation mass has been shown to increase up to two-fold in slow-growing cells compared to fast growing cells (Bipatnath et al. 1998). Interestingly, thymine-depletion has also been shown to induce DNA initiation in *E. coli* (Pritchard & Lark 1964), this premature firing of the origin of replication has been linked to cell death in thymine auxotrophs (Martín & Guzmán 2011).

1.7.2 Elongation of DNA

After DNA replication is initiated, two replication 'forks' progress in opposite directions along the chromosome. Helicase unwinds the DNA double-helix into single strands and new dNTPs incorporated by the rest of the replisome into the new strands in a fashion complementary to the original strands. The replication fork consists of a leading and lagging strand that are replicated by two polymerases in a continuous and discontinuous manner respectively, owing to the requirement for DNA replication to proceed in a 5' to 3' direction (Benkovic et al. 2001). Elongation of the DNA molecule is a costly

process, requiring many dNTPs, and while early studies showed that the rate of chromosomal replication in *E. coli* varied little under different conditions (Helmstetter & Cooper 1968), the lowest levels of nutrients used was too high to observe an effect (Bipatnath et al. 1998; Michelsen et al. 2003). In fact, if the availability of carbon is low enough then the rate of chromosomal replication decreases (Michelsen et al. 2003). The availability of thymine in auxotrophic *E. coli* has also been found to affect the rate of elongation (Churchward & Bremer 1977). Under amino acid starvation conditions, *B. subtilis* was found to produce higher levels of ppGpp, which in turn led to a global nondisruptive replication arrest (Wang et al. 2007). Replication fork arrest can occur in either a programmed or accidental fashion (Rothstein et al. 2000). Specific regions of the bacterial chromosome specifically arrest the replication forks as they progress in order to ensure that replication forks meet at the terminus site (Hill 1992). However, replication fork arrest can also be induced by DNA damage (Cox et al. 2000). Bacteria have dedicated replication fork restart proteins to help reload the replisome when replication has stalled and continue with replication (Windgassen et al. 2017).

1.7.3 Deconcatenation and segregation of DNA

After replication has completed, the two new chromosomes will be in an entangled state referred to as concatenation. The topoisomerase TopoIV is able to resolve these sister chromosomes into separate molecules that can be segregated apart (Wang et al. 2008). The toxin Fic has been found to inhibit TopoIV activity, in the presence of Fic, TopoIV is unable to deconcatenate the chromosomes, inhibiting segregation and division as a result (Harms et al.

2015). Segregation of the chromosomes in *E. coli* has been recently described as being dependent on the interplay between the structural maintenance of chromosomes complex (SMC) MukBEF, TopoIV and the DNA-binding protein MatP, which result in the timely segregation of the origin and terminus during and upon completion of replication (Nolivos et al. 2016). *B. subtilis* also has an SMC which interacts with ParB, itself bound to *parS* sequences on the chromosome to enable effective segregation of the sister chromosomes (Sullivan et al. 2009).

1.7.4 Cell division

Although several forms of division exist among bacteria, including budding in *Hyphomonas* and multiple fission in *Bdellovibrio*, binary fission is by far the most common and the best characterised (Angert 2005). In rod-shaped bacteria such as *E. coli* and *B. subtilis*, oligomerisation of FtsZ forms a ring at the midpoint of the cell (Bi & Lutkenhaus 1991). This ring acts as a scaffold for other division proteins and constricts forming the septum and ultimately allowing cytokinesis to occur (Adams & Errington 2009). FtsZ assembly and division have been observed in anucleate *E. coli* cells, suggesting that septum formation and cytokinesis are able to occur without the presence of DNA (Sun et al. 1998). However division and chromosome replication are clearly still coordinated, for instance, if cell division is inhibited it will in turn inhibit DNA synthesis and eventually lead to a ‘point of no return’ state, from which the bacterium can no longer reinitiate the normal cell cycle in order to proliferate (Arjes et al. 2014). In addition, if chromosomal segregation has not occurred in *E. coli* and *B. subtilis* then FtsZ ring formation

will in turn be inhibited in what is called nucleoid occlusion (Bernhardt & de Boer 2005; Adams et al. 2015).

There are no division proteins that appear to be dependent on nutrient availability (Wang & Levin 2009), it is more likely that the DNA replication and segregation serve as the major regulators in this regard. Expression of the division protein FtsL in *E. coli* is known to be repressed by DnaA (Goranov et al. 2005). While SlmA and Noc in *E. coli* and *B. subtilis* inhibit septum formation if the DNA has not segregated to the poles of the cell (Bernhardt & de Boer 2005; Adams et al. 2015). This presumably reduces the chances of anucleoid daughter cells resulting from division. In addition, if DNA replication itself is heavily regulated by nutrient availability, and division in turn is regulated by DNA replication, then a mechanism of regulating division through nutrient availability may not be necessary.

1.7.5 The bacterial cell cycle during pathogenesis

Many new genetic tools have become available in recent years, these coupled with advances in super resolution microscopy and single molecule tracking have boosted research into the bacterial cell cycle (Gahlmann & Moerner 2014; Robinson & van Oijen 2013). However most of these studies are *in vitro,* with few observing what occurs during infections. There have been many studies on the effects bacterial pathogens have on the host cell cycle, through toxin secretion and effector translocation (Oswald et al. 2005; Leitão et al. 2014), but few monitoring the cell cycle state of the bacterial cell itself. During infection, bacteria experience many stresses that are likely to

influence their cell cycle. Recently, the cell cycle of *Brucella abortus* was studied during infection, the bacteria were found to be blocked in the G1-like stage of growth until they are trafficked to the intracellular proliferation compartment, where growth and division is allowed to continue (Deghelt et al. 2014; De Bolle et al. 2015). This may be due to a lack of nutrient availability during the intermediate stages of intracellular trafficking. While not technically a pathogen, there has been research into the differentiation of *Rhizobium* into bacteroids inside root nodules, which involves several rounds of chromosome duplication without division (Mergaert et al. 2006). The cell cycle of intracellular *Salmonella* has not previously been studied. There are known to be differences between *E. coli* and *Salmonella* in the supercoiling of DNA *in vitro* due to the activity of the DNA-binding protein Fis under conditions such as low pH however, which may be related to *Salmonella* being better adapted more to an intracellular lifestyle (Cameron et al. 2011). It is known that during macrophage infection, *Salmonella* undergoes little proliferation until 6 h.p.i. (Helaine et al. 2010), this may be the length of time that is required for host processes to be manipulated into providing the bacteria with the nutrients it needs. Another factor that has not been investigated is the heterogeneity present in the states of cell cycle progression within a population of bacteria during infection. As *Salmonella* is known to exist in both a growing and a growth-arrested state during intracellular infection, it would be interesting to know the state of the cell cycle in these cells.

1.8 Aims and Objectives

To gain a greater understanding the physiological state of macrophage-induced *Salmonella* persisters and the host cells they inhabit; including the transcriptome, the state of the persister cell cycle and the reawakening from the persister state. This was achieved by:

- Dual RNA-seq of growing and nongrowing *Salmonella* during macrophage infection
- Observing active DNA synthesis with nongrowing *Salmonella* inside macrophages
- Examination of whether toxins with homologues known to effect DNA metabolism affect persister formation and growth
- Using ScanLag to study the ability of *Salmonella* persisters to regrow after antibiotic treatment during infection

Chapter Two

Materials and Methods

2.1 Bacterial strains, plasmids and primers

Table 2.1: *S.* Typhimurium strains

Name	Description	Source
Wild-type	*S.* Typhimurium 12023 wild-type	NTCC
Δ*parDE*	*S.* Typhimurium 12023 Δ*parDE::km*	Helaine, 2014
Δ*yhfG-fic*	*S.* Typhimurium 12023 Δ*yhfG-fic::km*	This study
Δ*parDE*Δ*yhfG-fic*	*S.* Typhimurium 12023 Δ*parDE::km* Δ*yhfG-fic::cat*	This study
Δ*relBE1*	*S.* Typhimurium 12023 Δ*relBE1::km*	Helaine, 2014
Δ*tacAT*	*S.* Typhimurium 12023 Δ*tacAT::km*	Helaine, 2014
Δ*phd-doc*	*S.* Typhimurium 12023 Δ*phd-doc::km*	Helaine, 2014
Δ*recA*	*S.* Typhimurium 12023 Δ*recA::km*	Hill, P.

Table 2.2: *E. coli* strains

Name	Description	Source
DH5**α**	*E. coli* DH5α	Invitrogen
Wild-type	*E. coli* str. K-12 substr. MG1655	*E. coli* Genetic Stock Center
Δ*yeaG*	*E. coli* K-12 MG1655 Δ*yeaG::km*	*E. coli* Genetic Stock Center

Table 2.3: Plasmids

Name	Description	Source
pDiGc	P_{BAD}*::DsRed.T3_S4T* and *rpsM::gfpmut3a* promoter fusions in pBAD18 (Amp)	Helaine *et al.*, 2010
pDiGi	P_{BAD}*::DsRed.T3_S4T* and P_{BAD}*::gfpmut3a* promoter fusions in pBAD18 (Amp)	Helaine *et al.*, 2010
pFCcGi	*rpsM::mCherry* and P_{BAD}*::gfpmut3a* (*bla*)	Helaine *et al.*, 2010
pMPM-A3-ΔP_{lac}-P_{ssaG}-*gfplva*	Transcriptional fusion of P_{ssaG} promotor to unstable GFP on pMPM-A3 plasmid	Ibarra *et al.*, 2009
pKD3	Chloramphenicol resistance cassette flanked by FLP sites (Cm)	Datsenko and Wanner, 2000
pKD4	Kanamycin resistance cassette flanked by FLP sites (Km)	Datsenko and Wanner, 2000
pKD46	Plasmid encoding arabinose-inducible λ red recombinase system; temperature-sensitive; retained at 30°C; cured at	Datsenko and Wanner, 2000

	≥37°C	
pBAD33	p15 *cat araC* P_{BAD}	Guzman *et al.*, 1995
pNDM220	R1 *bla lacIq* pA1/04/03	Gotfredsen & Gerdes, 1998
pCA24N	pMB1 *lacIq* T5-*lac* T*rrnB cat*	Kitagawa *et al.*, 2006
pBAD33-*fic*	pBAD33 P_{BAD}::*fic*	This study
pNDM220-*fic*	pNDM220 P_{lac}::*fic*	This study
pBAD33-*yhfG*	pBAD33 P_{BAD}::*yhfG*	This study
pCA24N-*yhfG*	pCA24N P_{lac}::*yhfG*	This study

Table 2.4: Primers

Name	5' to 3' nucleotide sequence	Description
F-delyhfGfic	**TATACTTGTGGTCAAGCACAGGC ATATTCAGGGAGGCCAG**GTGTAG GCTGGAGCTGCTTC	Deletion of *yhfG-fic*, homology to gene target in bold
R-delyhfGfic	**CAGGATCATGGCGGCTCCGGGT GAGTAGAACCGCACTATT**CATAT GAATATCCTCCTTAGT	Deletion of *yhfG-fic*, homology to gene target in bold
yhfGfic-ex-F	AAATCTCACAGGTACCGACGCAC GATGTCG	Homologous to upstream of *yhfG-fic*: mutant genotyping
yhfGfic-ex-R	TCGGCGTACAGGGGCCAGGAGA GATAACGA	Homologous to downstream of *yhfG-fic*: mutant genotyping
fic-in-F	AACTGCGGGAGGTCGATATT	Homologous to internal *fic* sequence: mutant genotyping
fic-in-R	ACCCGCTCCCAAAACGAAAC	Homologous to internal *fic* sequence: mutant genotyping
F-SalI-fic	CTCGTCGACCGAGCTTCGGAGGC ACT**ATG**	Amplication of *fic* for cloning into pBAD33 (SalI site underlined, start codon in bold)
R-HindIII-fic	CTCAAGCTTAGTAGAACCGCACTA TT**TTA**	Amplication of *fic* for cloning into pBAD33 (HindIII site underlined, stop codon in bold)
F-KpnI-fic	CTGGTACCCGAGCTTCGGAGGCA CT**ATG**	Amplication of *fic* for cloning into pNDM220 (KpnI site underlined, start codon in bold)
R-XhoI-fic	CTCTGAGCTCAGTAGAACCGCAC TATT**TTA**	Amplication of *fic* for cloning into pNDM220 (XhoI site underlined, stop codon in bold)
F-SalI-yhfG	CTCGTCGACATATTCAGGGAGGC CAG**GTG**	Amplication of *yhfG* for cloning into pBAD33 (SalI site underlined, start codon in bold)
R-HindIII-yhfG	CTCAAGCTTCGCGTCCTTCGCCA AAT**TTA**	Amplication of *yhfG* for cloning into pBAD33 (HindIII site underlined, stop codon in bold)
F-MfeI-yhfG	GGGCAATTGATATTCAGGGAGGC CAG**GTG**	Amplication of *yhfG* for cloning into pCA24N (MfeI site underlined, start codon in bold)
R-NotI-yhfG	GGGGCGGCCGCCGCGTCCTTCG CCAAAT**TTA**	Amplication of *yhfG* for cloning into pCA24N (NotI site underlined, stop codon in bold)
pNDM220-Seq-F	AGCAATTTCCGTTGCACCAG	Upstream of pNDM220 MCS: sequencing
pNDM220-Seq-R	GCGGGCCTCTTCGCTATTAC	Downstream of pNDM220 MCS: sequencing
pBAD33-Seq-F	AACTCTCTACTGTTTCTCCA	Upstream of pBAD33 MCS: sequencing
pBAD33-Seq-R	TGATTTAATCTGTATCAGGC	Downstream of pBAD33 MCS: sequencing
pCA24N-Seq-F	GGCGTATCACGAGGCCCTTTCGT CTTCACC	Upstream of pCA24N MCS: sequencing
pCA24N-Seq-R	TTGCATCACCTTCACCCTCTCCAC TGACAG	Downstream of pCA24N MCS: sequencing

2.2 Bacterial growth conditions

Bacteria were typically cultured in Lennox Broth (referred to as LB) (10 g/L Bactotryptone, 5 g/L yeast extract, 5 g/L NaCl, pH7.5) and on LB agar plates (LB containing 15 g/L bacteriological agar No. 1 (Oxoid, Basingstoke, GBR)). Both LB and LB agar were sterilised by autoclave prior to culturing bacteria. Antibiotics were added to medium when appropriate: carbenicillin (50 mg/L), kanamycin (50 mg/L) and chloramphenicol (30 mg/L). Bacteria were cultured in MgMES medium (5 mM KCl, 7.5mM $(NH_4)_2SO_4$, 1 mM KH_2PO_4, 8 mM $MgCl_2$, 38 mM glycerol, 0.5 mM K2SO4, 0.5 M 2-[*N*-morpholino]ethane-sulphonic acid) prior to infection and for *in vitro* assays when stated. When indicated MgMES medium was adjusted to pH 5 or 7 and filter-sterilised, or a low Mg^{2+} variant with 8 µM Mg_2Cl was used.

Medium was supplemented with 10 mM IPTG or 0.2% w/v L-arabinose to induce gene expression under the control of the P_{lac} and P_{BAD} promoters respectively.

For *E. coli* nitrogen starvation, bacteria were grown for 24 hours in Gutnick minimal medium (33.8 mM KH_2PO_4, 77.5 mM K_2HPO_4, 5.74 mM K_2SO_4, 0.41 mM $MgSO_4$) supplemented with 0.4% (w/v) glucose, Ho-LE trace elements and 3 mM NH_4Cl (Figueira et al. 2015). Bacteria were recovered on Gutnick agar plates (Gutnick medium containing 15 g/L bacteriological agar). Both Gutnick medium and agar was sterilised by autoclave.

2.3 Tissue culture conditions

RAW 264.7 murine macrophage-like cells were obtained from the European Collection of Cell Cultures (ECACC, cat. no. 91062702). RAW

264.7 macrophages were cultured in DMEM supplemented with 10% foetal calf serum (FCS; PAA laboratories).

Primary bone marrow-derived macrophages (BMM) were extracted from the tibias and femurs of sacrificed C57BL/6 mice (Racoosin & Swanson 1989). Red blood cells of isolated bone marrow were lysed in 0.83% NH_4Cl, and the remaining cells were differentiated in DMEM supplemented with 10% FCS, 1 mM sodium pyruvate, 10 mM HEPES, 0.05 M β-mercaptoethanol, 20% L929 cell-conditioned medium (LCM; National Institute of Medical Research) and 100 U/mol penicillin/streptomycin in 10 cm Petri dishes (Sterilin, Caerphilly, GBR) for 6 days at a density of 3 x 10^6 cells per 10 cm dish. Cells were detached in ice-cold PBS and centrifuged at 300 x *g* for 5 min before seeding for infection in the same medium as before but with no penicillin / streptomycin.

Immortalised bone marrow-derived macrophages (iBMMs) transformed using J2-Cre virus, were a gift from Dr. A. Shenoy and grown in the same medium as primary BMM. All mammalian cells were cultured in 5% CO_2 at 37^{o}C.

2.4 Plasmid extraction and Polymerase Chain Reaction (PCR)

The GenElute Plasmid Miniprep kit (Sigma-Aldrich, Missouri, USA) was used according to manufactor's specifications to extract plasmidic DNA from stationary phase bacterial cultures grown in LB. DNA was amplified for cloning and mutagenesis using the Expand High Fidelity (EHF) PCR System (Roche, Basel, CHE). Genotyping was carried out using PCR Taq DNA polymerase (Taq; Sigma-Aldrich, Missouri, USA) with standard reactions

contained 1.5 mM Mg^{2+}, 0.1 µM of forward and reverse primer each (Table 2.4), 0.8 µM of mixed dNTPs (Sigma-Aldrich, Missouri, USA) and 2.5 U of polymerase. Thermocycler parameters varied depending on the reaction, however typical parameters were 95°C for 5 min, 30 cycles of 95°C for 30 sec, 50°C for 30 sec, 68°C (EHF) or 72°C (Taq) for 1 min per kb of amplicon with a final 68°C (EHF) or 72°C (Taq) for 10 min. Electrophoresis was carried out to separate DNA through 1% agarose Tris-acetate EDTA buffer (TAE) gels in TAE buffer. DNA was visualised on gels with SYBR Safe stain (Invitrogen, California, USA), diluted to 1:10,000, using a Geneflash UV transilluminator (Syngene, Bangalore, IND) and compared to a HyperLadder (Bioline, London, GBR) marker to determine band size. Gel extraction of DNA from gels was carried out using a QIAquick Gel Extraction kit (Qiagen, Hilden, DEU) according to manufacturers specifications.

2.5 Deletion of *yhfG-fic* in *S.* Typhimurium

The one-step λred recombinase method (Datsenko & Wanner 2000) was used to delete the *yhfG-fic* TA module in wild-type and Δ*parDE S.* Typhimurium strains. Primers with homology to regions immediately upstream and downstream of *yhfG-fic* as well as homology to chloramphenicol and kanamycin resistance cassettes were used to amplify these cassettes by PCR from the pKD3 and pKD4 plasmids, respectively. After transformation of wild-type and Δ*parDE S*. Typhimurium with pKD46, bacteria were induced to express the λred recombinase with 0.2% arabinose and transformed by electroporation with the PCR fragments containing the antibiotic resistance cassettes with homology to sequences flanking the target region.

Recombinant mutants were subsequently selected with the appropriate antibiotic. PCR was used to confirmed the deletion mutants using the deletion primer as well as primers upstream, downstream and internal to the *yhfG-fic* sequence. Bacteria were cured of the pKD46 plasmid by overnight growth at 42^{o}C.

Figure 2.1

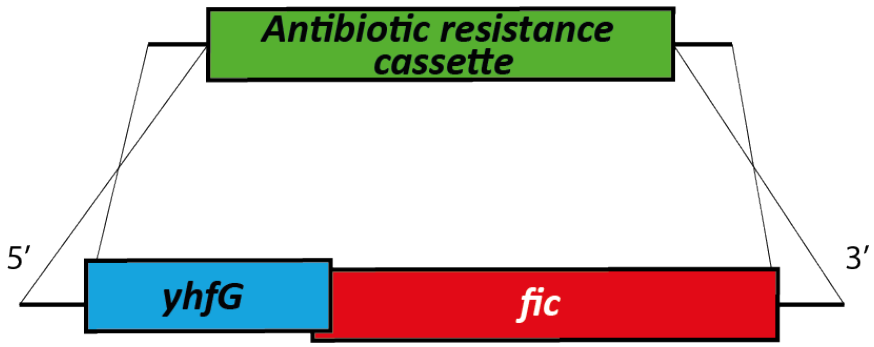


Figure 2.1: λRed recombinase-mediated site-directed mutagenesis of *yhfG-fic*. Diagram depicting recombination of sequences bordering an antibiotic resistance cassette with homologous sequences bordering the target gene on the chromosome (*yhfG-fic*). Recombination results in replacement of the target gene with the antibiotic resistance cassette.

2.6 Construction of toxin and antitoxin overexpression plasmids

The genes *fic* and *yhfG* were amplified taking care to include the ribosome-binding site within the amplicon. Primers adding the restriction site sequences of KpnI upstream and XhoI downstream of the amplicon were used for insertion into pNDM220 at the multiple cloning site (MCS), resulting in gene expression under the control of a P_{lac} promoter. SalI and HindIII restriction sites were added upstream and downstream of the amplicon respectively for insertion into pBAD33 at the MCS for gene expression under the control of a P_{BAD} promoter. MfeI and NotI restriction sites were added upstream and downstream of the amplicon respectively for insertion into pCA24N at the MCS for gene expression under the control of a P_{lac} promoter. Restriction enzymes (New England Biolabs [NEB], Massachusetts, USA) were added to DNA following the manufacturers guidelines and incubated at 37^{o}C for 1 h. DNA was purified by gel extraction (as previously described above) and ligation reactions were carried out using T4 DNA ligase (Invitrogen, California, USA) at 16^{o}C overnight and inactivated at 65^{o}C for 20 min before transformation into *E. coli* DH5α chemically competent cells. Transformants were selection on LB agar plates supplemented with appropriate antibiotics. Plasmid constructs were confirmed using Sanger sequencing carried out by GATC Biotech (GATC Biotech, Konstanz, DEU). All primers and plasmids are listed in tables 2.3 and 2.4 respectively**.**

2.7 Preparation and transformation of electro-competent bacterial cells

Salmonella strains grown overnight in LB medium were subcultured 1:33 in fresh LB and grown to 0.4-0.6 OD_{600nm} at 37^{o}C, or 30^{o}C supplemented

with 0.2% arabinose for strains harbouring pKD46. Bacteria were then chilled on ice, repetitively washed with ice-cold water and then with 10% glycerol reducing in volume at each wash to a final amount of 150 µL of electro-competent cells from an original 5 mL of culture. DNA to be transformed into cells was incubated with 50 µL of electro-competent cells on ice and added into a 2 mm electroporation cuvette (Molecular BioProducts, San Diego, USA). Electroporation was carried out as a 5 second pulse using a GenePulser (BioRad, California, USA) at 2.5kV, 200 Ω and 25 µF. After electroporation bacteria were recovered in SOC medium (20 g/L bacto-tryptone, 5 g/L yeast extract, 0.5 g/L NaCl, 2.5 mM KCl, 10 mM glucose) for 1 h at 37^{o}C (or 30^{o}C if transforming with pKD46), and plated on LB agar plates supplemented with appropriate antibiotics.

2.8 Toxin and antitoxin overexpression assays

E. coli or *S.* Typhimurium cells harbouring plasmids encoding either the *fic* toxin or *yhfG* antitoxin or both were grown to stationary phase overnight in LB without inducer unless grown in MgMES where stated. For protein overexpression in mid-exponential phase, cells were subcultured at 1:100 in fresh LB medium and grown shaking to an OD_{600nm} of 0.4 - 0.6 at 37^{o}C. The subculture was then diluted to an OD_{600nm} of 0.2 in fresh LB medium supplemented with 10 mM IPTG and 0.2% L-arabinose to induce expression of toxin and antitoxin. Cultures were then incubated shaking at 37^{o}C and bacterial growth monitored by OD_{600nm} readings at regular intervals. For protein overexpression in stationary phase, bacterial strains were grown

overnight to stationary phase, subcultured to an OD_{600nm} of 0.01 in inducing medium and grown and monitored as described above.

2.9 Bacterial growth curves

To monitor bacterial growth kinetics, *S.* Typhimurium wild-type, single ΔTA deletion mutants (Δ*parDE,* Δ*yhfG-fic)* and the double ΔTA deletion mutant Δ*parDE*Δ*yhfG-fic* were grown overnight to stationary phase in LB medium or MgMES medium and subcultured to an OD_{600nm} of 0.01 or 0.05 for long-term survival assays, in either LB medium or MgMES medium. Bacterial growth was then monitored by OD_{600nm} and colony forming units (CFU) measurements. CFU readings were taken by diluting culture in PBS and plated on LB plates that were incubated overnight at 37^{o}C for enumeration.

2.10 Macrophage infection with *S.* Typhimurium

For *Salmonella* infection of macrophages, cells were seeded in 6-well plates (Sterilin, Caerphilly, GBR) at a density of 1 x 10^6 cells per well. *S.* Typhimurium strains were grown overnight to stationary phase in MgMES pH5 supplemented with the relevant inducer for fluorescence dilution (FD) assays or LB for all other experiments. Prior to infection bacteria were opsonised with mouse serum for 20 min at a ratio of 45 parts bacterial culture, 170 parts DMEM (containing 10% FCS) and 20 parts mouse serum. 600 parts DMEM (containing 10% FCS) were added to the mix immediately before infection and each well of macrophages was then infected with 30 µL opsonised bacteria for non-FD infections (multiplicity of infection (m.o.i.) of ~10), 150 µL for dual RNA-seq infections (m.o.i. of ~5) and 300 µL for infections monitoring

bacterial DNA content (m.o.i of ~10). 6-well plates were subsequently centrifuged at 100 x *g* for 5 min and incubated for 30 min at 37^{o}C to allow phagocytosis to take place. Cells were then washed 3x with PBS and medium (as above) was added to the wells supplemented with gentamicin as standard (100 mg/L for 1 hour, then 20 mg/L for the remainder of the infection) or cefotaxime (100 mg/L for entire infection) to isolate nongrowing bacteria..

For whole macrophage cell sorting, cells were scraped off the wells and collected in cold PBS. Cell sorting was carried out by Dr. S. Helaine (for dual RNA-seq analysis) and Dr. P. Hill (for ScanLag analysis) using a BD FACSAria III (Becton Dickinson [BD], New Jersey, USA) using BD FACSDiva acquisition software (BD, New Jersey, USA) and FlowJo V10.1 (FlowJo LLC) for analysis.

For bacterial CFU or flow cytometry, macrophages were lysed in 0.1% Triton X-100 (Sigma-Aldrich, Missouri, USA) in PBS, centrifugated at 300 x *g* for 2 min to pellet nuclei and cells debris. The bacteria containing supernatant was then removed and plated for CFU measurements or fixed for 10 min in 3% paraformaldehyde in PBS, washed and resuspended in PBS for flow cytometry analysis.

2.11 Differentiation of growing and nongrowing *Salmonella* using fluorescence dilution (FD)

Macrophages were infected in 6-well plates (as described above) with *S.* Typhimurium harbouring an FD plasmid (pDiGc, pDiGc or pFCcGi). Bacteria were grown overnight in MgMES pH5 supplemented with relevant inducer (see 2.2). At selected time points, the macrophages were lysed and the

bacteria collected for flow cytometry analysis. Events were acquired on a BD LSRFortessa I (BD, New Jersey, USA), with red and green fluorescence detected at 561-610/20 nm and 488-530/30 nm respectively. BD FACSDiva (BD, New Jersey, USA) acquisition software was used in conjunction with the flow cytometer and FlowJo V10.1 (FlowJo LLC) was used for analysis.

2.12 DNA quantification of *S.* Typhimurium

Bacterial DNA staining with 4',6-diamidino-2-phenylindole (DAPI) was carried out by permeabilisation of fixed bacterial cells in 0.1% Triton for 5 min at room temperature, resuspension of the cells in DAPI (50 mg/L) in PBS and incubating for at least 1 hour in the dark at room temperature before flow cytometry measurement using a BD LSRFortessa I (as described above) with DAPI fluorescence detected at 405-450/50 nm. Hoescht 33342 dye (ThermoFisher Scientific, Massachusetts, USA) was used to stain bacteria for cell sorting and ScanLag, this was also detected at 405-450/50 nm.

Ethynyl deoxyuridine (EdU) from the Click-iT EdU Alexa Fluor 488 Imagine Kit (Thermo Fisher Scientific, Massachusetts, USA) was added to macrophages at a concentration of 10 μM at indicated intervals during *Salmonella* infection and washed out with PBS and replaced by fresh medium. Click reactions were carried out using the kit according to manufacturer's specifications, staining with DAPI after the click reaction (as described above).

2.13 *S.* Typhimurium DNA replication run-out

S. Typhimurium was grown overnight to stationary phase in MgMES pH5, subcultured into fresh LB medium and grown at 37°C (shaking) until exponential phase (an OD_{600nm} of 0.1-0.2) was reached. Samples of both the overnight stationary phase and exponential phase culture were then fixed with 3% PFA (as described above) as controls, while unfixed samples were supplemented with both rifampicin (150 mg/L) and cefalexin (10 mg/L) and incubated at 37°C for 4 hours before fixing. Samples were then stained with DAPI (as described above) and analysed by flow cytometry.

2.14 RNA extraction and dual RNA-seq analysis

Infection of macrophages and cell sorting for dual RNA-seq analysis was carried out as described above. RNA was extracted from sorted cells using the Ambion mirVana miRNA Isolation Kit, with phenol (Thermo Fisher Scientific, Massachusetts, USA) according to manufacturer's specifications. RNA was sent on dry ice to the Vogel laboratory at the University of Würzburg (Germany) for RNA sequencing and analysis (Westermann et al. 2016). Samples were ribo-depleted (except for the preliminary run) with a Ribo-Zero rRNA removal kit (Illumina, San Diego, USA), converted into a cDNA library and sequenced using an Illumina MiSeq platform. Sequencing reads were mapped to murine (GENCODE M2) and *S.* Typhimurium SL1344 (NC_016810.1, NC_017718.1, NC_017719.1, NC_017720.1) reference genomes and RPKM values were quantified using the READemption pipeline (Förstner et al. 2014). Differential expression analysis of RNA was carried out by Dr. K. Förstner at the University of Würzburg using the DESeq R package (Bioconducter). Subsequent analyses were carried out using Excel (Microsoft)

and Integrated Genome Browser. Gene enrichment lists were constructed by filtering for genes with an RPKM > 1 and fold changes above 2 and below 0.5 if there were no repeats of the experiment. For the n=3 analysis, genes were filtered based on having a log2(fold change) above 1 or below -1. Gene ontology analysis was carried out using Gene Ontology Enrichment Analysis and Visualisation Tool (GOrilla) and confirmed using the Database for Annotation, Visualization and Integrated Discovery (DAVID) (Huang et al. 2007).

2.15 P_{ssaG}-*gfplva* transcriptional fusion expression assay

To monitor SPI-2 expression during infection, *S.* Typhimurium harbouring the P_{ssaG}-*gfplva* transcriptional fusion (Ibarra & Steele-Mortimer 2009) on the pMPM-A3-ΔP_{lac}- P_{ssaG}-*gfplva* plasmid were used to infect BMMs as described above. *Salmonella* were labeled in the dark with the BacTrace anti-*Salmonella* CSA-1 antibody (Seracare, Massachusetts, USA), diluted 1:200 in PBS with 10% horse serum for 1 h at room temperature. Secondary antibody labelling using 1:500 diluted donkey anti-goat IgG (H+L) Cross-Absorbed, Alexa Fluor 647 far red-antibody (Thermo Fisher, Massachusetts, USA) was subsequently performed for 30 min at room temperature. Flow cytometry was performed using a BD LSRFortessa (BD, New Jersey, USA), BD FACSDiva acquisition software (BD, New Jersey, USA) and FlowJo V10.1 (FlowJo, Oregon, USA) for analysis, gating on CSA-1-positive cells and measuring the proportion of GFP-positive cells within that population.

2.16 ScanLag analysis

ScanLag analysis was adapted from Levin-Reisman et al. (2010). Bacterial samples were diluted appropriately in PBS (to produce ~100 colonies per plate) and spread on LB agar plates or Gutnick agar plates and dried inside a microbiological safety cabinet (MSC). Black cotton sheets were sandwiched inside the agar plates to stop light from the scanner reflecting and causing a double image and to improve contrast of the bacterial colonies against the agar in the scanned images. Plates were placed inside Epson Perfection V370 photo scanners (Epson, Suwa, JPN), which were connected to a computer running the Scanning Manager software (Levin-Reisman et al. 2010). The scanners were incubated at 33^{o}C (to not exceed the recommended safe temperature for running the scanners), typically for 2 days. Images were analysed using Matlab and software developed by the Balaban group (Levin-Reisman et al. 2010), with output scripts modified by M. Priestman (https://github.com/mountainpenguin/NQBMatlab**)**. Cell sorting prior to ScanLag analysis was carried out by Dr. L. Rigano (*E. coli*) and Dr. P. Hill (*Salmonella*) using a BD FACSAria (BD, New Jersey, USA).

2.17 Statistics

The software DESeq2 was used to determine *p*-values of fold changes in gene expression for dual RNA-seq analysis (Dr. K. Förstner). Student's t-tests were carried out on all normally distributed data to determine statistical significance differences in data sets. Mann-Whitney U tests carried out on data with skewed distributions (lag distributions of bacteria in ScanLag analysis). Statistical analysis was performed with the software Prism 7

(GraphPad). On figures, *p*-values are indicated as *<0.05, **<0.01, ***<0.001, ****<0.0001 and ns for >0.05.

Chapter Three

Transcriptomic analysis of both host and pathogen: Cell sorting and dual RNA-seq of macrophages infected with either growing or nongrowing *Salmonella*

3.1 Introduction

Microarrays have been heavily used in the recent past for transcriptomics studies, however the recently developed RNA-seq provides many improvements on this technique. An increased dynamic range and ability to detect novel transcripts makes RNA-seq invaluable for transcriptomics. Dual RNA-seq allows the analysis of both host and pathogen transcriptomes simultaneously, with both transcriptomes extracted and sequenced together and only separated at the *in silico* stage using mapping to reference genomes (Westermann et al. 2012). This allows the analysis of the global gene expression of the host cell and the pathogen at the time of RNA extraction. Theoretically, less time is allowed for the expression levels of genes to change, compared to techniques that first physically separate pathogen and host before RNA extraction. As our lab is interested in studying the transcriptome of *Salmonella* persisters present during macrophage infection, we combined dual RNA-seq with fluorescence dilution (FD) and cell sorting. By doing so, we were able to separate macrophages 18 h after inoculation with *Salmonella* carrying a FD plasmid into subpopulations based

on the growth state of the bacteria within each host cell (Figure 3.1). The plasmid pFCcGi was used for fluorescence dilution, which allows constitutive expression of mCherry whereas that of GFP is under the control of an arabinose-inducible promoter. Upon entry into macrophages the bacteria either start to proliferate after 6 h (Helaine et al. 2010), or remain in a nongrowing (NG) antibiotic tolerant state. It is important to stress that while the NG *Salmonella* present during macrophage infection are a source of persisters, they are not entirely composed of persisters (Helaine et al. 2014) (see chapter 6). Therefore the transcriptomic data retrieved from this NG population will be of a subpopulation that is enriched for persisters. Macrophages that contain *Salmonella* that proliferated over the course of the 18 h infection will have a higher level of the constitutively expressed mCherry compared to macrophages that contain *Salmonella* that did not proliferate. The levels of GFP should be the same between these two populations of macrophages, unless multiple bacteria were taken up during phagocytosis, in which case the GFP fluorescence will be higher. This allows us to isolate macrophages that only took up one bacterial cell at the start of the infection that then either proliferated or remained in a nongrowing state. Uninfected bystander macrophages, those with no mCherry or GFP fluorescence can also be isolated. In addition, it was realised that a fourth population of macrophages could be identified, those with no GFP but with mCherry fluorescence. These cells had degraded their *Salmonella*, and as GFP is less stable than mCherry, the former was degraded while the latter persisted in the host cell. Purity of the sorted fractions was confirmed by microscopy (data not shown).

Figure 3.1

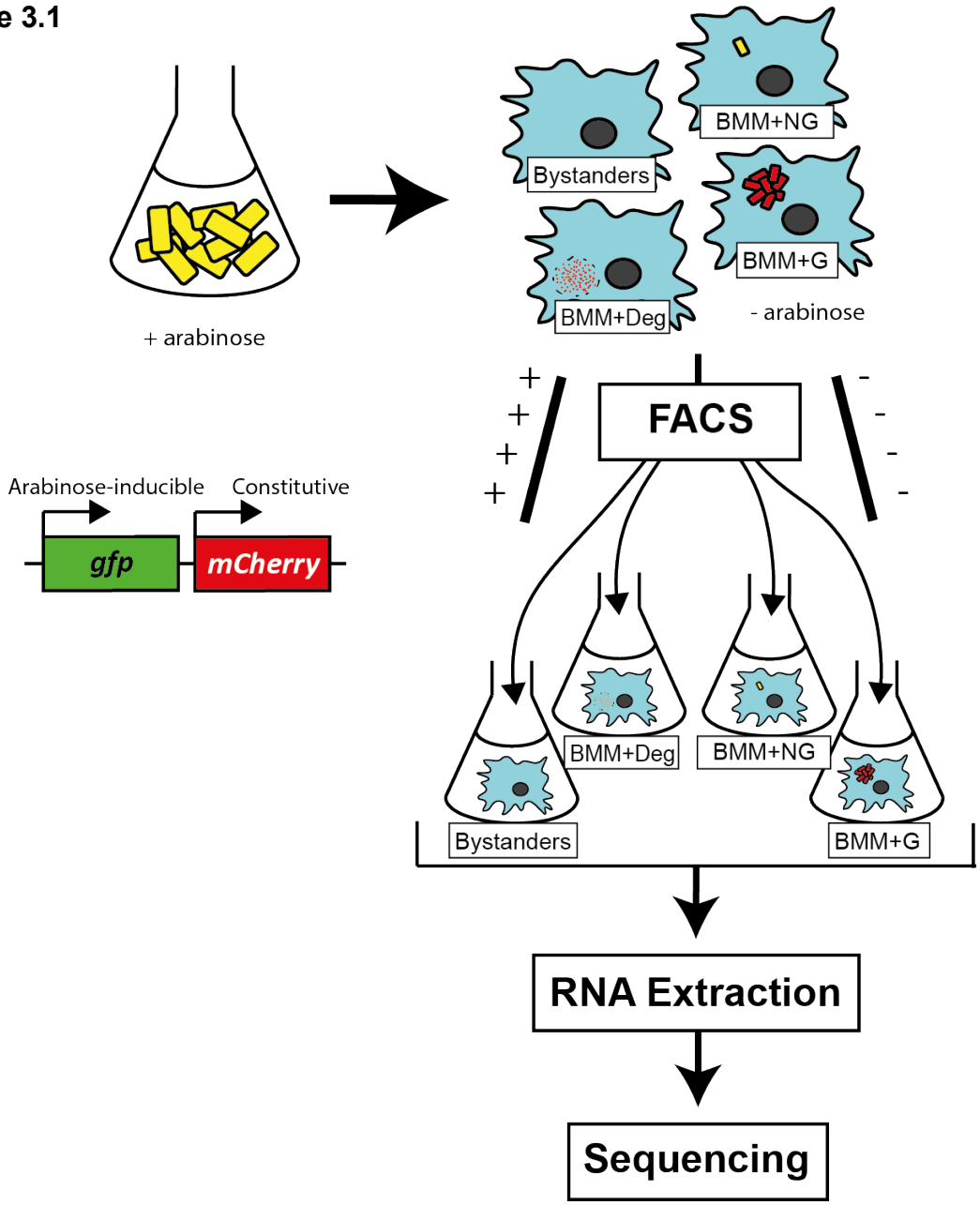


Figure 3.1: Schematic of dual RNA-seq experimental set up. *S.* Typhimurium SL1344 harbouring pFCcGi express *gfp* under the control of an arabinose inducible P_{BAD} promoter and express mCherry constitutively. These bacteria were grown overnight culture in MgMES pH5 medium with arabinose and used to infect BMMs for 18 h. BMMs were then sorted by FACS into four populations, uninfected bystanders BMMs, BMMs with degraded bacteria (BMM+Deg), BMMs with nongrowing *Salmonella* (BMM+NG) and BMMs with growing *Salmonella* (BMM+G). RNA was then extracted from these populations of cells, converted to cDNA and sequenced.

3.2.1.1 Preliminary run of dual RNA-seq and cell sorting

A preliminary trial run of the dual-RNA Seq cell sorting experiment was carried out to assess any issues that may need adjusting before further repeats were carried out. Primary bone marrow-derived macrophages (BMMs) were infected for 18 h with wild-type *S.* Typhimurium SL1344 carrying pFCcGi, induced overnight to express GFP, before collecting whole macrophages for FACS. Figure 3.2A shows the auto-fluorescence of uninfected control macrophages detected by flow cytometry. The fluorescence profile of the macrophage population collected after 18 h.p.i. is shown in figure 3.2B (Helaine, S.). At least 100,000 cells were sorted for each population before RNA extraction. These macrophages are made of four distinct subpopulations of BMMs containing growing *Salmonella* (BMM+G; GFP+, high mCherry), BMMs containing NG *Salmonella* (BMM+NG; GFP+, low mCherry), BMMs containing degraded *Salmonella* (BMM+Deg; mCherry+, GFP-) and uninfected bystander BMMs. At least 100 ng RNA was extracted from each population and converted to cDNA and sequenced using Illumina sequencing (collaboration with Vogel group; Dr. A. Westermann). The transcriptomic data of host and pathogen were then analysed using DESeq2 (Dr. K. Förstner, K; University of Würzburg, Germany).

Figure 3.2

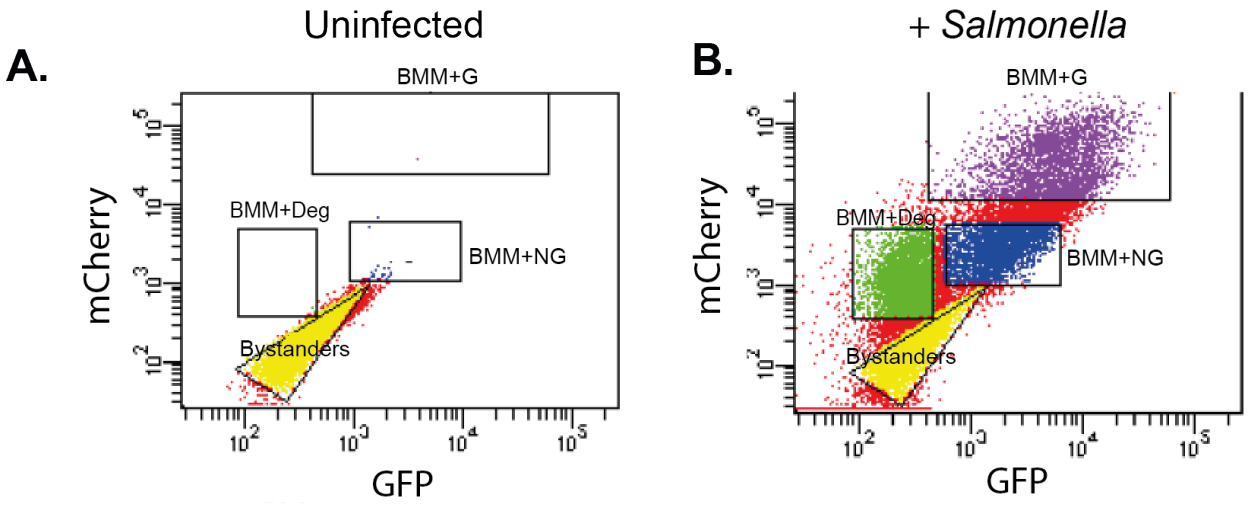


Figure 3.2: Different subpopulations of BMMs can be identified based on *Salmonella* fluorescence during infection (Preliminary test). Bivariate plots of the GFP and mCherry fluorescence of (A) uninfected BMMs and (B) BMMs infected with *S.* Typhimurium harbouring pFCcGi for 18 h. Gating for sorting (A) uninfected BMMs and, (B) uninfected bystanders (bottom triangle), BMM+Deg (left rectangle), BMM+NG (centre rectangle) and BMM+G (top rectangle) is overlaid onto the plots. Gates were validated using fluorescent microscopy. n=1 (Helaine, S.)

3.2.1.2 Proportions of RNA in sequencing

Figure 3.2A shows the proportions of *Salmonella* and macrophage RNA detected by sequencing in each sorted subpopulation of BMMs from infection. The majority of RNA in each sample is mouse (macrophage), this was to be expected owing to the far larger amount of RNA present in mammalian cells compared to bacterial cells. The high amount of macrophage RNA present in the inoculum is the result of host cell lysate being added to the sample to reduce biases during sequencing. No *Salmonella* RNA are detected in the bystander and uninfected control samples showing that there was no contamination between the samples. Low levels of bacterial RNA were still detectable in the BMM+Deg. Of the RNA extracted from the BMM+NG sample, 1.15% was found to belong to *Salmonella.* Previous RNA-seq studies have suggested a minimum of 1 million non-rRNA reads for the effective transcriptomic analysis of a bacteria sample (Westermann et al. 2012). There were 176,444,122 total aligned reads in the BMM+NG sample, of which, 2,022,921 reads were from *Salmonella* (Appendix table 1). As 1,135,083 aligned reads were non-rRNA, this is enough to carry out an effective analysis of the transcriptome belonging to NG *Salmonella*. 11.12% of the RNA in the BMM+G sample was found to be bacterial, constituting 6,525,090 million aligned non-rRNA reads. This proportion of bacterial RNA in the sample suggests an average number of 10 Salmonellae per macrophage cell in the BMM+G cells.

Figure 3.3

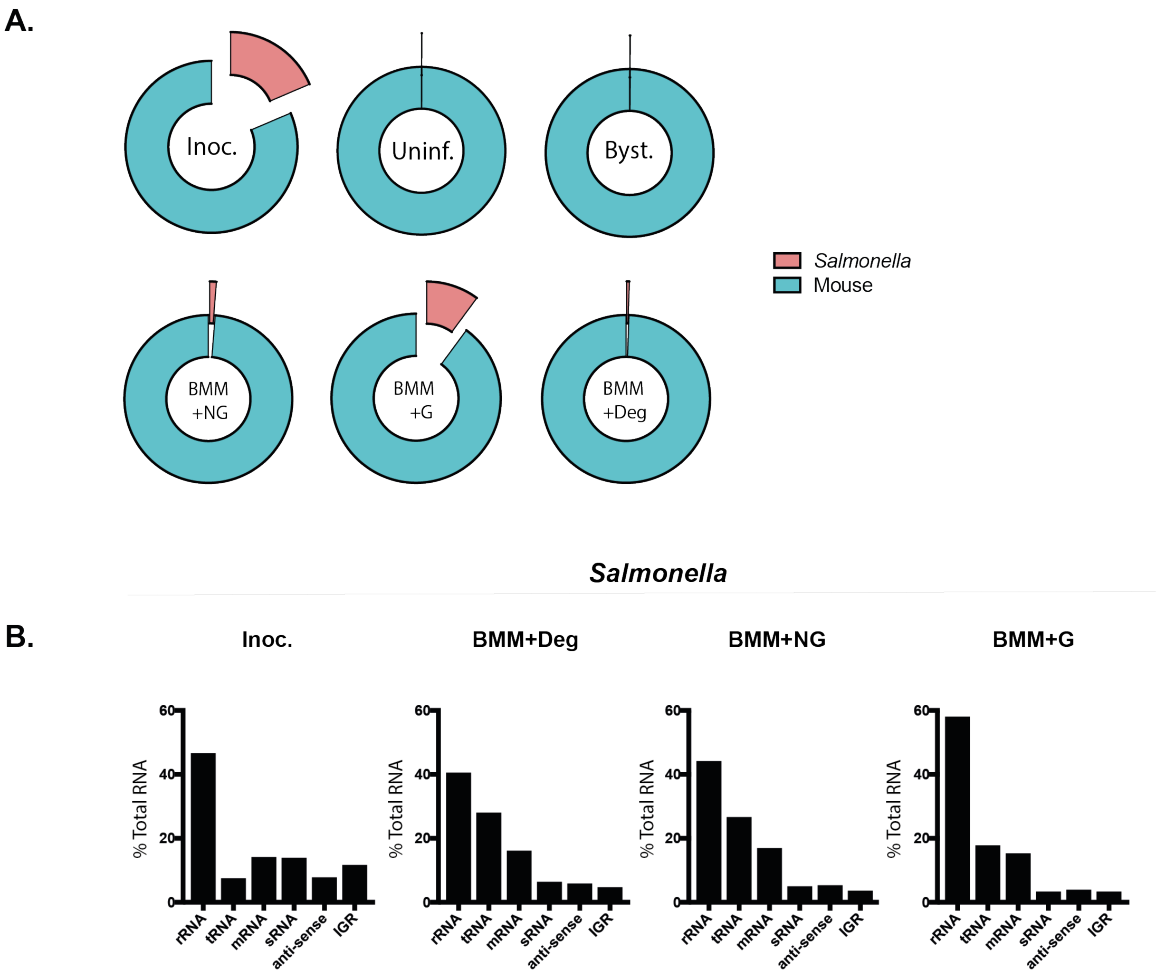

A.
Inoc.
Uninf.
Byst.
BMM +NG
BMM +G
BMM +Deg
Salmonella
Mouse
B.
Salmonella
Inoc.
BMM+Deg
BMM+NG
BMM+G
% Total RNA
0
20
40
60
rRNA
tRNA
mRNA
sRNA
anti-sense
IGR

Figure 3.3

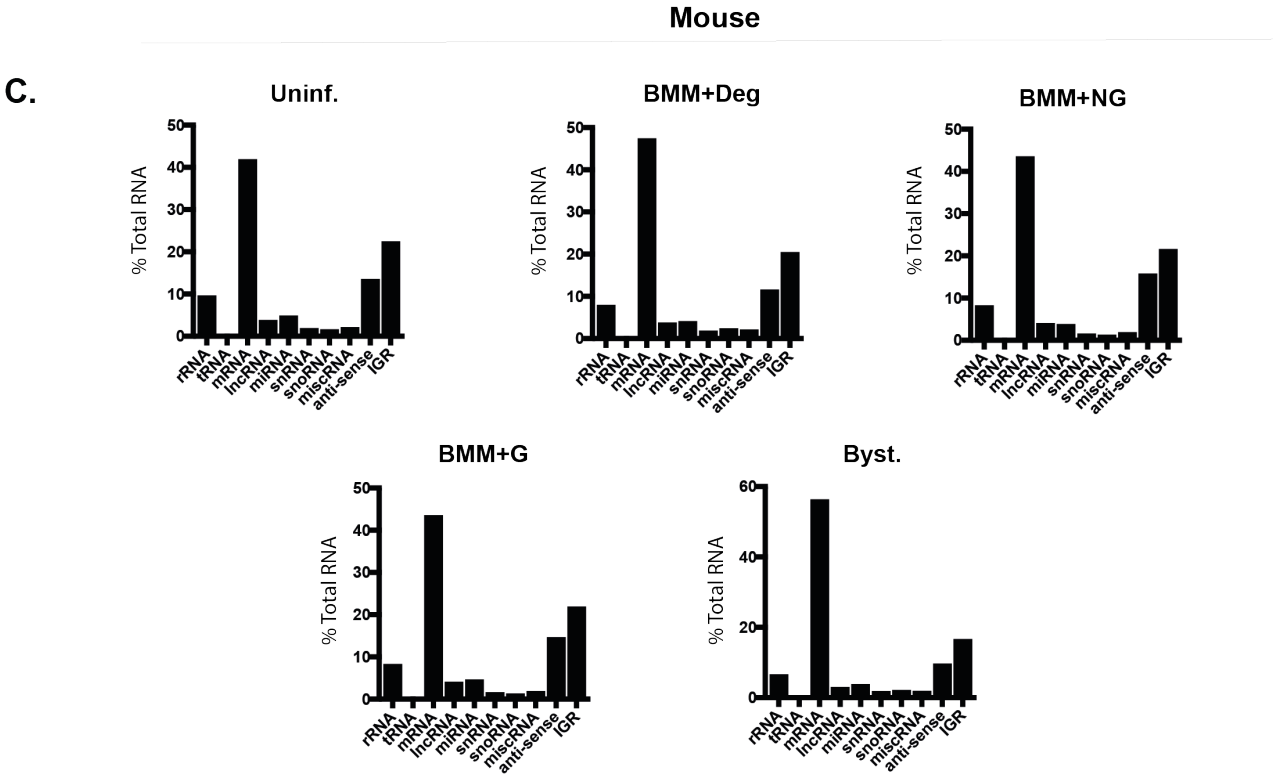


Figure 3.3: Proportions of RNA present in *Salmonella* and BMM transcriptomes (Preliminary test). A) Pie charts displaying proportions of bacterial (red) and mammalian (blue) RNA and (B,C) bar charts displaying proportions of different RNA species detected in (B) bacterial and (C) mouse transcriptomes. Samples are labelled as inoculum (Inoc.), uninfected mock control (Uninf.), uninfected bystanders (Byst.), BMMs with NG *Salmonella* (BMM+NG), BMMs with growing *Salmonella* (BMM+G) and BMMs with degraded *Salmonella* (BMM+Deg). RNA species labeled as follows: ribosomal RNA (rRNA), transfer RNA (tRNA) messenger RNA (mRNA), small RNA (sRNA), anti-sense transcripts (anti-sense), intergenic transcripts (IGR), long non-coding RNA (lncRNA), micro RNA (miRNA), small nuclear RNA (snRNA), small nucleolar (snoRNA) miscRNA

Figure 3.3B and 3.3C shows the proportions of different RNA species present in the *Salmonella* or mouse transcriptomes respectively. In *Salmonella*, rRNA is the most prevalent class at between 40 and 58% of the samples - no ribo-depletion procedure was carried out to enrich the coding RNA molecules in the sample. The highest proportion of rRNA is found in growing *Salmonella*, this is plausible considering the likely increased ribosomal activity in these bacteria required for growth. The next largest class of RNAs in the bacterial transcriptome during infection are tRNAs. Protein-coding mRNA makes up between 14% and 17% of each bacterial transcriptome. Transcripts annotated as sRNA, intergenic region (IGR) and anti-sense transcripts make up very little of the bacterial transcriptomes isolated from infection conditions, however they are at a higher proportion in the stationary phase (inoculum) control. This could reflect the large amount of gene silencing in these inactive bacteria, or could simply be a consequence of the decrease in amount of tRNA, rRNA and mRNA in these cells.

The proportions of different RNA classes present in the macrophage transcriptomes are very similar across all of the sorted subpopulations of BMMs. The most prevalent class was mRNA, making up around half of all sequenced transcripts, followed by IGR transcripts, anti-sense transcripts and rRNA. The bystander BMM transcriptome is differs the most from other subpopulations in terms of proportions of RNA species, with an increased proportion of mRNAs. The fractions of tRNA, lncRNA, miRNA, snRNA, snoRNA, and miscRNA classes are consistent across all samples, altogether making up between 11.7% and 13.3% of the BMM transcriptomes.

3.2.2.1 Differences in gene expression between growing and NG *Salmonella* during macrophage infection

The fold changes in gene expression from that of the inoculum to that of the NG or growing *Salmonella* were plotted against each other (Figure 3.4). Genes differentially regulated between the growing and NG populations are highlighted. There are many genes enriched in the NG population (Table 3.1), interestingly, a large number of these are tRNAs for various amino acids. In addition, several genes in the *psp* operon, involved in the response to membrane stress, were enriched in NG bacteria. Several ribosomal proteins were enriched in growing *Salmonella* as well as the SOS response repressor *lexA*, which could indicate that growing *Salmonella* are undergoing DNA damage while proliferating inside the macrophages.

Figure 3.4

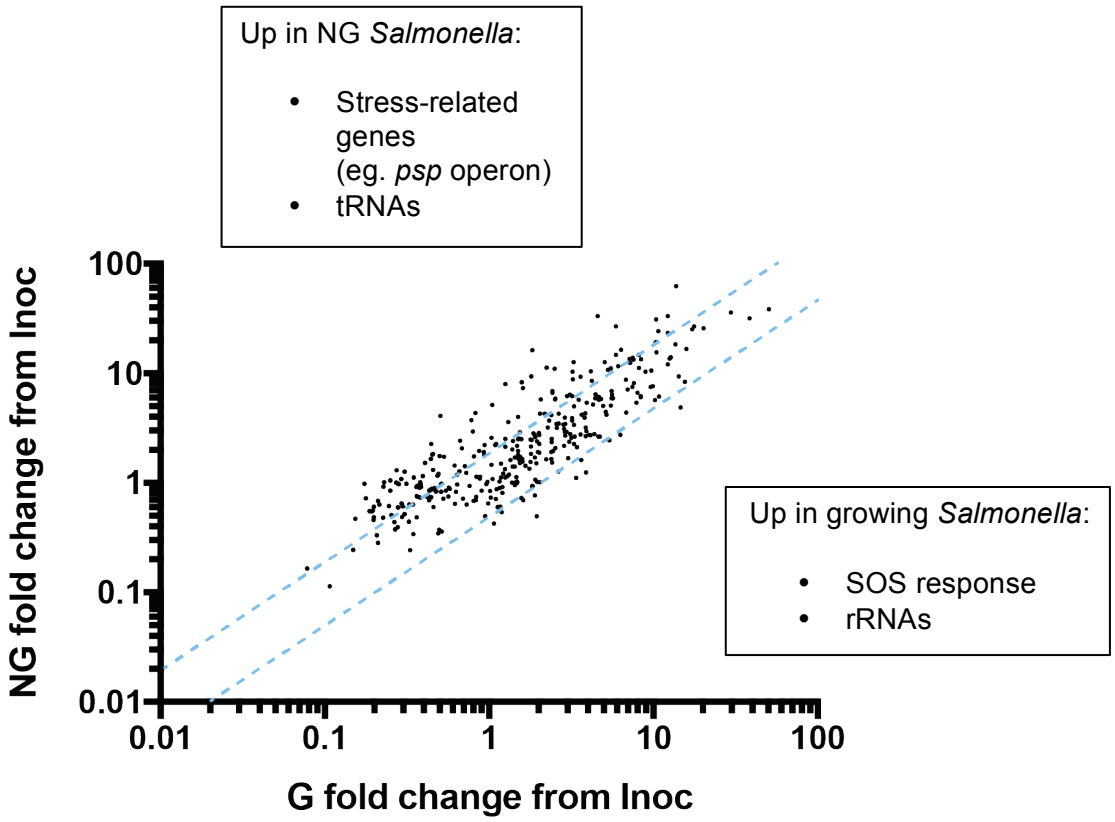


Figure 3.4: Comparison of growing and NG *Salmonella* transcriptomic profiles during BMM infection (Preliminary test). Scatter plot showing the expression of genes in growing and NG *Salmonella* at 18 h infection of BMMs shown as fold changes from inoculum transcript levels. Dashed lines show arbitrary cut-off of a two-fold difference in the fold changes of genes between growing and NG *Salmonella* from that of the inoculum. Boxes summarise genes upregulated in each subpopulation in relation to the other. n=1.

Table 3.1: Gene enrichment lists (abridged) for comparison of growing v NG *Salmonella* transcriptomes.
(0.5 > fold change threshold > 2), n=1.

Enriched in growing *Salmonella*			Enriched in NG *Salmonella*		
Gene	**Function**	**Fold change**	**Gene**	**Function**	**Fold change**
asr	putative secreted stress response protein	3.49	umuD	DNA repair protein	0.112595964
SL1344_P1_0044	hypothetical protein	3.11	SL1344_1210	membrane protein	0.123609925
finO	thr operon leader peptide	3.04	pspB	bacteriophage shock protein B	0.138356372
slyB	outer membrane lipoprotein SlyB	2.99	SL1344_1722	hypothetical protein	0.157659881
SL1344_4339	hypothetical protein	2.51	SL1344_tRNA0053	-	0.177315843
csrA	carbon storage regulator	2.48	mobA	molybdopterin-guanine dinucleotide biosynthesis protein MobA	0.189843281
SL1344_1768	hypothetical protein	2.31	SL1344_tRNA0064	-	0.191707284
SL1344_1767	hypothetical protein	2.28	SL1344_tRNA0003	-	0.192269083
pagK	bacteriophage encoded pagK %28phoPQ-activated protein%29	2.24	SL1344_0845	putative tetR family transcriptional regulator	0.194704026
rpsO	30S ribosomal protein S15	2.21	slyD	FKBP-type peptidyl-prolyl cis-trans isomerase	0.195506348
rpsM	30S ribosomal protein S13	2.19	SL1344_tRNA0004	-	0.199155851
traS	hypothetical protein	2.15	SL1344_tRNA0068	-	0.20131399
lppA	major outer membrane lipoprotein	2.08	SL1344_1098	hypothetical protein	0.203298268
lexA	LexA repressor	2.08	SL1344_3354	hypothetical protein	0.20910679
rplL	50S ribosomal protein L7%2FL12	2.01	priB	primosomal replication protein N	0.210040303
-	-		SL1344_1425	hypothetical protein	0.220052402
-	-		pspA	bacteriophage shock protein A	0.220714185
-	-		pspC	bacteriophage shock protein C	0.221097335
-	-		SL1344_tRNA0055	-	0.22630605
-	-		trbE	DnaJ protein	0.228501556

3.2.2.2 Differences in macrophage gene expression

Figure 3.5 shows the comparisons between the macrophage transcriptomes, as fold changes in gene expression from the uninfected control. The transcriptomic profiles of the BMM+G and BMM+NG samples appear relatively similar (Figure 3.5). Few genes are enriched in the BMM+NG subpopulation compared to BMM+G, including nischarin, and the pro-inflammatory genes gadd45g and spp1 (Table 3.2). Nischarin has been previously reported to be important for the proliferation of *Salmonella* (Kuijl et al. 2013), it is interesting therefore that it is observed to be upregulated in BMM+NG compared to BMM+G cells rather than the other way around. A large number of miRNAs appear to be enriched in the BMM+G population when compared to BMM+NG. Gene ontology enrichment analysis reports that these are involved in the response to lipopolysaccharide (LPS), this is plausible as macrophages exposed to growing *Salmonella* are more likely to have a stronger response compared to those infected only with a single nongrowing bacterium.

Figure 3.5

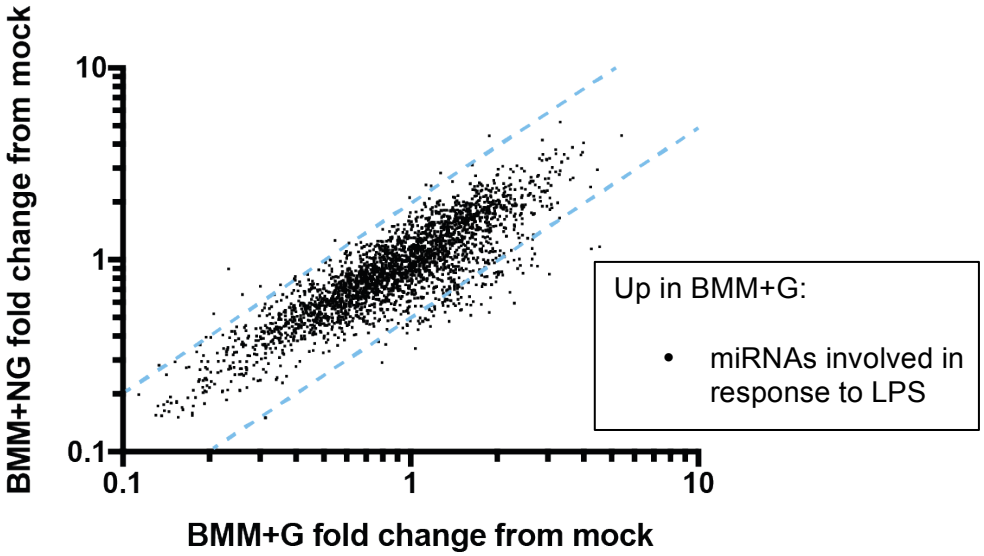


Figure 3.5: Comparison of macrophage BMM+G and BMM+NG transcriptomic profiles during infection with *Salmonella* (Preliminary test). Scatter plot showing the expression of genes in macrophage subpopulations BMM+G and BMM+NG at 18 h.p.i. with *Salmonella* shown as fold changes from uninfected mock infection macrophage transcript levels. Dashed lines show arbitrary cut-off of a two-fold difference in the fold changes of genes between growing and NG *Salmonella* from that of the inoculum. Box states miRNAs involved in the LPS response as being upregulated in the BMM+G population. n=1.

Table 3.2: Gene enrichment lists (abridged) for comparison of BMM+G v BMM+NG transcriptomes.
(0.5 > fold change threshold > 2), n=1.

Enriched in BMM+G			Enriched in BMM+NG		
Gene	**Function**	**Fold change**	**Gene**	**Function**	**Fold change**
Mir328	microRNA 328	0.40	Nisch	nischarin	3.84
mmu-let-7j	mmu-let-7j	0.40	Gadd45g	growth arrest and DNA-damage-inducible 45 gamma	2.53
Mir1249	microRNA 1249	0.40	Gm14328	predicted gene 14328	2.53
Mir350	microRNA 350	0.40	Mt1	metallothionein 1	2.42
Gm24148	Unknown function	0.40	Snora69	small nucleolar RNA, H/ACA box 69	2.35
Gm24016	Unknown function	0.40	Gm15432	predicted gene 15432	2.31
Mir148b	Unknown function	0.39	Scarna6	small Cajal body-specific RNA 6	2.23
Gm25744	Unknown function	0.39	Snora75	small nucleolar RNA, H/ACA box 75	2.17
Gm25789	Unknown function	0.39	HOTAIRM1_5	HOX antisense intergenic RNA myeloid 1 conserved region 5	2.13
Mir151	microRNA 151	0.39	Dusp2	dual specificity phosphatase 2	2.11
mt-Td	mitochondrially encoded tRNA aspartic acid	0.38	Odc1	ornithine decarboxylase, structural 1	2.10
Gm22455	Unknown function	0.38	Gm23297	predicted gene, 23297	2.06
n-R5s195	nuclear encoded rRNA 5S 195	0.38	Map1lc3b	microtubule-associated protein 1 light chain 3 beta	2.05
Snord23	small nucleolar RNA, C/D box 23	0.37	Spp1	secreted phosphoprotein 1	2.03
Mir1981	microRNA 1981	0.37	Ecm1	extracellular matrix protein 1	2.02
Mir146b	microRNA 146b	0.37	-	-	-
Gm25122	Unknown function	0.37	-	-	-
Gm24463	Unknown function	0.36	-	-	-
Gm24105	Unknown function	0.36	-	-	-
Snord35a	small nucleolar RNA, C/D box	0.36	-	-	-

Interestingly, the bystanders appear to have a more divergent transcriptomic profile compared to both the BMM+NG and BMM+G subpopulations (Appendix figure 1; Appendix table 5-6). Many of these genes are miRNAs and gene ontology enrichment analysis suggests that they are chiefly involved in the response to LPS. This indicates that perhaps the immune response in bystanders is stronger than that of infected macrophages, perhaps owing to the immunosuppressive effect of *Salmonella*. This proposes an interesting question, while it is known than growing *Salmonella* uses T3SS to influence host gene expression with effector translocation, are NG *Salmonella* doing the same?

3.3.1 Repeat of optimised dual RNA-seq experiment to produce a larger data set

After the preliminary run of the dual RNA-seq experiment following FACS, three more repeats were carried out with a few alterations to the technique. Ribo-depletion was carried out on the RNA samples to enrich the protein-coding RNAs and decrease the level of deep sequencing required for statistical analysis. The gating strategy was altered slightly to make the isolation of each subpopulation of BMMs more stringent. Differential expression analysis was primarily carried out with direct comparisons between samples, rather than comparing fold changes from a bacteria-only or macrophage-only control, as it was decided that the gene expression profiles in these controls were very different to every other sample and this may not be the most useful way to present the data. I carried out repeats of the infection as previously described (Figure 3.6).

Figure 3.6

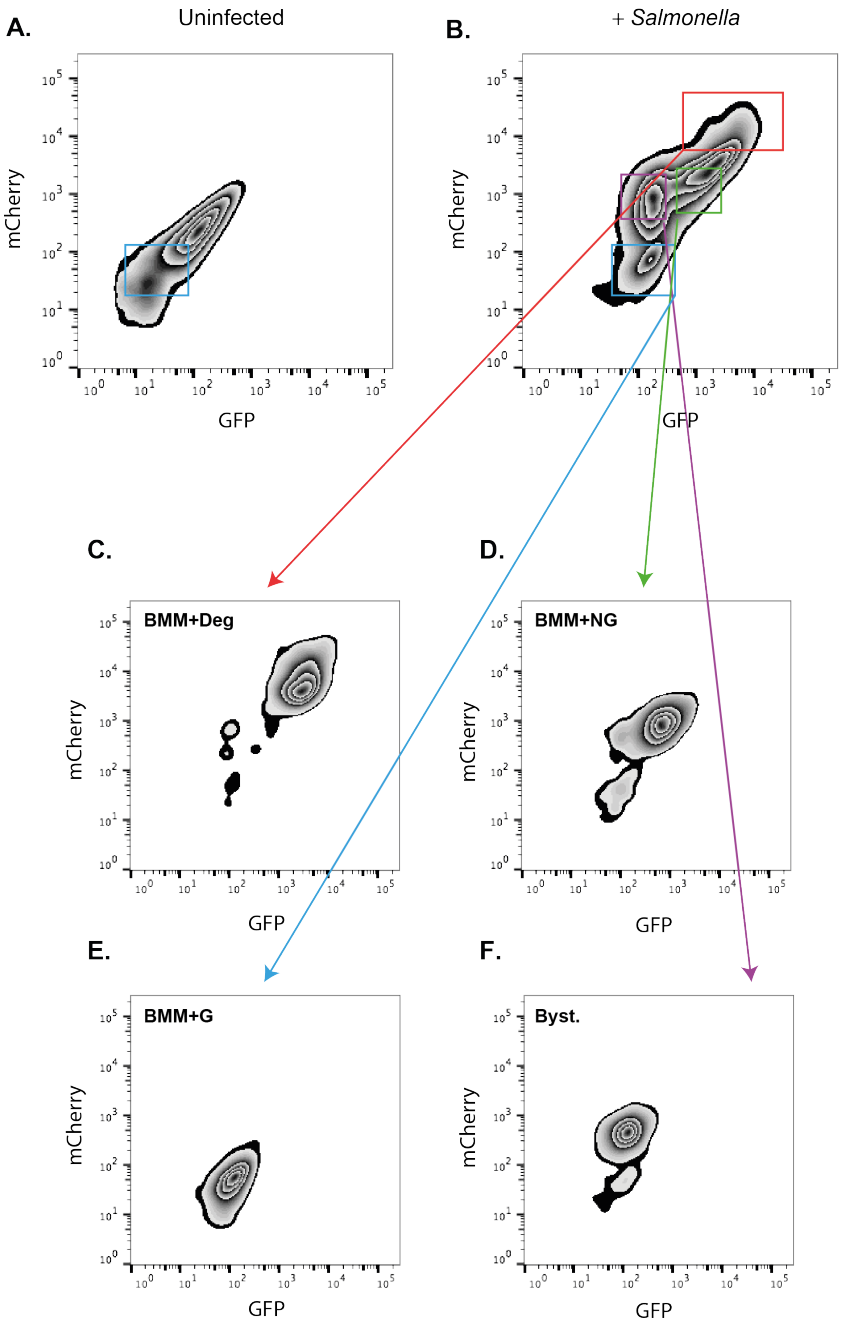

A.
Uninfected
B.
+ Salmonella
mCherry
GFP
C.
BMM+Deg
D.
BMM+NG
E.
BMM+G
F.
Byst.

Figure 3.6

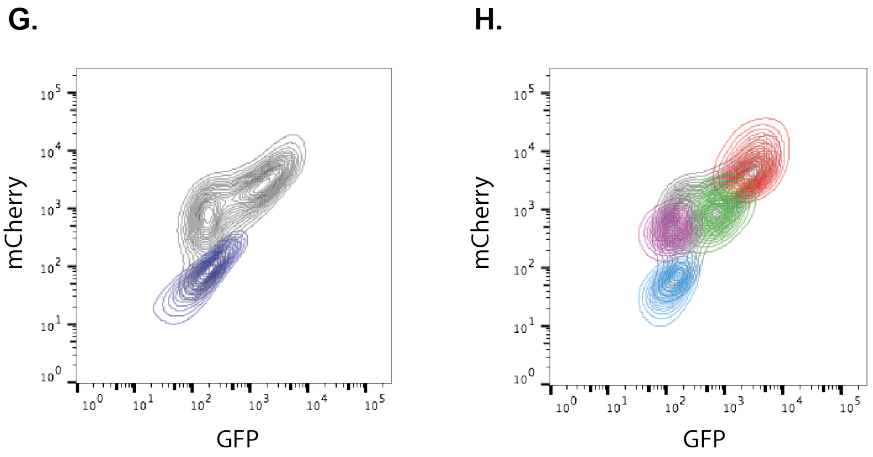


Figure 3.6: Subpopulations of BMMs can be identified based on *Salmonella* fluorescence during infection (Repeated experiment). Bivariate plots of the GFP and mCherry fluorescence of (A) uninfected BMMs and (B) BMMs infected with *S.* Typhimurium harbouring pFCcGi for 18 h (B). Gating for sorting (A) uninfected BMMs and (B), uninfected bystanders (blue), BMM+Deg (purple), BMM+NG (green) and BMM+G (red) is overlaid onto the plots and arrows directing to reanalysed samples of (C) BMM+G, (D) BMM+NG, (E) bystanders, (F) BMM+Deg. G) Fluorescence profiles of uninfected mock overlaid onto fluorescence of pre-sort BMMs 18 h.p.i.. H) Reanalysed subpopulations of sorted BMMs overlaid onto total population of pre-sort BMMs 18 h.p.i.. Plots representative of three independent experiments.

The proportions of bacterial and mammalian RNA in each sample were similar to that of the preliminary run of the dual RNA-seq experiment (Figure 3.7A). One exception was the inoculum sample, this was due to a reduced amount of host cell lysate being added to this sample. BMM+NG had 0.65% and BMM+G had 4.01% bacterial RNA. BMM+Deg contained 0.54% bacterial RNA, which was presumably yet to be fully degraded within the macrophage, and bystanders and uninfected macrophages contained <0.5% bacterial RNA (Figure 3.7A). The sequencing depth used for these repeats was much lower, resulting in around 10 times less aligned reads for the bacterial samples. However as ribo-depletion was employed to enrich the coding transcripts and as there were three repeats with which to carry out statistical analysis, this no. of aligned reads was considered adequate (Appendix table 2).

The proportions of different RNA classes amongst the *Salmonella* transcriptome differ to those of the preliminary run due to the ribo-depletion carried out on the RNA samples (Figure 3.7B). Protein-coding mRNAs are the most prevalent class, with the highest proportions found in the stationary phase control (inoculum) and growing *Salmonella* during infection. A higher proportion of rRNA was detected in the NG *Salmonella* and the RNA belonging to degraded bacteria. This likely reflects the less efficient ribo-depletion going on in samples with smaller amounts of RNA. The increase in tRNA upon infection is not observed, and sRNA and anti-sense RNA appear to increase upon infection - the opposite observation compared to the preliminary test. The proportions of RNA detected following ribo-depletion must be considered unreliable indicators of the proportions present in the original transcriptomes as the biases of such treatments are not completely

understood. This is one disadvantage of using enrichment techniques, however if the main target of interest is coding RNA, then this is likely not a problem. The enrichment of mRNA in the macrophage population was very effective, with mRNA making up around 60-77% across all samples. All other classes make up only a minority of the transcriptomes.

Figure 3.7

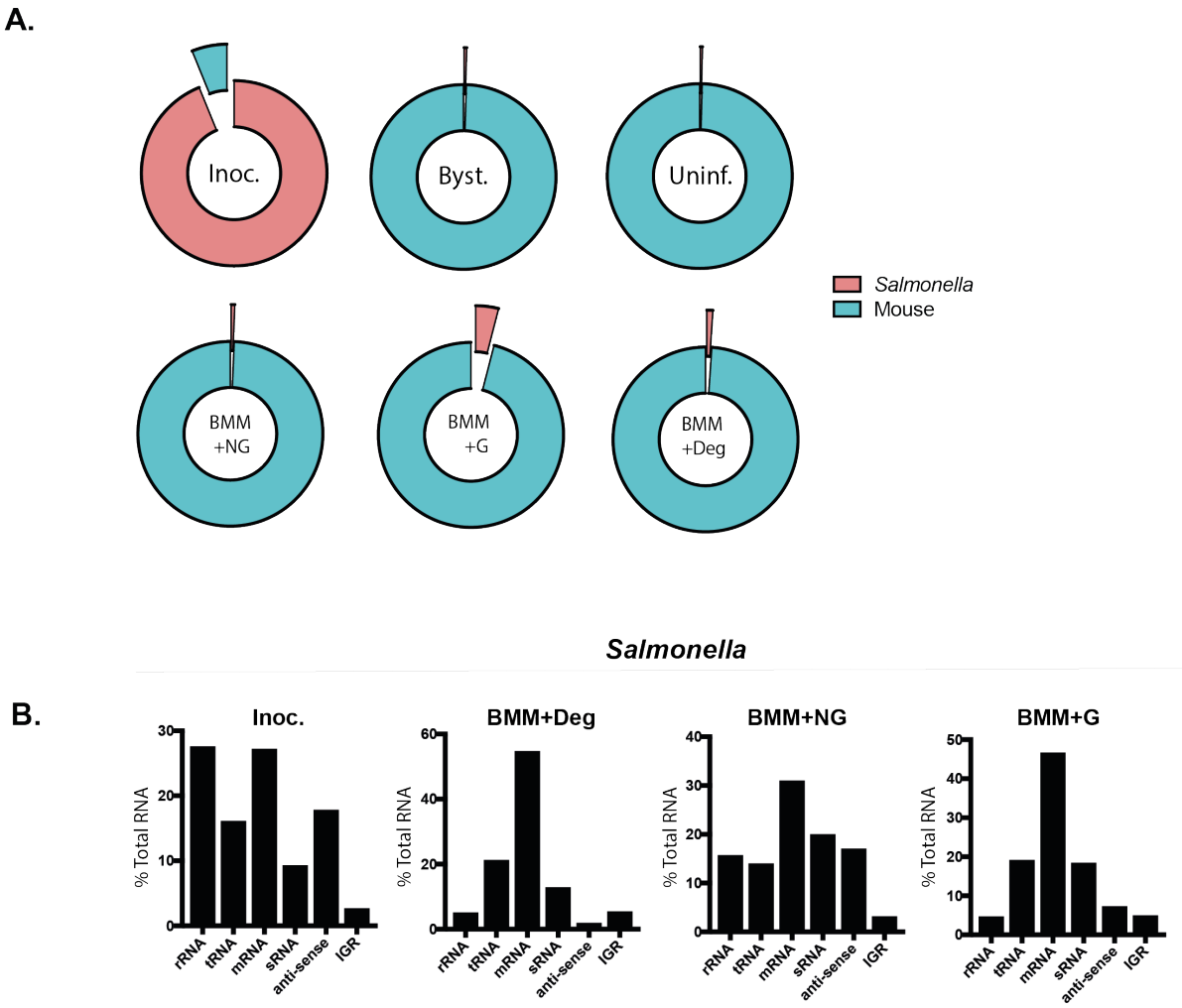


Figure 3.7

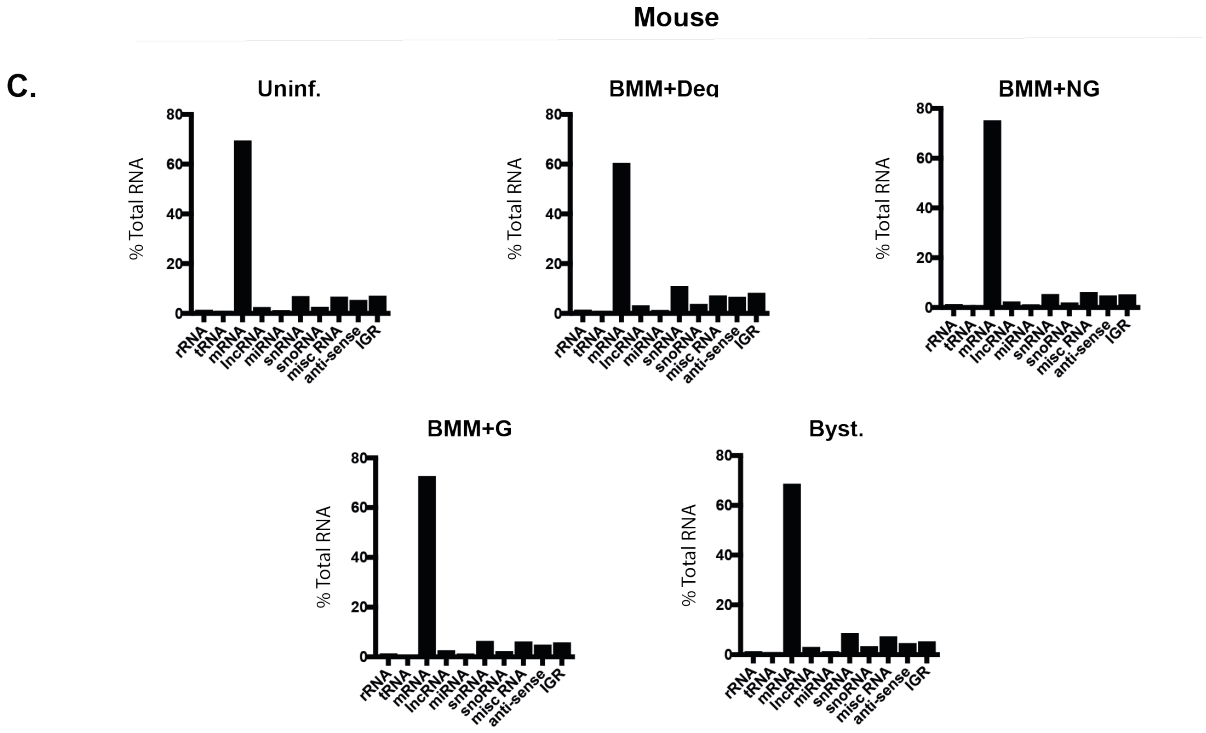


Figure 3.3: Proportions of RNA present in *Salmonella* and BMM transcriptomes (Preliminary test). A) Pie charts displaying proportions of bacterial (red) and mammalian (blue) RNA and (B,C) bar charts displaying proportions of different RNA species detected in (B) bacterial and (C) mouse transcriptomes. Samples are labelled as inoculum (Inoc.), uninfected mock control (Uninf.), uninfected bystanders (Byst.), BMMs with NG *Salmonella* (BMM+NG), BMMs with growing *Salmonella* (BMM+G) and BMMs with degraded *Salmonella* (BMM+Deg). RNA species labeled as follows: ribosomal RNA (rRNA), transfer RNA (tRNA) messenger RNA (mRNA), small RNA (sRNA), anti-sense transcripts (anti-sense), intergenic transcripts (IGR), long non-coding RNA (lncRNA), micro RNA (miRNA), small nuclear RNA (snRNA), small nucleolar (snoRNA) miscRNA

3.3.2.1 Differences in gene expression between growing and NG *Salmonella* during macrophage infection

Principal component analysis was carried out to determine how related the transcriptomes of each subpopulation of macrophages and *Salmonella* were to each other (Figure 3.8). The *Salmonella* transcriptome during infection varies greatly compared to the extracellular control. Within these *Salmonella*, the NG and growing bacteria vary from each other significantly also, with the exception of one of the NG samples.

Figure 3.8

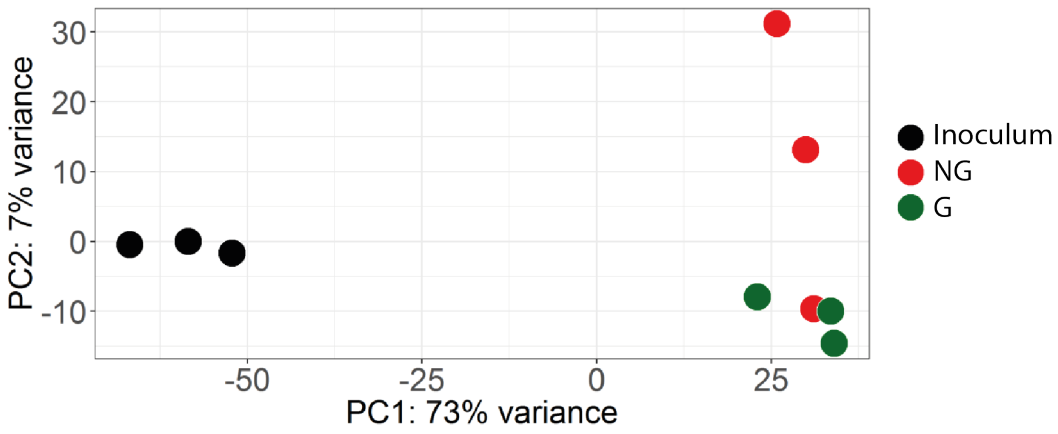


Figure 3.8: Principal component analysis of transcriptomes belonging to growing and NG *Salmonella* during infection and the inoculum. Transcriptomic data sets belonging to samples of inoculum (black), NG (red) and growing (green) bacteria from three independent BMM infections were subjected to 2D principal component analysis to separate each sample based on levels of variance from one another in gene expression. The 1st principal component (PC1) is given on the x-axis while the 2nd principal component is plotted on the y-axis (Dr. P. Hill).

Direct comparisons of the gene expression in growing, NG *Salmonella,* and that of the inoculum (stationary phase bacteria) were carried out. When comparing the transcriptomes of growing and NG *Salmonella* (Figure 3.9), several genes are enriched in one of the two subpopulations. In growing *Salmonella*, these include genes involved in LPS synthesis and DNA metabolism such as *rfaQ* and *recF*, as well as genes involved in pathogenesis and antibiotic resistance (*iagB* and *marB*; Table 3.3). The transcriptional repressor *trpR* was found to be upregulated in growing cells compared to NG *Salmonella*. Genes enriched in the NG *Salmonella* included the global regulator *fis* and genes involved in the biosynthesis of tryptophan. From these results it can be assumed that the NG *Salmonella* are limited for tryptophan while growing *Salmonella* are not. Interestingly, several SPI-2 effectors were enriched in the NG *Salmonella* when compared to growing *Salmonella.* Considering that *Salmonella* is already known to express SPI-2 genes and translocate effectors during proliferation within macrophages, it was fascinating to find that they are also expressed in NG *Salmonella*, and to a relatively higher extent when compared to growing bacteria.

Figure 3.9

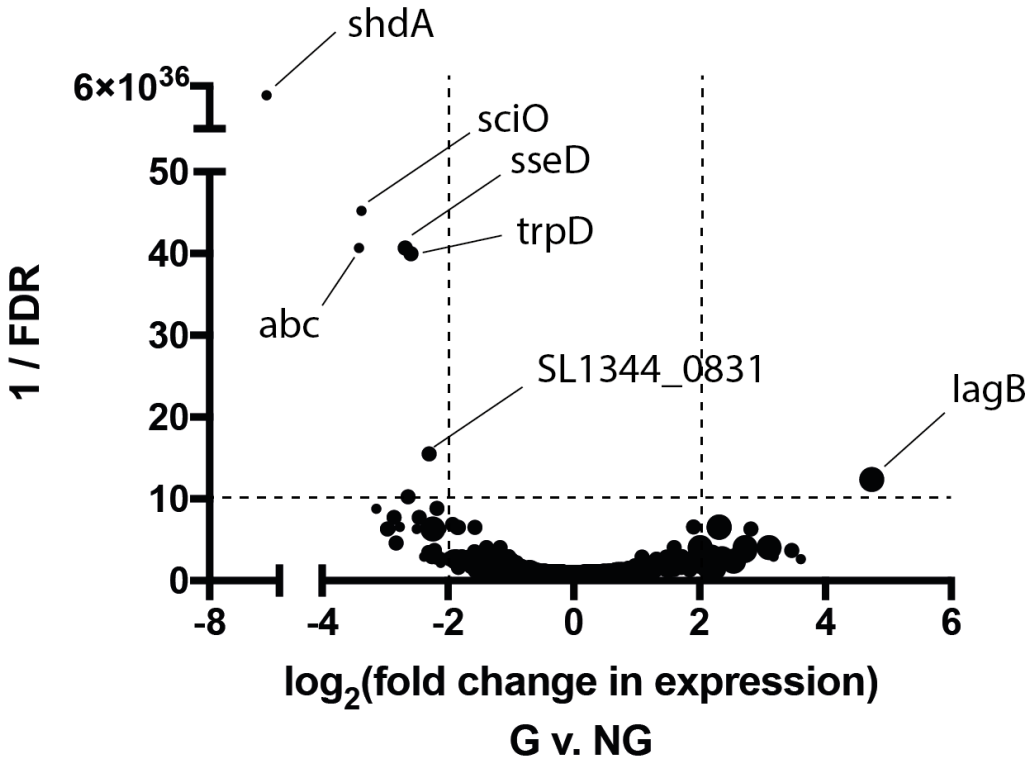


Figure 3.9: Direct comparison of growing and NG *Salmonella* transcriptomic profiles during BMM infection (repeated experiment). Volcano plot showing the **fold change in** expression of genes in growing *Salmonella* compared to NG *Salmonella* at 18 h infection of BMMs as $\log_2$(fold change in expression). Dashed lines show arbitrary cut-off of a four-fold difference in the expression (vertical) and a false discovery rate of over 10 (horizontal) in genes in growing *Salmonella* from those of NG *Salmonella*. Significant hits are labelled, size of dots correlates with coverage of gene annotation. Plots representative of three independent experiments.

Table 3.3: Gene enrichment lists (abridged) for direct comparison of growing v NG *Salmonella* transcriptomes.
(-1 > log_2FC threshold > 1), n=3.

Enriched in NG *Salmonella*			**Up in growing *Salmonella***		
Gene	**Function**	**log2FC**	**Gene**	**Function**	**log2FC**
shdA	host colonisation factor	6.36	iagB	cell invasion protein	-4.74
abc	ABC transporter	3.41	uraA	uracil permease	-3.61
sciO	hypothetical protein	3.37	fruK	1-phosphofructokinase	-3.46
trpB	tryptophan synthase beta chain	3.14	SL1344_4420	putative ATP-dependent Lon protease	-3.18
SL1344_3979	hypothetical protein	2.96	marB	multiple antibiotic resistance protein MarB	-3.10
SL1344_3107	hydrolase	2.91	birA	biotin operon repressor	-2.81
sseE	pathogenicity island protein	2.85	trpR	trp operon repressor	-2.73
sirA	invasion response-regulator	2.82	SL1344_3023	hypothetical protein	-2.71
SL1344_3540	hypothetical protein	2.76	SL1344_3744	putative DNA-binding protein	-2.54
trpD	anthranilate phosphoribosyltransferase	2.68	ybfA	hypothetical protein	-2.41
SL1344_0083	secreted protein	2.64	SL1344_2579	putative antitermination protein	-2.36
sseD	pathogenicity island effector protein	2.58	sicP	chaperone	-2.31
misL	autotransporter	2.50	tehB	tellurite resistance protein	-2.31
hisI	histidine biosynthesis	2.46	lolA	lipoprotein carrier protein	-2.22
sseF	pathogenicity island effector protein	2.38	rfaQ	lipopolysaccharide core biosynthesis protein	-2.19
alr	alanine racemase	2.36	SL1344_3575	hypothetical protein	-2.18
SL1344_1301	hypothetical protein	2.30	SL1344_P1_0036	putative transglycosylase	-2.09
SL1344_0831	putative electron transfer flavoprotein	2.30	recF	recF protein	-2.01
rph	RNase PH	2.26	dedA	DedA protein %28dsg-1 protein%29	-2.00
pagM	virulence factor	2.24	yifK	amino acid permease	-1.94
SL1344_1593	hypothetical protein	2.21	flrD	anaerobic nitric oxide reductase flavorubredoxin	-1.93
SgrS		2.21	SL1344_3867	hypothetical protein	-1.90
fruR	fructose repressor	2.18	traN	conjugative transfer aggregate stability protein	-1.90
fis	Fis DNA-binding protein	2.18	SL1344_2781	putative transcriptional regulator	-1.89
StyR-88		2.18	treF	cytoplasmic trehalase	-1.88
trpE	anthranilate synthase component I	2.17	SL1344_1662	hypothetical protein	-1.85
RUF_247c		2.11	rfbX	putative O-antigen transporter	-1.81
SL1344_2302	putative transporter	2.11	sinR	LysR family regulator	-1.78
SL1344_1780	hypothetical protein	2.11	tehA	tellurite resistance protein	-1.72
SL1344_3198	membrane transport protein	2.10	spoU	tRNA guanosine-2-O-methyltransferase	-1.72

Analysis of both growing and NG *Salmonella* compared to the inoculum (stationary phase) confirm what is observed in the principal component analysis in that *Salmonella* from infection conditions vary greatly in their gene expression when compared to extracellular stationary phase bacteria (Appendix figure 2). A similar pattern is observed in both comparisons however the statistical significance in fold changes of gene expression is much higher when comparing the growing *Salmonella* to the inoculum, likely due to the greater number of reads gained from sequencing growing *Salmonella* compared to NG bacteria. Flagellin genes and chemotaxis genes are down in the growing and NG *Salmonella* compared to the inoculum and virulence genes are enriched. Perhaps the most striking finding in analysing growing and NG *Salmonella* is that despite their very different phenotypes, their transcriptomes are relatively similar, with both expressing high levels of virulence genes, including the SPI-2 island and effectors.

3.3.2.2 Differences in macrophage gene expression

Principal component analysis showed the variance between the macrophage transcriptomes to follow a similar pattern to that observed across the bacterial transcriptomes, with uninfected control samples varying the most compared to all subpopulations of macrophages present during infection (Figure 3.10). The replicate samples of each macrophage subpopulation transcriptome extracted during infection cluster together, with the exception of one BMM+G sample that is similar to the BMM+NG samples.

Figure 3.10

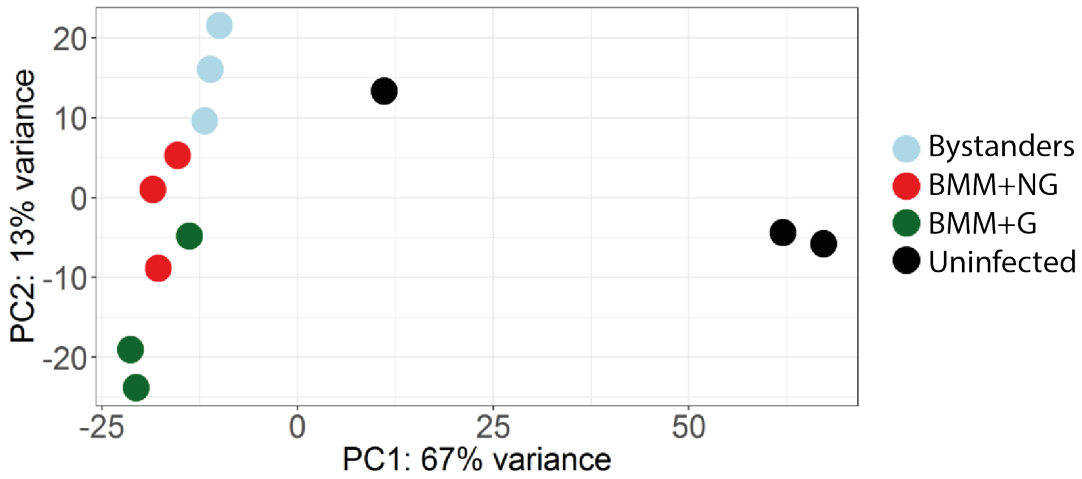


Figure 3.10: Principal component analysis of transcriptomes belonging to BMM+G, BMM+NG, bystanders and uninfected control BMMs infected with *Salmonella*. Transcriptomic data sets belonging to samples of bystander BMMS (blue), BMM+NG (red), BMM+G (green) and uninfected control BMMs from three independent infections with *Samonella* were subjected to 2D principal component analysis to separate each sample based on levels of variance from one another in gene expression. The 1st principal component (PC1) is given on the x-axis while the 2nd principal component is plotted on the y-axis (Dr. P. Hill).

Direct comparisons of the transcriptomes belonging to the different sorted BMM subpopulations were carried out. As was expected, genes upregulated in BMMs infected with NG or growing *Salmonella* when compared to uninfected cells, were found to have genes involved in the immune response upregulated. Uninfected cells had genes involved in the cell cycle and DNA replication upregulated. The profiles of bystanders and BMM+Deg appear to be very similar (data not shown). Direct comparisons of the BMM+G and BMM+NG transcriptomes (Figure 3.11) identified genes enriched in the BMM+NG transcriptome associated with the gene ontology term ‘cell differentiation’. As reported by Saliba et al. (2016), it appears that many genes enriched in the BMM+NG subpopulation of macrophages are associated with an M1 activation state (Tnf, Il1b, Nlrp), while many genes enriched in the BMM+G are associated with polarisation to an M2-like activation state (Mrc1, Fcgr2b, Arg1, Spp1, Il4ra, Timp1). Additionally, bystander macrophages appear to have M1 markers upregulated compared to BMM+G and BMM+NG. This suggests that the strength of polarisation of macrophages to an M2-like phenotype is dependent on bacterial number, with bystanders being more M1-like, BMM+G being more M2-like and BMM+NG having an intermediate phenotype between the two. This observation was also made using single cell RNA-seq data and confirmed on the protein level using IL1b and IL4Ra as markers of M1 and M2 polarisation respectively (Saliba et al. 2016). In this study, principal component analysis of the transcriptomic data showed that 69% BMM+NG macrophages had an M1 profile, while 31% had an M2 phenotype. This may explain why an intermediate phenotype is observed in this study, with a mix of the RNA from

these different subpopulations of cells. M1 macrophages are primarily anti-bacterial and inflammatory whereas M2 macrophages are anti-inflammatory and more permissive to bacterial proliferation (Benoit et al. 2008). This raises the question of whether polarisation of the macrophages is what causes some bacteria to grow and some to not grow, or is it that growing bacteria are able to effect the polarisation of their host macrophages to a phenotype that is more permissive for growth.

Figure 3.11

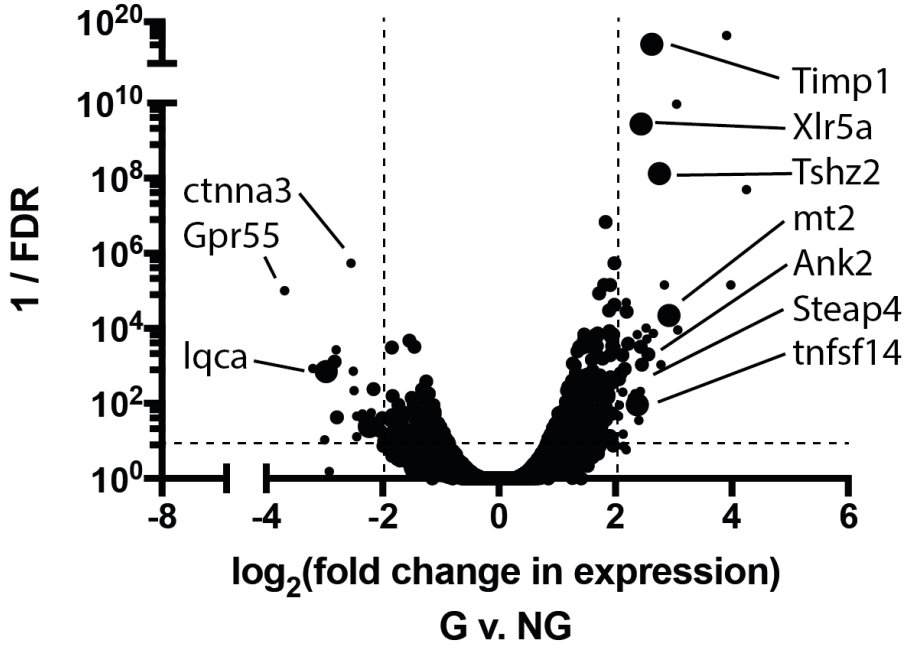


Figure 3.11: Direct comparison of BMM+G and BMM+NG transcriptomic profiles during infection with *Salmonella* (repeated **experiment).** Volcano plot showing the **fold change in**expression of genes in macrophage subpopulations BMM+G compared to BMM+NG at 18 h infection with *Salmonella* as $\log_2$(fold change in expression). Dashed lines show arbitrary cut-off of a four-fold difference in the expression (vertical) and a false discovery rate of over 10 (horizontal) in genes in growing *Salmonella* from those of NG *Salmonella*. Significantly upregulated genes are upregulated for each population. Size of dots correlates with read coverage of gene annotation. Plots representative of three independent experiments.

Table 3.4: Gene enrichment lists (abridged) for direct comparison of BMM+NG v BMM+G *Salmonella* transcriptomes.

(-1 > log_2FC threshold > 1), n=3.

Enriched in BMM+NG			Enriched in BMM+G		
Gene	**Function**	**log2FC**	**Gene**	**Function**	**log2FC**
Iqca	protein_coding	3.68	Xlr5a	protein_coding	-5.30
Zpld1	protein_coding	3.20	Tshz2	protein_coding	-4.61
RP24-231P10.4	TEC	3.00	Kctd17	protein_coding	-4.25
Gpr55	protein_coding	2.96	Cish	protein_coding	-3.98
Cux2	protein_coding	2.91	Ank2	protein_coding	-3.91
Fam213a	protein_coding	2.82	Rnf165	protein_coding	-3.07
Gm17782	unprocessed_pseudogene	2.80	Fam19a1	protein_coding	-3.05
Tdgf1-ps1	processed_pseudogene	2.78	Steap4	protein_coding	-2.92
Ctnna3	protein_coding	2.54	Enpp2	protein_coding	-2.84
Atp5d	protein_coding	2.50	Ccdc92	protein_coding	-2.79
Defb42	protein_coding	2.49	Tnfsf14	protein_coding	-2.76
Tgfbr3	protein_coding	2.45	Rasip1	protein_coding	-2.66
Fam196a	protein_coding	2.45	Timp1	protein_coding	-2.63
Gm14780	processed_pseudogene	2.36	Ocstamp	protein_coding	-2.56
Dynlt1b	protein_coding	2.34	Entpd3	protein_coding	-2.54
Gm18953	unprocessed_pseudogene	2.23	Wdr63	protein_coding	-2.52
Ntrk2	protein_coding	2.19	Gm16194	lincRNA	-2.45
Dnah12	protein_coding	2.16	Mt2	protein_coding	-2.44
Iqck	protein_coding	2.14	Ier5l	protein_coding	-2.44
Rnf170-ps	processed_pseudogene	2.04	Socs2	protein_coding	-2.43
Gm2904	processed_pseudogene	2.00	Marveld1	protein_coding	-2.41
Nudt14	protein_coding	1.99	Il1f5	protein_coding	-2.38
4930405A21Rik	processed_transcript	1.97	Mir511	miRNA	-2.38
Xlr4b	protein_coding	1.93	Acvr1c	protein_coding	-2.34
Tmem40	protein_coding	1.86	Cd28	protein_coding	-2.29
Cyp2b13	protein_coding	1.85	Pgf	protein_coding	-2.22
Gm23623	snRNA	1.85	Selp	protein_coding	-2.19

3.4 NG *Salmonella* express SPI-2 during macrophage infection

The finding that SPI-2 genes are expressed in NG *Salmonella* as well as growing *Salmonella* was striking (Figure 3.12A). To find that certain SPI-2 genes (*sseD, sseE* and *sseF*) were more highly expressed compared to growing bacteria was unexpected as SPI-2 T3SS activity have been previously associated with intracellular growth (Helaine et al. 2010). To confirm this result from the RNA-seq analysis, BMMs were infected with wild-type *Salmonella* harbouring a plasmid expressing an unstable variant of *gfp* under the transcriptional control of the promoter for *ssaG* – the gene encoding the needle protein of the SPI-2 T3SS apparatus (Figure 3.12B) (Ibarra & Steele-Mortimer 2009). The proportion of *Salmonella* extracted from BMMs incubated in gentamicin (including both growing and NG bacteria) and in cefotaxime (NG bacteria only; see chapter 4) at 2, 8 and 24 h.p.i. that were GFP-positive was measured by flow cytometry to assess the levels of *ssaG* expression, from which SPI-2 expression across the bacterial population could be inferred (Figure 3.12C). Only 10% of bacterial cells in stationary phase (inoculum) were GFP-positive, however upon infection the expression of *ssaG* increases to 35% in NG and growing *Salmonella*, and in NG *Salmonella* isolated in cefotaxime. The proportion of GFP-positive cells peaks at 8 h.p.i. in *Salmonella* extracted from BMMs with gentamicin present, this then reduces by 24 h.p.i. to 50%. In contrast, the proportion of GFP-positive NG *Salmonella* isolated during BMM infection in cefotaxime increases by 24 h.p.i. to 80%. This confirms the results of the dual RNA-seq analysis in terms of SPI-2 expression. The decrease in *ssaG* expression in the population of *Salmonella* present during infection of macrophages incubated in gentamicin

could be the result of the antibiotic interfering with the bacteria. Alternatively, the growing *Salmonella* may decrease expression of SPI-2 later during infection while the expression of SPI-2 in NGs remains high.

Figure 3.12

A.

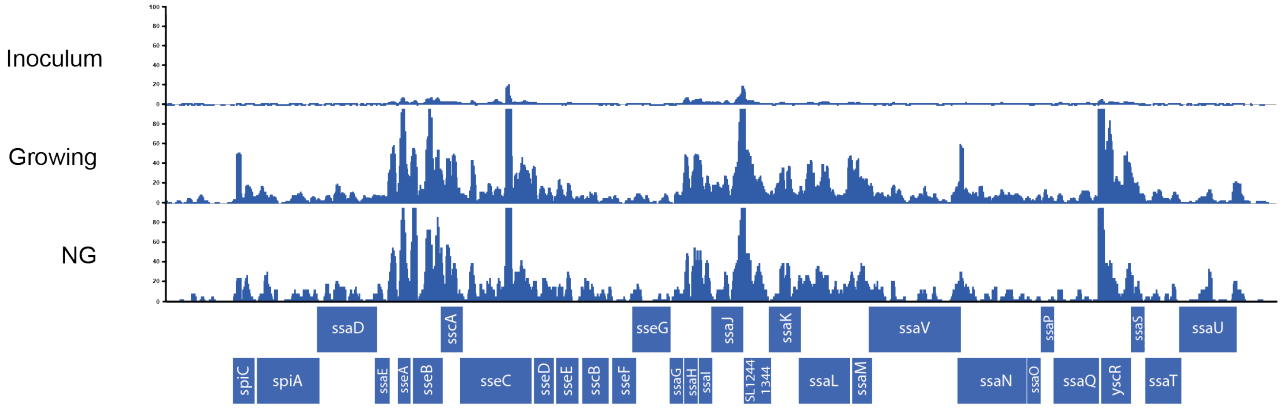


Figure 3.12

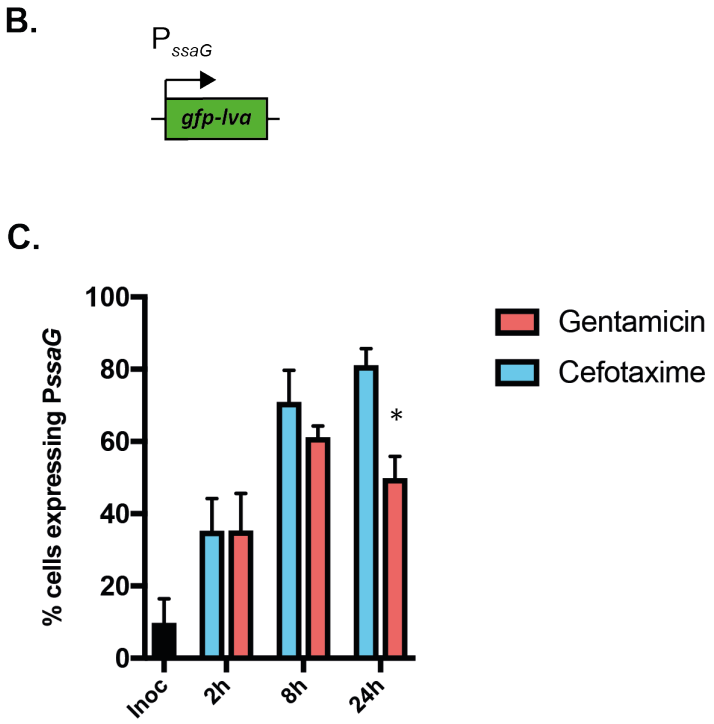


Figure 3.4: NG and growing *Salmonella* express SPI-2 through infection of BMMs. A) Plot showing levels (arbitrary units) of reads mapped to SPI-2 island for the inoculum, growing *Salmonella* and NG *Salmonella* 18 h.p.i. in BMMs with genes annotated along x-axis. Representative of three independent experiments. B) Diagram of transcriptional fusion of P_{ssaG} and *gfp-lva* present on the pMPM-A3-ΔPlac-PssaG-*gfplva* plasmid transformed into wild-type *Salmonella* for this experiment. C) Bar graph showing proportion of bacteria expressing *ssaG,* a gene encoding the needle protein of the SPI-2 T3SS apparatus during infection of BMMs incubated in cefotaxime (blue) to isolate NG *Salmonella* only or in gentamicin (red) with both NG and growing *Salmonella* present. Data are mean ±s.e.m. n =3. p-values indicated as *<0.05.

3.5 Conclusion

The work shown here describes the use of fluorescence dilution, cell sorting and dual RNA-seq to analyse the transcriptomes of growing and NG *Salmonella* as well as the transcriptomes of their host macrophages simultaneously during infection. The NG *Salmonella* population is enriched for persisters, but it is important to stress that the NG population of bacteria are not all necessarily persisters, as persisters are defined by an ability to regrow after a period of antibiotic tolerance, often associated with a lack of growth. It is not possible to assess the ability of these NG *Salmonella* to regrow and then extract RNA as the transcriptome would revert to that of growing bacteria. A preliminary run of the dual RNA-seq experiment was carried out to highlight any potential changes to be made before repeating the experiment several times for increased statistical power. The preliminary run appeared to be a success, however it was decided that ribo-depletion of the bacteria RNA would decrease the depth of sequencing required to obtain enough data for analysis, thus vastly decreasing the cost of the experiment. The gating used for sorting was made more stringent also, in the hope of more easily identifying differences between the subpopulations of BMMs. The bacterial transcriptomic analysis from the preliminary run highlighted stress-related genes and tRNAs to be up in NG *Salmonella* and chiefly ribosomal genes and DNA replication genes to be up in growing *Salmonella*. Some of the same genes were picked up as hits in the repeats of the experiment that followed, however large differences included LPS synthesis genes detected as being upregulated in growing *Salmonella*, pathogenesis genes such as *iagB* and stress regulatory genes such as *marB* being upregulated in growing

Salmonella. In addition, many SPI-2 genes were identified as being upregulated in NG *Salmonella* in comparison to growing bacteria during infection. This was confirmed using a transcriptional fusion of the promoter of *ssaG* to an unstable *gfp* variant (Ibarra & Steele-Mortimer 2009) and flow cytometry. A major reason for the difference in results is likely that many genes were discarded from the analysis of the preliminary experiment as being unreliable owing to a low RPKM value. This quality control step was not necessary for the next run of repeats due to the ability to reliably calculate p-values for each gene in the transcriptomes analysed. In addition, one interesting finding was that tryptophan biosynthesis appears to be upregulated in NG *Salmonella* and repressed in growing *Salmonella* during infection. One microarray study on chlamydia persisters found this also to be the case in this species (Belland et al. 2003) and a previous investigation discovered that the addition of tryptophan to the infection medium enabled the resumption of growth in these NG *Chlamydia* (Beatty et al. 1994). It would be interesting to observe whether the addition of tryptophan to the medium during infection reduced the proportion of NG *Salmonella* during infection of macrophages.

The major findings of the preliminary RNA-seq run analysing the macrophage transcriptomes observed a higher LPS response in bystander macrophages BMM+NGs and BMM+Gs. The 'response to LPS' gene ontology term was highlighted based mainly on the enrichment of a large number of miRNA genes. As a quality control step was selection based on RPKM values being higher than 1, it is possible that this leads to a bias towards the enrichment of small transcripts such as miRNAs that are more likely to have complete read coverage than larger genes, this may explain the

absence of this result in subsequent experiments. This could also explain the enrichment of tRNAs in NG *Salmonella* observed in the preliminary run and not in the three subsequent repeats. The pro-inflammatory genes upregulated in BMMs highlighted by the preliminary run do fit with the finding from the three subsequent repeats of the experiment that BMM+NGs and to a greater extent, BMM+Gs are polarised towards a M2 phenotype. This result has been confirmed using single cell RNA-seq on macrophages infected with *Salmonella* using the same experimental set up (Saliba et al. 2016). Our group now has produced evidence that the polarisation of host macrophages to an M2 phenotype is SPI-2-dependent, with expression of M2 markers correlating with the number of intracellular *Salmonella*. The effector responsible for this polarisation phenotype has recently been identified (Stapels, D., unpublished data).

From the dual RNA-seq analysis, we found that both NG and growing *Salmonella* express SPI-2 genes and macrophages containing bacteria are polarised to an M2 (anti-inflammatory) phenotype rather than an M1 (anti-bacterial) phenotype. Enrichment of coding RNA species is advised to decrease the depth of sequencing required, which is necessary to reduce the costs involved in repeating the experiment several times. Repetition of RNA-Seq is advised to increase the statistical power and the reliability of the results from the transcriptomic analysis.

Chapter four

DNA synthesis occurs in nongrowing *Salmonella* during macrophage infection

4.1 Introduction

The cell cycle of bacteria during infection is still currently little understood. However research is beginning to explore this aspect of the pathogenic bacterial life-cycle. *Brucella abortus* is known to undergo arrest in the G1-like phase of its cell cycle, not undergoing growth for the first 4-6 h of infection in HeLa cells (Deghelt et al. 2014). Several other pathogens, including *Salmonella* are known to have a lag between initial infection and subsequent proliferation. There is also heterogeneity in the levels of growth of *Salmonella* after this initial lag during infection of macrophages, with some bacterial cells starting to proliferate and others remaining in a nongrowing (NG) state (Helaine et al. 2010; Helaine et al. 2014). These NG *Salmonella* are thought to be a source of antibiotic-tolerant persisters, responsible for treatment failure and recurrent infection (Helaine et al. 2014; Helaine & Kugelberg 2014; Fisher et al. 2017). Interestingly, different proportions of *Salmonella* persisters are isolated from infected macrophages depending on the class of antibiotic. For instance, treatment of *Salmonella,* released from macrophages, with the fluoroquinolones ciprofloxacin, isolates persisters an order of magnitude less frequently when compared to treatment with gentamicin or cefotaxime (Helaine et al. 2014). As antibiotic tolerance is

thought to be owing to the shutting down or slowing down of certain metabolic processes in bacteria, the increased activity of fluoroquinolones against NG *Salmonella* indicates that the target of the antibiotic, DNA gyrase may be active in these bacteria. Indeed, there is already evidence for active transcription and translation in nongrowing *Salmonella* during macrophage infection – demonstrated by the production of DsRed in response to the addition of an arabinose inducer (Helaine et al. 2014). However, the presence of active DNA synthesis in these bacteria had not yet been investigated. Therefore, I sought to test the hypothesis that NG *Salmonella* during macrophage infection carried out DNA replication.

4.2 *In vitro* detection of differential levels of DNA content in *Salmonella*

In order to ensure the ability to differentiate between varying levels of DNA replication in NG *Salmonella* cells during macrophage infection, I first needed to test whether I could detect increasing DNA content in bacteria grown *in vitro*. Fixed *Salmonella* were stained with 4',6-diamidino-2-phenylindole (DAPI). DAPI is a fluorescent dye that binds to the minor grooves of a DNA molecule, increasing in fluorescence intensity when bound. Rifampicin and cefalexin were used in order to carry out a run-out experiment on *Salmonella* cells grown to either exponential or stationary phase in minimal media. This involves adding a small, sub-lethal dose of both cephalexin and rifampicin to inhibit division and indirectly inhibit the initiation of DNA synthesis respectively and incubating for 2h at 37^{o}C. This allows any currently active replication forks to continue DNA synthesis to completion, resulting in an integer number of chromosomes within each cell. This allows the visualisation

of easily distinguishable peaks of fluorescence by flow cytometry following fixing with paraformaldehyde (PFA) and DAPI-staining. Figure 4.1A shows the histograms of *Salmonella* in exponential and stationary phase without the addition of antibiotics. Figure 4.1B shows exponential and stationary phase *Salmonella* following the rif-cef run out. In exponential phase *Salmonella*, more defined peaks of DAPI fluorescence can be distinguished following the run-out (figure 4.1B) when compared to before the addition of the antibiotics (figure 4.1A), indicating that the active replication forks present were allowed to continue to completion. The stationary phase samples are identical to each other before and after the addition of the antibiotics, suggesting that there is little to no active DNA synthesis in these bacteria. It can be assumed that the two peaks visible in stationary phase *Salmonella* grown in minimal media represent 1 or 2 chromosomes (1N or 2N), as is the case in *E. coli* when grown in poor growth conditions (Ferullo et al. 2009). From these results, we can be satisfied that differential levels of DNA replication can be detected using DAPI-staining *in vitro*. In addition, *Salmonella* grown to stationary phase in minimal media exhibit little or no DNA replication and contain either 1 or 2 chromosomes.

Figure 4.1

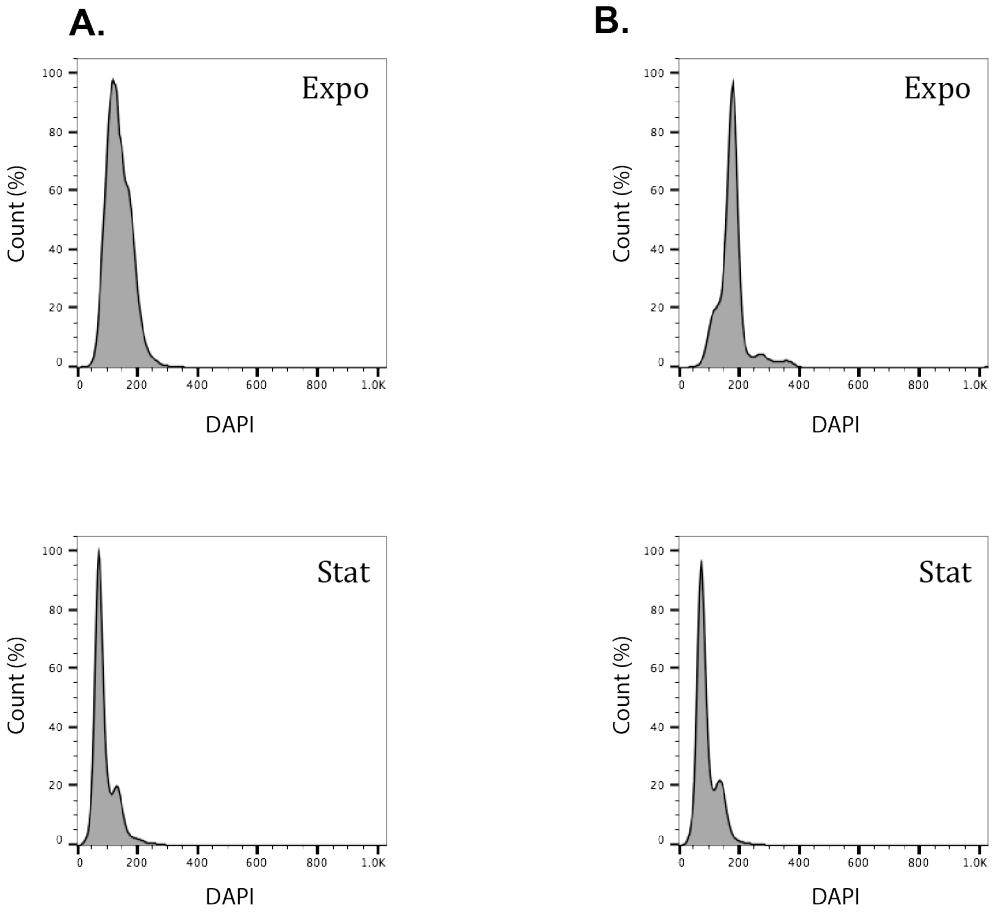


Figure 4.1: Flow cytometry analysis of DAPI-stained run-out *Salmonella* grown to exponential phase and stationary phase in minimal medium. DNA content of *Salmonella* in exponential phase (Expo) and stationary phase (Stat) grown in MgMES pH5 minimal medium was quantified in the absence of antibiotics (A) and after 2 h of incubation in a low dose of rifampicin and cephalexin (B) allowing any active DNA replication forks to run to completion while inhibiting any further initiation of DNA replication.

4.3.1 DNA replication occurs in *Salmonella* during infections of RAW 264.7 macrophages

To test whether DNA replication was occurring in *Salmonella* cells in the absence of cell division during macrophage infection, DAPI-staining was combined with fluorescence dilution (FD) of *Salmonella* during macrophage infection (Figure 4.2). RAW 264.7 macrophages (RAWs) were infected with wild-type *Salmonella* carrying the pDiGc FD plasmid (Figure 4.3). Bacteria harbouring the pDiGc plasmid (Figure 4.2) express GFP constitutively while also expressing DsRed under the control of an arabinose-inducible P_{BAD} promoter. Figure 4.3A contains bivariate plots of the levels of GFP and DsRed fluorescence in the *Salmonella* within the inoculum as well as *Salmonella* extracted at 4 and 8 h.p.i. from macrophages. The levels of GFP stayed constant in the population throughout the infection, which was to be expected. However, as expression of DsRed is only induced prior to infection (Figure 4.2), the levels of DsRed dilute as the bacteria divide. A population of NG *Salmonella* (high DsRed) is clearly distinguishable from the growing bacteria (low DsRed) levels by 8 h.p.i. (Figure 4.3A). Proliferation of *Salmonella* in RAWs is particularly unrestricted compared to in other macrophages. It begins almost immediately in contrast to bone marrow-derived macrophages that usually display a 6 h lag between the initial infection and the start of bacterial proliferation (Helaine et al. 2010). The pie charts in Figure 4.3B show the proportions of growing to NG *Salmonella* present at each timepoint of infection. At 4 h.p.i., only 11% of *Salmonella* have undiluted DsRed fluorescence, indicating that they have not divided, whereas at 8 h.p.i., this proportion is just 4%, as the growing population is increasing in proportion

during infection. Bivariate histograms of DAPI and DsRed fluorescence levels over time (Figure 4.3C) show that by 4 h.p.i., the bacteria that contain the highest levels of DsRed have increased their DAPI content. The levels of DAPI fluorescence in the NG subpopulation have further increased by 8 h.p.i., suggesting that the NG *Salmonella* indeed have active DNA replication, at least early on during infection. Histograms of DAPI fluorescence of the *Salmonella* in each sample can be found in Figure 4.3D, the histogram for 8 h.p.i. compares the DAPI fluorescence for growing and NG bacteria (gating shown in Figure 4.3A). Most of the NG *Salmonella* have increased their DNA content from that of the inoculum and that of the growing bacteria in the same sample. Figure 4.3E is a bar chart displaying the DAPI fluorescence of all bacteria at each time point, along with the DAPI fluorescence levels for growing and NG bacteria. The DNA content of the total population changes little throughout the infection. The growing bacteria, which make up most of the population, appear to cycle between 1N and 2N as they proliferate. The NG bacteria however (red bars), increase their DNA content greatly during infection. This can be seen to be almost two-fold compared to that of the growing *Salmonella* (Figure 4.3F) suggesting there are up to four chromosomes in these NG bacteria. These results appear to support the hypothesis that NG *Salmonella* undergo DNA replication in macrophages.

Figure 4.2

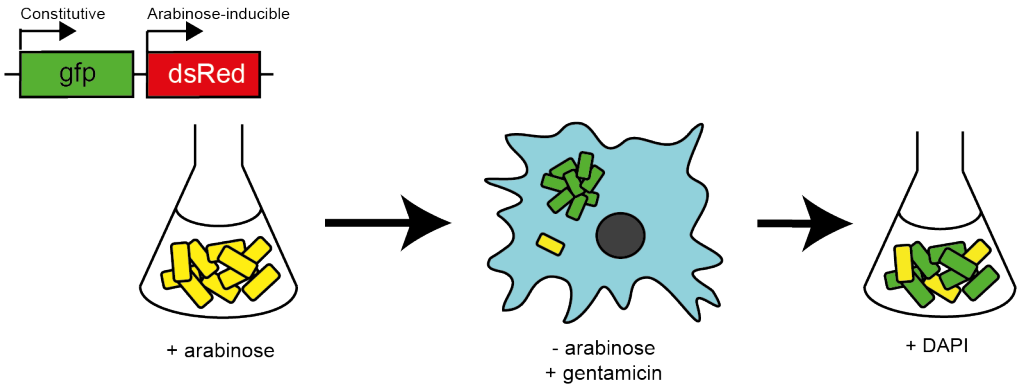


Figure 4.2: Experimental design for quantifying *Salmonella* proliferation and DNA content during macrophage infection. Wild-type *Salmonella* carrying the pDiGc fluorescence dilution plasmid expressing GFP constitutively and DsRed under the control of an arabinose-inducible P_{BAD} promoter were grown overnight in MgMES pH5 minimal medium to stationary phase in the presence of arabinose. During infection of macrophages in the absence of arabinose, any dividing bacteria will dilute their DsRed fluorescence allowing the differentiation between growing and nongrowing bacteria. The addition of gentamicin to the infection medium prevents the growth of extracellular *Salmonella* that could interfere with the assay. Samples are taken at different time points during infection by lysing the macrophages and collecting the *Salmonella* cells for DAPI-staining and flow cytometry.

Figure 4.3

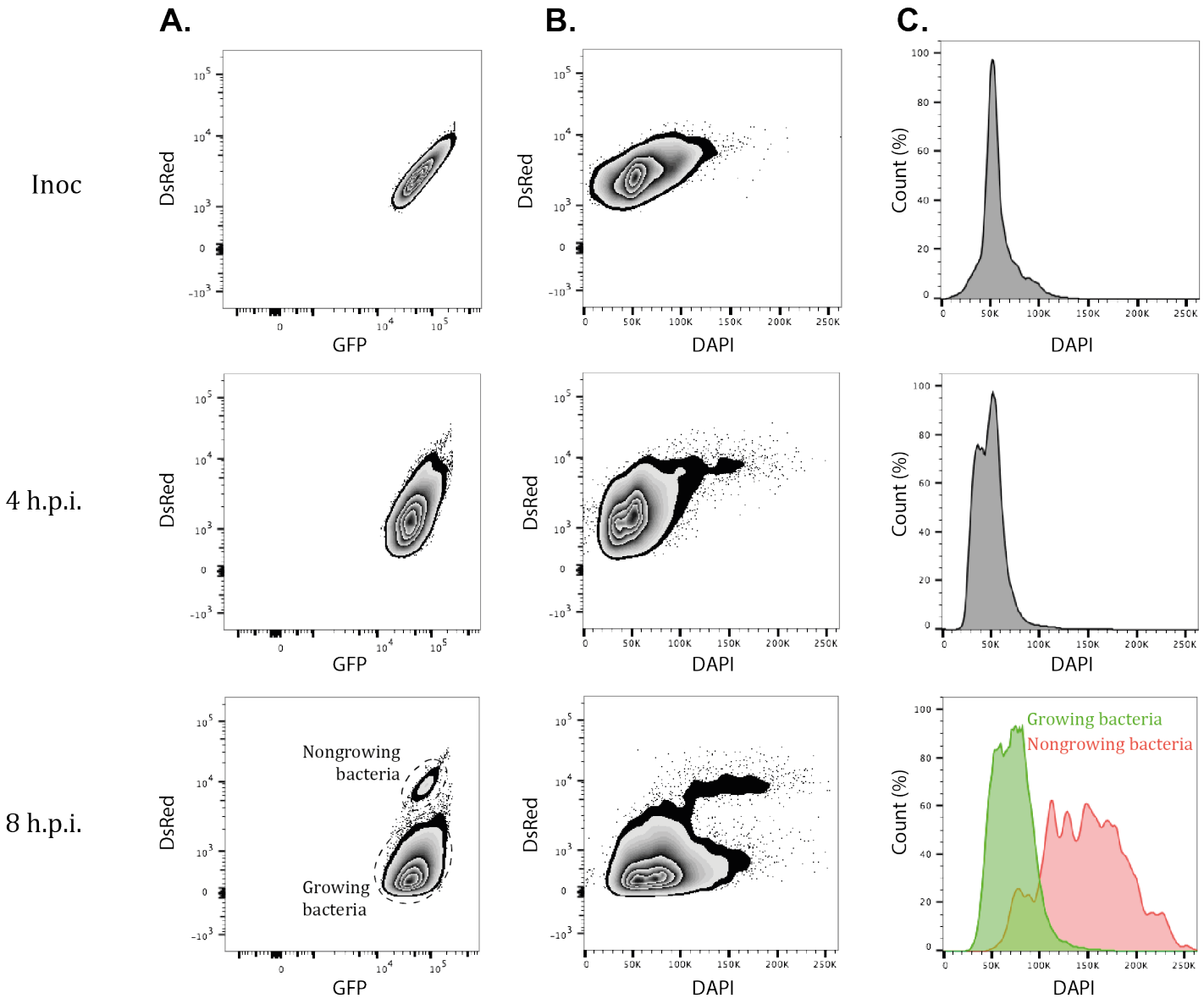

A.
B.
C.
Inoc
4 h.p.i.
8 h.p.i.
DsRed
GFP
DAPI
Count (%)
Nongrowing bacteria
Growing bacteria
Growing bacteria
Nongrowing bacteria

Figure 4.3

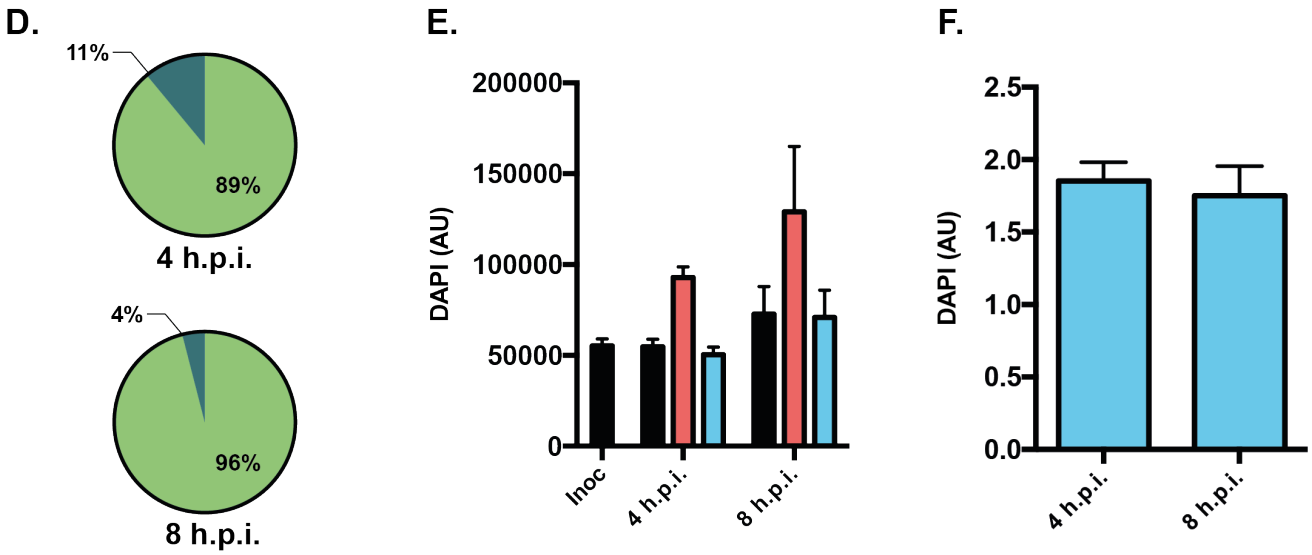


Figure 4.3: Infection of RAW 264.7 macrophages with *Salmonella* for fluorescence dilution and DNA quantification. Fluorescence dilution profiles as measured by flow cytometry are shown for the inoculum, 4 h.p.i. and 8 h.p.i. as bivariate histograms of GFP and DsRed fluorescence (A). Bacterial growth is shown in combination with DNA content as bivariate histograms of DsRed and DAPI fluorescence (B) DNA content alone is shown as DAPI histograms (C). Proportions of growing and nongrowing *Salmonella* at 4 h.p.i. and 8 h.p.i. displayed in pie charts (D). Arithmetic mean DAPI fluorescence values of the total bacteria population (black), nongrowing bacteria (red) and growing bacteria (blue) are shown as mean ± SEM (n=3) (E), an example of the gating used is visible (A). Values are also shown for nongrowing bacteria normalised to those of growing bacteria mean ± SEM (n=3) (F).

4.3.2 DNA replication occurs in *Salmonella* during infections of iBMM macrophages

It could be argued that RAWs are not particularly physiologically relevant, due to the large amounts of mutations and rearrangements that have taken place in their genomes. To test for the presence of DNA replication in NG *Salmonella* during infection of a more relevant cell type, immortalised bone marrow-derived macrophages (iBMMs) were used. These are cells that have been differentiated from murine bone marrow progenitor cells and then infected with a transforming virus in order to immortalise the cell line. The iBMMs can be infected for longer than RAWs as less cell lysis occurs throughout. The iBMMs were infected with wild-type *S.* Typhimurium carrying pDiGc for 24 h.p.i., taking samples at 8 h.p.i., 12 h.p.i. and 24 h.p.i. to monitor the bacteria for FD and DNA content with DAPI-staining (Figure 4.4). Bivariate histograms of the GFP and DsRed fluorescence of *Salmonella*, detected by flow cytometry, in each of these samples are shown in Figure 4.4A. The FD profiles are similar at 8 h.p.i. between the infection of RAWs (Figure 4.3A) and iBMMs (Figure 4.4A), as are the proportions of growing and NG bacteria present (Figure 4.4B). At 12 h.p.i. and 24 h.p.i., the NG population of *Salmonella* is still detectable. The DAPI fluorescence levels, shown alongside DsRed levels as bivariate plots (Figure 4.4C) and alone as univariate histograms for all samples (Figure 4.4D) follow the same pattern as that observed during infection of RAWs; the DNA content of NG *Salmonella* increases in comparison to the growing bacteria. By 8 h.p.i., it appears that a maximum amount of 4N is reached in the nongrowing bacteria. After 8 h.p.i. however this level of DNA appears to decrease, while the population is still

identifiable by high GFP and DsRed fluorescence. The DsRed and GFP fluorescence suggests that the bacteria are most likely alive but the low DAPI level suggests that little to no DNA is present. It is possible that this reduction in DAPI-staining is not due to a reduction in the levels of DNA but the increase in total number of cells present titrating out the stain as this low-DAPI population is also observed in the 24 h sample. The absolute DAPI fluorescence levels and those of the NG *Salmonella* normalised to the growing bacteria averaged across three experiments are presented in Figures 4.4E and 4.4F. These show a clear increase in the levels of NG *Salmonella* DNA in comparison to the growing *Salmonella* by 8 h.p.i., however this reduces by 12 h.p.i. and further reduces to levels representing less than 1N by 24 h.p.i., this must be due either to compaction of the DNA or cell death.

Figure 4.4

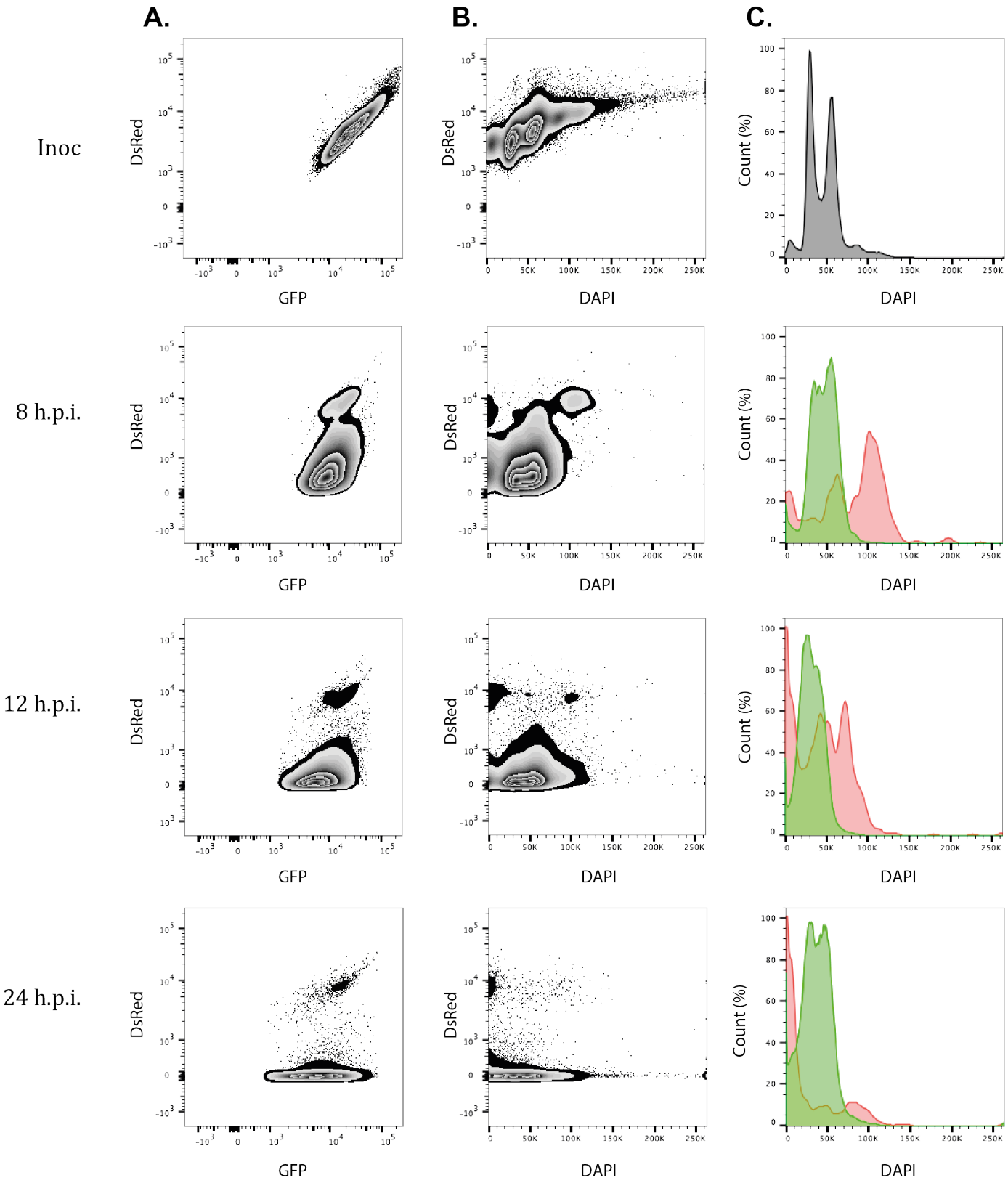


Figure 4.4

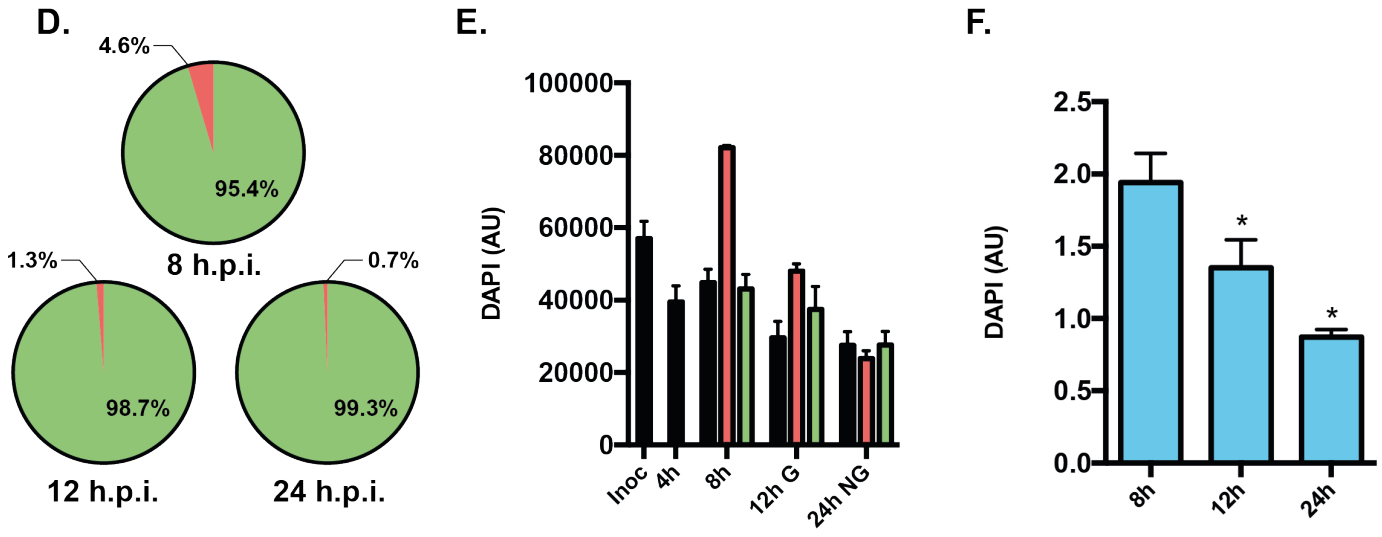


Figure 4.4: Infection of immortalised bone marrow-derived macrophages (iBMMs) with *Salmonella* for fluorescence dilution and DNA quantification. Fluorescence dilution profiles as measured by flow cytometry are shown for the inoculum, 4 h.p.i. and 8 h.p.i. as bivariate histograms of GFP and DsRed fluorescence (A) with the proportions of growing and nongrowing *Salmonella* at 4 h.p.i. and 8 h.p.i. displayed in pie charts (B). Bacterial growth is shown in combination with DNA content as bivariate histograms of DsRed and DAPI fluorescence (C) DNA content alone is shown as DAPI histograms (D). Arithmetic mean DAPI fluorescence values of the total bacteria population (black), nongrowing bacteria (red) and growing bacteria (blue) are shown as mean ± SEM (n=3) (E), an example of the gating used is visible (A). Values are also shown for nongrowing bacteria normalised to those of growing bacteria mean ± SEM (n=3) (F).

4.3.3 DNA replication occurs in *Salmonella* during infections of primary BMMs

Finally, I tested whether this increase of DAPI-staining (and decrease at later time points of infection) also occurred in nongrowing *Salmonella* during infection of primary bone marrow-derived macrophages (BMMs). BMMs are macrophages that have been differentiated from freshly extracted bone marrow macrophage progenitor cells. As a result of this, they have accumulated fewer mutations and are likely to be more similar to cells found inside the host. Samples were taken at 4 h.p.i. to monitor DNA levels early in infection, as well as at 8 h.p.i. and 24 h.p.i. to monitor levels later during infection. The fluorescence dilution profiles of the *Salmonella* during infection of BMMs are starkly different to both RAWs and iBMMs (Figure 4.5A). The BMMs are far more restrictive to bacterial growth than immortalised macrophage-variants, with only 21.7% of the bacterial population having diluted any DsRed by 8 h.p.i. and only 38.9% by 24 h.p.i.. However, the DAPI fluorescence levels of the NG *Salmonella* during BMM infection show a similar profile to those during RAWs and iBMM infection (Figure 4.5C), with an increase by 8 h.p.i. and a decrease in the DAPI levels later in infection (24 h.p.i.). The increase in DAPI levels occurs in the ‘high DsRed’ subpopulation indicating that they have not divided. The univariate DAPI fluorescence histograms show this increase clearly in the total population of bacteria present (Figure 4.5D) as the NG bacteria are no longer a minority in these infections. Figure 4.5E shows the mean DAPI fluorescence levels of the total bacteria and the NG and growing *Salmonella* during BMM infection averaged across three experiments, the DAPI levels are clearly higher in NG

Salmonella than in growing bacteria, however this is lost later in infection. It is possible that the NG bacteria with high levels of DNA are simply slow-growing *Salmonella* that then go on to divide and as a result reduce their DNA content. It is possible that the NG persisters present during infection could be the NG bacteria that do not increase their DNA level. To investigate this further, I decided to observe the NG *Salmonella* during infection in isolation, with the eradication of all growing *Salmonella*.

Figure 4.5

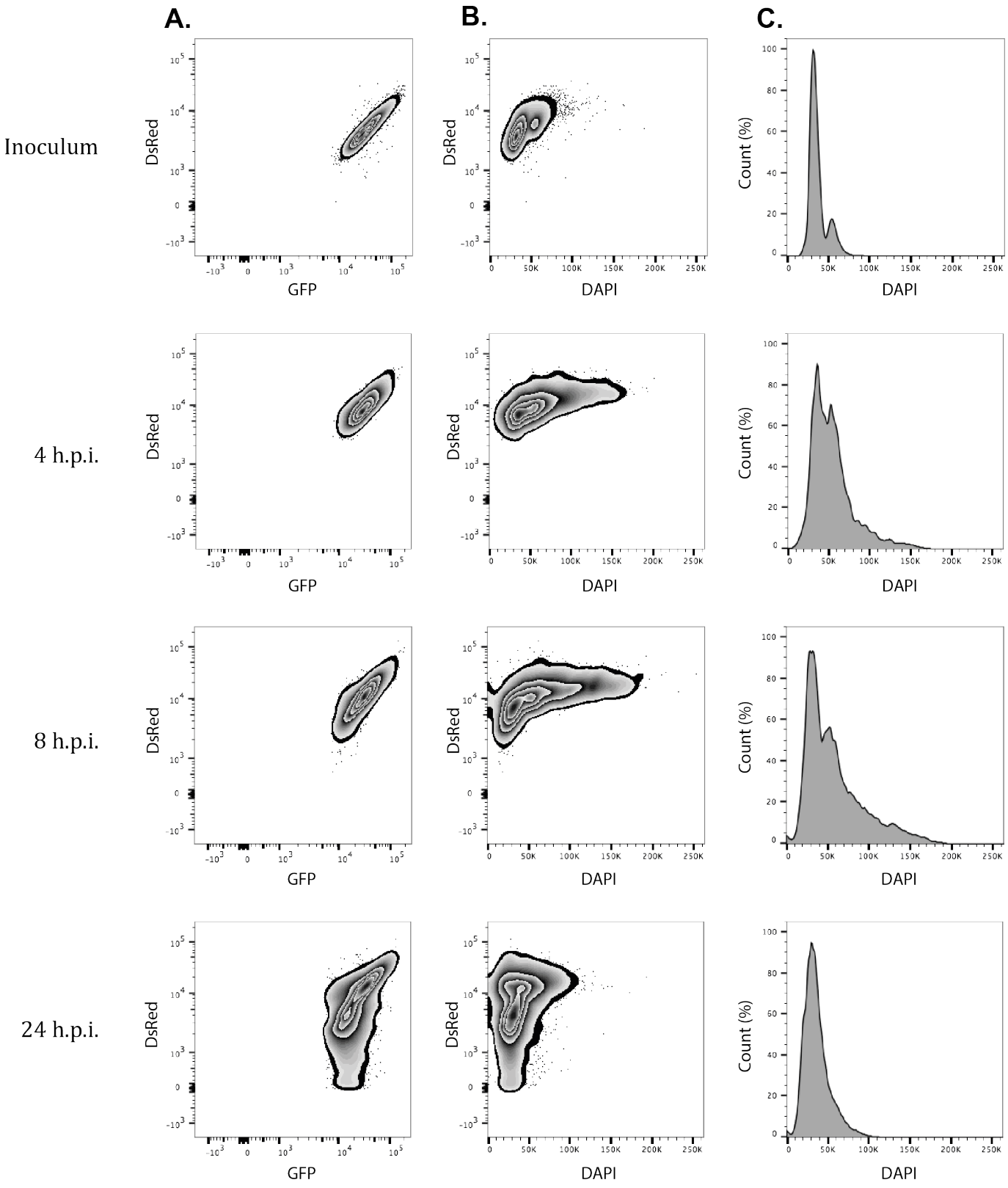


Figure 4.5

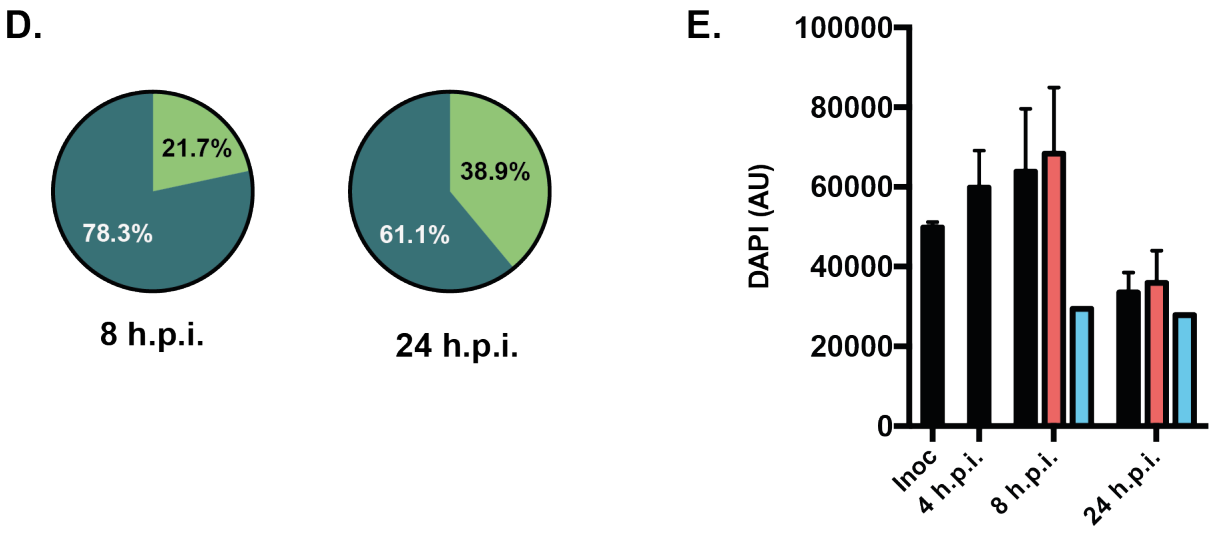


Figure 4.5: Infection of primary bone marrow-derived macrophages (BMMs) with *Salmonella* for fluorescence dilution and DNA quantification. Fluorescence dilution profiles as measured by flow cytometry are shown for the inoculum, 4 h.p.i. and 8 h.p.i. as bivariate histograms of GFP and DsRed fluorescence (A). Bacterial growth is shown in combination with DNA content as bivariate histograms of DsRed and DAPI fluorescence (B) DNA content alone is shown as DAPI histograms (C). Proportions of growing and nongrowing *Salmonella* at 4 h.p.i. and 8 h.p.i. displayed in pie charts (D) Arithmetic mean DAPI fluorescence values of the total bacteria population (black), nongrowing bacteria (red) and growing bacteria (blue) are shown as mean ± SEM (n=3) (E), an example of the gating used is visible (A). Values are also shown for nongrowing bacteria normalised to those of growing bacteria mean ± SEM (n=3) (F).

4.4 DNA synthesis in nongrowing *Salmonella* can be more effectively monitored by using cefotaxime isolation to kill growing *Salmonella*

Traditionally, infecting macrophages with *Salmonella* is carried out under gentamicin-protection, in which the antibiotic is added post-phagocytosis to inhibit the growth of extracellular bacteria, as aminoglycosides are not easily taken up by mammalian cells. However, in order to measure the DNA content of nongrowing *Salmonella* in the absence of growing *Salmonella*, macrophages were infected with wild-type *Salmonella* carrying an FD plasmid in the presence of cefotaxime. In contrast to aminoglycosides, cephalosporin antibiotics are easily taken up by mammalian cells and are able to act intracellularly on any growing bacteria present. However, assuming any intracellular NG *Salmonella* would not be synthesising peptidoglycan in order to grow and divide, they should be left unharmed by the antibiotic. As infection of BMMs resulted in a higher proportion of NG bacteria in the population and is arguably the most physiologically relevant cell type out of the three macrophage cell lines used so far, I chose to continue their use for this experiment. The FD plasmid pDiGi was used, with GFP acting as the diluting fluorophore, being induced before but not during infection (see schematic for metabolic activity assay in Figure 4.8). The infection was followed for over two days with either the standard gentamicin-protection protocol (containing both growing and NG *Salmonella*) or by adding cefotaxime to the cell culture medium after phagocytosis instead (NG bacteria only), with samples taken at 8 h.p.i., 24 h.p.i. and 52 h.p.i. to measure FD and DNA content of the bacterial cells through flow cytometry (Figure 4.6). The FD and DAPI profiles of the growing and NG *Salmonella*

present in the gentamicin-protection assay were the same as previously observed in BMMs (Figure 4.5). In particular, the mean DAPI fluorescence of the NG *Salmonella* showed an increase, followed by a decrease in levels when averaged over three experiments (Figure 4.6C). These differences are not statistically significant and merely represent a reproducible trend. If the infection was carried out with the addition of cefotaxime post-phagocytosis, the results are strikingly different however (Figures 4.6D-F). As was expected, there is no dilution of GFP visible, as dividing bacteria will have been killed by the cefotaxime (Figure 4.6D). The levels of DAPI fluorescence appear to increase up until 28 h.p.i. however, and remain at this level for a further 24 h (Figure 4.6D-E). Individual peaks in the DAPI fluorescence that could represent whole numbers of chromosomes are not distinguishable (Figure 4.6E), as in most previous experiments. This suggests that perhaps while DNA replication is occurring early on during infection, replication fork arrest may occur before completion of whole chromosomes (Figure 4.6E). The mean DAPI fluorescence levels in NG *Salmonella* during BMM infection in the presence of cefotaxime increases significantly by 8 h.p.i. and 28 h.p.i. when compared to the inoculum. There is also a significant increase in the DNA content again between 28 h.p.i. and 8 h.p.i., when no significant increase is observed in when gentamicin is also used. In infection assays with growing also bacteria present, the increase in DNA content over time in NG *Salmonella* may be underestimated owing to the reduction in the efficiency of DAPI-staining as bacterial numbers increase. This is not an issue in infections in the presence of cefotaxime as the numbers of NG *Salmonella* remain relatively constant through infection. While it is difficult for gentamicin to enter

mammalian cells, it does occur (Van der Auwera et al. 1988). It is therefore possible that gentamicin is becoming intracellular during infection and having an effect on the NG *Salmonella* translation, subsequently affecting DNA metabolism. Owing to the continued presence of NG *Salmonella* in the same SCV over extended periods of time, in comparison to growing *Salmonella* having to renew the SCVs at each division, gentamicin may accumulate to a greater extent in NG SCVs consequently inhibiting more cellular processes than in the absence of cefotaxime. It would be ideal to observe the NG *Salmonella* without either antibiotic present, however such an experiment would be difficult because of the rapid proliferation of extracellular bacteria in the infection medium.

Figure 4.6

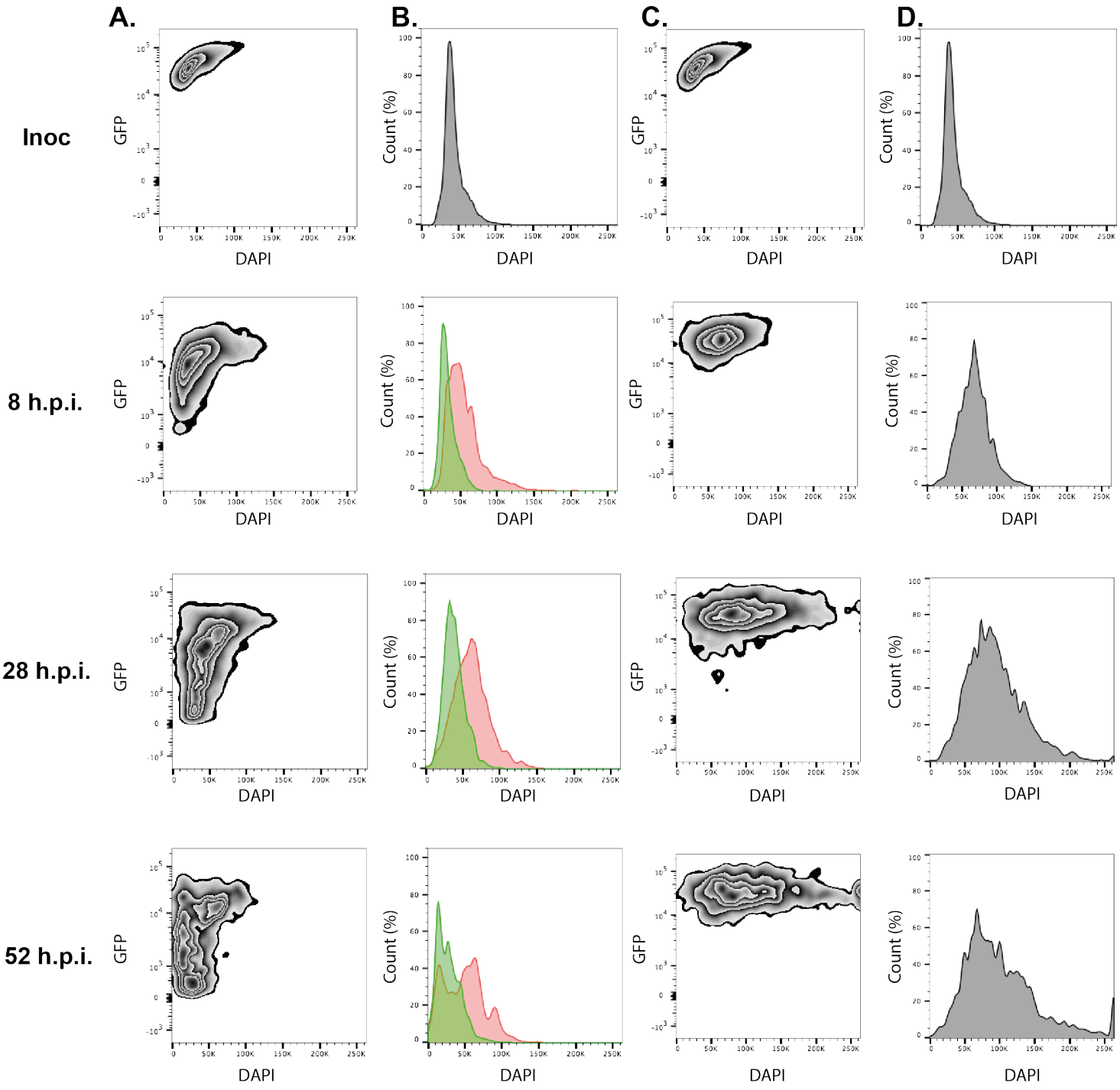


Figure 4.6

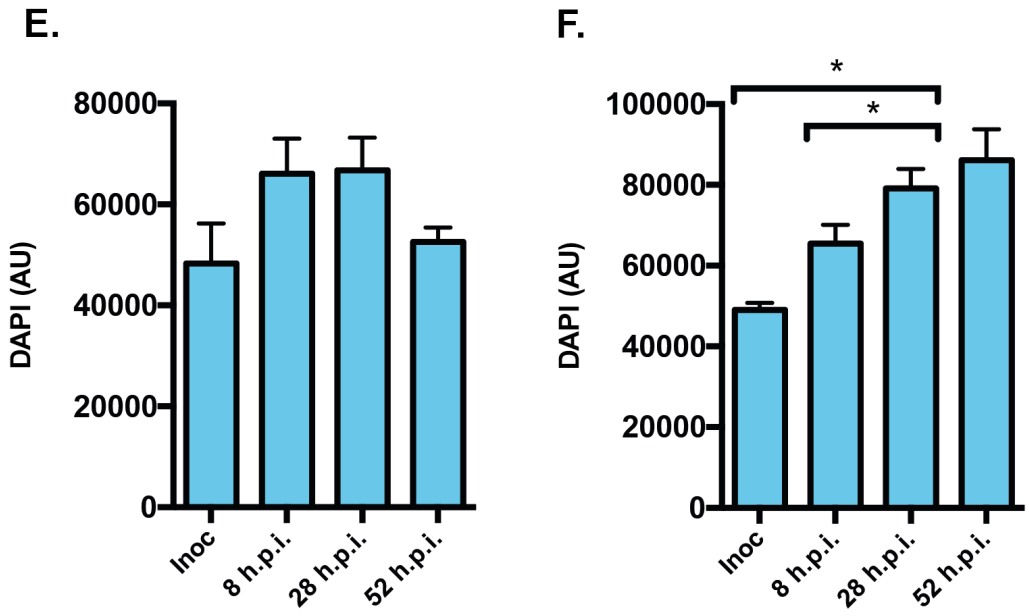


Figure 4.6: Comparison of the quantification of DNA in nongrowing bacteria during infection in the presence of either gentamicin or cefotaxime. Fluorescence dilution and DNA content measured by flow cytometry are shown for the inoculum, 8 h.p.i., 28 h.p.i. and 52 h.p.i. in the presence of gentamicin (A) and cefotaxime (C) as bivariate histograms of GFP and DAPI fluorescence. DNA content of total bacteria (grey) growing (green) and nongrowing (red) bacteria during infection with gentamicin (B) and cefotaxime (D) is shown as histograms of DAPI fluorescence. Arithmetic mean DAPI fluorescence values of the nongrowing bacterial population with gentamicin (E) and cefotaxime (F) are shown as mean ± SEM (n=3).

As the focus of this study is on the cellular state of the NG *Salmonella* during macrophage infection, I chose to continue using cefotaxime during infection experiments to obtain clearer results regarding this particular subpopulation. DAPI-staining is a reliable method of measuring an increase in the DNA content of the nongrowing *Salmonella*, that I wanted to complement using 5-Ethynyl-2´-deoxyuridine (EdU) to monitor directly *de novo* synthesis in NG *Salmonella*. EdU is a thymidine analogue that incorporates into DNA as it is replicating. Click chemistry can then be used to covalently bind a fluorescent azide to the EdU, which can be detected by flow cytometry. EdU was added to the cell culture medium during infection of BMMs with wild-type *Salmonella* expressing mCherry in the presence of cefotaxime in intervals of 2-4 h.p.i. and 4-6 h.p.i. to observed whether DNA replication is occurring early in and infection (Figure 4.7). EdU was also added between 6 and 24 h.p.i. to assess whether DNA is occurring later in infection, when growing *Salmonella* are known to start proliferating. The DNA increase in the NG population was detected by DAPI simultaneously. The *Salmonella* exposed to EdU for the longest period 6-24 h.p.i., showing a reduced level of DNA increase, owing to the cytotoxicity of prolonged EdU exposure (Figure 4.7A). A small level of *de novo* synthesis was detected between 2 and 4 h.p.i. (7% of cells displaying a fluorescent profile higher than the inoculum) and between 4 and 6 h.p.i. (12% of cells). The highest level of EdU incorporation was detected when adding EdU between 6 and 24 h.p.i., with 32% of bacteria displaying increased EdU-azide fluorescence. This suggests that the DNA synthesis is occurring gradually over time up until at least 24 h.p.i., and that this DNA replication makes use of nucleotides transported from the host to the bacteria.

Figure 4.7

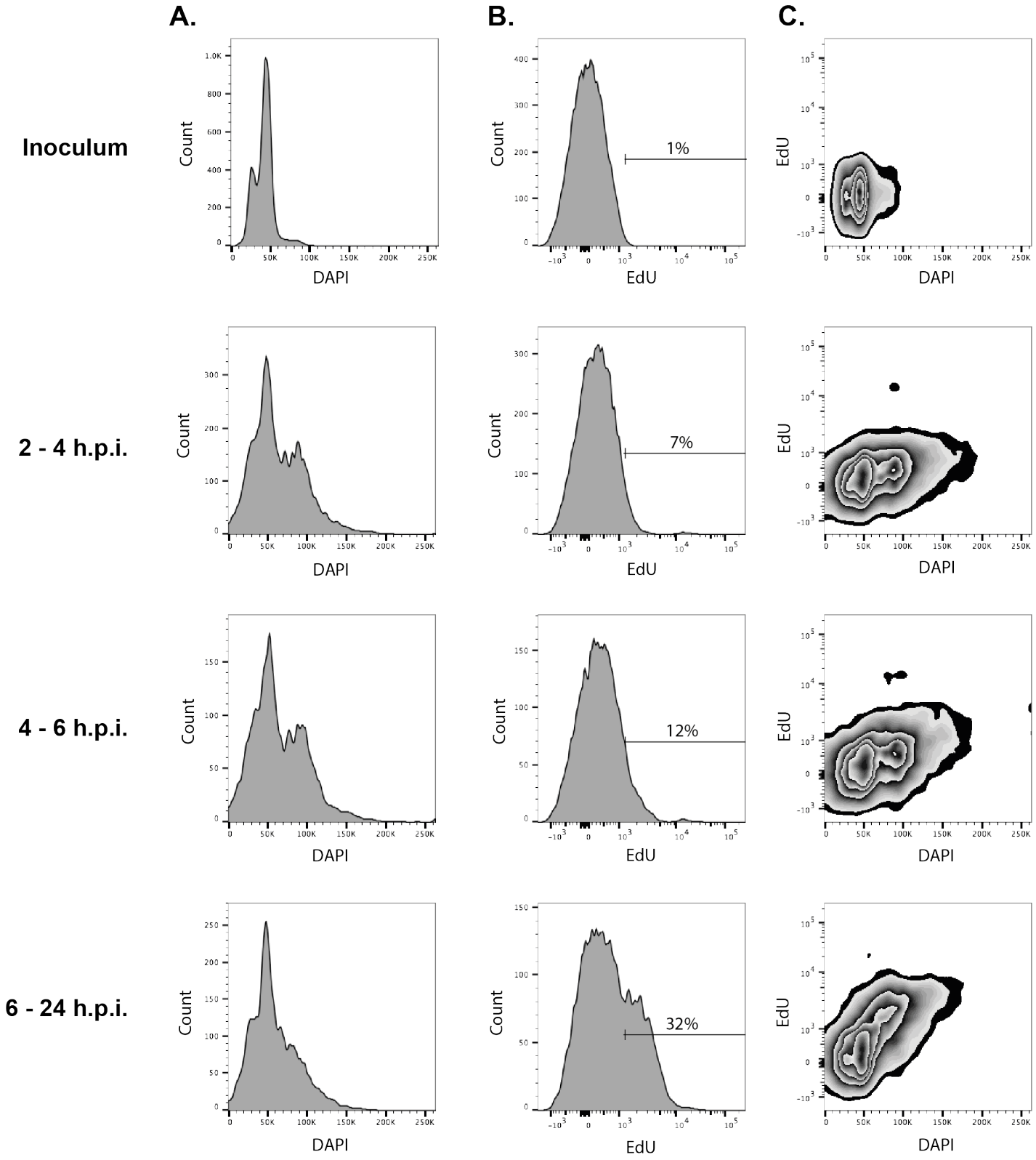


Figure 4.7: EdU incorporation into DNA of NG *Salmonella* during infection. Univariate histograms of DNA content (A) and EdU incorporation (B) and bivariate histograms of both together (C) shown for the inoculum and *Salmonella* extracted 24 h.p.i., exposed to EdU from 2 - 4 h.p.i., 4 - 6 h.p.i., and between 6 – 24 h.p.i. Infection was carried out in the presence of cefotaxime. Percentage increases in fluorescence normalised to a non-EdU treated control are shown (B).

4.5 Nongrowing *Salmonella* that undergo DNA synthesis during macrophage infection are metabolically active

Our lab previously showed that NG *Salmonella* are a heterogeneous population made up of metabolically active bacteria, able to respond to the presence of an inducer, and unresponsive bacteria (Helaine et al. 2014). To test the hypothesis that NG *Salmonella* are able to respond to the addition of an arabinose-inducer to produce DsRed, BMMs were infected with wild-type *Salmonella* carrying pDiGi (expressing GFP under the control of an IPTG-inducible promoter and DsRed under the control of an arabinose-inducer). 4 h before bacteria were extracted from the BMMs, arabinose was added to the infection medium, to allow time for the inducer to enter the host cell, be taken up into bacterial cells, induce expression of the fluorescent protein and allow time for the protein to fold correctly (Figure 4.8). The production of DsRed can be used as an indicator of metabolic activity.

Figure 4.8

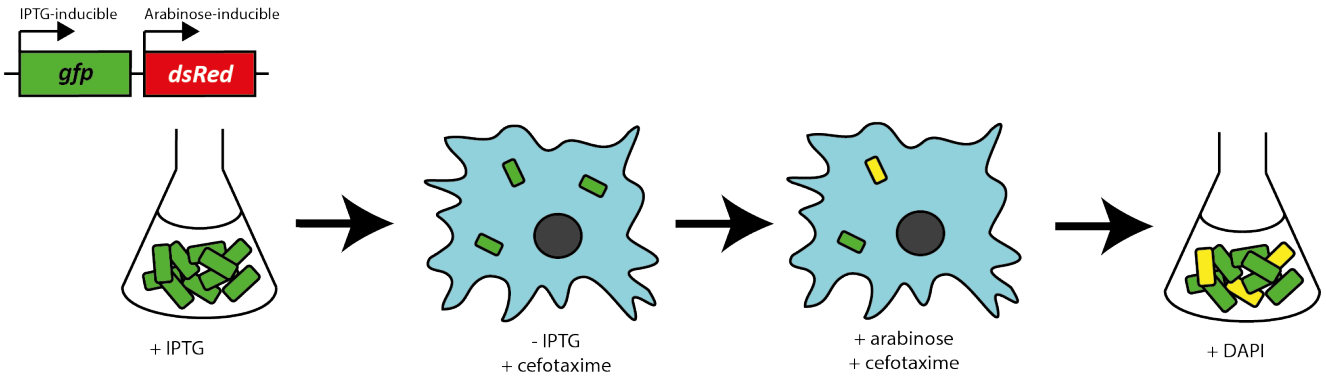


Figure 4.8: Experimental design for measuring metabolic responsiveness and DNA content of nongrowing *Salmonella* during macrophage infection. Wild-type *Salmonella* carrying the pDiGi fluorescence dilution plasmid expressing GFP under the control of an IPTG-inducible promoter and DsRed under the control of an arabinose-inducible P_{BAD} promoter was grown overnight in MgMES pH5 minimal medium to stationary phase in the presence of IPTG. During infection of macrophages in the absence of IPTG and in the presence of cefotaxime, any dividing bacteria should be killed by the antibiotic but will dilute their GFP fluorescence allowing the differentiation between growing and nongrowing bacteria if this does not occur. 4 h before the bacteria are extracted, arabinose is added to the medium to induce DsRed expression to be used as a read-out of metabolic responsiveness. Samples are taken at various time points during infection by lysing the macrophages and collecting the *Salmonella* cells for DAPI-staining and flow cytometry.

GFP expression was induced with IPTG prior to but not during the infection, in order to monitor fluorescence dilution. Bacteria were extracted from the macrophages at 8 h.p.i., 28 h.p.i. and 52 h.p.i. for flow cytometry (Figure 4.9). The reduction in GFP fluorescence throughout the infection is negligible (Figure 4.9A), the little that is observed likely represents dead cells resultant from aberrant division owing to the presence of cefotaxime. These low-GFP bacteria also did not respond to the arabinose inducer and produce DsRed as live, growing *Salmonella* was observed to (Figure 6.5B). The heterogeneity previously reported in the ability to respond to an inducer (Helaine et al. 2014) within the intracellular NG *Salmonella* population was confirmed as many NG *Salmonella* produced DsRed upon arabinose-induction while many did not (Figure 4.9A). 55% of NG *Salmonella* responded to arabinose induction by 28 h.p.i. and 62% were responsive by 52 h.p.i., the high proportion (74%) of metabolically responsive bacteria observed at 8 h.p.i. is likely owing to the presence of growing bacteria that were yet to divide, which were then subsequently killed by the cefotaxime upon division (figure 4.9B). DAPI levels increase and are stable by 24 h.p.i. as was observed previously (Figure 4.9C), the NG *Salmonella* that increased their cellular DNA content chiefly belonged to the metabolically responsive population (Figure 4.9D-E).

Figure 4.9

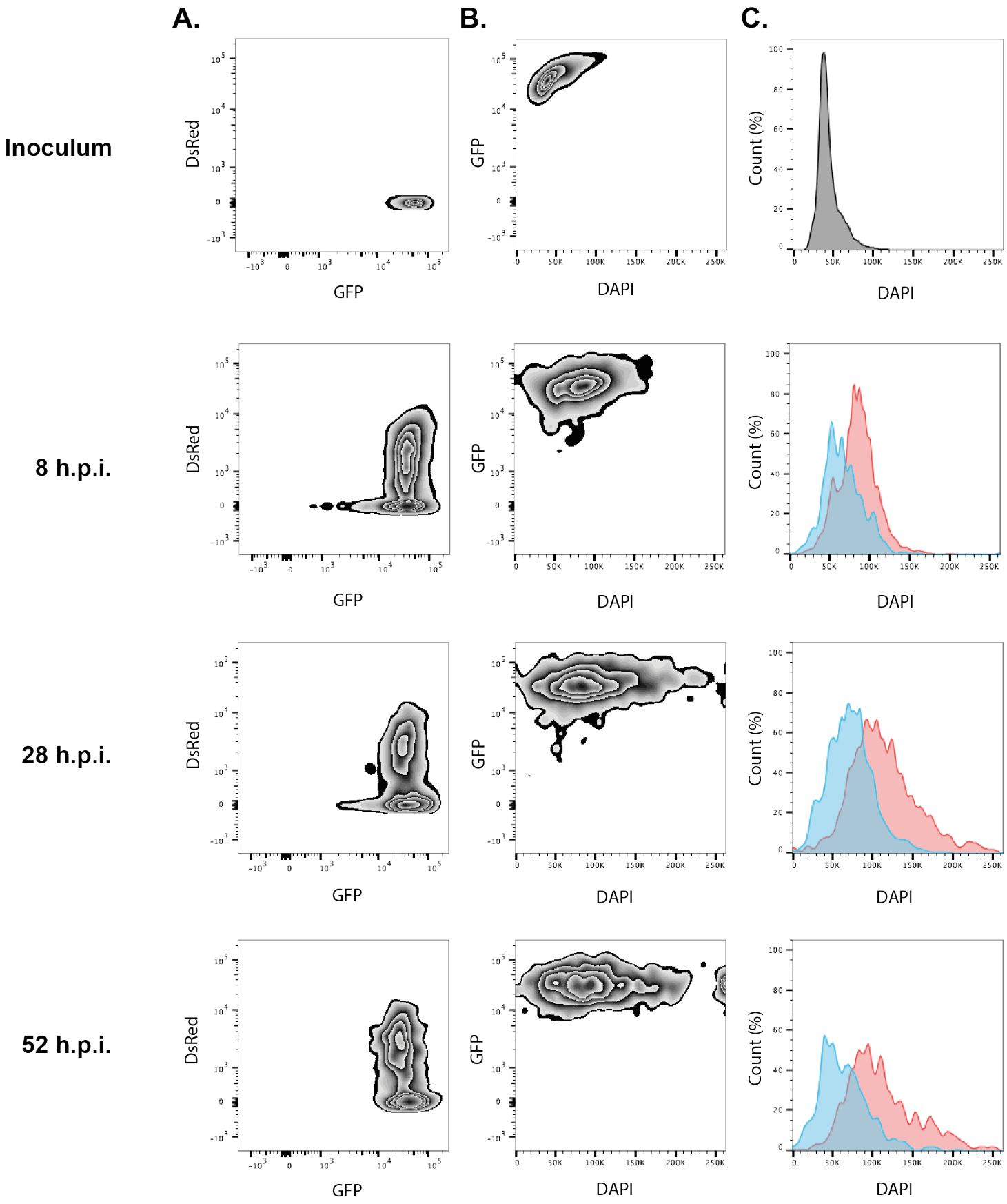


Figure 4.9

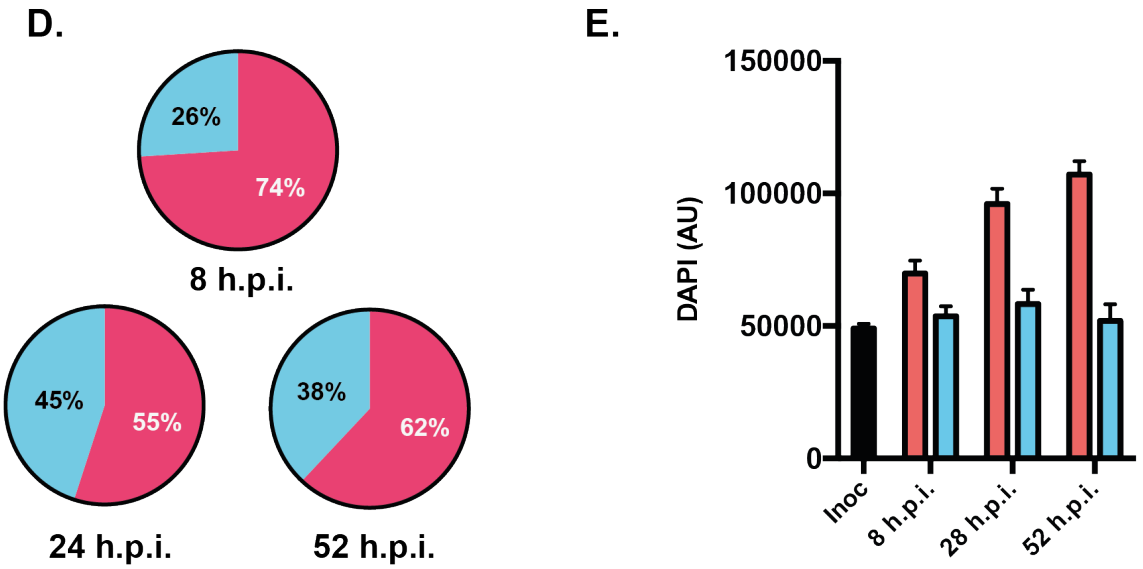


Figure 4.9: Metabolic response and DNA content of nongrowing *Salmonella* during BMM infection. Fluorescence dilution profiles and metabolic response of *Salmonella* measured by flow cytometry are shown for the inoculum, 8 h.p.i., 28 h.p.i. and 52 h.p.i. as bivariate histograms of GFP and DsRed fluorescence (A) with the proportions of metabolically active and metabolic unresponsive *Salmonella* displayed in pie charts (B). Bacterial growth is shown in combination with DNA content as bivariate histograms of DsRed and DAPI fluorescence (C) DNA content alone is shown as DAPI histograms (D) of metabolically active (red) and unresponsive bacteria (blue). Arithmetic mean DAPI fluorescence values of the total bacterial population (black), metabolically active (red) and unresponsive bacteria (blue) are shown as mean ± SEM (n=3) (E).

4.6 Recovery of nongrowing *Salmonella*

Persisters are antibiotic-tolerant NG bacteria that are able to regrow after the resolution of some internal block to the division, or the removal of a limiting environmental condition. I wanted to test whether *Salmonella* persisters from macrophages are more likely to belong to the population of high DNA NG bacteria than those with low DNA. NG *Salmonella* were extracted from macrophages incubated in with cefotaxime over a period of 24 h. The NG *Salmonella* were then resuspended in LB with no antibiotic present and placed in a shaking incubator taking samples for flow cytometry after 1 and 2 h. As previously observed the DNA content of the NG population increased from that of the inoculum (Figure 4.10A) up to 28 h.p.i. (Figure 4.10B). At 1h after recovery in LB there was little FD of GFP observed, however the DNA content appears to have increased further (Figure 4.10C). This is then followed by proliferation by 2h in LB, as observed by the reduction in GFP and DNA (Figure 4.10D). These newly divided cells appear to have originated from the high DNA nongrowing population (with a small amount of division appearing to originate from the low DNA population). This suggests that the persisters may be more likely to emerge from the high DNA, metabolically active population. However it is difficult to prove the origin of these new populations of bacteria, and the experiment is further limited by the inability to follow the progress of the NG regrowth past 2 h in LB as the culture is quickly overrun by early-regrowing bacteria. Cell sorting can overcome the former problem, and ScanLag, an experiment based on timelapse images of colony formation on agar plates may solve the latter (see chapter 6).

Figure 4.10

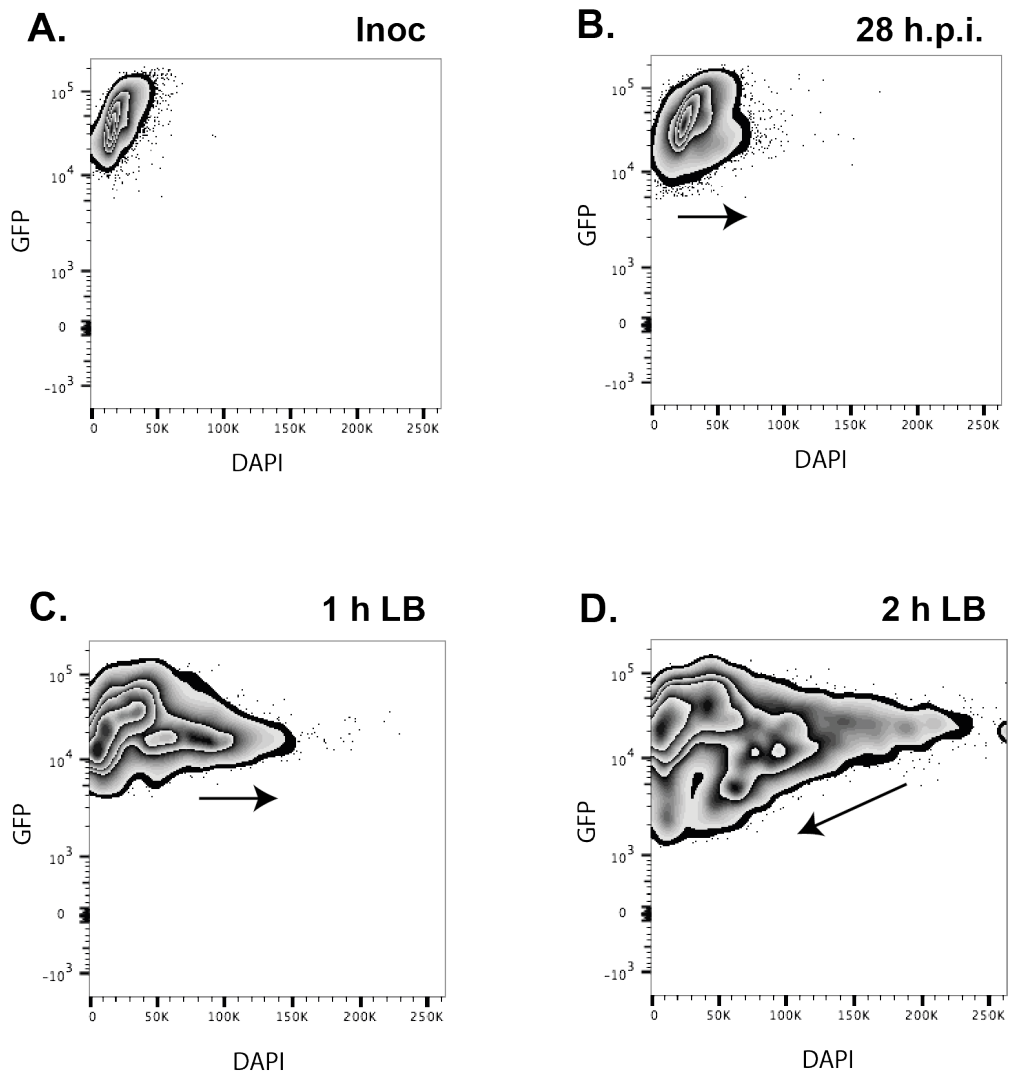


Figure 4.8: Recovery of NG *Salmonella* post-infection in LB broth. GFP and DAPI fluorescence bivariate histograms displayed for the inoculum (A), 28 h.p.i. (B), 1h after recovery in LB broth (C) and 2 h after recovery in LB broth (D). Arrows indicated likely direction changes in the fluorescence levels of the bacterial population. Plots representative of three independent experiments.

4.9 Conclusion

The work described here presents evidence for active DNA replication in NG *Salmonella* during infection of macrophages. This DNA synthesis appears to halt by 24 h.p.i., likely not running to completion as integer numbers of chromosomes are often not easily distinguished by DAPI-staining. It could be that this replication arrest is occurring due to starvation. The population of high DNA nongrowing *Salmonella* primarily overlaps with the previously described metabolically responsive population present (Helaine *et al.,* 2014). The persisters present during infection (defined as the NG *Salmonella* able to survive antibiotic treatment and regrow at a later time) may chiefly originate from the high DNA and metabolically responsive population as observed by flow cytometry. However to prove that persisters are originating from one subpopulation over another will require cell sorting and ScanLag may also provide a method of observing the recovery of NG *Salmonella* over a longer period of time than just 2 hours in LB (see chapter 6).

Chapter Five

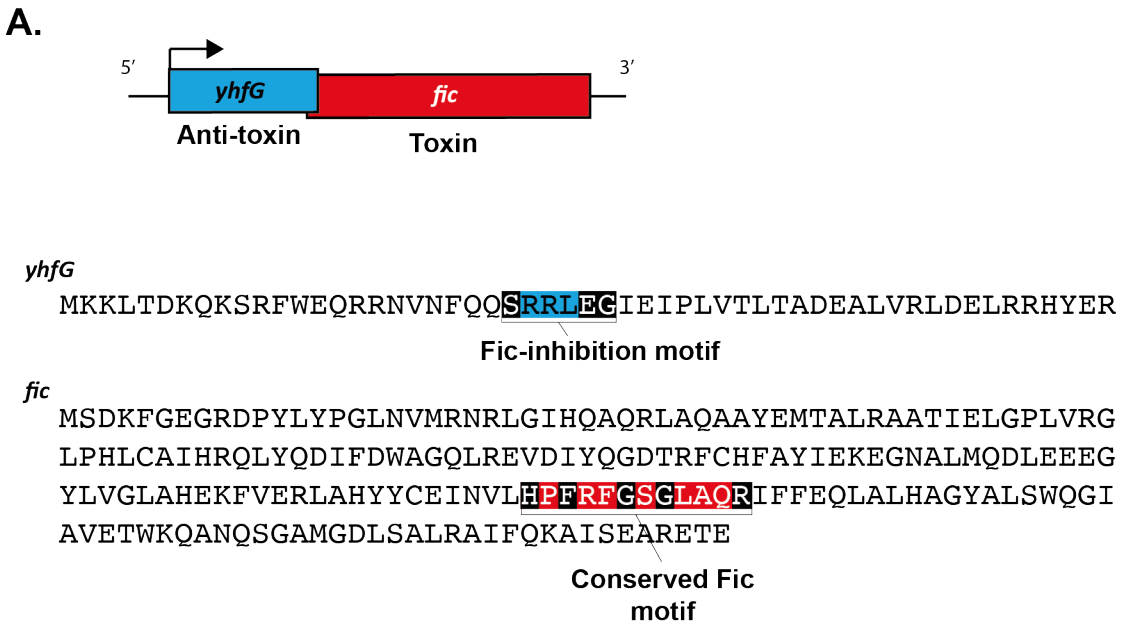
Characterising the *yhfG-fic* toxin-antitoxin module

5.1 Introduction

Toxin-antitoxin (TA) modules have been linked to persister formation by several studies (Keren, Shah, et al. 2004; Shah et al. 2006; Maisonneuve et al. 2013; Germain et al. 2015). Different toxins from TA modules have wide-ranging activities, targeting diverse sections of bacterial metabolism (Page & Peti 2016). A relatively small group of TA modules reversibly inhibit DNA metabolism. Currently three TA modules are known to target enzymes involved in the supercoiling of DNA, as well as deconcatenation of bacterial chromosomes; the ParDE, CcdAB and FicAT modules (Page & Peti 2016; Harms et al. 2015). The ParE toxin encoded on the RK2 plasmid and the F-plasmid toxin CcdB in *E. coli* both inhibit DNA gyrase to induce cell death after loss of the plasmid, what is known as post-segregational killing (PSK) (Jiang et al. 2002; Bernard et al. 1993). Three ParE toxins were also found to be involved in PSK in *Vibrio cholerae,* inhibiting DNA gyrase, leading to cell death upon loss of chromosome II after division (Yuan et al. 2011). A recent study described how FicT toxins from *Bartonella*, *Yersinia* and *Pseudomonas* inhibited the B subunits of DNA gyrase and TopoIV to reversibly inhibit negative supercoiling and deconcatenation of chromosomes following replication. The filamentation induced by cAMP (FIC) domain that gives Fic toxins their name is ubiquitous, found throughout all three domains of life. It is mostly involved in forms of NMPylation, commonly AMPylation, although other activities have been found in more diverse forms of the FIC domain. The toxin

Doc, for example, has a noncanonical FIC domain that catalyses phosphorylation, rather than NMPylation. The most commonly found FIC domain proteins are the FicT toxins of bacteria. Interestingly, the FicT toxins of the Enterobacteriaceae have a conserved but noncanonical (when compared to that of other bacteria) FIC domain (Figure 5.1A), which has been predicted to be unable to catalyse NMPylation (Harms, Stanger, et al. 2016). These include FicT toxins found in *E. coli* and *Salmonella* belonging to the TA modules named *yhfG-fic* (Harms et al. 2015; Harms, Stanger, et al. 2016). *Salmonella* has the TA module homologues *parDE* and *yhfG-fic* encoded on the chromosome (Figure 5.1). My lab has previously reported that a deletion mutant *parDE* of *Salmonella* yielded lower levels of persisters after transient infection of macrophages, indicating thus a role of ParDE in host-induced persister formation. The role of the *yhfG-fic* module had not been tested. A *ccdAB* homologue is present on the pSLT virulence plasmid, however it was found to be nontoxic due to a mutation (Lobato-Márquez et al. 2015).

Figure 5.1



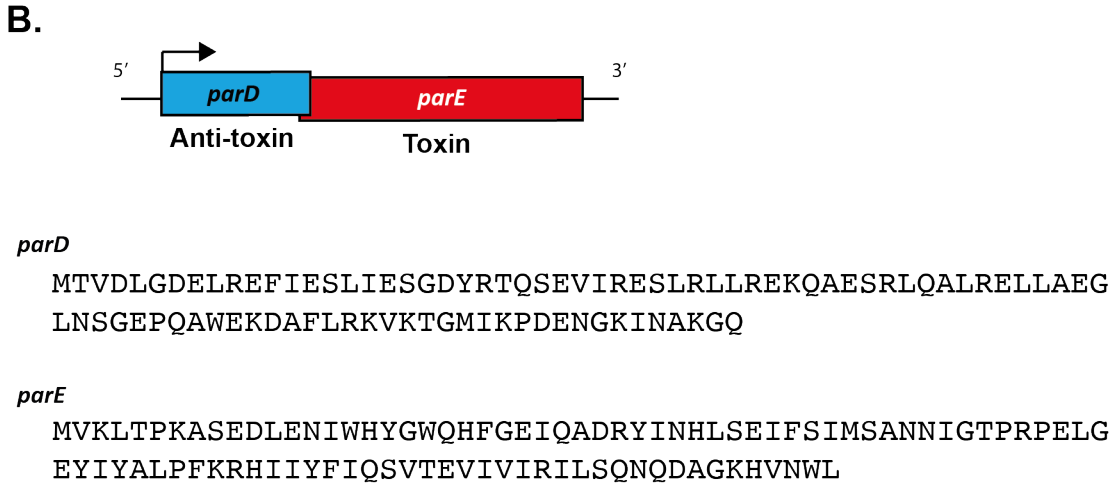


Figure 5.1: Genomic arrangement of *parDE* and *yhfG-fic* operons and amino acid sequences of toxin and antitoxin proteins. Diagram representing the orientation and the amino acid sequences of the putative antitoxin *yhfG* and putative toxin *fic* (A) and putative antitoxin *parD* and putative toxin *parE* (B). Predicted Fic-inhibition motif in the YhfG sequence and core Fic motif in the Fic sequence are annotated (A).

5.2 Deletion of both *parDE* and *yhfG-fic* in *Salmonella* leads to a growth defect in RAW 267.4 macrophages

The single TA module deletion mutant Δ*yhfG-fic* was constructed using λred mutagenesis in *S.* Typhiumrium 12023 along with a double-deletion mutant, Δ*parDE*Δ*yhfG-fic*. These mutants were used alongside the wild-type and the single ΔTA mutant Δ*parDE* (Helaine et al. 2014) to infect RAW 264.7 macrophages (RAWs), and CFU measurements were made at 2, 8 and 24 h.p.i. during infection. The CFU values at 8 and 24 h.p.i. were normalised to those at 2 h.p.i. (Figure 5.2A) to assess the difference in survival after 2 h of infection. By 8 h.p.i., there was no clear difference in CFUs between the wild-type, Δ*parDE* Δ*yhfG-fic* and Δ*parDE*Δ*yhfG-fic* strains. However by 24 h.p.i., there was a significant difference in the CFUs of the Δ*parDE*Δ*yhfG-fic* strain when compared to the wild-type and each of the single ΔTA mutants. This experiment was repeated in primary BMMs to test if there was still a difference in CFU in an environment more restrictive to *Salmonella* growth. As the BMMs survive for longer than RAWs during infection, an extra time point of 48 h.p.i. was used to take samples for CFU measurement (Figure 5.2B). There was no significant difference between the strains in this experiment based on CFU measurements. It may be that due to the more restrictive environment of BMMs compared to RAWs, the growth defect in the Δ*parDE*Δ*yhfG-fic* strain during infection was obscured, as all strains grow slowly, not just the double ΔTA mutant. The deletion of multiple TA modules impacting growth in macrophages was intriguing, so it was decided to attempt to characterise the effect of these TA modules on *Salmonella* growth.

Figure 5.2

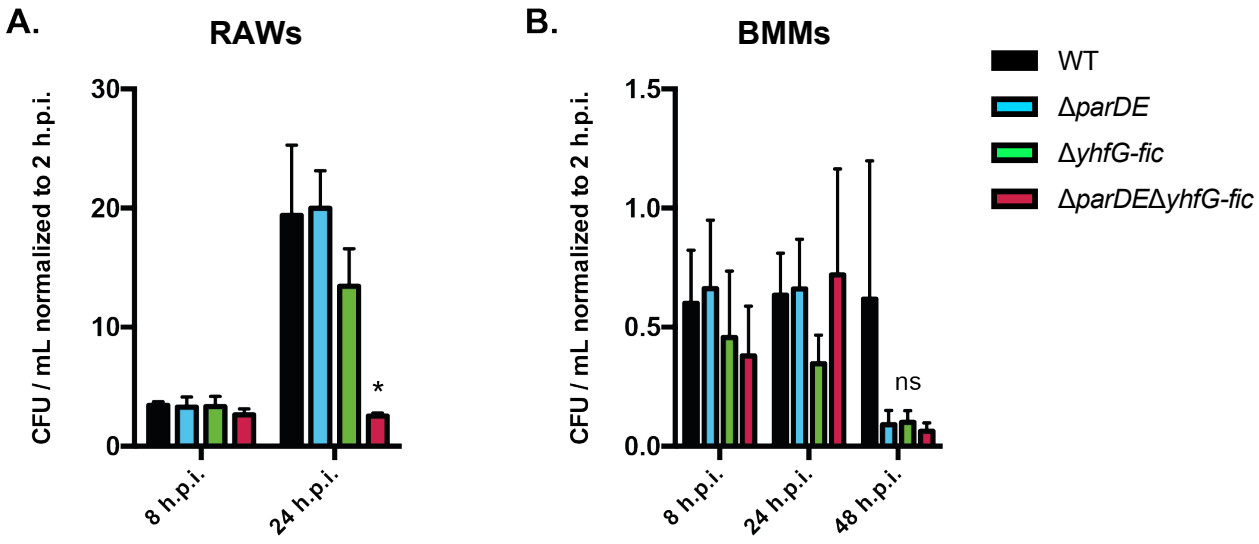


Figure 5.2: *S.* Typhimurium Δ*parDE*Δ*yhfG-fic* has a growth defect during infection of RAW 267.4 macrophages but not during infection of BMMs. Bar chart displaying CFUs at 8 and 24 h.p.i. during infection of RAWs (A) and at 8, 24 and 48 h.p.i. during infection of BMMs (B) normalised to CFUs at 2 h.p.i. of wild-type (black), Δ*parDE* (blue), Δ*yhfG-fic* (green), Δ*parDE*Δ*yhfG-fic* (red). Error bars are mean ±S.E.M (n=3), p-values indicated as *<0.05, **<0.01, ***<0.001, ****<0.0001 and ns for >0.05.

5.3.1 Overexpression of *fic* inhibits growth in *E. coli* DH5α but not in *S.* Typhimurium

The *fic* toxin gene was inserted onto a pBAD33 plasmid enabling the expression of the toxin under the control of an arabinose inducer (Figure 5.3). *E. coli* DH5α carrying either an empty pBAD33 vector or pBAD33-*fic* were grown to exponential or stationary phase, and then added to fresh media with arabinose. As the *yhfG-fic* TA module is absent from this strain of *E. coli*, there was no concern of interference from any native toxin. Inhibition of growth was observed in both phases of growth when overexpressing *fic* in *E. coli* DH5α (Figure 5.4).

Figure 5.3

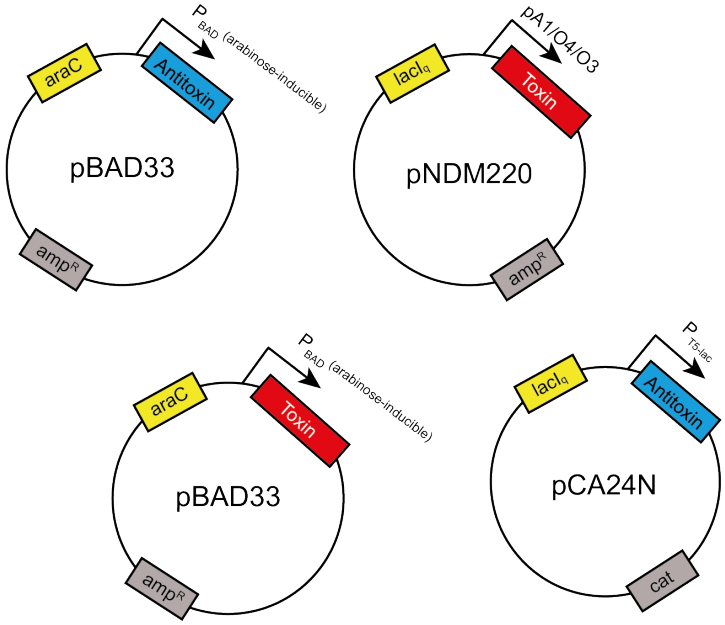


Figure 5.3: Maps of toxin and antitoxin overexpression plasmids. Representative plasmid maps of pBAD33 harbouring toxin or antitoxin genes, pNDM220 harbouring toxin genes and pCA24N harbouring antitoxin genes used for the overexpression of putative toxins *parE* and *fic* and the putative antitoxins *parD and yhfG.*

Figure 5.4

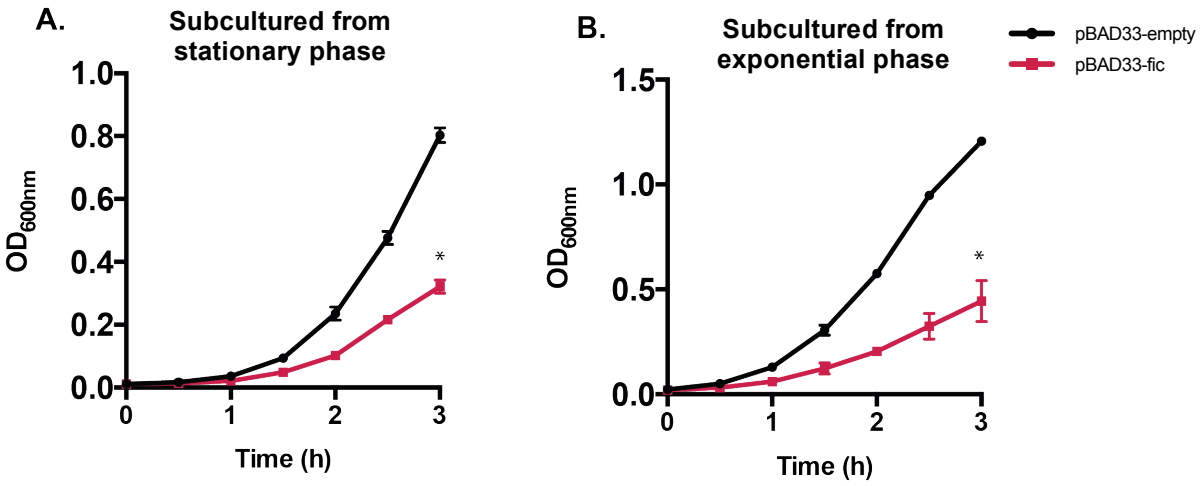


Figure 5.3.2: Overexpression of *fic* inhibits growth in *E. coli* DH5α. *E. coli* DH5α carrying either an empty pBAD33 vector or pBAD33 harbouring the *fic* gene were either grown to stationary phase (A) and subcultured to an OD_{600nm} of 0.2 or grown to exponential phase (B) and subcultured to an OD_{600nm} of 0.1 in fresh LB medium + arabinose (0.2%) to induce toxin expression. OD_{600nm} readings were taken every 30 min, starting from 0 h. Data represent mean ±S.E.M (n=3), p-values indicated as *<0.05.

To test whether Fic was also toxic in *Salmonella*, pBAD33-*fic* was transformed into *S.* Typhimurium ∆*yhfG-fic* to allow overexpression of the toxin without the interference of the native toxin or antitoxin. Growth of *Salmonella* overexpressing *fic* and *Salmonella* harbouring an empty vector were monitored in LB and MgMES pH5 (Figure 5.5A-B). In contrast to in *E. coli* DH5α, no difference was observed in growth when overexpressing the toxin in these conditions. As it has previously been reported that expression of *yhfG-fic* is highly upregulated when magnesium (Mg^{2+}) levels are low (Kröger et al. 2013), I hypothesised that the toxin may only affect growth in these conditions in *Salmonella*, say if the target is only affected by the toxin under this limitation. Low Mg^{2+} MgMES pH5 will expose the *Salmonella* to similar conditions experienced inside the macrophage during infection. Growth while overexpressing *fic* in low Mg^{2+} conditions did not affect growth however (figure 5.5C). Starving the bacteria of Mg^{2+} overnight before conducting the growth curve in LB or MgMES pH5 also did not increase toxicity of Fic (figure 5.5D-E), effectively disproving this hypothesis.

Figure 5.5

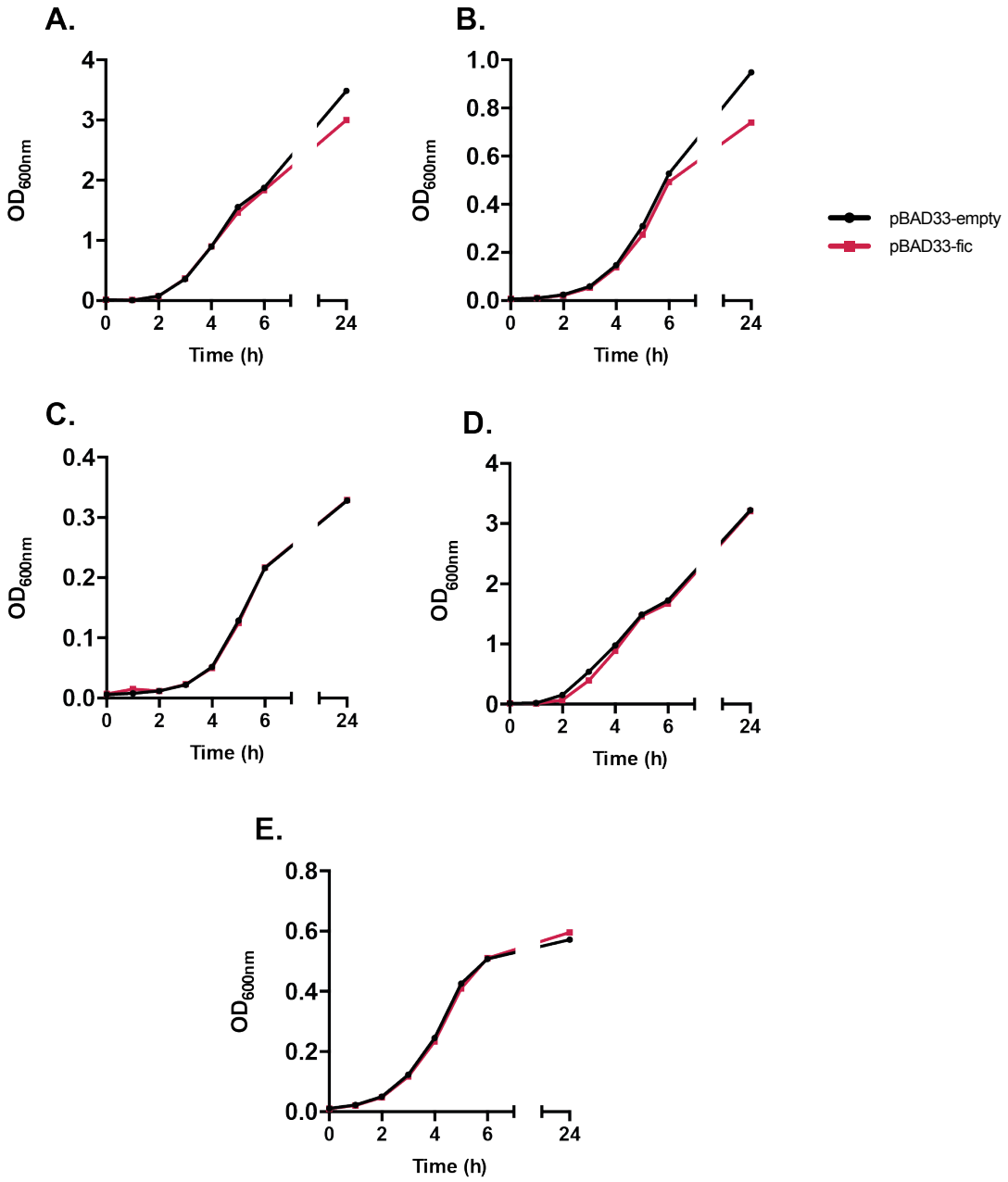


Figure 5.5: Fic is not toxic in *S.* Typhimurium Δ*yhfG-fic*. *S.* Typhimurium Δ*yhfG-fic* carrying either an empty pBAD33 vector or pBAD33 harbouring the *fic* gene were grown to stationary phase in LB and subcultured to an OD_{600nm} of 0.1 in fresh LB (A), MgMES pH5 (B) or MgMES pH5 [low Mg^{2+}] (C) medium with arabinose to induce toxin expression. Strains were also grown overnight in MgMES pH5 [low Mg^{2+}] before being subcultured as above in LB (D) or MgMES pH5 [low Mg^{2+}] (E) medium. F) Overexpression of *fic* in *S.* Typhimurium Δ*parDE*Δ*yhfG-fic* background. OD_{600nm} readings were taken every 30 min, starting from 0 h. Data represent mean ±S.E.M (n=3).

As there is a growth defect in the Δ*parDE*Δ*yhfG-fic* mutant but not in single ΔTA mutants of each individual module during infection, *fic* was overexpressed in this double ΔTA genetic background, in case the presence of the *parDE* TA module was interfering with the toxicity of the Fic toxin. However, there was no impact of Fic on *Salmonella* growth in this background (Figures 5.5F). From these experiments I conclude that the activity of Fic may not be that of a standard type II toxin in that overexpressing the protein does not inhibit growth or that detoxifying factors might be at play in *Salmonella*.

Figure 5.6

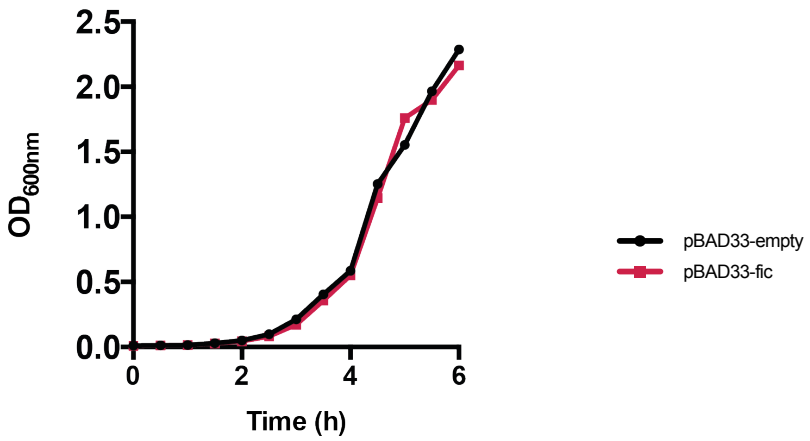


Figure 5.6: Fic is not toxic in *S.* Typhimurium Δ*parDE*Δ*yhfG-fic*. *S.* Typhimurium Δ*parDE*Δ*yhfG-fic* carrying either an empty pBAD33 vector or pBAD33 harbouring the *fic* gene were grown to stationary phase in LB and subcultured to an OD_{600nm} of 0.1 in fresh LB medium with arabinose to induce toxin expression. OD_{600nm} readings were taken every 30 min, starting from 0 h. Data represent mean ±S.E.M (n=3).

5.3.2 Toxicity of Fic and YhfG observed in *E. coli* is likely a non-specific effect of overexpression

In order to test whether the effect of Fic on the growth of *E. coli* DH5α could be counteracted by its predicted cognate antitoxin YhfG, *fic w*as overexpressed from the IPTG-inducible expression vector pNDM220 and *yhfG* was overexpressed from pCA24N in *E. coli* DH5α (Figure 5.7). The vector pNDM220 has a lower copy number than pCA24N, meaning the antitoxin should be produced to a greater extent than the toxin allowing a greater probability of successful toxin counteraction. Fic toxicity was not observed when expressed from pNDM220 in *E. coli* DH5α however, suggesting that the toxicity observed when expressed from pBAD33 was not due to the activity of the toxin but non-specific effects of Fic overproduction. Interestingly, overexpression of *yhfG* was toxic to the growth of *E. coli* DH5α. Overexpression of *fic* did inhibit the growth when expressed from pNDM220 in *E. coli* K-12 MG1655 (Figure 5.8). However, this toxicity was not counteracted by *yhfG* expression. No toxicity was observed in *Salmonella* when expressing *fic* from the pNDM220 vector (Figure 5.9). These results suggest that the toxicity of Fic observed when in *E. coli* is non-specific, further giving evidence to the hypothesis that Fic is not a standard toxin in that it does not have a specific mechanism to inhibit growth, at least not in any of the conditions tested.

Figure 5.7

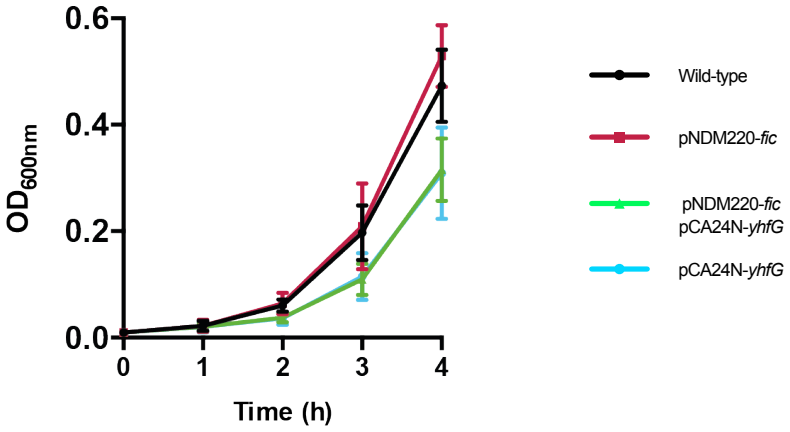


Figure 5.7: Fic is not toxic in *E. coli* DH5α when expressed from pNDM220. *E. coli* DH5α with no plasmid (black), with pNDM220 harbouring the *fic* gene (red), with pCA24N harbouring the *yhfG* (blue) and with both pNDM220 harbouring the *fic* gene and pCA24N harbouring the *yhfG* (green) were grown to stationary phase in LB and subcultured to an OD_{600nm} of 0.1 in fresh LB with arabinose and IPTG to induce expression of the toxin and antitoxin genes. OD_{600nm} readings were taken every hour, starting from 0 h. Data represent mean ±S.E.M (n=3).

Figure 5.8

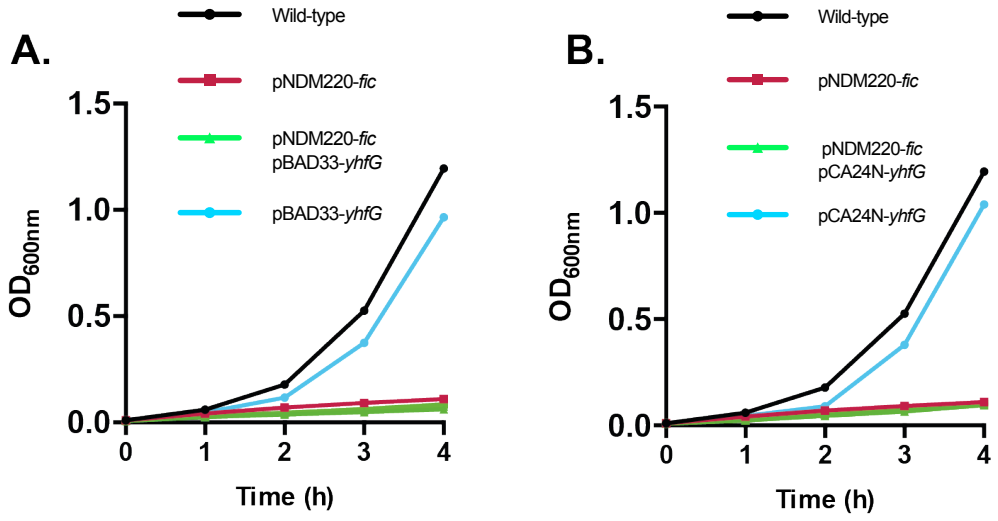


Figure 5.8: Fic is toxic in *E. coli* K-12 MG1655 when expressed from pNDM220. *E. coli* K-12 MG1655 with no plasmid (black), with pNDM220 harbouring the *fic* gene (red), with pBAD33 (A) or pCA24N (B) harbouring the *yhfG* (blue) and with both pNDM220 harbouring the *fic* gene and pBAD33 (A) or pCA24N (B) harbouring the *yhfG* (green) were grown to stationary phase in LB and subcultured to an OD_{600nm} of 0.1 in fresh LB with arabinose and IPTG to induce expression of the toxin and antitoxin genes. OD_{600nm} readings were taken every hour, starting from 0 h. Data represent mean ±S.E.M (n=1).

Figure 5.9

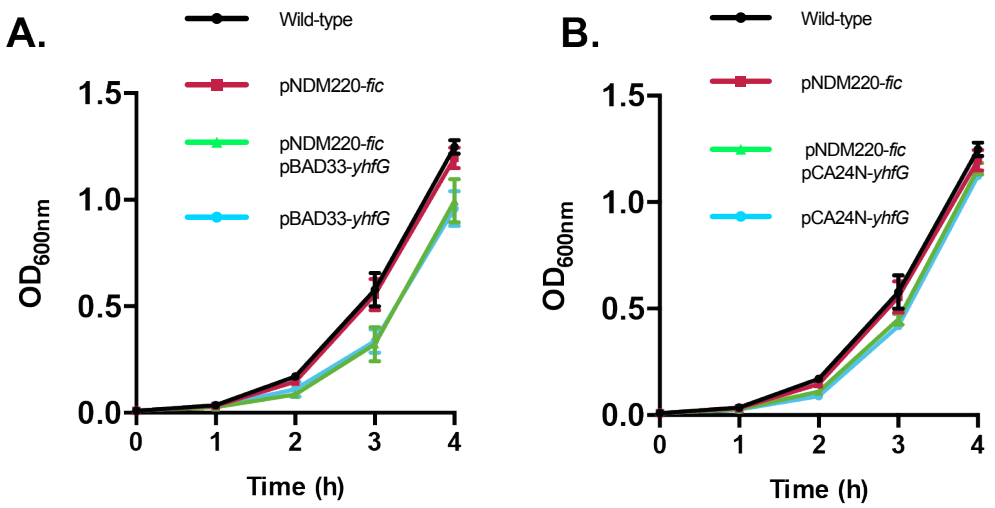


Figure 5.9: Fic is not toxic in *S.* Typhimurium when expressed from pNDM220. *S.* Typhimurium Δ*yhfG-fic* with no plasmid (black), with pNDM220 harbouring the *fic* gene (red), with pBAD33 (A) or pCA24N (B) harbouring the *yhfG* (blue) and with both pNDM220 harbouring the *fic* gene and pBAD33 (A) or pCA24N (B) harbouring the *yhfG* (green) were grown to stationary phase in LB and subcultured to an OD_{600nm} of 0.1 in fresh LB with arabinose and IPTG to induce expression of the toxin and antitoxin genes. OD_{600nm} readings were taken every hour, starting from 0 h. Data represent mean ±S.E.M (n=3).no plasmid (black), with pNDM220 harbouring the *fic* gene (red), with pCA24N harbouring the *yhfG* (blue) and with both pNDM220 harbouring the *fic* gene and pCA24N harbouring the *yhfG* (green) were grown to stationary phase in LB and subcultured to an OD_{600nm} of 0.1 in fresh LB with arabinose and IPTG to induce expression of the toxin and antitoxin genes. OD_{600nm} readings were taken every hour, starting from 0 h. Data represent mean ±S.E.M (n=3).

5.4.1 *S.* Typhimurium Δ*parDE*Δ*yhfG-fic* has a growth defect in minimal medium

As little information was gained from attempting to characterise the *yhfG-fic* and *parDE* TA modules using plasmid expression, it was decided to further attempt to characterise the phenotype of the Δ*parDE*Δ*yhfG-fic* strain instead. No difference was found in the growth of wild-type *Salmonella*, the single TA mutants Δ*parDE* and Δ*yhfG-fic* and the double TA mutant Δ*parDE*Δ*yhfG-fic* in LB medium when monitored by OD_{600nm} and CFU measurements (Figures 5.10A-B). In contrast, when grown in MgMES pH5 medium, a significant growth defect was observed by OD_{600nm} measurements in the Δ*parDE*Δ*yhfG-fic* strain when compared to the wild-type or the single ΔTA mutants. However, this growth defect was not observed by CFU measurements (Figure 5.10D). No obvious difference in cell size was observable by light microscopy that could account for this difference however (data not shown). To test whether the low pH was responsible for the growth defect in the Δ*parDE*Δ*yhfG-fic* strain, all strains were grown in MgMES pH7 medium (Figures 5.10E,F). Again, Δ*parDE*Δ*yhfG-fic* displayed a defect in growth, although it was not a significant difference. This trend suggests that the low pH accentuates the growth defect in Δ*parDE*Δ*yhfG-fic* but is likely not the root cause. I continued using MgMES pH5 as it produced the most difference in growth while also closely simulating the environment of the SCV during macrophage infection (low pH and low nutrient availability). Figure 5.11 shows the OD_{600nm} and CFU measurements of wild-type *Salmonella*, single ΔTA mutants of Δ*parDE* and Δ*yhfG-fic* as well as the double ΔTA mutant Δ*parDE*Δ*yhfG-fic* grown in MgMES pH5 over 12 h. A significantly lower OD

was observable for the Δ*parDE*Δ*yhfG-fic* between 6 and 8 h, OD of this strain caught up with the others when reaching stationary phase however. Once more the CFU measurements did not reveal a significant different however.

Figure 5.10

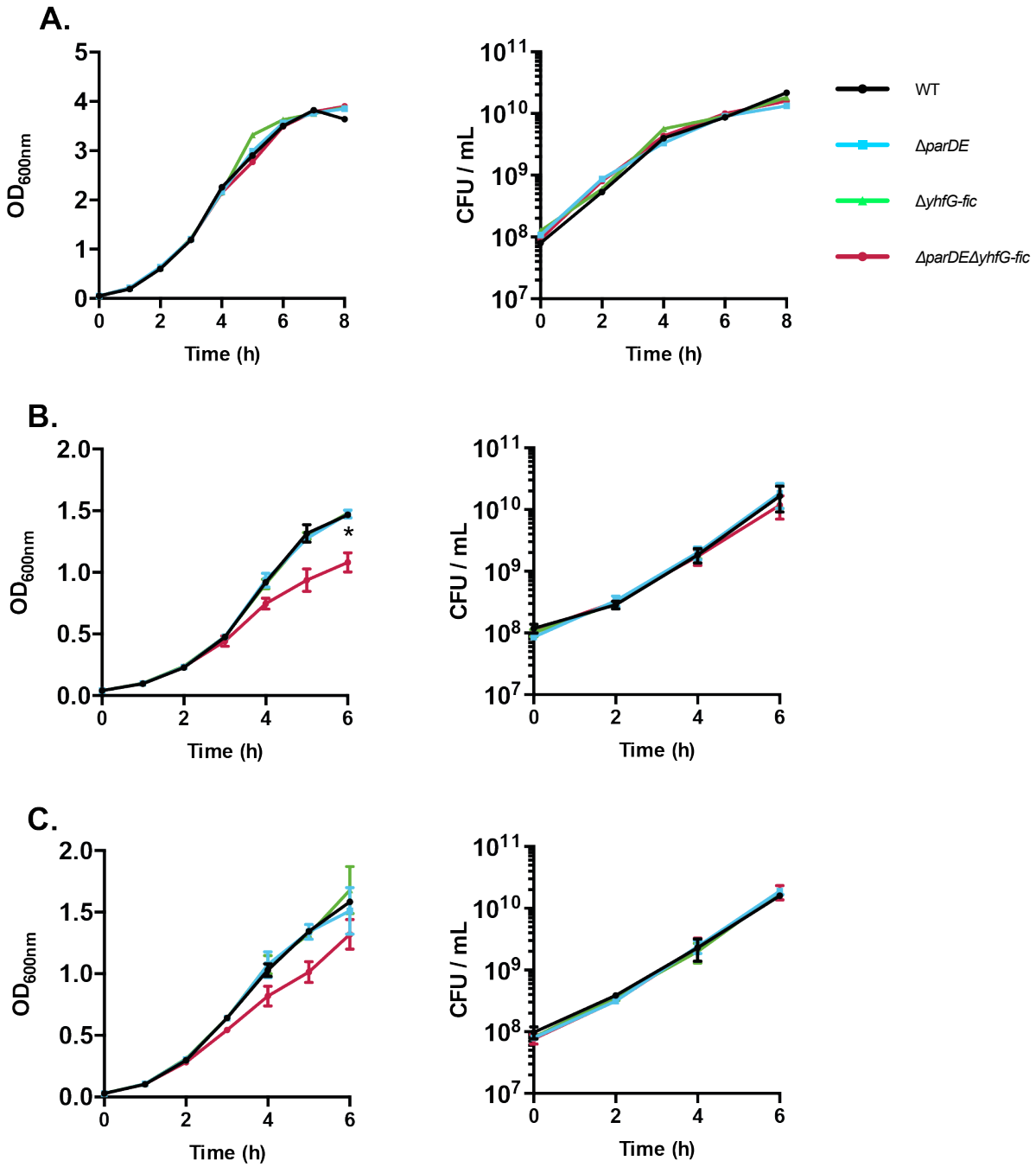


Figure 5.10: Deletion of *parDE* and *yhfG* leads to a growth defect in MgMES pH5 medium when monitored by OD_{600nm} but not by CFU. *S.* Typhimurium wild-type (black), Δ*parDE* (blue), Δ*yhfG-fic* (green), Δ*parDE*Δ*yhfG-fic* (red), were grown to stationary phase in LB and subcultured to an OD_{600nm} of 0.1 in fresh LB (A), MgMES pH5 (B) and MgMES pH7 (C). OD_{600nm} and CFU readings were taken every 30 min, starting from 0 h. Data represent mean ±S.E.M (n=3).

Figure 5.11

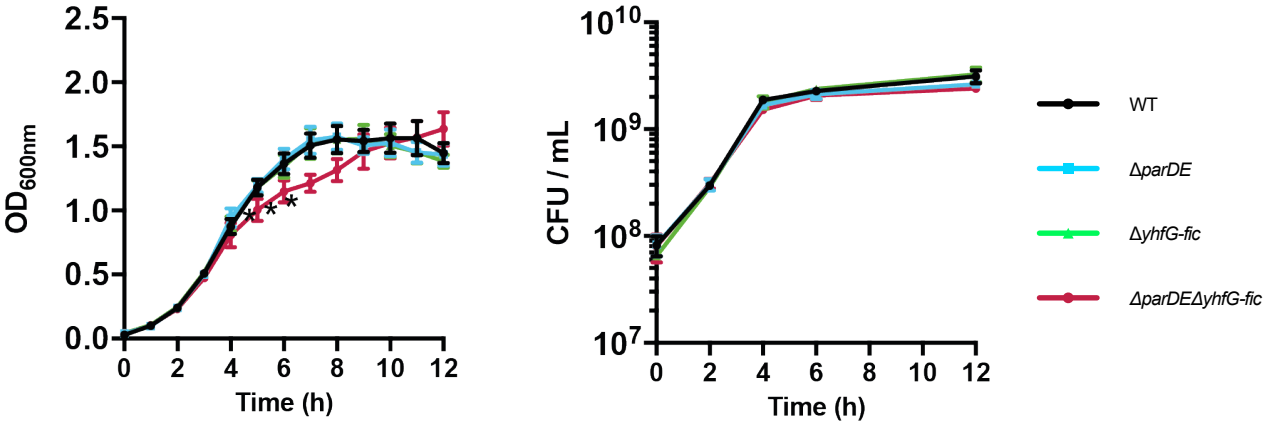


Figure 5.11: Growth of *S.* Typhimurium Δ*parDE*Δ*yhfG-fic* ultimately reaches same level as wild-type in stationary phase in MgMES pH5 medium. *S*. Typhimurium wild-type (black), Δ*parDE* (blue), Δ*yhfG-fic* (green), Δ*parDE*Δ*yhfG-fic* (red) were grown to stationary phase in LB and subcultured to an OD_{600nm} of 0.1 in fresh MgMES pH5. OD_{600nm} and CFU readings were taken every 30 min, starting from 0 h. Data represent mean ±S.E.M (n=3).

5.4.2 Deletion of both *parDE* and *yhfG-fic* leads to a greater variability in survival during long-term growth in nutrient limiting and acidic conditions

I hypothesised that the TA modules may be important for growth in stressful conditions, if this is the case, it follows that the phenotype belonging to these TA modules would be more easily detectable over a longer exposure to such conditions. To test whether the deletion of *parDE* and *yhfG-fic* affected long-term survival during *in vitro* culture, wild-type *S.* Typhimuirum 12023, Δ*parDE,* Δ*yhfG-fic* and Δ*parDE*Δ*yhfG-fic* were grown in LB and MgMES pH5 for 72 h, measuring the number of viable cells using CFU measurements (Figure 5.12). As the variability in the results gathered from these experiments proved to be high, each individual repeat is shown. There was no observable difference between the survival of any of the strains while cultured in LB for 72 h (Figures 5.12A,C,E). However, if either of the single ΔTA mutants were cultured for a long period of time in MgMES pH5 they generally did not survive to as high a number by 72 h (Figures 5.12B,D). Interestingly, the survival of the double ΔTA mutant Δ*parDE*Δ*yhfG-fic* was highly variable, with some repeats showing higher CFU values than the wild-type by 72 h and some showing lower CFU values by this time. As the TA modules have homologues to those known to affect DNA metabolism, this variability could be owing to an increased chance of mutation, with some allowing greater survival and some leading to decreased survival. Mutations that slowed growth for example may have had a beneficial effect on survival in the double ΔTA mutant when grown in starvation or acidic conditions when compared to the wild-type.

Figure 5.12

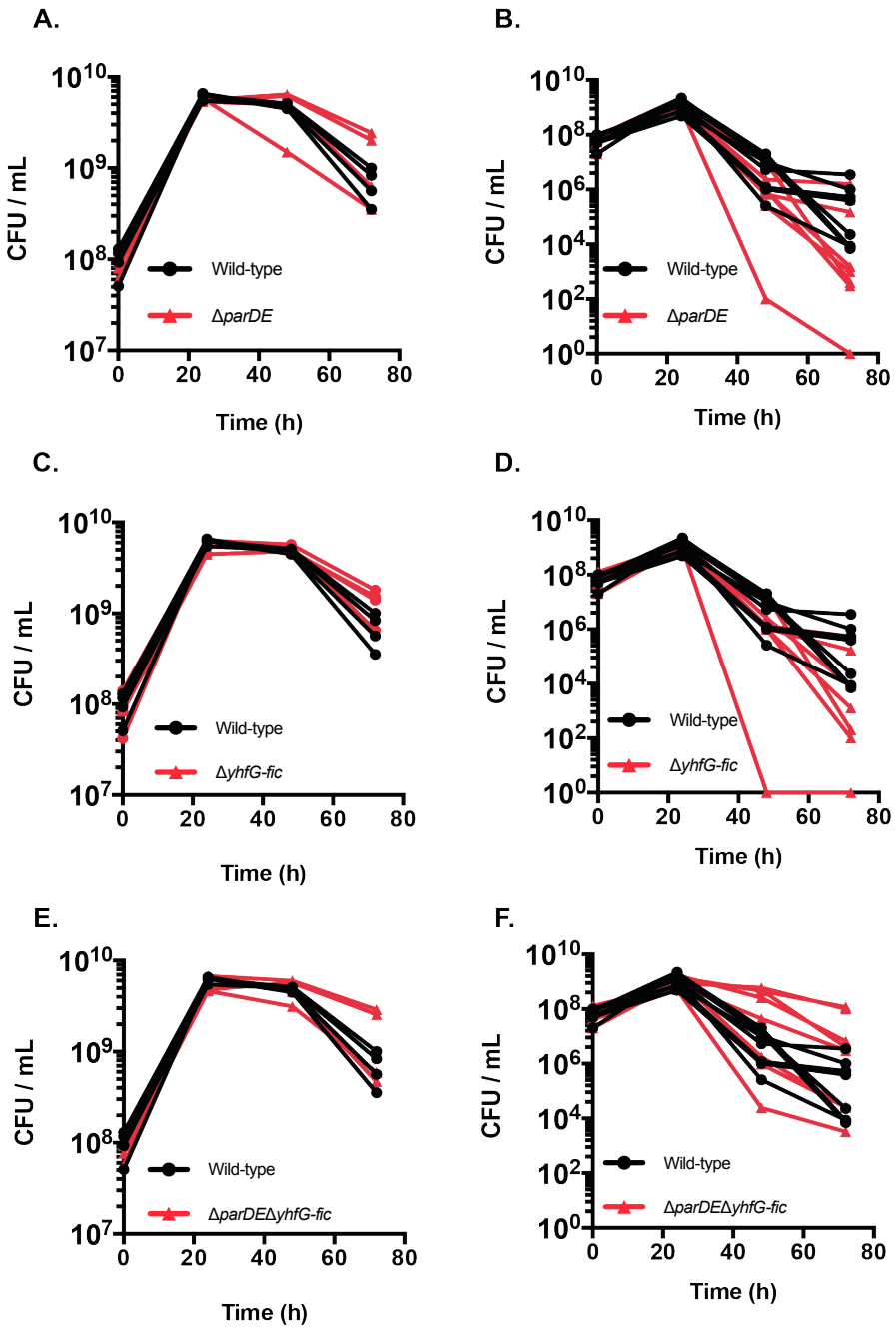


Figure 5.12: Long-term survival of *S.* Typhimurium Δ*parDE* and Δ*yhfG-fic* is reduced and is more variable for Δ*parDE*Δ*yhfG-fic* compared the wild-type. *S.* Typhimurium wild-type (black) and ΔTA mutant (red) Δ*parDE* (A,B), Δ*yhfG-fic* (C,D), Δ*parDE*Δ*yhfG-fic* (E,F) were grown to stationary phase in LB and subcultured to an OD_{600nm} of 0.5 in fresh LB (A,C,E) MgMES pH5 (B,D,F). CFU readings were taken every 24 h, starting from 0 h. Each repeat from six independent experiments is displayed.

5.4.3 The growth defect in *S.* Typhimurium Δ*parDE*Δ*yhfG-fic* is the result of a polar effect on the expression of the *pabA* gene

To investigate whether the growth defect of the Δ*parDE*Δ*yhfG-fic* strain in minimal medium is due to nutrient limitation or acidic conditions, the strain was grown overnight in LB and MgMES at both pH5 and pH7 (Figure 5.13). The Δ*parDE*Δ*yhfG-fic* strain grown overnight in LB pH5 or pH7 and recovered in the same medium grew the same as the wild-type and single ΔTA mutants (Figure 5.13A,B). However, the Δ*parDE*Δ*yhfG-fic* strain had a significant growth defect compared to the wild-type and single ΔTA mutants when grown in minimal medium overnight, in pH5 or pH7 and recovered in the same medium (Figure 5.13C,D), although acidic conditions again increased this effect. The fact that the growth defect was greatly accentuated after growth in minimal medium overnight was reminiscent of a starvation phenotype. It is possible that this defect was the result of an essential nutrient present in LB and not in MgMES (at least to a high extent) being produced at a lower level in the Δ*parDE*Δ*yhfG-fic* strain.

Figure 5.13

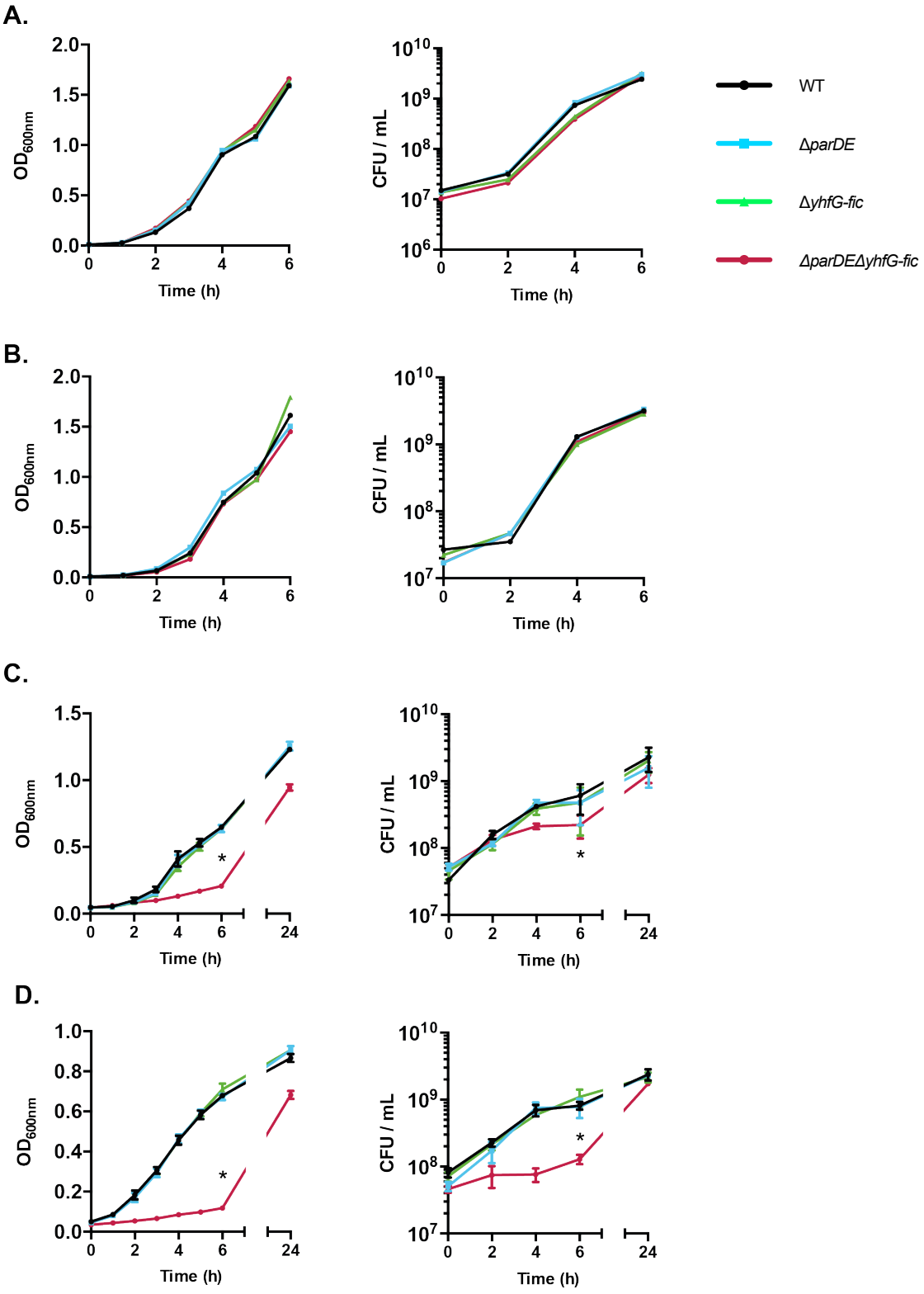


Figure 5.13: Growth defect upon deletion of *parDE* and *yhfG-fic* is dependent on nutrient limitation rather than low pH5 and is accentuated if grown overnight in minimal medium. *S*. Typhimurium wild-type (black), Δ*parDE* (blue), Δ*yhfG-fic* (green), Δ*parDE*Δ*yhfG-fic* (red) were grown to stationary phase in LB pH7 (A), LB pH5 (B), MgMES pH7 (C) and MgMES pH5 (D) and subcultured to an OD_{600nm} of 0.1 in fresh corresponding medium. OD_{600nm} and CFU readings were taken every hour, starting from 0 h. Data represent mean ±S.E.M (n=3).

The *pabA* gene that synthesises para-aminobenzoate (PABA), a precursor for the synthesis of the essential nutrient folate, is located directly downstream of the *yhfG-fic* operon. I hypothesised that a polar effect on the expression of this gene may be occurring in the Δ*parDE*Δ*yhfG-fic* strain and resulting in a defect in growth in minimal medium as a consequence. To test this hypothesis, I compared growth overnight, followed by recovery in MgMES pH5 with and without PABA added to the medium (Figure 5.14). The growth defect occurred without PABA added, but this was complemented when PABA was present in the medium. This suggests that the growth defect is not directly the result of the deletion of Δ*parDE* and Δ*yhfG-fic* but a polar effect of the *yhfG-fic* deletion on *pabA*. The reason this defect was present in the double ΔTA mutant and not in the single Δ*yhfG-fic* mutant is likely due to the difference in antibiotic resistance cassette used between the two strains. The single mutant has a kanamycin cassette inserted in place of the *yhfG-fic* TA module while the double ΔTA mutant has a chloramphenicol cassette inserted in this location (Figure 5.15). The chloramphenicol cassette may interfere with the expression of the *pabA* gene while the kanamycin cassette does not. Or, if the promoter for the kanamycin resistance gene is stronger than that of chloramphenicol, the native promoter of the *pabA* gene could be disrupted in both deletion strains, but with the promoter for the kanamycin cassette is still driving enough expression of the downstream *pabA* in the single deletion mutant to allow growth.

Figure 5.14

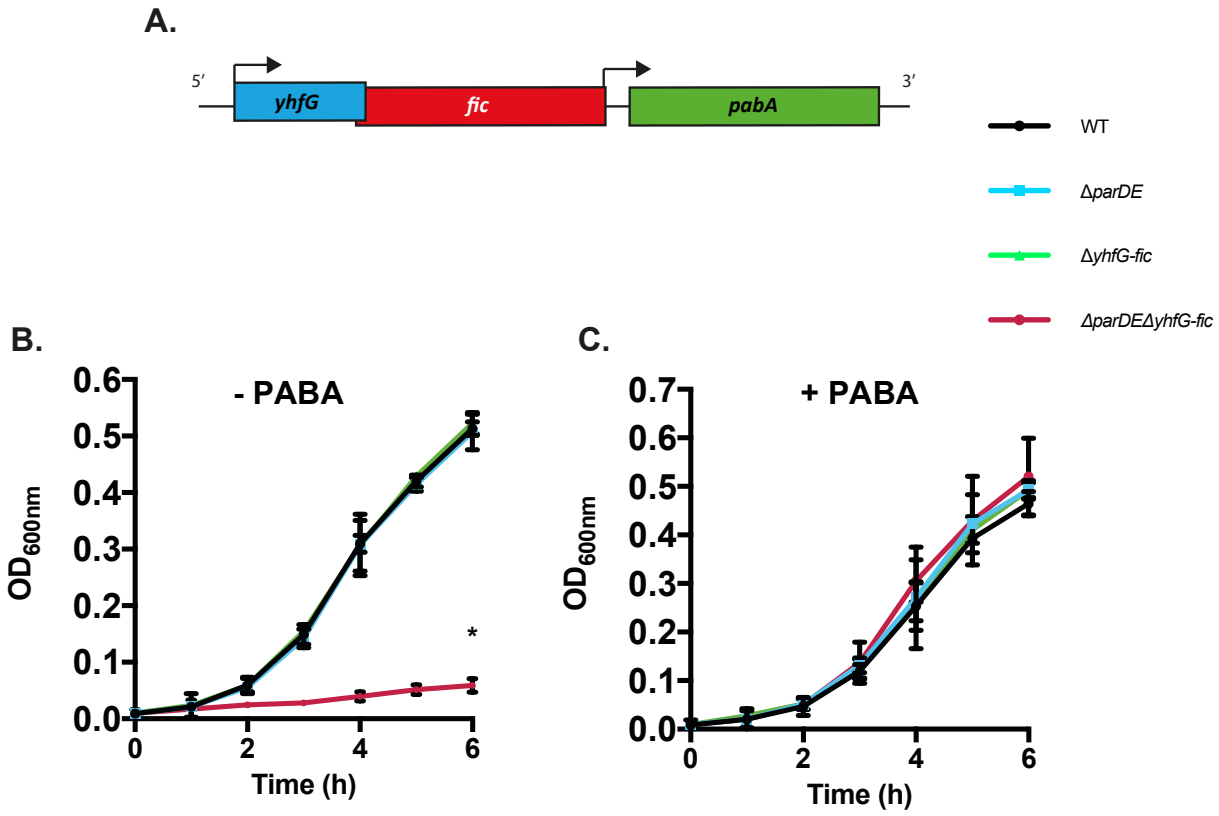


Figure 5.14: Growth defect of *S.* Typhimurium Δ*parDE*Δ*yhfG-fic* is complemented by *para*-aminobenzoate suggesting that a polar effect is taking place in the mutant strain. (A) Diagram depicting the location of the *pabA* gene in respect to the *yhfG-fic* TA module. *S*. Typhimurium wild-type (black), Δ*parDE* (blue), Δ*yhfG-fic* (green), Δ*parDE*Δ*yhfG-fic* (red) were grown to stationary phase in MgMES pH5 and subcultured to an OD_{600nm} of 0.1 in fresh MgMES pH5 with no PABA (B) or with PABA supplementation (C). OD_{600nm} readings were taken every hour, starting from 0 h. Data represent mean ±S.E.M (n=3).

Figure 5.15

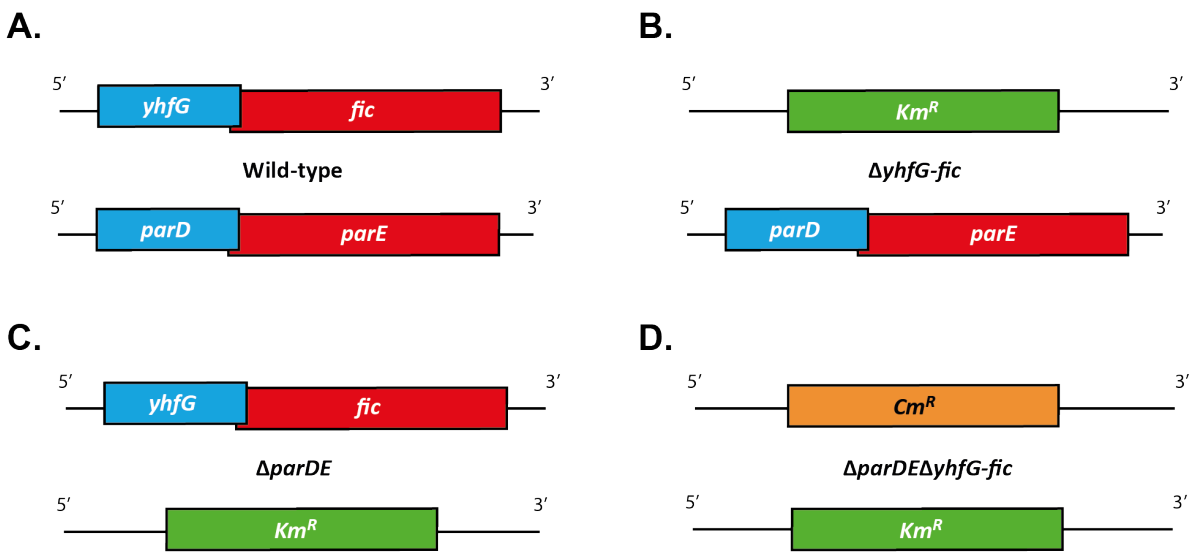


Figure 5.15: Arrangement of antibiotic resistance cassettes in *S.* Typhimurium wild-type, Δ*parDE*, Δ*yhfG-fic* and Δ*parDE*Δ*yhfG-fic* strains. Diagrams displaying the presence of the TA modules genes or antibiotic resistance cassettes (Km^R – kanamycin resistance; Cm^R – chloramphenicol resistance) in *S.* Typhimurium (A) wild-type, (B) Δ*parDE*, (C) Δ*yhfG-fic* and (D) Δ*parDE*Δ*yhfG-fic* strains.

5.5 Conclusion

The deletion of both *parDE* and *yhfG-fic* were found to result in a growth defect in RAWs, while the single mutants of each module did not show this defect. The possibility of two TA modules possibility involved in targeting similar parts of bacterial DNA metabolism being required for intra-macrophage growth was exciting, so an attempt was made to characterise mutants in these TA modules. However plasmid overexpression assays did not find Fic toxic in *Salmonella*. I then decided to explore whether the presence of these TA modules on the chromosome were required for stressful conditions in general in *Salmonella*. Growth curves of *Salmonella* conducted in MgMES pH5, which closely resembles conditions to those found within the SCV during macrophage infection, found that the double ΔTA mutant had a growth defect while the wild-type single mutants Δ*parDE* and Δ*yhfG-fic* did not. If these TA modules were important for survival and growth in stressful conditions, then perhaps a longer incubation in these conditions would produce a more apparent phenotype upon their deletion. Deletion of the single TA modules *parDE* and *yhfG-fic* appear to negatively effect survival slightly over 72 h as measured by CFU. However the double Δ*parDE*Δ*yhfG-fic* strain had highly variable levels of survival between experimental repeats compared to the wild-type, perhaps due to different mutations arising within the population.

It was found that growing the Δ*parDE*Δ*yhfG-fic* strain overnight in minimal media before resuming growth in fresh minimal media greatly accentuated the growth defect in comparison to the wild-type or single deletion mutants. This growth defect was due to nutrient limitation and not the result of pH. This resembled the phenotype of a strain deficient in an essential

nutrient. The *pabA* gene, responsible for synthesising *para*-aminobenzoate (PABA), which is required for synthesis of the essential nutrient folate, is found immediately downstream of the *yhfG-fic* operon. A recent review of bacterial FIC proteins from the Dehio group mentioned unpublished data stating that the promoter of *pabA* is found within the *fic* gene in *E. coli.* The genomic arrangement of these genes in *Salmonella* is extremely similar, so it is highly likely that this is also the case in *S.* Typhimurium. I previously had not considered that a polar effect could be taking place in the double ΔTA mutant as the single ΔTA mutants did not have a growth defect. However, concerned that this double ΔTA strain had deficient expression of the *pabA* gene, I cultured the double mutant in MgMES pH5 supplemented with PABA. This fully complemented the growth defect, strongly suggesting that a lack of PABA production as a result of the promoter of *pabA* being disrupted was the cause of the phenotype observed. The reason the single Δ*yhfG-fic* mutant did not have a growth defect, is likely due to the presence of a kanamycin resistance cassette in place of the *yhfG-fic* module. This cassette has a strong promoter that is likely driving expression of the downstream *pabA* gene, counteracting the disruption of the native *pabA* promoter. The chloramphenicol cassette present in place of the *yhfG-fic* module in the double deletion strain has a weaker promoter and is likely unable to drive the expression of *pabA.* This could be tested by either removing the antibiotic resistance cassettes from the mutants, or reconstructing the strains, leaving the end of the *fic* gene sequence containing the *pabA* promoter intact.

Chapter Six

Phenotypic heterogeneity in the lag times of stressed *E. coli* and macrophage-induced *Salmonella* persisters

6.1 Introduction

One aspect of persister biology that is currently not well understood is the ability of persister cells to transition from a nongrowing, antibiotic-tolerant state to a growing, antibiotic-susceptible one. While some experiments have been carried out investigating persister regrowth they are generally only capable of monitoring the recovery of the first persisters to reawaken (Helaine et al. 2014). The experiment is quickly overrun by early-regrowing bacteria, making observations of late-regrowers difficult by methods such as microfluidics or flow cytometry (Levin-Reisman et al. 2010). As a result, the distribution of awakening times in persister populations has been difficult to observe. However, recently the Balaban group developed a new technique, ScanLag, which uses time-lapse imaging of agar plates in desktop computer scanners to allow the measurement of colony appearance times (Levin-Reisman et al. 2010). If it is assumed that the times at which colonies are first visible to the scanners reflect the lag times of the founding bacterial cells from the original sample, then the distribution of lag times can be effectively measured (Levin-Reisman et al. 2010). This technique has already been used to successfully investigate the link between lag time and antibiotic tolerance

as well as the link between tolerance and antibiotic resistance in *E. coli* (Fridman et al. 2014; Levin-Reisman et al. 2017). I adapted the ScanLag technique in our lab in order to answer questions about the lag time distributions of intra-macrophage *Salmonella* persisters after extraction from their host cells. To confirm the ability of ScanLag to observe phenotypic heterogeneity through the distributions of colony appearance times, I first used the technique to investigate two examples of phenotypic heterogeneity in *E. coli*.

6.2.1 Heterogeneity in metabolic activity of stationary phase *E. coli* can be linked to heterogeneity in lag time distribution

To carry out ScanLag analysis, the bacterial sample to be measured is spread on agar plates at the appropriate dilution (resulting in ~100 colonies per plate). The plates are then placed onto desktop computer scanners, which are incubated while connected to a computer and programmed to take images at regular intervals over a period of days - long enough for both early and late appearing colonies to appear (Figure 6.1A). The resultant images are analysed in time-lapse format, detecting and tracking the size of colonies over time. The first time point at which any colony is first visible is then recorded. These ‘colony appearance time’ values can be used to reflect the lag time distribution of the original colony-founding bacterial cells present in the sample. The growth rate of colonies can also be measured, however this metric was found to be highly variable (Appendix figure 5) as it is likely influenced by the proximity of neighbouring colonies and unlikely to give reliable information about the bacteria present in the original sample.

Figure 6.1

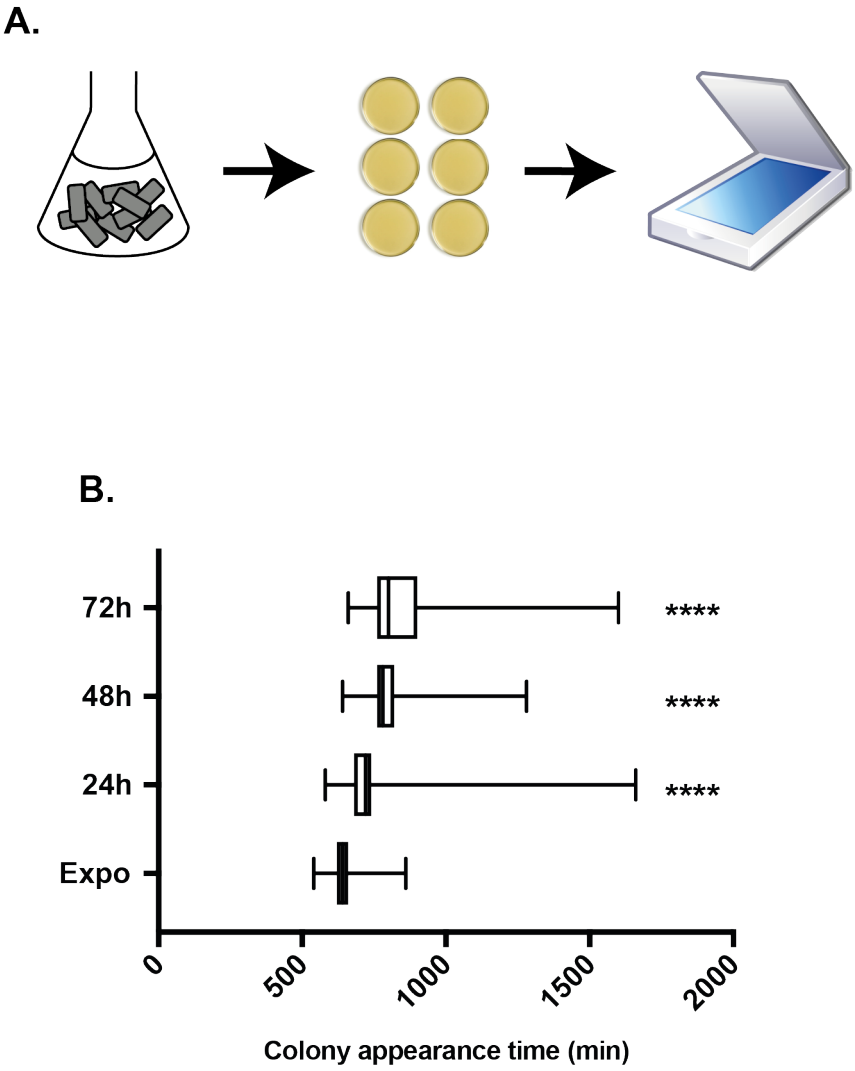


Figure 6.1. ScanLag analysis shows stationary phase *E. coli MG1655* has increased heterogeneity lag. A) Schematic of ScanLag technique: Bacterial sample is plated out on agar and incubated inside desktop computer scanners that repetitively take images through the control of a computer. Time-lapse analysis allows the time colonies first appear to be recorded as a measure of the lag time of the founding cells. B) Box and whisker plots of colony appearance time distributions for *E. coli* grown to exponential phase and stationary phase (grown in minimal media for 24 h, 48 h and 72 h). Data was pooled for three independent experiments and samples of 752 colonies were randomly selected for each condition. Statistical significance was tested using Mann-Whitney U; p-values indicated as ****<0.0001 and ns for >0.05.

To test whether the ScanLag technique in our hands could reveal increased heterogeneity in lag times, two forms of phenotypic heterogeneity currently under investigation in *E. coli* were used. It was recently found that *E. coli* in long stationary phase is made of fast and slow responders to the presence of an inducer, as assessed by inducing GFP expression (Rigano, L. *et al.,* unpublished data, personal communication; Figure. 6.1B). To assess whether this population was also heterogeneous in the lag times of individual cells, *E. coli* was grown to varying lengths of time in Gutnick minimal media and plated for ScanLag analysis. The average lag time significantly increased with each extra day of culture (Figure 6.1B), with the range of lag times, one indicator of population heterogeneity, also increasing during this time.

To test whether the heterogeneous response in GFP production and lag times were associated, *E. coli* was grown to stationary phase in minimal media, induced for GFP fluorescence and then cell sorted based on this level of fluorescence (Figure 6.2A) [collaboration with Dr. L. Rigano]. Figure 6.2B shows the gating used to sort the metabolically heterogeneous population of *E. coli*, with Figure 6.2C displaying the resultant re-analysed high-GFP population and Figure 6.2D displaying the re-analysed low-GFP population. The high- and low-GFP *E. coli* were plated for ScanLag analysis, along with exponential phase, stationary phase and pre-sort samples as controls. As observed previously, the median and range values of the appearance times increased dramatically between exponential phase and stationary phase populations of *E. coli* (Figure 6.2E). The induction of GFP expression involves a 30 min incubation in fresh minimal media with an arabinose inducer. As a result of this the range and median appearance times in the pre-sort sample

are predictably lower than in stationary phase owing to the alleviation of the nutrient limitation present during stationary phase, however there was still greater heterogeneity than in exponential phase. After cell sorting, the high-GFP population of *E. coli* was found to have very little variation in the appearance times of colonies, with a median value similar to that of exponential phase. In contrast, the low-GFP subpopulation in contrast had the greatest median colony appearance time (1000 min) and the largest range of values, it was significantly different to the pre-sort sample while the high-GFP population was not. This suggests that this metabolically slow-responding population is largely responsible for the heterogeneity in individual bacterial cell lag times within the stationary phase *E. coli* population. The slow response to produce a fluorescent protein in reaction to the presence of an inducer is directly linked to heterogeneity in the lag times of regrowth in stationary phase *E. coli*.

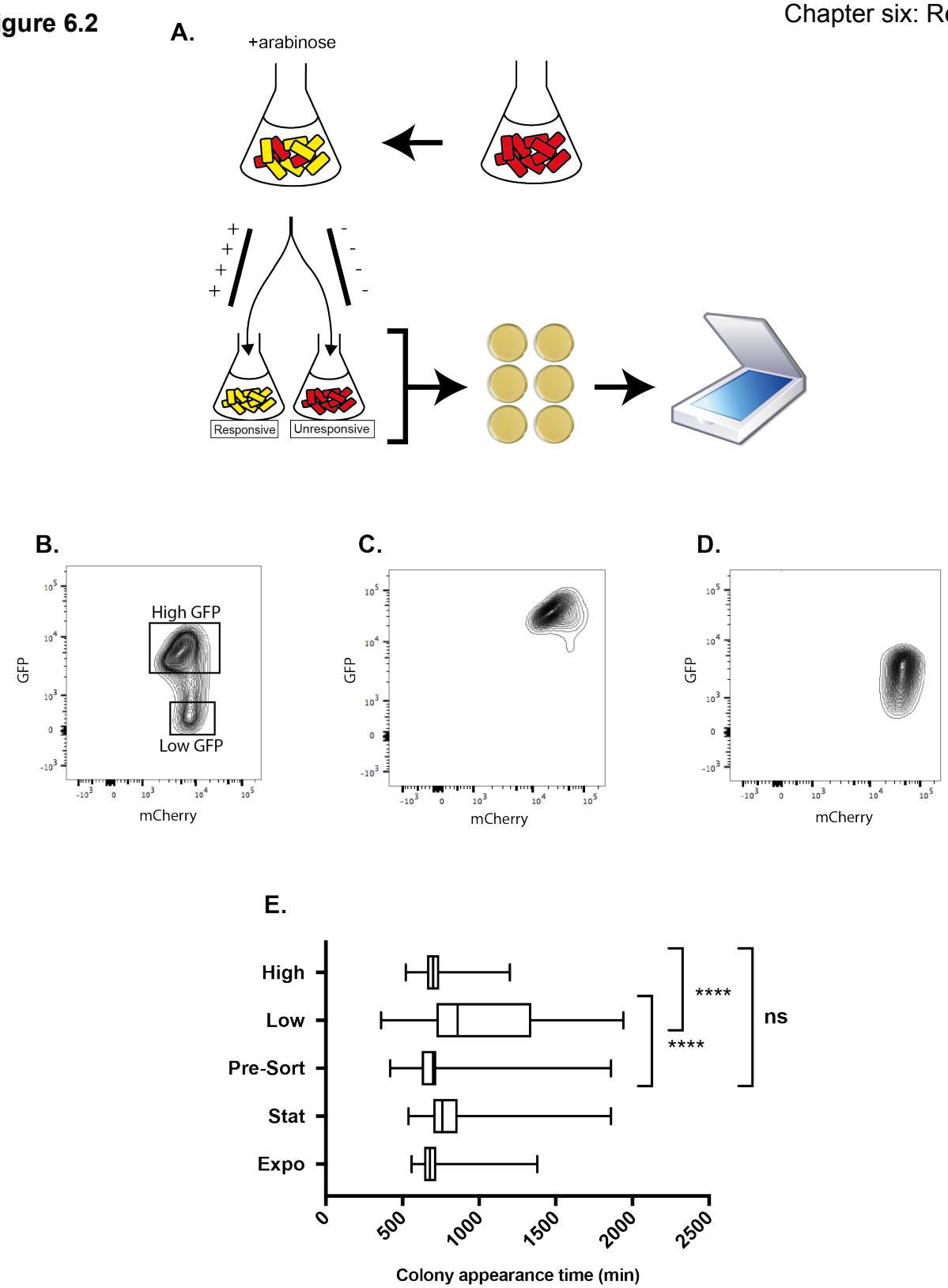


Figure 6.2. ScanLag analysis of stationary phase *E. coli* after FACS based on metabolic activity. A) Schematic of experimental design: *E. coli* carrying pFCcGi was grown to stationary phase, GFP expression was induced with arabinose and the bacteria were sorted based on GFP fluorescence and plated for ScanLag analysis. B) Bivariate plot of mCherry (constitutive) and GFP (arabinose-inducible) fluorescence in stationary phase *E. coli* pFCcGi, gating used for cell-sorting is overlaid onto the plot. Bivariate plots of mCherry and GFP fluorescence also shown for 'high-GFP' (C) and 'low-GFP' *E. coli* reanalysed by flow cytometry post-sorting. E) Box and whisker plots of colony appearance time distributions for exponential phase, stationary phase (24 h), pre-sort (post-induction) *E. coli*, and sorted 'high-GFP' and 'low-GFP' cells. Data was pooled for three independent experiments and samples of 728 colonies were randomly selected for each condition. Statistical significance was tested using Mann-Whitney U; p-values indicated as ****<0.0001 and ns for >0.05.

6.2.2 ScanLag can reveal a decrease in heterogeneity of lag in *E. coli* Δ*yeaG* compared to wild-type

To further test the ability of ScanLag to investigate phenotypic heterogeneity through lag time distribution, another example of phenotypic heterogeneity known in *E. coli* was utilised. The *yeaGH* operon is associated with increasing heterogeneity in metabolic activity and whole population lag time following recovery from nitrogen starvation (Figueira et al. 2015). It was previously reported that upon deletion of *yeaG*, *E. coli* regrows faster in fresh minimal media following nitrogen-starvation compared to the wild-type. *E. coli* Δ*yeaG* was also found to be more homogeneous in the metabolic response to an inducer (Figueira et al. 2015). It was hypothesised that perhaps a greater number of individual cells have lower lag times in growth within the mutant population compared to the wild-type, something detectable by ScanLag analysis. *E. coli* wild-type and Δ*yeaG* were starved of nitrogen for 24h before being plated on minimal medium agar with 3 mM NH_4Cl acting as an available nitrogen source for ScanLag analysis (Collaboration with Dr R. Figueira; Figure 6.3A). As expected the wild-type displayed more heterogeneity in lag when compared to the Δ*yeaG* mutant, with many more late-regrowers present in the wild-type population following nitrogen-starvation. Surprisingly, there were several early appearing colonies belonging to the wild-type population compared to the mutant, although this was a minority of the population. Presumably however, in liquid culture these early regrowers would lead to a faster recovery from nitrogen-starvation in the wild-type rather than the Δ*yeaG* mutant. There may be factors that differ between solid and liquid phase media that could affect the lag of these *E. coli*, this is potentially difficult to control for.

This highlights that ScanLag restricts the study of growth to solid-phase medium and differences in growth will exist between solid media, liquid phase or during infection. Nevertheless, a reduction in heterogeneity in lag times was observed in the Δ*yeaG* mutant when compared to the wild-type with more of the population regrowing earlier. This shows that heterogeneity in lag times within a population as measured by ScanLag appears to be readily linked to phenotypic heterogeneity observed using other techniques within bacterial populations.

Figure 6.3

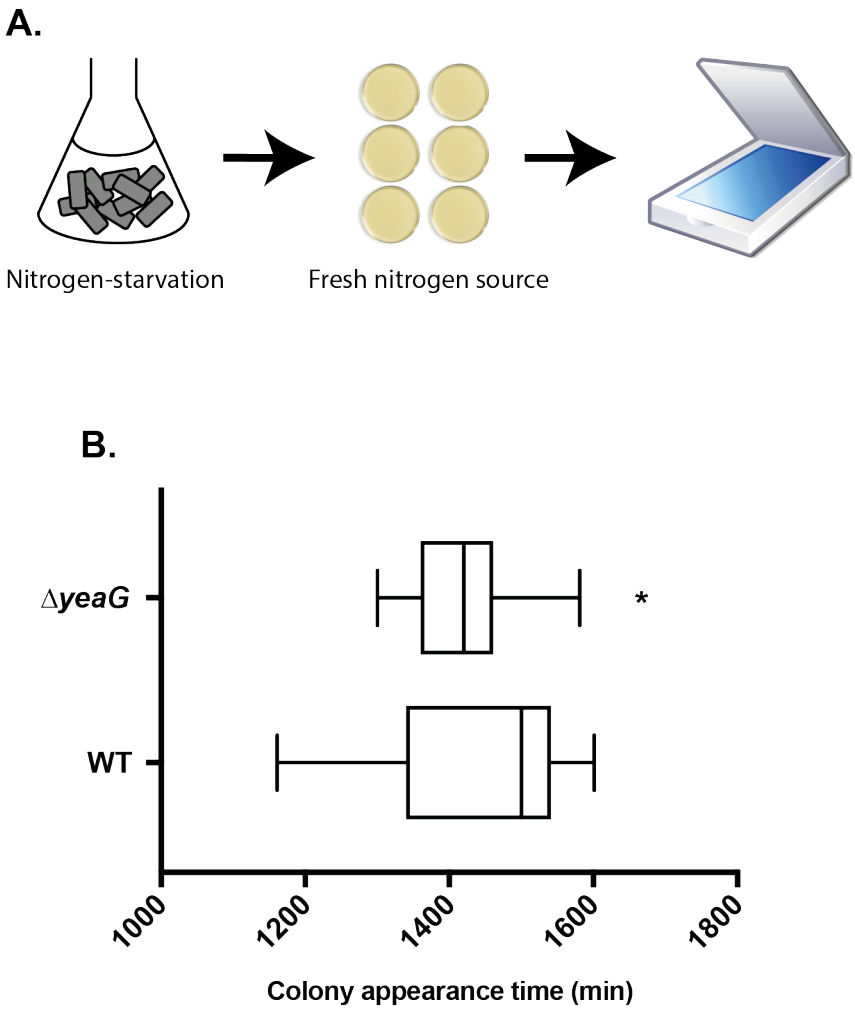


Figure 6.3. *E. coli* Δ*yeaG* is more homogeneous in lag time than wild-type. A) Schematic of experimental design: *E. coli* were starved of nitrogen for 24 h, then plated onto minimal medium agar with a fresh nitrogen source, and incubated in scanners for ScanLag analysis. B) Box and whisker plots of colony appearance time distributions for *E. coli* Δ*yeaG* and wild-type strains. Data was pooled for three independent experiments and samples of 59 colonies were randomly selected for each condition. Statistical significance was tested using Mann-Whitney U; p-values indicated as *<0.05.

6.3.1 ScanLag analysis reveals no difference in regrowth depending on DNA content of NG *Salmonella*

I hypothesised in chapter 4 that a higher DNA content in NG *Salmonella* during macrophage infection may lead to a faster recovery from a persister state. To test this hypothesis, macrophages were infected with wild-type *S.* Typhimurium carrying the pDiGi plasmid for 24 h in presence of cefotaxime in order to isolate NG *Salmonella* and allow enough time for DNA replication. Arabinose was added to the infection medium 4 h before the bacteria were extracted from macrophages to allow time for DsRed expression and maturation, to act as an indicator of metabolic activity. After extraction from macrophages, the NG *Salmonella* were sorted based on DsRed and DAPI fluorescence in order to isolate metabolically active NG *Salmonella* that had a high DNA content (compared to the inoculum) and a lower DNA content (Collaboration with Dr P. Hill). The third population isolated was that of cells that did not respond to the inducer to make DsRed. All three populations and a stationary phase control sample were plated out on LB agar for ScanLag analysis (Figure 6.4A). Figures 6.4B and 6.4D show the DAPI levels in the inoculum and at 28 h.p.i. respectively, the DNA increase in the NG *Salmonella* present during macrophage infection occurred as previously reported in chapter 4. Figures 6.4C and 6.4E show the DsRed levels in both these samples plotted against the DAPI fluorescence levels. No DsRed is detectable in the inoculum, as it was not exposed to arabinose (Figure 6.4C). The NG *Salmonella* present at 28 h.p.i. displayed a heterogeneous production of DsRed (Figure 6.4E) as previously reported - the gating used for sorting these different subpopulations is shown in Figure 6.4E. Figure 6.4F shows the

proportions of regrowth after cell sorting (adjusting for the dilution used before plating) along with a sorted stationary phase control. This proportion of regrowth can be referred to as the recovery rates of the samples. Only 2.7% of the unresponsive *Salmonella* were able to regrow while 12% and 16% of the high DNA and low DNA content nongrowing *Salmonella* regrew after sorting respectively, indicating that the metabolically responsive NGs are the greater source of regrowing persisters after infection. Figure 6.4G shows the appearance times of colonies recorded after cell sorting. There is a difference between the lag time distributions of stationary phase *Salmonella* and all *Salmonella* extracted from macrophages, with a greater median lag time observed after infection. While there was a difference in the lag time distribution of the responsive and unresponsive subpopulations there was no difference observed between subpopulations of high and low DNA contents. This suggests that the DNA content of *Salmonella* persisters does not affect the speed of recovery after infection, at least not to a degree that is detectable by ScanLag.

Figure 6.4

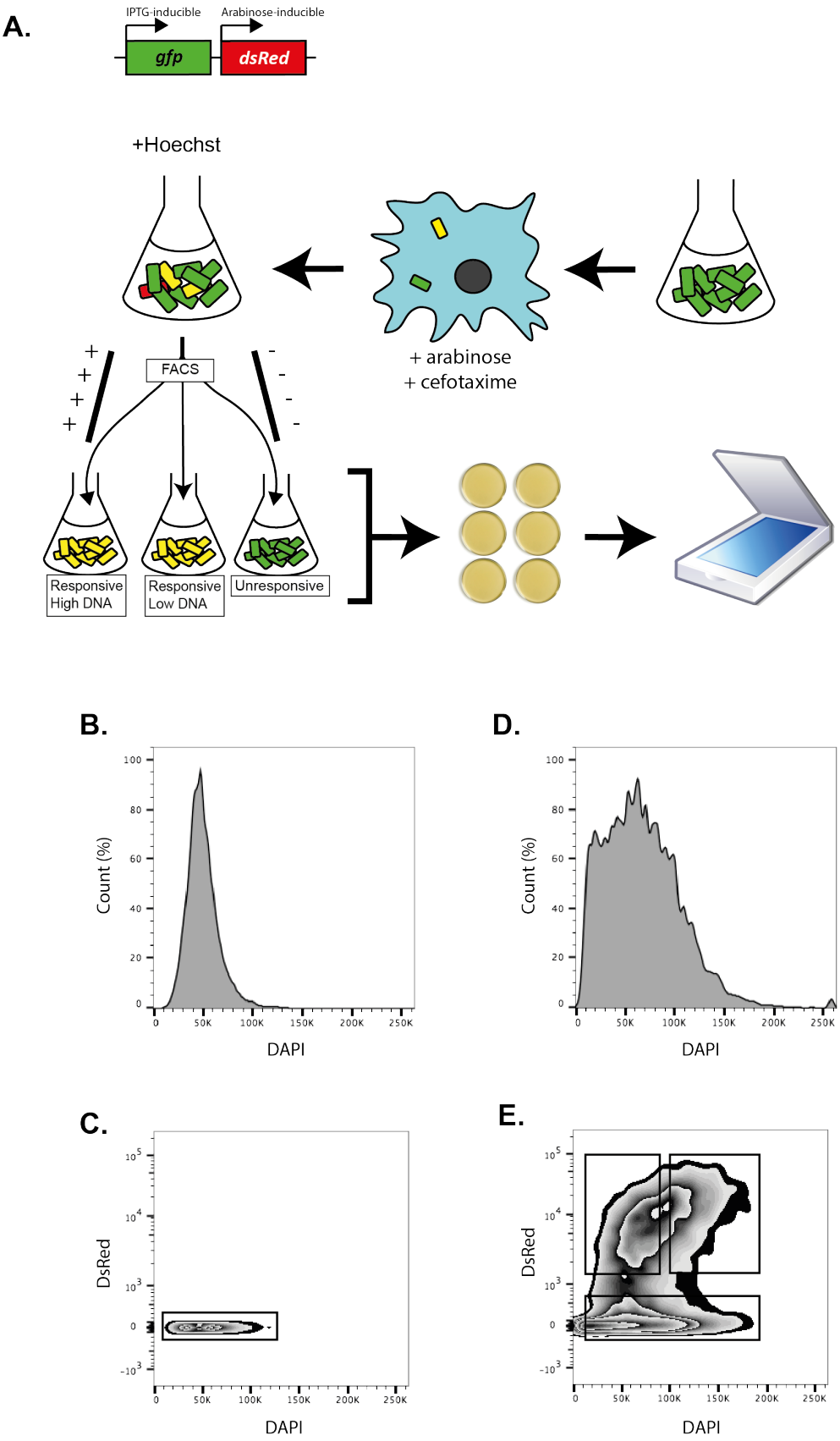

A.
IPTG-inducible
Arabinose-inducible
gfp
dsRed
+Hoechst
+ arabinose
+ cefotaxime
FACS
Responsive High DNA
Responsive Low DNA
Unresponsive
B.
Count (%)
DAPI
D.
Count (%)
DAPI
C.
DsRed
DAPI
E.
DsRed
DAPI

Figure 6.4

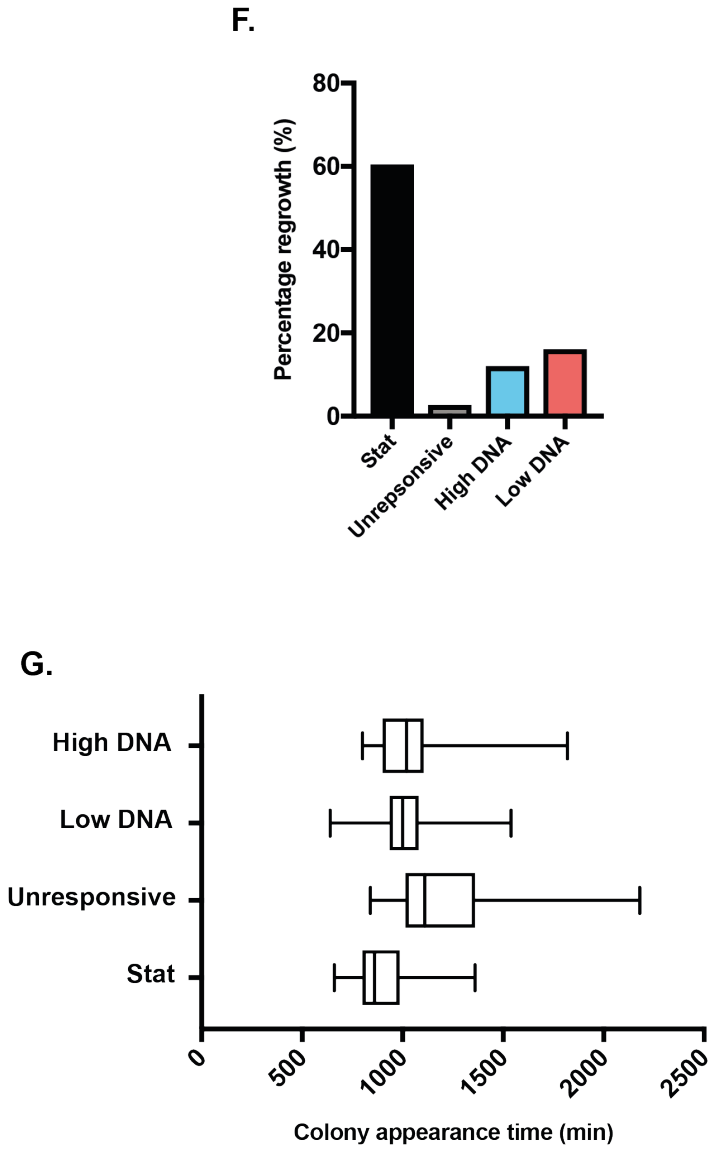


Figure 6.4. DNA content of NG *Salmonella* does not affect lag post-infection. A) Schematic of experimental design: *Salmonella* carrying pDiGi was infected into BMMs. Arabinose was added to medium 4 h before extraction of bacteria. After extraction, bacteria were staining with Hoechst dye and sorted into cells that did not respond to the arabinose, and responsive cells that were 'high' or 'low' in DNA content. These three samples and a stationary phase control were plated on LB and analysed by ScanLag. Histograms of Hoechst fluorescence in stationary phase (inoculum) *Salmonella* (B) and 28 h.p.i. (D) and bivariate plots displaying Hoechst and DsRed fluorescence together for stationary phase (C) and 28 h.p.i. (E) are shown, gating is overlaid on plots. F) Bar chart of recovery rates of bacteria post-infection and after cell sorting (G) box and whisker plots of colony appearance time distributions for stationary phase (Stat), unresponsive NGs and responsive NGs 'high' and 'low' in DNA content, n=1.

6.3.2 ScanLag analysis reveals no difference in regrowth of NG ΔTA *Salmonella* but does in growing ΔTA *Salmonella*

Toxin-antitoxin (TA) modules have been implicated in persister formation by many studies, however many of these experiments are reliant on CFU measurements and do not attempt to differentiate between the formation of persisters and their regrowth (Fisher et al. 2017). In order to test whether TA modules are involved in the ability of *Salmonella* persisters to regrow after macrophage infection, single *S.* Typhimurium ΔTA mutants (Δ*phd-doc*, Δ*relBE* and Δ*tacAT*) were used to infect BMMs for 24 h in the presence of either gentamicin or cefotaxime and sorted based on metabolic responsiveness and growth (collaboration with Dr. P. Hill). These cells were then plated on LB agar for ScanLag analysis alongside a stationary phase control. Figures 6.5A-E show the DsRed and GFP fluorescence profiles for stationary phase and wild-type, Δ*relBE1*, Δ*tacAT* and Δ*phd-doc* post-infection in gentamicin, with gating shown for sorting metabolically unresponsive subpopulations (low DsRed), metabolically active and growing subpopulations (high DsRed, low GFP) and metabolically active and NG subpopulations (high DsRed, high GFP). Similarly, figures 6.5F-I show the DsRed and GFP fluorescence profiles for wild-type, Δ*relBE1*, Δ*tacAT* and Δ*phd-doc* post-infection in cefotaxime, isolating only the NG *Salmonella*. The gating is shown for sorting the metabolically unresponsive subpopulations (low DsRed) and the metabolically responsive and NG subpopulations (high DsRed, high GFP). Figure 6.5J shows the regrowth rates for the wild-type and ΔTA mutants following macrophage infection. After cell sorting the GFP-positive bacteria in the stationary phase *Salmonella* sample, the number of resultant colonies only

corresponded to ~60% of the cells present in the sample (after correcting for the dilution made before plating). The metabolically unresponsive subpopulations only regrew at a rate of between 0 and 1.8% whether infected in the presence of gentamicin or cefotaxime, with no significant differences between any mutant and the wild-type strain. In contrast, all metabolically active subpopulations had substantially higher recovery rates. There were no significant differences in the recovery rates between any of the strains within each subpopulation. However there were significant differences in the recovery rates between subpopulations, with growing bacteria regrowing at the highest frequency and metabolically active NG bacteria in the presence of cefotaxime or gentamicin regrowing at the lowest frequency. All strains infected in the presence of cefotaxime had recovery rates of between 12.1% (*relBE1*) and 23.9% (*tacAT*) on average.

Figure 6.5

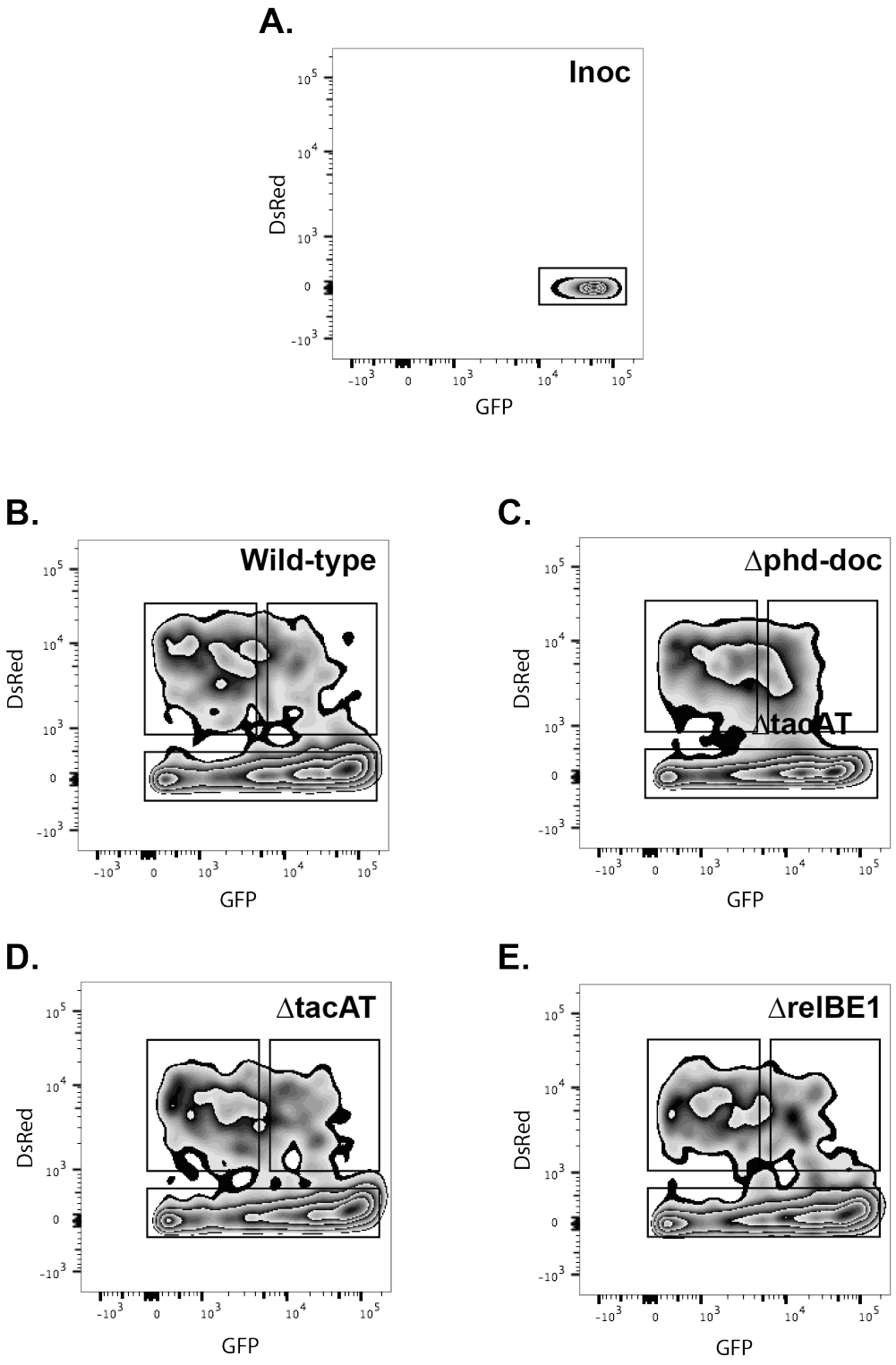

A.
Inoc
DsRed
GFP
B.
Wild-type
DsRed
GFP
C.
Δphd-doc
ΔtacAT
DsRed
GFP
D.
ΔtacAT
DsRed
GFP
E.
ΔrelBE1
DsRed
GFP

Figure 6.5

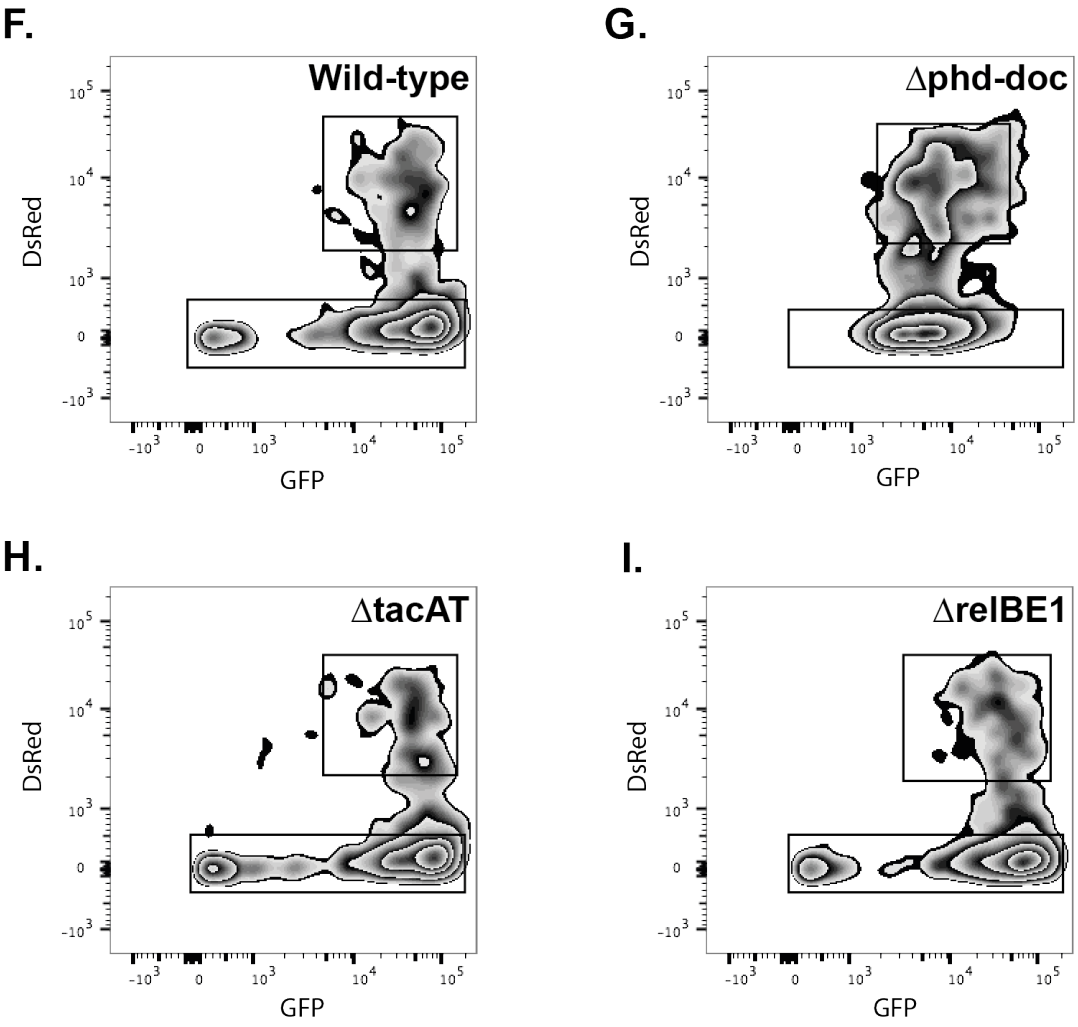


Figure 6.5

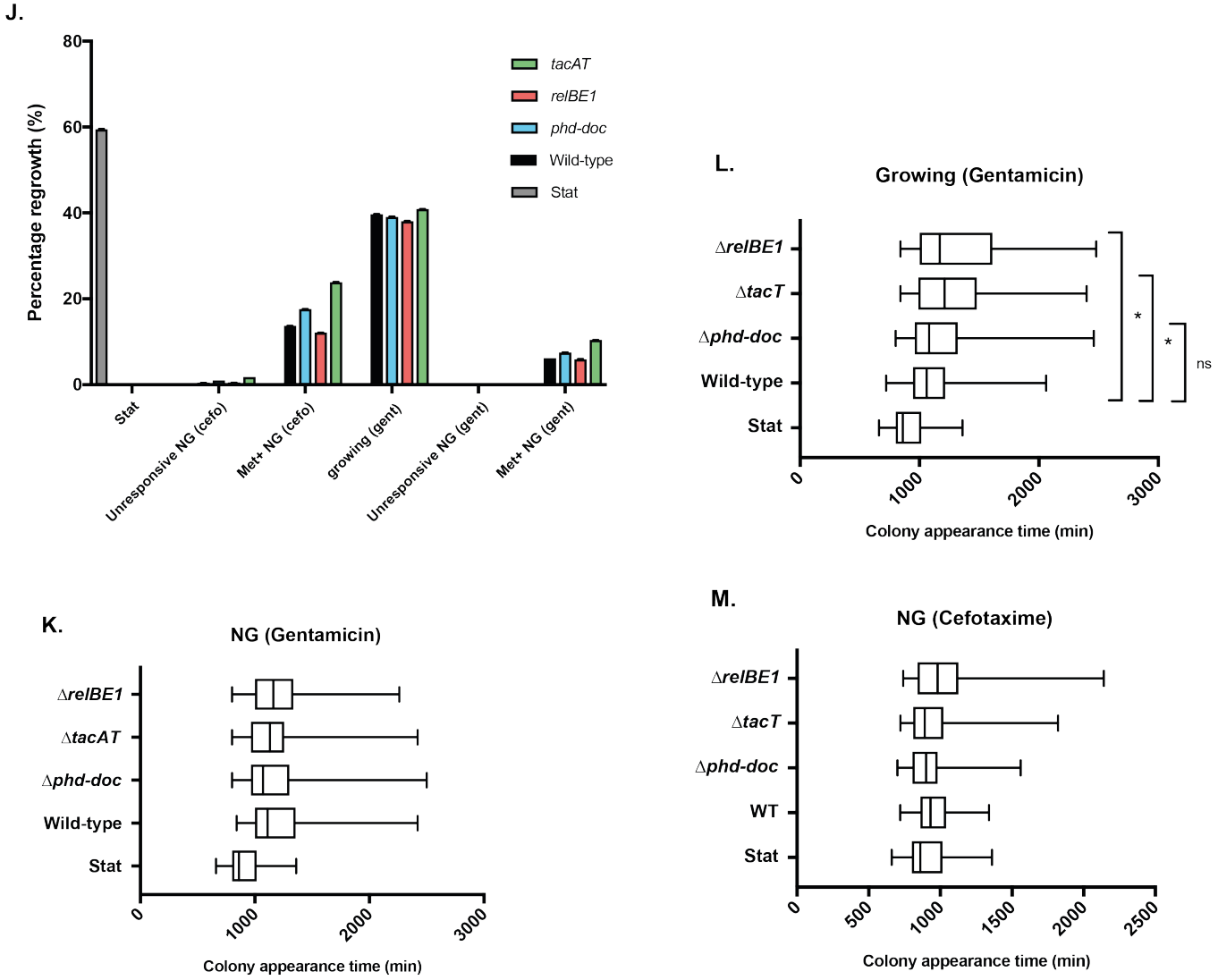


Figure 6.5. Deleting single TA modules affects lag in growing but not NG *Salmonella.* Bivariate plots of GFP (constitutive) and DsRed (arabinose-inducible) fluorescence levels in the inoculum (A), wild-type (B), Δ*phd-doc* (C), Δ*tacAT* (D), Δ*relBE1* (E) post-infection in gentamicin and wild-type (F), Δ*phd-doc* (G), Δ*tacAT* (H), Δ*relBE1* (I) post-infection in cefotaxime, gating for sorting responsive NG, growing and unresponsive populations overlaid on plots. J) Bar chart of recovery rates of bacteria post-infection and after cell sorting of stationary phase (Stat) *Salmonella*, unresponsive and responsive bacteria post-infection with cefotaxime and unresponsive, responsive NGs and growing bacteria post-infection with gentamicin belonging to wild-type, Δ*phd-doc*, Δ*tacAT*, Δ*relBE1* strains, values are mean ±S.E.M.. Box and whisker plots of colony appearance time distributions for stationary phase (Stat) and wild-type (WT), Δ*phd-doc*, Δ*tacAT*, Δ*relBE1* post-infection for responsive NGs with gentamicin (K), growing bacteria with gentamicin (L) and responsive NGs with cefotaxime (M) added during infection. Statistical significance was tested using Mann-Whitney U; p-values indicated as *<0.05 and ns for >0.05.

Figure 6.5K shows the distribution of colony appearances times for the NG *Salmonella* belonging to the wild-type and each ΔTA mutant after being sorted post-infection in the presence of gentamicin as well as a stationary phase wild-type *Salmonella* control. There was a significant difference between the lag distributions of the stationary phase bacteria and all other strains post-infection as previously observed (Figure 6.4G), with all NG *Salmonella* post-infection displaying an increased average lag time. However there were no differences in the median or range of colony appearance times between the ΔTA strains and the wild-type. Figure 6.5L shows the distributions of colony appearance times for the growing bacteria belonging to each ΔTA strain and the wild-type, with a stationary phase total bacteria control. Once more, all bacteria post-infection showed an extended lag distribution compared to stationary phase bacteria. *S.* Typhimurium Δ*phd-doc* did display an extended lag distribution but this was not a significant change compared to the wild-type post-infection. Interestingly, both Δ*tacAT* and Δ*relBE1* displayed a significant change in their lag distributions within growing bacterial subpopulations post-infection when compared to the wild-type, with both subpopulations taking longer to regrow. Figure 6.5M shows lag distributions for all samples post-infection in the presence of cefotaxime and after cell sorting based on metabolic responsiveness. There were no significant changes between the lag distributions of the different strains in this subpopulation. To conclude, the deletion of TA modules did not have any significant effect on the recovery rate or the distribution of lag times in NG *Salmonella* post-infection. However, deletion of TA modules, in particular *relBE1* and *tacAT* appeared to increase the average lag time of growing

Salmonella post-infection. As TA modules are known to be important in managing stressful conditions, perhaps more damage has occurred to these mutants during infection than to the wild-type, leading to increased lag times as repair mechanisms take place before recovery can occur. Another possibility is that if any genetic damage that has taken place in these mutants at a higher frequency than to the wild-type, this may increase the likelihood of 'slow colony-formers' arising, passing down mutations that affect their growth through successive generations and thus affecting the growth rate of the entire colony. Whole-genome sequencing could be used to check for the presence of these mutations.

6.3.3 The SOS response is important for recovery of *Salmonella* post-infection

If single TA modules are not directly involved in the lag time of *Salmonella* persisters released from macrophages then perhaps another mechanism is responsible. Alternatively, if redundancy in the action of multiple TA modules is blocking the ability to observe a phenotype upon the deletion of single modules, then a mechanism that is acting upstream of TA modules may be easier to investigate. Such a mechanism could be the SOS response, a global change that occurs upon the detection of DNA damage by RecA that is known to lead to TA activation and involved in antibiotic tolerance (Dörr et al. 2010; Theodore et al. 2013). Deletion mutants for *recA*, should not be able to activate the SOS response. If it is responsible for the changes in the lag distribution in NG *Salmonella*, it may give clues as to how to wake persisters early, or perhaps inhibit their recovery. Indeed, a recent study described how

the *recA* gene is important for the recovery of persisters in *E. coli* (Völzing & Brynildsen 2015).

Infection of BMMs was carried out as previously described, with wild-type *S.* Typhimurium and a Δ*recA* mutant in the presence of gentamicin or cefotaxime, to allow both growing and NG *Salmonella* to be monitored in the same infection and NG bacteria to be monitored in isolation. Figures 6.6A-E show the DsRed and GFP fluorescence levels for *S*. Typhimurium wild-type and Δ*recA* strains in stationary phase and post-infection. The gating strategy used to isolate the unresponsive (low DsRed), metabolically responsive and NG (high DsRed, high GFP) and metabolically responsive and growing subpopulations (high DsRed, low GFP) of *Salmonella* is shown overlaid on the bivariate histograms (Collaboration with Dr Hill, P.). There was no difference in intracellular growth as seen by fluorescence dilution between the wild-type and Δ*recA* (Figure 6.6D,E).

Figure 6.6

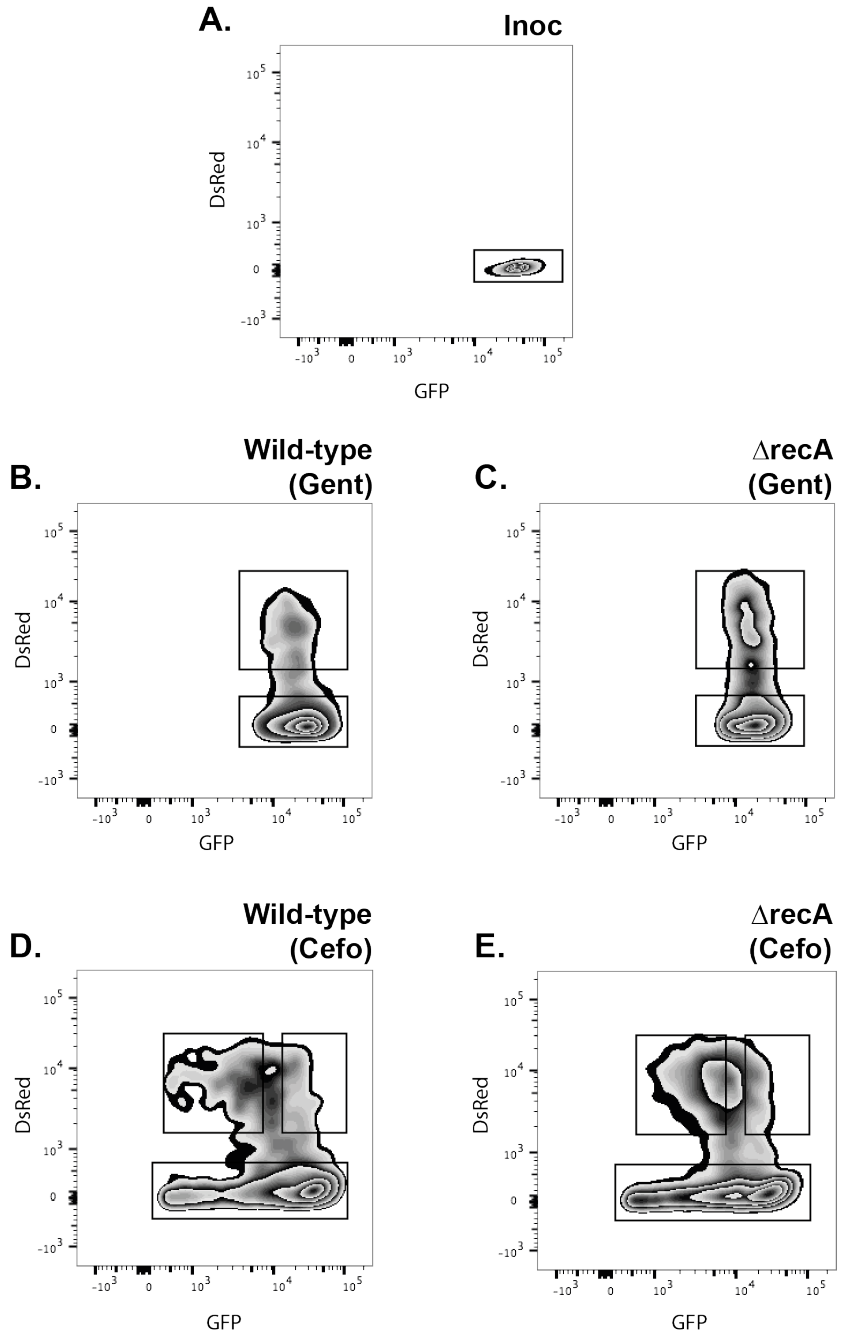

A.
Inoc
B.
Wild-type
(Gent)
C.
ΔrecA
(Gent)
D.
Wild-type
(Cefo)
E.
ΔrecA
(Cefo)
DsRed
GFP

Figure 6.6

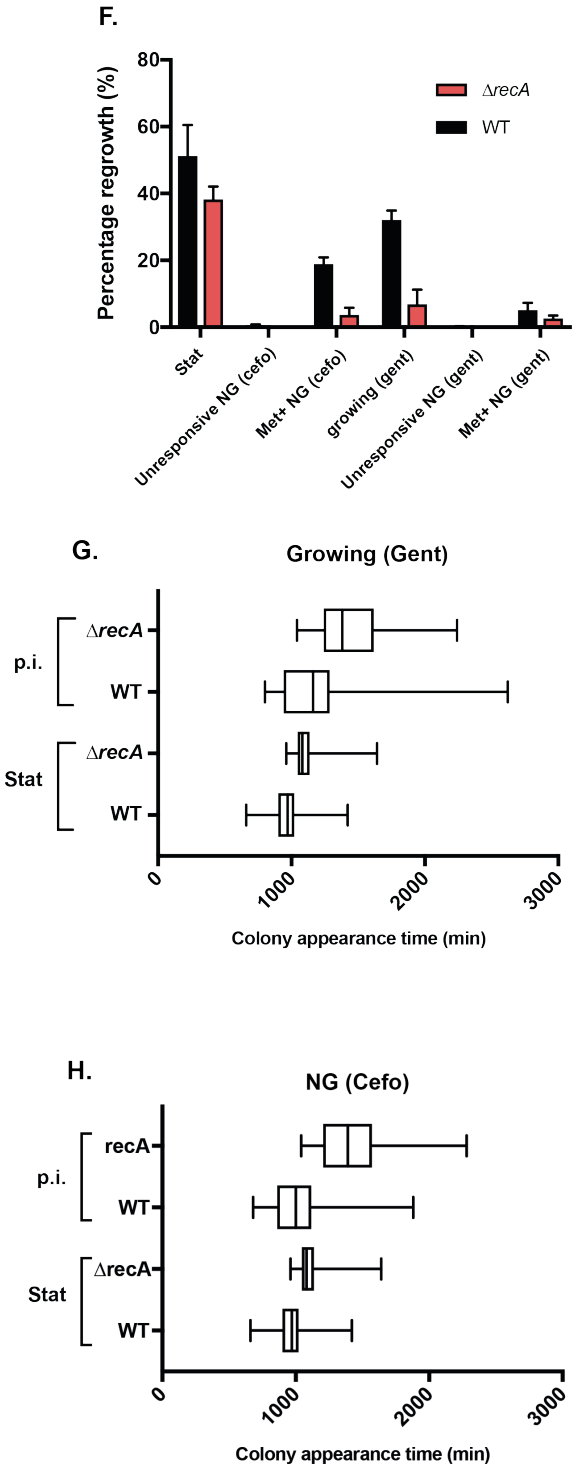


Figure 6.6. **The SOS response is important for reducing lag times in growing and NG *Salmonella* post-infection.** Bivariate plots of GFP (constitutive) and DsRed (arabinose-inducible) fluorescence levels in the inoculum (A), wild-type (B), Δ*recA* (C), post-infection in cefotaxime and wild-type (D) and Δ*recA* (E) post-infection in gentamicin, gating for sorting responsive NG, growing and unresponsive populations overlaid on plots. F) Bar chart of recovery rates of bacteria post-infection and after cell sorting of stationary phase (Stat) *Salmonella*, unresponsive and responsive bacteria post-infection with cefotaxime and unresponsive, responsive NGs and growing bacteria post-infection with gentamicin belonging to wild-type and Δ*recA* strains, values are mean ±S.E.M.. Box and whisker plots of colony appearance time distributions for stationary phase (Stat) and bacteria post-infection (p.i.) that are growing bacteria (gentamicin infection) (G) and responsive NGs (cefotaxime infection) (H) belonging to *S.* Typhimurium wild-type and Δ*recA*.

The recovery rates of the *S.* Typhimurium wild-type and Δ*recA* strains, in stationary phase (inocula) or post-infection are shown in figure 6.6F. The recovery rate was slightly lower for the Δ*recA* mutant from stationary phase than the wild-type, although the difference was not significant. However post-infection the Δ*recA* mutant had a much lower recovery rate than the wild-type, in both the growing population and with the NG bacteria isolated in cefotaxime. This result is in line with that made by a recent paper from the Brynildsen group (Völzing & Brynildsen 2015), however that study only made reference to persisters and did not measure the recovery of growing bacteria under stress. It is intriguing that the recovery rate of the growing *Salmonella* is so much lower post-infection and after cell sorting but the level of fluorescence dilution during infection is roughly the same as the wild-type strain. One hypothesis could be that the stress of release from the host macrophages or the cell-sorting could be responsible, however the difference in recovery rates between the sorted stationary phase samples belonging to the wild-type and the Δ*recA* strains was not large, meaning this could only be partially responsible. Alternatively, growth may be allowed to continue within the macrophage, however DNA damage that occurs may not be repaired in the Δ*recA* mutant, resulting in a large number of nonviable progeny.

The lag distributions for the *S.* Typhimurium wild-type and Δ*recA* strains based on colony appearance times as measured by ScanLag are displayed in figures 6.6G and 6.6H. As observed previously, all strains post-infection had an increased averaged colony appearance time (Figure 6.6G). Both growing and NG bacteria Δ*recA Salmonella* had significantly increased lag distributions compared to the wild-type, both in stationary phase and post-

infection. This is likely due to the inability to repair DNA damage accumulated in stationary phase or within the macrophage. The NG Δ*recA* bacteria had the longest colony appearance times, however the SOS response is unlikely to be specifically involved in the recovery of persisters as it affects the ability to regrow in all conditions tested and unlike with the TA modules mutants, the rate of growth *in vitro* is considerably slower in Δ*recA* (data not shown). This means that the colony appearance time may not be a good indicator of lag time in the founding cells, but an indicator of slower growth in general. However, the reduction in recovery rate post-infection and sorting in the Δ*recA* mutant while still exhibiting an FD profile similar to the wild-type is an interesting observation.

6.4 Conclusion

I adapted the ScanLag technique, developed by the Balaban group to our laboratory and used it to observe phenotypic heterogeneity in *E. coli* and *Salmonella* through recording the times colonies take to become visible to a scanner using time-lapse analysis. Two examples of phenotypic heterogeneity currently under investigation in *E. coli*, (i) the response to an inducer during stationary phase growth and (ii) the whole population lag in liquid culture and heterogeneous metabolic response of wild-type *E. coli* compared to a Δ*yeaG* mutant following nitrogen-starvation, could be linked to heterogeneity in individual cell lag times using ScanLag. No difference was detected in the ability of NG *Salmonella* following macrophage infection to recovery based on cellular DNA content, suggesting that the hypothesis made in chapter 4 that it decreases the time to recovery is invalid. It is however possible that this

increase in DNA is required for effective DNA repair during infection. It would therefore be interesting to measure the recovery rates of Δ*recA* NG bacteria that have undergone DNA replication during macrophage infection. Single deletions of TA modules do not appear to affect the recovery or lag time of NG *Salmonella*, however the deletion of *relBE1* and *tacAT* increased heterogeneity in the lag times of growing *Salmonella* post-infection, perhaps due to decreased ability to manage the stress of the SCV during infection. The role of the SOS response in NG *Salmonella*, as assessed through the deletion of Δ*recA*, appears to be important for recovery and reducing lag times, however this appeared to be true for growing bacteria also, indicating that it is likely not specific to persister recovery only. ScanLag is an effective method of measuring phenotypic heterogeneity in bacteria through lag times. One major caveat of the system that is difficult to control for the difference between lag time of colony-founding cells and the growth rate of a colony. Colony growth rate is difficult to measure using the technique due to the effect of neighbouring colonies, however this is likely only affecting the latter phase of colony growth, after the colony has become visible. Whole genome sequencing could be used alongside the technique to differentiate between genotypic (more likely affecting colony growth rate) and phenotypic heterogeneity (lag times) amongst bacterial populations, which is especially important to do when placing bacteria under the stress of infection.

Chapter Seven

Discussion

7.1 Dual RNA-seq reveals SPI-2 activity in NG *Salmonella* and polarisation towards an M2 phenotype in macrophages infected with viable *Salmonella*

The ability of NG *Salmonella* to produce fluorescent proteins (Helaine et al. 2014) provided evidence that active transcription was taking place in these bacteria, allowing comparative transcriptomic analysis against growing *Salmonella* to be possible. This inspired the recently developed dual RNA-seq technique (Westermann et al. 2012; Westermann et al. 2016) to be combined with fluorescence dilution and FACS to allow the heterogeneity present during macrophage infection with *Salmonella* to be dissected through transcriptomic analysis. A large gene expression data set was produced by this technique in both growing and NG *Salmonella* and the host macrophages they inhabit during infection. Immediate analysis was able to identify striking behaviours in both pathogen and host, including SPI-2 activity in NG *Salmonella* and polarisation of infected macrophages to an M2 phenotype. Expression of SPI-2 in NG *Salmonella* is particularly interesting as it has previously been reported that SPI-2 expression is associated with the intracellular proliferation of *Salmonella* (Helaine et al. 2010). It has recently been confirmed in our lab that SPI-2 is required for the metabolic activity of NGs. This subpopulation of metabolically active NG *Salmonella* expressing SPI-2 have been shown to induce an M2-like state of their host macrophages, while metabolically inactive NG *Salmonella* reside in M1 macrophages (Dr. P. Hill, Dr. D. Stapels,

unpublished data). The polarisation of macrophages containing *Salmonella* towards an anti-inflammatory M2 phenotype is fascinating. There are two major forms of activation described for macrophages, characterised by the expression of specific markers. M1 macrophages are activated by LPS or pro-inflammatory cytokines such as IFN-γ and produce IL-1b. M2 macrophages, also referred to as 'alternately-activated' macrophages are stimulated by cytokines such as IL-4 or IL-10. Increased expression of the receptor IL-4R is often used as a marker for these cells. They are connected to an T_h2 anti-parasitic response and are generally not considered competent for clearing bacterial pathogens (Martinez & Gordon 2014). Many bacteria are known to interfere with parts of the M1 response in macrophages such as phagosomal maturation in order to survive post-phagocytosis (this has been well reviewed by Scott et al. 2003). However there are also bacteria that appear to specifically induce an M2 transcriptional program. For example, *Yersinia enterocolitis* polarises host macrophages to an M2 phenotype during infection, this is dependent on expression of the Yop T3SS and the virulence factor LcrV (Hoffmann et al. 2004; Brubaker 2003). At first glance, this polarisation may explain the growth of *Salmonella* in BMM+G cells as an M2 phenotype would be more permissive for bacterial growth than M1 cells (Benoit et al. 2008). However, M2 markers are upregulated in BMM+NGs also, and SPI-2 is expressed with effectors being translocated by NG *Salmonella* into host cells (Dr. D. Stapels, unpublished data), therefore illustrating that another limitation to growth may be bacteria-driven, rather than a host factor. Furthermore, if BMMs are polarised towards an M2 state with IL-4 prior to infection, the same proportion of NG *Salmonella* are present compared to if no polarisation takes

place, indicating that the M1/M2 polarisation is not the key factor effecting *Salmonella* growth during infection (Dr. D. Stapels, unpublished data). The limitation could potentially be the result of TA module activity. It is interesting to note that tryptophan biosynthesis genes were upregulated in NG *Salmonella* and the *trpR* repressor was upregulated in growing *Salmonella* when these two transcriptomes were compared to one another. Upregulation of tryptophan biosynthesis genes has been recorded in chlamydia persisters present during infection of IFN-γ activated macrophages (Belland et al. 2003). The addition of tryptophan to the medium during infection reduced the level of NG persisters present during infection in this experimental set up (Beatty et al. 1994). Perhaps amino acid starvation could be leading to the activation of TA modules that inhbit bacterial growth in NG *Salmonella.*

Interestingly, the SPI-2 genes *sseD, sseE* and *sseF* were expressed at higher levels in NG *Salmonella* than in growing *Salmonella*. SseF is an effector translocated by SPI-2 that has been implicated in tethering the SCV to the Golgi apparatus in HeLa cells and affecting the migration of dendritic cells (Jennings et al. 2017). It is possible that the role of this effector is somehow important for NG *Salmonella.* The screening of SPI-2 effector mutants has revealed the effector responsible for the polarisation of macrophages to an M2 phenotype during infection of macrophages with *Salmonella,* although the mechanism is yet to be characterised (Dr. D. Stapels, unpublished data). While the concept of M1/M2 polarity in macrophage activation is useful in many contexts, it is also generally considered quite simplistic with a continuum of activation states thought to be possible (Martinez & Gordon 2014). Recent findings in our lab suggest that

the *Salmonella*-induced M2-like state is similar to both the M2a and M2b forms, induced by IL-4 and IL-10 respectively (Dr. D. Stapels, unpublished data).

Far more substantial results were gained from later three repeats of the dual RNA-seq compared to the preliminary trial run carried out. This could be partly due to the more stringent gating used during cell-sorting to ensure less contamination of the subpopulations with each other. However the quality control measures used to discard unreliable data in the preliminary run (selection of genes with RPKM values > 1) greatly reduced the number of genes in the analysis. This may have also introduced a bias for enriching small transcripts, such as miRNA and tRNAs. Directly comparing transcriptomes to each other rather than comparing via fold changes in expression from a control (inoculum or mock-infected macrophages) made observations of similar patterns of gene expression from one population to another (SPI-2 expression in NG and growing *Salmonella*) easier to make. Enrichment of coding RNAs is recommended for dual RNA-seq to reduce the depth of sequencing required as multiple samples are sequenced for each experiment, this is especially important if multiple runs of an experiment are to be carried out in order to reduce cost and time. The data set produced by this study will be useful for reference and further analysis in the future. Examples of potential further analysis of the data could be comparative transcriptomic analysis carried out without the removal of unwanted variables, or with the removal of certain outlying subpopulations. This could help identify phenotypes that exist only in two repeats within a subpopulation of bacteria or BMMs but not all three. Dual RNA-seq could also be carried out isolating

BMMs infected only with metabolically active NG *Salmonella*, as this subpopulation of NG bacteria has the greatest recovery rate post-infection, being more enriched for persisters.

The use of transcriptional studies on host gene expression during bacterial infection has previously identified polarisation to an M2 phenotype (Benoit et al. 2008). However, the simultaneous observation that macrophages infected with NG *Salmonella* had M2 markers upregulated in comparison to bystanders and that M2 polarisation correlates with SPI-2 expression (D. Stapels *et al.* unpublished data, personal communication) was made due to the powerful combination of FD, cell sorting and dual RNA-seq. This highlights the importance of considering heterogeneity during infection and not simply making observations on the whole population level. Using fluorescent reporters and cell sorting can allow for the transcriptional analysis of subpopulations of cells to reveal phenotypes that would have been missed during analysis of the entire population owing to averaging of data. Emerging techniques such as single cell RNA-seq promise to take this one step further by analysing the transcriptomes of individual cells, this technique has already confirmed the results made in this study (Saliba et al. 2016), however the technology is not yet capable of single cell bacterial transcriptomics. Previous transcriptional studies of persister-enriched fractions have been carried out *in vitro* (Keren, Shah, et al. 2004; Shah et al. 2006; Hansen et al. 2008). However, as persisters are generally studied owing to their link to persistent infections, the finding that NG *Salmonella* express SPI-2 during infection highlights the need to study these antibiotic tolerant cells in the context of infection.

7.2 NG *Salmonella* are capable of DNA replication during infection

The increased activity of ciprofloxacin against macrophage-induced *Salmonella* persisters compared to cefotaxime and gentamicin *in vitro* led us to investigate whether DNA replication was occurring in these cells. Ciprofloxacin is a fluoroquinolone antibiotic that targets DNA gyrase leading to double-stranded breaks in DNA during transcription and DNA synthesis. Evidence for active transcription in NG *Salmonella* during macrophage infection had already been reported (Helaine et al. 2014) through the production of a fluorescent protein encoded on a plasmid. However the possibility of DNA replication had not been ruled out. Using DAPI-staining combined with fluorescence dilution, NG *Salmonella* were found to increase in DNA content during infection. However late in infection of BMMs this NG *Salmonella* population reduced in DAPI levels, seemingly to that lower than 1N. The increasing proportion of growing bacteria during infection may have affected the ability to stain and observe the DNA in the NG bacteria properly. Cefotaxime was added to the infection medium in place of gentamicin, which is used in a standard *Salmonella* infection assay, in order to isolate only the NG intracellular *Salmonella.* This is due to the ability of cefotaxime to easily enter macrophage cells and kill any growing bacteria present. In contrast, gentamicin does not readily enter macrophage cells, which is why this antibiotic is used in infection assays, in order to inhibit extracellular bacterial growth only, although small amounts of the antibiotic may enter the host cell (Van der Auwera et al. 1988). By DAPI-staining NG *Salmonella* isolated in cefotaxime, the DNA content could be observed to increase in many NG bacteria during macrophage infection by 24 h.p.i. and remain at this high

level. Further experiments were carried out in these conditions as it provided the best opportunity to study the phenotype of DNA synthesis in NG *Salmonella* effectively. However it would be interesting to know whether the difference between the observations in NG *Salmonella* during a standard gentamicin-protection assay and an infection using cefotaxime isolation was due to technical difficulties (ie. staining efficiency) or biological (owing to the effect of small amounts of gentamicin). It is difficult to control for this effectively as an infection assay cannot be carried out without the presence of one of these antibiotics owing to the extracellular bacterial proliferation that would inevitably take place, resulting in macrophage cell death early on in infection. One experiment that could shed light on this scenario is the addition of both antibiotics to the infection media, compared to the addition of just each antibiotic singly. If the DAPI-staining reduces in the NG *Salmonella* population isolated in cefotaxime with gentamicin also added, as is observed in a standard gentamicin-protection assay using FD, but this does not occur during infection with only cefotaxime added to the medium, then it is likely owing to the gentamicin that the DAPI levels reduce. Exactly why this happens is another question, for the DAPI should not be lower than 1N, and could be the result of condensation of the bacterial chromosome. It is important to understand if NG *Salmonella* are being affected by the presence of gentamicin during infection to ensure results are not biased. This could be the case considering the recovery rate of metabolically active NG *Salmonella* isolated from a gentamicin protection assay was lower than that of metabolically active NG *Salmonella* isolated in cefotaxime during infection. In addition to this, further experimentation using EdU and click chemistry could

determine the timing of the DNA replication in these NG *Salmonella* more precisely.

The reason for the continued replication of DNA in NG *Salmonella* bacteria is elusive. I hypothesised that it may lead to faster recovery in these bacteria when whatever environmental condition limiting their growth is alleviated. When recovering of these NG bacteria in LB broth and flow cytometry, it appeared that this could be the case, as regrowing bacteria seemed to chiefly originate from a high-DNA, metabolically active population of NG bacteria. However, ScanLag was unable to detect any difference in the lag of colonies after sorting based on DNA content. What may be the most likely scenario is that DNA replication that is initiated after exposure to fresh medium immediately prior to phagocytosis is simply allowed to continue until resources become limited (such as amino acids - for example tryptophan). The fact that no defined peaks of DAPI fluorescence are usually visible in the NG *Salmonella* population post-macrophage infection suggests that DNA synthesis does not continue to completion of whole chromosomes, but becomes stalled part-way through. Attempts were made to use qPCR and primers targeting the origin and the terminus of the *Salmonella* chromosome on isolated NG *Salmonella* DNA to determine the *ori* / *ter* ratio in these bacteria. This ratio should be a value of 1 if all DNA synthesis was allowed to continue to completion (as the first part of a bacterial chromosome to be replicated is the origin and the last part is the terminus). However these experiments were largely inconclusive owing to an inability to isolate enough of the NG *Salmonella* DNA (data not shown). Another method that could be utilised is that of automated fluorescence microscopy with constructs enabling

the formation of fluorescent foci on *ori* and *ter* sequences, allowing the numbers of each to be counted in NG *Salmonella*. As this last method would allow the actual number of chromosomes to be counted also, it may help determine whether or not the DNA replication observed is chromosomal and not episomal or phage sequences. The presence of active DNA synthesis in NG *Salmonella* may explain why the ciprofloxacin was found to isolate less persisters than gentamicin and cefotaxime after exposure to macrophages (Helaine et al. 2014).

7.3 The toxin-antitoxin modules *yhfG-fic* and *parDE*

A defect during infection of RAW macrophages was observed in the double ΔTA Δ*parDE*Δ*yhfG-fic* mutant when compared to single mutants in each module or the wild-type. It was decided that if two TA modules with predicted similar activities, notably likely to be inhibiting DNA metabolism, were important to proliferation during infection it would be worth investigating. This growth defect was determined to be owing to a nutrient deficiency in minimal medium, and subsequently found that it could be complemented by the addition of *para*-aminobenzoate (PABA), a compound necessary for the biosynthesis of folate – an essential nutrient in bacterial growth. PABA is synthesised by the gene *pabA*, which is found immediately downstream of the toxin *fic.* A recent review from the Dehio group describes how in *E. coli*, a species in which this genomic region shares a remarkably similar identity with *Salmonella*, the promoter for the *pabA* gene is found within the *fic* gene itself (Harms, Stanger, et al. 2016). Hence deletion of this gene in my study likely resulted in a polar effect on the expression of the *pabA* gene, resulting in a

growth defect in minimal medium or during infection - environments where sources of folate are low. The possibility of a polar effect upon the deletion of the *yhfG-fic* was not investigated at first owing to the fact that this growth defect was not observed in the single deletion mutant of *S.* Typhimurium ∆*yhfG-fic*. As the resistance cassettes were not removed from these deletion strains, the promoter for the kanamycin resistance cassette is likely compensating for the removal of the native P_{pabA} promoter in the single ∆*yhfG-fic* deletion mutant. By contrast, the resistance cassette present in place of the *yhfG-fic* module in the ∆*parDE*∆*yhfG-fic* double deletion mutant was a chloramphenicol resistance cassette, it may be that the promoter for this gene is less strong than a kanamycin resistance cassette and may not be able to compensate for the disruption of the native P_{pabA} promoter. This could be tested by reconstructing the mutant strains leaving the *pabA* promoter intact within the end of the *fic* sequence. This highlights the importance, firstly, of removing antibiotic resistance cassettes upon deletion of genes in bacteria and secondly, ensuring the comparison of isogenic mutant strains.

The Fic toxin still remains an interesting candidate for study due to its noncanonical FIC domain, the activity of which is not likely to be UMPylation like most other bacterial Fic toxins (Harms, Stanger, et al. 2016). While study of the toxin seems to have been hampered by the probability of disrupting the expression of the essential *pabA* gene downstream (Harms, Stanger, et al. 2016), is interesting that the promoter for an essential gene is found within a toxin gene. The *ccdAB* module has been implicated in the regulation of downstream genes contributing to the stability of the pSLT virulence plasmid in *S*. Typhimurium (Lobato-Márquez, Molina-García, et al. 2016). Perhaps

yhfG-fic is somehow involved in the regulation of *pabA*. Fic was found to be nontoxic in *Salmonella*, implying its role may be unlike other type II TA modules studied. Interestingly, the single ΔTA mutants *S.* Typhimurium Δ*parDE* and Δ*yhfG-fic* appear to have defects in long-term survival in MgMES pH5, suggesting a role for these modules in dealing with stressful conditions over a long period of time. There is evidence that TA modules may have a role in virulence (Lobato-Márquez, Díaz-Orejas, et al. 2016). As long-term survival in the host will likely require exposure to similar conditions as long-term survival in MgMES pH5 medium, this may be the case for *parDE* and *yhfG-fic*. Mouse infections will likely be able to show whether a virulence defect in these ΔTA mutants exists.

7.4 The ScanLag technique is useful for studying bacterial heterogeneity through lag time distributions

One issue with experiments attempting to monitor the regrowth of persisters is the inability to make observations over a long period of time owing to 'early regrowing bacteria' overrunning an experiment. For example, using fluorescence dilution, any persisters that regrow upon recovery in LB broth post-macrophage infection quickly expand in size to make observations of the remaining NG bacteria present impossible due to the small proportion of their subpopulation within the sample. The ScanLag technique, developed by the Balaban group, offered a solution this problem. By spreading the bacterial sample on an agar plates and taking images for time-lapse analysis, the lag times of each persister cell present can be indirectly monitored by measuring the time taken for colonies to appear that form after cells resume

growth. As the growth of a colony will slow considerably after a certain amount of time and not just keep expanding over the agar plate, it allows the colonies formed by late-regrowing bacteria to be observed, increasing the amount of time allowed to observe regrowth from a persister sample from a few hours to several days (Levin-Reisman et al. 2010). It was decided that this technique would be of great use to the research of macrophage-induced *Salmonella* persisters.

After adapting the technique to our lab, it was used first to investigate forms of heterogeneity currently being studied in *E. coli*. ScanLag effectively showed that metabolic heterogeneity and the population level lag could be observed as heterogeneity in the lag distribution of individual cells indirectly through the formation of colonies. It could not however, reveal any difference in the lag time distributions of *Salmonella* with higher or lower DNA content post-macrophage infection. This gives evidence against the hypothesis that the continuation of DNA synthesis could be part of a bet-hedging strategy of *Salmonella* persisters to decrease lag time upon recovery. As many experiments linking TA modules to persister formation involved using CFU measurements, they did not effectively test whether a reduction in CFU could be due to late recovery or less recovery of NG cells. Using ScanLag to monitor the lag distribution of ΔTA mutants, I found no effect upon their deletion in NG *Salmonella* post-infection. However it did show a significant shift in lag towards later recovery times of cells when deleting TA modules in growing bacteria post-infection. This could be owing to TA modules having a role in dealing with the stress of macrophage-infection during growth. Alternatively, it could be hypothesised they are important in the transition from

one environment to another; for example moving from within a macrophage cell to an agar surface. In addition, the SOS response was found to be important in the recovery of both growing and NG *Salmonella* following macrophage infection. Interestingly, the recovery rates of *S.* Typhimurium Δ*recA* growing bacteria post-infection were exceptionally low, despite the same level of fluorescence dilution being observed in the growing bacteria as the wild-type. These bacteria deficient in the SOS response may be proliferating but generating nonviable progeny, likely the result of DNA damage sustained within the host cell. Evidence of the importance of the SOS response is furthered by the observed that the SOS gene *lexA* was observed to be upregulated in the RNA-seq data for growing *Salmonella* during infection.

One problem with adapting the ScanLag method I identified was a large amount of variation in the growth rate of colonies owing to the presence of neighbouring colonies on the agar plate, making this metric unreliable. Strangely, this was not observed to be the case in experiments in the Balaban lab. As genetic factors are likely the major reason for a slow-growing colony, the combination of this technique with whole-genome sequencing is recommended to increase its ability to separate phenotypic (affecting lag times) and genetic effects (effecting lag times or colony growth rate) on bacterial cells.

One serendipitous finding from using the technique was the usefulness of the recovery rate of bacteria post-infection. By monitoring the proportions of bacterial cells that did regrow after cell sorting it was clear that the metabolically active subpopulation of NG *Salmonella* were the major source of

persister regrowth following infection. This result is substantial as it is now known that these persisters are not dormant in any sense other than that of growth, but in fact synthesise and utilise the SPI-2 T3SS, and can undergo DNA synthesis, transcription and translation. This potentially provides ways of targeting these bacteria, either inhibiting their virulence (as SPI-2 is required for persister survival) or corrupting on going processes in order to kill them. Beta-lactam antibiotics are clearly not ideal for this job as they only target growing bacteria that are synthesising peptidoglycan. Aminoglycosides do not enter the cells efficiently enough to reach bactericidal levels. Ciprofloxacin has been reported to have higher activity against these NG *Salmonella*, however it does not eradicate them, perhaps because not all metabolically active NG *Salmonella* are replicating DNA. As regrowth of NG *Salmonella* originates from the subpopulation of metabolically active cells able to produce fluorescent proteins upon induction, improving the entry of antibiotics that inhibit bacterial transcription or translation into host cells and into the bacterial cells is likely a key issue to be tackled in order to effectively eradicate of this reservoir of persisters during infection.

Bibliography

Aballay, A., Yorgey, P. & Ausubel, F.M., 2000. *Salmonella* typhimurium proliferates and establishes a persistent infection in the intestine of *Caenorhabditis elegans*. *Current Biology*, 10(23), pp.1539–1542.

Adams, D.W. & Errington, J., 2009. Bacterial cell division: assembly, maintenance and disassembly of the Z ring. *Nature Reviews Microbiology*, 7, p.642.

Adams, D.W., Wu, L.J. & Errington, J., 2015. Nucleoid occlusion protein Noc recruits DNA to the bacterial cell membrane. *The EMBO Journal*, 34(4), pp.491–501.

Albrecht, M. et al., 2010. Deep sequencing-based discovery of the *Chlamydia trachomatis* transcriptome. *Nucleic Acids Research*, 38(3), pp.868–877.

Allison, K.R., Brynildsen, M.P. & Collins, J.J., 2011. Metabolite-enabled eradication of bacterial persisters by aminoglycosides. *Nature*, 473(7346), pp.216–220.

Amato, S. et al., 2014. The role of metabolism in bacterial persistence. *Frontiers in Microbiology*, 5, p.70.

Amato, S.M. & Brynildsen, M.P., 2015. Persister Heterogeneity Arising from a Single Metabolic Stress. *Current Biology*, 25(16), pp.2090–2098.

Amato, S.M., Orman, M.A. & Brynildsen, M.P., 2013. Metabolic Control of Persister Formation in *Escherichia coli*. *Molecular Cell*, 50(4), pp.475–487.

Angert, E.R., 2005. Alternatives to binary fission in bacteria. *Nat Rev Micro*, 3(3), pp.214–224.

Arjes, H.A. et al., 2014. Failsafe Mechanisms Couple Division and DNA Replication in Bacteria. *Current Biology*, 24(18), pp.2149–2155.

Armour, C.D. et al., 2009. Digital transcriptome profiling using selective hexamer priming for cDNA synthesis. *Nat Meth*, 6(9), pp.647–649.

Atlung, T., Clausen, E.S. & Hansen, F.G., 1985. Autoregulation of the dnaA gene of *Escherichia coli* K12. *Molecular and General Genetics MGG*, 200(3), pp.442–450.

Van der Auwera, P., Matsumoto, T. & Husson, M., 1988. Intraphagocytic penetration of antibiotics. *Journal of Antimicrobial Chemotherapy*, 22(2), pp.185–192.

Baba, T. et al., 2006. Construction of *Escherichia coli* K-12 in-frame, single-gene knockout mutants: the Keio collection. *Molecular Systems Biology*, 2(1), pp. 2006-2012.

Balaban, N.Q. et al., 2004. Bacterial Persistence as a Phenotypic Switch. *Science* , 305(5690), pp.1622–1625.

Barthel, M. et al., 2003. Pretreatment of Mice with Streptomycin Provides a *Salmonella* enterica Serovar Typhimurium Colitis Model That Allows Analysis of Both Pathogen and Host. *Infection and Immunity*, 71(5), pp.2839–2858.

Bäumler, A.J. et al., 1998. Evolution of Host Adaptation in *Salmonella* enterica. *Infection and Immunity*, 66(10), pp.4579–4587.

Bäumler, A.J., 1997. The record of horizontal gene transfer in *Salmonella*. *Trends in Microbiology*, 5(8), pp.318–322.

Bayer-Santos, E. et al., 2016. The *Salmonella* Effector SteD Mediates

MARCH8-Dependent Ubiquitination of MHC II Molecules and Inhibits T Cell Activation. *Cell Host & Microbe*, 20(5), pp.584–595.
Beaber, J.W., Hochhut, B. & Waldor, M.K., 2004. SOS response promotes horizontal dissemination of antibiotic resistance genes. *Nature*, 427(6969), pp.72–74.
Beatty, W.L. et al., 1994. Tryptophan depletion as a mechanism of gamma interferon-mediated chlamydial persistence. *Infection and Immunity* , 62(9), pp.3705–3711.
Belland, R.J. et al., 2003. Transcriptome analysis of chlamydial growth during IFN-γ-mediated persistence and reactivation. *Proceedings of the National Academy of Sciences* , 100(26), pp.15971–15976.
Benkovic, S.J., Valentine, A.M. & Salinas, F., 2001. Replisome-Mediated DNA Replication. *Annual Review of Biochemistry*, 70(1), pp.181–208.
Benoit, M., Desnues, B. & Mege, J.-L., 2008. Macrophage Polarization in Bacterial Infections. *The Journal of Immunology*, 181(6), p.3733-3739.
Van den Bergh, B. et al., 2016. Frequency of antibiotic application drives rapid evolutionary adaptation of *Escherichia coli* persistence. *Nature Microbiology*, 1, p.16020.
Bernard, P. et al., 1993. The F Plasmid CcdB Protein Induces Efficient ATP-dependent DNA Cleavage by Gyrase. *Journal of Molecular Biology*, 234(3), pp.534–541.
Bernhardt, T.G. & de Boer, P.A.J., 2005. SlmA, a Nucleoid-Associated, FtsZ Binding Protein Required for Blocking Septal Ring Assembly over Chromosomes in *E. coli*. *Molecular cell*, 18(5), pp.555–564.
Bhan, M.K., Bahl, R. & Bhatnagar, S., 2005. Typhoid and paratyphoid fever. *The Lancet*, 366(9487), pp.749–762.
Bi, E. & Lutkenhaus, J., 1991. FtsZ ring structure associated with division in Escherichia coli. *Nature*, 354, p.161.
Bigger, J.W., 1944. Treatment of Staphylococcal Infections with Penicillin by Intermittant Sterilisation. *Lancet*, 244(6320), pp.497–500.
Bingen, E. et al., 1992. DNA restriction fragment length polymorphism differentiates recurrence from relapse in treatment failures of *Streptococcus pyogenes* pharyngitis. *Journal of Medical Microbiology*, 37(3), pp.162–164.
Bipatnath, M., Dennis, P.P. & Bremer, H., 1998. Initiation and Velocity of Chromosome Replication in *Escherichia coli* B/r and K-12. *Journal of Bacteriology*, 180(2), pp.265–273.
Blair, J.M.A. et al., 2015. Molecular mechanisms of antibiotic resistance. *Nat Rev Micro*, 13(1), pp.42–51.
De Bolle, X. et al., 2015. *Brucella abortus* Cell Cycle and Infection Are Coordinated. *Trends in Microbiology*, 23(12), pp.812–821.
Boye, E. & Nordström, K., 2003. Coupling the cell cycle to cell growth. *EMBO reports*, 4(8), p.757 LP-760.
Brandt, S.M. et al., 2004. Secreted Bacterial Effectors and Host-Produced Eiger/TNF Drive Death in a *Salmonella*-Infected Fruit Fly. *PLOS Biology*, 2(12), p.e418.
Braun, R.E., O'Day, K. & Wright, A., 1985. Autoregulation of the DNA replication gene dnaA in *E. coli* K-12. *Cell*, 40(1), pp.159–169.
Brauner, A. et al., 2016. Distinguishing between resistance, tolerance and persistence to antibiotic treatment. *Nat Rev Micro*, 14(5), pp.320–330.

Brendler, T., Abeles, A. & Austin, S., 1995. A protein that binds to the P1 origin core and the oriC 13mer region in a methylation-specific fashion is the product of the host seqA gene. *The EMBO journal*, 14(16), p.4083—4089.

Brooun, A., Liu, S. & Lewis, K., 2000. A Dose-Response Study of Antibiotic Resistance in *Pseudomonas aeruginosa* Biofilms. *Antimicrobial Agents and Chemotherapy*, 44(3), pp.640–646.

Brubaker, R.R., 2003. Interleukin-10 and Inhibition of Innate Immunity to Yersiniae: Roles of Yops and LcrV (V Antigen). *Infection and Immunity* , 71(7), pp.3673–3681.

Bruno, V.M. et al., 2009. *Salmonella* Typhimurium Type III Secretion Effectors Stimulate Innate Immune Responses in Cultured Epithelial Cells. *PLOS Pathogens*, 5(8), p.e1000538.

Bryers, J.D., 2008. Medical biofilms. *Biotechnology and Bioengineering*, 100(1), pp.1–18.

Buckle, G.C., Walker, C.L.F. & Black, R.E., 2012. Typhoid fever and paratyphoid fever: Systematic review to estimate global morbidity and mortality for 2010. *Journal of Global Health*, 2(1), p.10401.

Burmølle, M. et al., 2010. Biofilms in chronic infections – a matter of opportunity – monospecies biofilms in multispecies infections. *FEMS Immunology Medical Microbiology*, 59(3), p.324-336.

Cameron, A.D.S., Stoebel, D.M. & Dorman, C.J., 2011. DNA supercoiling is differentially regulated by environmental factors and FIS in *Escherichia coli* and *Salmonella* enterica. *Molecular Microbiology*, 80(1), pp.85–101.

Cammarota, G. et al., 2012. Review article: biofilm formation by Helicobacter pylori as a target for eradication of resistant infection. *Alimentary Pharmacology & Therapeutics*, 36(3), 222–230.

Carter, P.B. & Collins, F.M., 1974. The Route of Enteric Infection in Normal Mice. *The Journal of Experimental Medicine*, 139(5), pp.1189–1203.

Castro-Roa, D. et al., 2013. The Fic protein Doc uses an inverted substrate to phosphorylate and inactivate EF-Tu. *Nat Chem Biol*, 9(12), pp.811–817.

Cataudella, I. et al., 2012. Conditional cooperativity in toxin–antitoxin regulation prevents random toxin activation and promotes fast translational recovery. *Nucleic Acids Research* , 40(14), pp.6424–6434.

Caygill, C.P.J. et al., 1994. Cancer mortality in chronic typhoid and paratyphoid carriers. *The Lancet*, 343(8889), pp.83–84.

Cheverton, A.M. et al., 2016. A *Salmonella* Toxin Promotes Persister Formation through Acetylation of tRNA. *Molecular Cell*, 63(1), pp.86–96.

Chiaramello, A.E. & Zyskind, J.W., 1989. Expression of *Escherichia coli* dnaA and mioC genes as a function of growth rate. *Journal of Bacteriology* , 171(8), pp.4272–4280.

Chowdhury, N., Kwan, B.W. & Wood, T.K., 2016. Persistence Increases in the Absence of the Alarmone Guanosine Tetraphosphate by Reducing Cell Growth. *Scientific Reports*, 6, p.20519.

Christensen-Dalsgaard, M., Jørgensen, M.G. & Gerdes, K., 2010. Three new RelE-homologous mRNA interferases of *Escherichia coli* differentially induced by environmental stresses. *Molecular Microbiology*, 75(2), pp.333–348.

Christensen, S.K. et al., 2003. Toxin–antitoxin Loci as Stress-response-elements: ChpAK/MazF and ChpBK Cleave Translated RNAs and are

Counteracted by tmRNA. *Journal of Molecular Biology*, 332(4), pp.809–819.
Christensen, S.K. & Gerdes, K., 2003. RelE toxins from bacteria and Archaea cleave mRNAs on translating ribosomes, which are rescued by tmRNA. *Mol Microbiol*, 48, pp.1389–1400.
Churchward, G. & Bremer, H., 1977. Determination of deoxyribonucleic acid replication time in exponentially growing *Escherichia coli* B/r. *Journal of Bacteriology*, 130(3), pp.1206–1213.
Claudi, B. et al., 2014. Phenotypic Variation of *Salmonella* in Host Tissues Delays Eradication by Antimicrobial Chemotherapy. *Cell*, 158(4), pp.722–733.
Coburn, B. et al., 2005. *Salmonella enterica* Serovar Typhimurium Pathogenicity Island 2 Is Necessary for Complete Virulence in a Mouse Model of Infectious Enterocolitis . *Infection and Immunity*, 73(6), pp.3219–3227.
Coburn, B., Grassl, G.A. & Finlay, B.B., 2006. *Salmonella*, the host and disease: a brief review. *Immunol Cell Biol*, 85(2), pp.112–118.
Cohen, N.R., Lobritz, M.A. & Collins, J.J., 2013. Microbial Persistence and the Road to Drug Resistance. *Cell Host & Microbe*, 13(6), pp.632–642.
Conlon, B.P. et al., 2013. Activated ClpP kills persisters and eradicates a chronic biofilm infection. *Nature*, 503(7476), pp.365–70.
Conlon, B.P. et al., 2016. Persister formation in *Staphylococcus aureus* is associated with ATP depletion. *Nature Microbiology*, 1, p.16051-16055.
Costerton, J.W., Stewart, P.S. & Greenberg, E.P., 1999. Bacterial biofilms: A common cause of persistent infections. *Science*, 284, pp.1318–1322.
Cox, M.M. et al., 2000. The importance of repairing stalled replication forks. *Nature*, 404, p.37.
Crawford, R.W. et al., 2010. Gallstones play a significant role in *Salmonella* spp. gallbladder colonization and carriage. *Proceedings of the National Academy of Sciences of the United States of America*, 107(9), pp.4353–4358.
Crosa, J.H. et al., 1973. Molecular Relationships Among the Salmonelleae. *Journal of Bacteriology*, 115(1), pp.307–315.
Crump, J.A. & Mintz, E.D., 2010. Global Trends in Typhoid and Paratyphoid Fever. *Clinical Infectious Diseases*, 50(2), pp.241–246.
Datsenko, K.A. & Wanner, B.L., 2000. One-step inactivation of chromosomal genes in *Escherichia coli* K-12 using PCR products. *PNAS*, 97, pp.6640–6645.
Davies, J.C., 2002. *Pseudomonas aeruginosa* in cystic fibrosis: pathogenesis and persistence. *Paediatric Respiratory Reviews*, 3(2), pp.128–134.
Deghelt, M. et al., 2014. G1-arrested newborn cells are the predominant infectious form of the pathogen Brucella abortus. *Nature Communications*, 5, p.4366.
Desai, P.T. et al., 2013. Evolutionary Genomics of *Salmonella enterica* Subspecies. *mBio* , 4(2). pp. 579-582
Domenech, M. et al., 2013. Biofilm Formation Avoids Complement Immunity and Phagocytosis of *Streptococcus pneumoniae* L. Pirofski, ed. *Infection and Immunity*, 81(7), pp.2606–2615.
Donegan, N.P. & Cheung, A.L., 2009. Regulation of the mazEF Toxin-Antitoxin Module in *Staphylococcus aureus* and Its Impact on *sigB*

Expression . *Journal of Bacteriology* , 191(8), pp.2795–2805.
Dörr, T., Lewis, K. & Vulić, M., 2009. SOS Response Induces Persistence to Fluoroquinolones in *Escherichia coli*. *PLOS Genetics*, 5(12), p.e1000760.
Dörr, T., Vulić, M. & Lewis, K., 2010. Ciprofloxacin Causes Persister Formation by Inducing the TisB toxin in *Escherichia coli*. *PLoS Biol*, 8(2), p.e1000317.
Eberth, C.J., 1880. Die Organismen in den Organen bei Typhus abdominalis. *Archiv für pathologische Anatomie und Physiologie und für klinische Medicin*, 81(1), pp.58–74.
Edsall, G. et al., 1960. Studies of Infection and Immunity in Experimental Typhoid Fever. *The Journal of Experimental Medicine*, 112(1), p.143-166.
Eriksson, S. et al., 2003. Unravelling the biology of macrophage infection by gene expression profiling of intracellular *Salmonella enterica*. *Molecular Microbiology*, 47(1), pp.103–118.
Eslick, G.D. et al., 1999. Association of *Helicobacter pylori* infection with gastric carcinoma: a meta-analysis. *Am J Gastroenterol*, 94(9), pp.2373–2379.
Fasani, R.A. & Savageau, M.A., 2013. Molecular mechanisms of multiple toxin–antitoxin systems are coordinated to govern the persister phenotype. *Proceedings of the National Academy of Sciences* , 110(27), pp.2528–2537.
Feasey, N.A. et al., 2012. Invasive non-typhoidal *Salmonella* disease: an emerging and neglected tropical disease in Africa. *Lancet*, 379(9835), pp.2489–2499.
Ferullo, D.J. et al., 2009. Cell cycle synchronization of *E. coli* using the stringent response, with fluorescence labeling assays for DNA content and replication. *Methods (San Diego, Calif.)*, 48(1), pp.8–13.
Ferullo, D.J. & Lovett, S.T., 2008. The Stringent Response and Cell Cycle Arrest in *Escherichia coli*. *PLOS Genetics*, 4(12), p.e1000300.
Figueira, R. et al., 2015. Adaptation to sustained nitrogen starvation by *Escherichia coli* requires the eukaryote-like serine/threonine kinase YeaG. *Scien*, 5, p.17524.
Figueira, R. & Holden, D.W., 2012. Functions of the *Salmonella* pathogenicity island 2 (SPI-2) type III secretion system effectors. *Microbiology*, 158(5), pp.1147–1161.
Fisher, R.A., Gollan, B. & Helaine, S., 2017. Persistent bacterial infections and persister cells. *Nat Rev Micro*, advance on.
Fodor, S.P.A. et al., 1993. Multiplexed biochemical assays with biological chips. *Nature*, 364(6437), pp.555–556.
Forbes, J.R. & Gros, P., 2003. Iron, manganese, and cobalt transport by Nramp1 (Slc11a1) and Nramp2 (Slc11a2) expressed at the plasma membrane. *Blood*, 102(5), p.1884-1892.
Förstner, K.U., Vogel, J. & Sharma, C.M., 2014. READemption—a tool for the computational analysis of deep-sequencing–based transcriptome data. *Bioinformatics*, 30(23), pp.3421–3423.
Foxman, B., 1990. Recurring urinary tract infection: incidence and risk factors. *American Journal of Public Health*, 80(3), pp.331–333.
Frandsen, J.L. et al., 2008. *Salmonella* pathogenesis reveals that BMP signaling regulates blood cell homeostasis and immune responses in Drosophila. *Proceedings of the National Academy of Sciences*, 105(39),

pp.14952–14957.
Fridman, O. et al., 2014. Optimization of lag time underlies antibiotic tolerance in evolved bacterial populations. *Nature*, 513(7518), pp.418–421.
Fu, Z. et al., 2009. Overexpression of MazFSa in *Staphylococcus aureus* Induces Bacteriostasis by Selectively Targeting mRNAs for Cleavage . *Journal of Bacteriology* , 191(7), pp.2051–2059.
Funnell, B.E., Baker, T.A. & Kornberg, A., 1987. In vitro assembly of a prepriming complex at the origin of the *Escherichia coli* chromosome. *Journal of Biological Chemistry* , 262(21), pp.10327–10334.
Gaffky, G., 1884. Zur Ätiologie des Abdominal-Typhus. *Mitteilungen aus dem kaiserlichen Gesundheitsamte, Berlin*, 2:, pp.372–420.
Gahlmann, A. & Moerner, W.E., 2014. Exploring bacterial cell biology with single-molecule tracking and super-resolution imaging. *Nat Rev Micro*, 12(1), pp.9–22.
Gaines, S. et al., 1968. Studies on Infection and Immunity in Experimental Typhoid Fever: VII. The Distribution of *Salmonella* typhi in Chimpanzee Tissue following Oral Challenge, and the Relationship between the Numbers of Bacilli and Morphologic Lesions. *The Journal of Infectious Diseases*, 118(3), pp.293–306.
Galán, J.E. & Curtiss, R., 1989. Cloning and molecular characterization of genes whose products allow *Salmonella* typhimurium to penetrate tissue culture cells. *Proceedings of the National Academy of Sciences* , 86(16), pp.6383–6387.
Gerdes, K., Christensen, S.K. & Lobner-Olesen, A., 2005. Prokaryotic toxin-antitoxin stress response loci. *Nat Rev Microbiol*, 3, pp.371–382.
Gerdes, K., Rasmussen, P.B. & Molin, S., 1986. Unique type of plasmid maintenance function: postsegregational killing of plasmid-free cells. *Proceedings of the National Academy of Sciences*, 83(10), pp.3116–3120.
Germain, E. et al., 2013. Molecular Mechanism of Bacterial Persistence by HipA. *Molecular Cell,* 52(2), pp.248-54.
Germain, E. et al., 2015. Stochastic induction of persister cells by HipA through (p)ppGpp-mediated activation of mRNA endonucleases. *Proceedings of the National Academy of Sciences* , 112(16), pp.5171–5176.
Giudice, E. & Gillet, R., 2013. The task force that rescues stalled ribosomes in bacteria. *Trends in Biochemical Sciences*, 38(8), pp.403–411.
Gomez, J.E. & McKinney, J.D., 2004. *M. tuberculosis* persistence, latency, and drug tolerance. *Tuberculosis*, 84(1–2), pp.29–44.
Gonçalves-Pereira, J. & Póvoa, P., 2011. Antibiotics in critically ill patients: a systematic review of the pharmacokinetics of β-lactams. *Critical Care*, 15(5), pp.1–17.
Gondwe, E.N. et al., 2010. Importance of antibody and complement for oxidative burst and killing of invasive nontyphoidal *Salmonella* by blood cells in Africans. *Proceedings of the National Academy of Sciences of the United States of America*, 107(7), pp.3070–3075.
Gonzalez-Escobedo, G., Marshall, J.M. & Gunn, J.S., 2011. Chronic and acute infection of the gall bladder by *Salmonella* Typhi: understanding the carrier state. *Nat Rev Micro*, 9(1), pp.9–14.
Goodman, M.F., 2002. Error-Prone Repair DNA Polymerases in Prokaryotes

and Eukaryotes. *Annual Review of Biochemistry*, 71(1), pp.17–50.
Goranov, A.I. et al., 2005. A transcriptional response to replication status mediated by the conserved bacterial replication protein DnaA. *Proceedings of the National Academy of Sciences of the United States of America* , 102(36), pp.12932–12937.
Gordon, M.A., 2011. Invasive Non-typhoidal *Salmonella* Disease – epidemiology, pathogenesis and diagnosis. *Current opinion in infectious diseases*, 24(5), pp.484–489.
Gordon, M.A. et al., 2010. Invasive Non-typhoid Salmonellae Establish Systemic Intracellular Infection in HIV-Infected Adults: An Emerging Disease Pathogenesis. *Clinical Infectious Diseases*, 50(7), pp.953–962.
Gordon, M.A., 2008. *Salmonella* infections in immunocompromised adults. *Journal of Infection*, 56(6), pp.413–422.
Gotuzzo, E. et al., 1987. Association between specific plasmids and relapse in typhoid fever. *Journal of Clinical Microbiology*, 25(9), pp.1779–1781.
Grant, A.J. et al., 2012. Attenuated *Salmonella* Typhimurium Lacking the Pathogenicity Island-2 Type 3 Secretion System Grow to High Bacterial Numbers inside Phagocytes in Mice. *PLOS Pathogens*, 8(12), p.e1003070.
Grant, S.S. & Hung, D.T., 2013. Persistent bacterial infections, antibiotic tolerance, and the oxidative stress response. *Virulence*, 4(4), pp.273–283.
Hall, A.M.J., Gollan, B. & Helaine, S., 2017. Toxin–antitoxin systems: reversible toxicity. *Current Opinion in Microbiology*, 36, pp.102–110.
Hannemann, S., Gao, B. & Galán, J.E., 2013. *Salmonella* Modulation of Host Cell Gene Expression Promotes Its Intracellular Growth. *PLOS Pathogens*, 9(10), p.e1003668.
Hansen, S., Lewis, K. & Vulić, M., 2008. Role of Global Regulators and Nucleotide Metabolism in Antibiotic Tolerance in *Escherichia coli* . *Antimicrobial Agents and Chemotherapy* , 52(8), pp.2718–2726.
Hapfelmeier, S. et al., 2004. Role of the *Salmonella* Pathogenicity Island 1 Effector Proteins SipA, SopB, SopE, and SopE2 in *Salmonella* enterica Subspecies 1 Serovar Typhimurium Colitis in Streptomycin-Pretreated Mice . *Infection and Immunity*, 72(2), pp.795–809.
Harms, A. et al., 2015. Adenylylation of Gyrase and Topo IV by FicT Toxins Disrupts Bacterial DNA Topology. *Cell Reports*, 12(9), pp.1497–1507.
Harms, A., Maisonneuve, E. & Gerdes, K., 2016. Mechanisms of bacterial persistence during stress and antibiotic exposure. *Science*, 354(6318).
Harms, A., Stanger, F. V & Dehio, C., 2016. Biological Diversity and Molecular Plasticity of FIC Domain Proteins. *Annual Review of Microbiology*, 70(1), pp.341–360.
Harris, J. & Keane, J., 2010. How tumour necrosis factor blockers interfere with tuberculosis immunity. *Clinical and Experimental Immunology*, 161(1), pp.1–9.
Harrison, J.J. et al., 2009. The Chromosomal Toxin Gene yafQ Is a Determinant of Multidrug Tolerance for *Escherichia coli* Growing in a Biofilm . *Antimicrobial Agents and Chemotherapy* , 53(6), pp.2253–2258.
Hayashi, M. et al., 2005. Bacillus subtilis YabA is involved in determining the timing and synchrony of replication initiation. *FEMS Microbiology Letters*, 247(1), pp.73–79.

Helaine, S. et al., 2010. Dynamics of intracellular bacterial replication at the single cell level. *Proceedings of the National Academy of Sciences of the United States of America*, 107(8), pp.3746–51.
Helaine, S. et al., 2014. Internalization of *Salmonella* by Macrophages Induces Formation of Nonreplicating Persisters. *Science* , 343(6167), pp.204–208.
Helaine, S. & Kugelberg, E., 2014. Bacterial persisters: Formation, eradication, and experimental systems. *Trends in Microbiology*, 22(7), pp.417–424.
Helmstetter, C.E. & Cooper, S., 1968. DNA synthesis during the division cycle of rapidly growing *Escherichia coli* Br. *Journal of Molecular Biology*, 31(3), pp.507–518.
Hensel, M. et al., 1995. Simultaneous identification of bacterial virulence genes by negative selection. *Science*, 269(5222), pp.400–403.
Hill, T.M., 1992. Arrest of Bacterial DNA Replication. *Annual Review of Microbiology*, 46(1), pp.603–633.
Hinton, J.C.D. et al., 2004. Benefits and pitfalls of using microarrays to monitor bacterial gene expression during infection. *Current Opinion in Microbiology*, 7(3), pp.277–282.
Hobby, G.L., Meyer, K. & Chaffee, E., 1942. Observations on the Mechanism of Action of Penicillin. *Experimental Biology and Medicine* , 50(2), pp.281–285.
Hoffmann, R. et al., 2004. Transcriptional responses of murine macrophages to infection with Yersinia enterocolitica. *Cellular Microbiology*, 6(4), pp.377–390.
Huang, D.W. et al., 2007. The DAVID Gene Functional Classification Tool: a novel biological module-centric algorithm to functionally analyze large gene lists. *Genome Biology*, 8(9), p.R183.
Hunstad, D.A. & Justice, S.S., 2010. Intracellular Lifestyles and Immune Evasion Strategies of Uropathogenic *Escherichia coli*. *Annual Review of Microbiology*, 64(1), pp.203–221.
Ibarra, J.A. & Steele-Mortimer, O., 2009. *Salmonella* – the ultimate insider. *Salmonella* virulence factors that modulate intracellular survival. *Cellular Microbiology*, 11(11), pp.1579–1586.
Ina, K., Kusugami, K. & Ohta, M., 2003. Bacterial hemorrhagic enterocolitis. *Journal of Gastroenterology*, 38(2), pp.111–120.
Jennings, E., Thurston, T.L.M. & Holden, D.W., 2017. *Salmonella* SPI-2 Type III Secretion System Effectors: Molecular Mechanisms And Physiological Consequences. *Cell Host & Microbe*, 22(2), pp.217–231.
Jernberg, C. et al., 2010. Long-term impacts of antibiotic exposure on the human intestinal microbiota. *Microbiology*, 156(11), pp.3216–3223.
Jesaitis, A.J. et al., 2003. Compromised Host Defense on Pseudomonas aeruginosa Biofilms: Characterization of Neutrophil and Biofilm Interactions . *The Journal of Immunology* , 171(8), pp.4329–4339.
Jiang, Y. et al., 2002. ParE toxin encoded by the broad-host-range plasmid RK2 is an inhibitor of *Escherichia coli* gyrase. *Molecular Microbiology*, 44(4), pp.971–979.
de Jong, H.K. et al., 2012. Host–Pathogen Interaction in Invasive Salmonellosis. *PLOS Pathogens*, 8(10), p.e1002933.
Kardas, P., 2002. Patient compliance with antibiotic treatment for respiratory

tract infections. *Journal of Antimicrobial Chemotherapy* , 49(6), pp.897–903.
Kaspy, I. et al., 2013. HipA-mediated antibiotic persistence via phosphorylation of the glutamyl-tRNA-synthetase. *Nature Communications*, 4, p.3001.
Katayama, T. et al., 1998. The Initiator Function of DnaA Protein Is Negatively Regulated by the Sliding Clamp of the *E. coli* Chromosomal Replicase. *Cell*, 94(1), pp.61–71.
Kato, J. & Katayama, T., 2001. Hda, a novel DnaA-related protein, regulates the replication cycle in *Escherichia coli*. *The EMBO Journal*, 20(15), p.4253 LP-4262.
Kauffmann, F., 1972. *Serological diagnosis of Salmonella-species. Kauffmann-White-Schema.*, Munksgaard, Copenhagen, Denmark.
Keren, I., Kaldalu, N., et al., 2004. Persister cells and tolerance to antimicrobials. *FEMS Microbiol Lett*, 230, pp.13–18.
Keren, I., Shah, D., et al., 2004. Specialized persister cells and the mechanism of multidrug tolerance in *Escherichia coli*. *J Bacteriol*, 186, pp.8172–8180.
Kingsley, R.A. et al., 2009. Epidemic multiple drug resistant *Salmonella* Typhimurium causing invasive disease in sub-Saharan Africa have a distinct genotype. *Genome Research* , 19(12), pp.2279–2287.
Kingsley, R.A. & Bäumler, A.J., 2000. Host adaptation and the emergence of infectious disease: the *Salmonella* paradigm. *Molecular Microbiology*, 36(5), pp.1006–1014.
Kint, C. et al., 2014. Bacterial Obg proteins: GTPases at the nexus of protein and DNA synthesis. *Critical Reviews in Microbiology*, 40(3), pp.207–224.
Kitagawa, R. et al., 1998. Negative control of replication initiation by a novel chromosomal locus exhibiting exceptional affinity for *Escherichia coli* DnaA protein. *Genes & Development* , 12(19), pp.3032–3043.
Kodzius, R. et al., 2006. CAGE: cap analysis of gene expression. *Nat Meth*, 3(3), pp.211–222.
Kröger, C. et al., 2013. An Infection-Relevant Transcriptomic Compendium for *Salmonella* enterica Serovar Typhimurium. *Cell Host & Microbe*, 14(6), pp.683–695.
Kronstad, J.W., 2006. Serial Analysis of Gene Expression in Eukaryotic Pathogens. *Infectious Disorders - Drug Targets*, 6(3), pp.281–297.
Kuijl, C. et al., 2013. Rac and Rab GTPases dual effector Nischarin regulates vesicle maturation to facilitate survival of intracellular bacteria. *The EMBO Journal*, 32(5), pp.713–727.
Labrousse, A. et al., 2000. *Caenorhabditis elegans* is a model host for *Salmonella* typhimurium. *Current Biology*, 10(23), pp.1543–1545.
LaFleur, M.D., Qi, Q. & Lewis, K., 2010. Patients with Long-Term Oral Carriage Harbor High-Persister Mutants of Candida albicans . *Antimicrobial Agents and Chemotherapy* , 54(1), pp.39–44.
Lan, R., Reeves, P.R. & Octavia, S., 2009. Population structure, origins and evolution of major *Salmonella* enterica clones. *Infection, Genetics and Evolution*, 9(5), pp.996–1005.
Laub, M.T., Shapiro, L. & McAdams, H.H., 2007. Systems Biology of Caulobacter. *Annual Review of Genetics*, 41(1), pp.429–441.
Lawn, S.D., Butera, S.T. & Shinnick, T.M., 2002. Tuberculosis unleashed: the

impact of human immunodeficiency virus infection on the host granulomatous response to *Mycobacterium tuberculosis*. *Microbes and Infection*, 4(6), pp.635–646.

Layton, J.C. & Foster, P.L., 2003. Error-prone DNA polymerase IV is controlled by the stress-response sigma factor, RpoS, in *Escherichia coli*. *Molecular Microbiology*, 50(2), pp.549–561.

Leitão, E. et al., 2014. *Listeria monocytogenes* induces host DNA damage and delays the host cell cycle to promote infection. *Cell Cycle*, 13(6), pp.928–940.

Levin-Reisman, I. et al., 2017. Antibiotic tolerance facilitates the evolution of resistance. *Science*, 355(6327), pp.826–830.

Levin-Reisman, I. et al., 2010. Automated imaging with ScanLag reveals previously undetectable bacterial growth phenotypes. *Nat Meth*, 7(9), pp.737–739.

Levin, J.Z. et al., 2010. Comprehensive comparative analysis of strand-specific RNA sequencing methods. *Nat Meth*, 7(9), pp.709–715.

Levine, M.M., Black, R.E. & Lanata, C., 1982. Precise Estimation of the Numbers of Chronic Carriers of *Salmonella* typhi in Santiago, Chile, an Endemic Area. *Journal of Infectious Diseases* , 146(6), pp.724–726.

Lewis, K., 2010. Persister Cells. *Annual Review of Microbiology*, 64(1), pp.357–372.

Libby, S.J. et al., 2010. Humanized nonobese diabetic-scid IL2rγnull mice are susceptible to lethal *Salmonella* Typhi infection. *Proceedings of the National Academy of Sciences* , 107(35), pp.15589–15594.

Lobato-Márquez, D. et al., 2015. Distinct type I and type II toxin-antitoxin modules control *Salmonella* lifestyle inside eukaryotic cells. *Scientific Reports*, 5, p.9374.

Lobato-Márquez, D., Molina-García, L., et al., 2016. Stabilization of the Virulence Plasmid pSLT of *Salmonella* Typhimurium by Three Maintenance Systems and Its Evaluation by Using a New Stability Test. *Frontiers in Molecular Biosciences*, 3, p.66.

Lobato-Márquez, D., Díaz-Orejas, R. & García-del Portillo, F., 2016. Toxin-antitoxins and bacterial virulence. *FEMS Microbiology Reviews*, 40(5), pp.592–609.

Lyczak, J.B., Cannon, C.L. & Pier, G.B., 2002. Lung Infections Associated with Cystic Fibrosis. *Clinical Microbiology Reviews* , 15(2), pp.194–222.

MacLennan, C.A. et al., 2010. Dysregulated humoral immunity to nontyphoidal *Salmonella* in HIV-infected African adults. *Science (New York, N.Y.)*, 328(5977), pp.508–512.

Maisonneuve, E. et al., 2011. Bacterial persistence by RNA endonucleases. *Proceedings of the National Academy of Sciences* , 108(32), pp.13206–13211.

Maisonneuve, E., Castro-Camargo, M. & Gerdes, K., 2013. (p)ppGpp controls bacterial persistence by stochastic induction of toxin-antitoxin activity. *Cell*, 154(5), pp.1140–1150.

Majowicz, S.E. et al., 2010. The Global Burden of Nontyphoidal *Salmonella* Gastroenteritis. *Clinical Infectious Diseases*, 50(6), pp.882–889.

Manina, G., Dhar, N. & McKinney, J.D., 2015. Stress and Host Immunity Amplify *Mycobacterium tuberculosis* Phenotypic Heterogeneity and Induce Nongrowing Metabolically Active Forms. *Cell Host & Microbe*,

17(1), pp.32–46.
Martín, C.M. & Guzmán, E.C., 2011. DNA replication initiation as a key element in thymineless death. *DNA Repair*, 10(1), pp.94–101.
Martinez, F.O. & Gordon, S., 2014. The M1 and M2 paradigm of macrophage activation: time for reassessment. *F1000Prime Reports*, 6, p.13.
Matsumura, H. et al., 2012. SuperSAGE: Powerful Serial Analysis of Gene Expression. In H. Jin & W. Gassmann, eds. *RNA Abundance Analysis: Methods and Protocols*. Totowa, NJ: Humana Press, pp. 1–17.
Maudet, C. et al., 2014. Functional high-throughput screening identifies the miR-15 microRNA family as cellular restriction factors for *Salmonella* infection. *Nature Communications*, 5, p.4718.
Mäurer, A.P. et al., 2007. Gene Expression Profiles of *Chlamydophila pneumoniae* during the Developmental Cycle and Iron Depletion–Mediated Persistence. *PLOS Pathogens*, 3(6), p.e83.
Maurizi, M.R., 1992. Proteases and protein degradation in *Escherichia coli*. *Experientia*, 48(2), pp.178–201.
McClelland, M. et al., 2001. Complete genome sequence of *Salmonella* enterica serovar Typhimurium LT2. *Nature*, 413(6858), pp.852–856.
Mechler, L. et al., 2015. A Novel Point Mutation Promotes Growth Phase-Dependent Daptomycin Tolerance in *Staphylococcus aureus*. *Antimicrobial Agents and Chemotherapy* , 59(9), pp.5366–5376.
Menendez, A. et al., 2009. *Salmonella* Infection of Gallbladder Epithelial Cells Drives Local Inflammation and Injury in a Model of Acute Typhoid Fever. *The Journal of Infectious Diseases*, 200(11), pp.1703–1713.
Mergaert, P. et al., 2006. Eukaryotic control on bacterial cell cycle and differentiation in the Rhizobium–legume symbiosis. *Proceedings of the National Academy of Sciences of the United States of America*, 103(13), pp.5230–5235.
Merrell, D.S. et al., 2002. Host-induced epidemic spread of the cholera bacterium. *Nature*, 417(6889), pp.642–645.
Metchnikoff, E. & Besredka, A., 1911. Recherches sur la fievre typhoide experimental. *Annales de l'Institut Pasteur*, 25, pp.814–865.
Metzker, M.L., 2010. Sequencing technologies [mdash] the next generation. *Nat Rev Genet*, 11(1), pp.31–46.
Michelsen, O. et al., 2003. Precise determinations of C and D periods by flow cytometry in *Escherichia coli* K-12 and B/r. *Microbiology*, 149(4), pp.1001–1010.
Michiels, J. & Fauvart, M. eds., 2016. *Bacterial Persistence - Methods and Protocols*, Springer New York.
Michiels, J.E. et al., 2017. Molecular mechanisms and clinical implications of bacterial persistence. *Drug Resistance Updates*, 29, pp.76–89.
Le Minor, L. et al., 1986. Individualisation d'une septième sods-espèce de *Salmonella*: s. choleraesuis subsp. indica subsp. nov. *Annales de l'Institut Pasteur / Microbiologie*, 137(1), pp.211–217.
Mizusawa, S. & Gottesman, S., 1983. Protein degradation in *Escherichia coli*: the lon gene controls the stability of sulA protein. *Proceedings of the National Academy of Sciences* , 80(2), pp.358–362.
Monack, D.M., Mueller, A. & Falkow, S., 2004. Persistent bacterial infections: the interface of the pathogen and the host immune system. *Nature reviews. Microbiology*, 2(9), pp.747–765.

Mott, M.L. & Berger, J.M., 2007. DNA replication initiation: mechanisms and regulation in bacteria. *Nature Reviews Microbiology*, 5, p.343.

Mouton, J.M. et al., 2016. Elucidating population-wide mycobacterial replication dynamics at the single-cell level. *Microbiology*, 162(6), pp.966–978.

Moyed, H.S. & Bertrand, K.P., 1983. *hipA*, a newly recognized gene of *Escherichia coli* K-12 that affects frequency of persistence after inhibition of murein synthesis. *J Bacteriol*, 155, pp.768–775.

Mulcahy, L.R. et al., 2010. Emergence of *Pseudomonas aeruginosa* Strains Producing High Levels of Persister Cells in Patients with Cystic Fibrosis . *Journal of Bacteriology* , 192(23), pp.6191–6199.

Nairz, M. et al., 2010. The struggle for iron – a metal at the host–pathogen interface. *Cellular Microbiology*, 12(12), pp.1691–1702.

Nakagawa, I. et al., 2004. Transcriptome analysis and gene expression profiles of early apoptosis-related genes in *Streptococcus pyogenes*-infected epithelial cells. *Cellular Microbiology*, 6(10), pp.939–952.

Nguyen, D. et al., 2011. Active Starvation Responses Mediate Antibiotic Tolerance in Biofilms and Nutrient-Limited Bacteria. *Science*, 334(6058), pp.982–986.

Nolivos, S. et al., 2016. MatP regulates the coordinated action of topoisomerase IV and MukBEF in chromosome segregation. *Nature Communications*, 7, p.10466.

Nomura, A. et al., 1994. *Helicobacter pylori* Infection and the Risk for Duodenal and Gastric Ulceration. *Annals of Internal Medicine*, 120(12), pp.977–981.

Nordstrom, K., Bernander, R. & Dasgupta, S., 1991. The *Escherichia coli* cell cycle: one cycle or multiple independent processes that are co-ordinated? *Molecular Microbiology*, 5(4), pp.769–774.

Norris, S.J., 2006. Antigenic variation with a twist – the *Borrelia* story. *Molecular Microbiology*, 60(6), pp.1319–1322.

Ochman, H. & Wilson, A.C., 1987. Evolution in bacteria: Evidence for a universal substitution rate in cellular genomes. *Journal of Molecular Evolution*, 26(4), p.74-86.

Ogura, T. & Hiraga, S., 1983. Mini-F plasmid genes that couple host cell division to plasmid proliferation. *Proceedings of the National Academy of Sciences* , 80(15), pp.4784–4788.

Oh, J.D., Karam, S.M. & Gordon, J.I., 2005. Intracellular *Helicobacter pylori* in gastric epithelial progenitors. *Proceedings of the National Academy of Sciences of the United States of America* , 102(14), pp.5186–5191.

Okoro, C.K. et al., 2012. High-Resolution Single Nucleotide Polymorphism Analysis Distinguishes Recrudescence and Reinfection in Recurrent Invasive Nontyphoidal *Salmonella* Typhimurium Disease. *Clinical Infectious Diseases* , 54(7), pp.955–963.

Österlund, A. et al., 1997. Intracellular Reservoir of *Streptococcus pyogenes* In Vivo: A Possible Explanation for Recurrent Pharyngotonsillitis. *The Laryngoscope*, 107(5), pp.640–647.

Oswald, E. et al., 2005. Bacterial toxins that modulate host cell-cycle progression. *Current Opinion in Microbiology*, 8(1), pp.83–91.

Overgaard, M. et al., 2008. Messenger RNA interferase RelE controls relBE transcription by conditional cooperativity. *Molecular Microbiology*, 69(4),

pp.841–857.
Ozsolak, F. et al., 2009. Direct RNA sequencing. *Nature*, 461(7265), pp.814–818.
Page, R. & Peti, W., 2016. Toxin-antitoxin systems in bacterial growth arrest and persistence. *Nat Chem Biol*, 12(4), pp.208–214.
Pan, J. et al., 2012. Reverting Antibiotic Tolerance of *Pseudomonas aeruginosa* PAO1 Persister Cells by (Z)-4-bromo-5-(bromomethylene)-3-methylfuran-2(5H)-one. *PLOS ONE*, 7(9), p.45778.
Pandey, D.P. & Gerdes, K., 2005. Toxin-antitoxin loci are highly abundant in free-living but lost from host-associated prokaryotes. *Nucleic Acids Res*, 33, pp.966–976.
Park, S.E. et al., 2016. The Relationship Between Invasive Nontyphoidal *Salmonella* Disease, Other Bacterial Bloodstream Infections, and Malaria in Sub-Saharan Africa . *Clinical Infectious Diseases*, 62(suppl_1), pp.S23–S31.
Parry, C.M. et al., 2002. Typhoid Fever. *New England Journal of Medicine*, 347(22), pp.1770–1782.
Passalacqua, K.D. et al., 2009. Comparative Transcriptional Profiling of Bacillus cereus Sensu Lato Strains during Growth in CO2-Bicarbonate and Aerobic Atmospheres. *PLOS ONE*, 4(3), p.e4904.
Pearl Mizrahi, S. et al., 2016. Persistence to anti-cancer treatments in the stationary to proliferating transition. *Cell Cycle*, pp.1–12.
Pecota, D.C. et al., 1997. Combining the hok/sok, parDE, and pnd postsegregational killer loci to enhance plasmid stability. *Applied and Environmental Microbiology* , 63(5), pp.1917–1924.
Pedersen, K. et al., 2003. The bacterial toxin RelE displays codon-specific cleavage of mRNAs in the ribosomal A site. *Cell*, 112, pp.131–140.
Pedersen, K., Christensen, S.K. & Gerdes, K., 2002. Rapid induction and reversal of a bacteriostatic condition by controlled expression of toxins and antitoxins. *Mol Microbiol*, 45, pp.501–510.
Perkins, T.T. et al., 2009. A Strand-Specific RNA–Seq Analysis of the Transcriptome of the Typhoid Bacillus *Salmonella* Typhi. *PLOS Genetics*, 5(7), p.e1000569.
Pritchard, R.H. & Lark, K.G., 1964. Induction of replication by thymine starvation at the chromosome origin in *Escherichia coli*. *Journal of Molecular Biology*, 9(2), pp.288–307.
Prouty, A.M., Schwesinger, W.H. & Gunn, J.S., 2002. Biofilm Formation and Interaction with the Surfaces of Gallstones by *Salmonella* spp. *Infection and Immunity*, 70(5), pp.2640–2649.
Racoosin, E.L. & Swanson, J.A., 1989. Macrophage colony-stimulating factor (rM-CSF) stimulates pinocytosis in bone marrow-derived macrophages. *The Journal of Experimental Medicine*, 170(5), p.1635-1648.
Radzikowski, J.L. et al., 2016. Bacterial persistence is an active σS stress response to metabolic flux limitation. *Molecular Systems Biology*, 12(882), pp.1–18.
Rappuoli, R., 2000. Pushing the limits of cellular microbiology: Microarrays to study bacteria–host cell intimate contacts. *Proceedings of the National Academy of Sciences* , 97(25), pp.13467–13469.
Reddick, L.E. & Alto, N.M., 2014. Bacteria Fighting Back – How Pathogens Target and Subvert the Host Innate Immune System. *Molecular cell*,

54(2), pp.321–328.
Redpath, S., Ghazal, P. & Gascoigne, N.R.J., 2001. Hijacking and exploitation of IL-10 by intracellular pathogens. *Trends in Microbiology*, 9(2), pp.86–92.
Reeves, M.W. et al., 1989. Clonal nature of *Salmonella* Typhi and its genetic relatedness to other Salmonellae as shown by multilocus enzyme electrophoresis, and proposal of *Salmonella bongori* comb. nov. *Journal of Clinical Microbiology* , 27(2), pp.313–320.
Revel, A.T., Talaat, A.M. & Norgard, M. V, 2002. DNA microarray analysis of differential gene expression in Borrelia burgdorferi, the Lyme disease spirochete. *Proceedings of the National Academy of Sciences* , 99(3), pp.1562–1567.
Rhen, M. et al., 2003. The basis of persistent bacterial infections. *Trends in Microbiology*, 11(2), pp.80–86.
Robinson, A. & van Oijen, A.M., 2013. Bacterial replication, transcription and translation: mechanistic insights from single-molecule biochemical studies. *Nat Rev Micro*, 11(5), pp.303–315.
Rotem, E. et al., 2010. Regulation of phenotypic variability by a threshold-based mechanism underlies bacterial persistence. *Proceedings of the National Academy of Sciences* , 107(28), pp.12541–12546.
Rothstein, R., Michel, B. & Gangloff, S., 2000. Replication fork pausing and recombination or “gimme a break.” *Genes & Development* , 14(1), pp.1–10.
Russo, T.A. et al., 1995. Chromosomal Restriction Fragment Length Polymorphism Analysis of *Escherichia coli* Strains Causing Recurrent Urinary Tract Infections in Young Women. *Journal of Infectious Diseases*, 172(2), pp.440–445.
Ryan, V.T. et al., 2004. *Escherichia coli* prereplication complex assembly is regulated by dynamic interplay among Fis, IHF and DnaA. *Molecular Microbiology*, 51(5), pp.1347–1359.
Sabbagh, S.C. et al., 2010. So similar, yet so different: uncovering distinctive features in the genomes of *Salmonella enterica* serovars Typhimurium and Typhi. *FEMS Microbiology Letters*, 305(1), pp.1–13.
Salama, N.R., Hartung, M.L. & Muller, A., 2013. Life in the human stomach: persistence strategies of the bacterial pathogen *Helicobacter pylori*. *Nat Rev Micro*, 11(6), pp.385–399.
Saliba, A.-E. et al., 2014. Single-cell RNA-seq: advances and future challenges. *Nucleic Acids Research* , 42(14), pp.8845–8860.
Saliba, A.-E. et al., 2016. Single-cell RNA-seq ties macrophage polarisation to growth rate of intracellular *Salmonella*. *Nature Microbiology*, 2, p.16206
Van Der Sar, A.M. et al., 2003. Zebrafish embryos as a model host for the real time analysis of *Salmonella* typhimurium infections. *Cellular Microbiology*, 5(9), pp.601–611.
Schena, M. et al., 1995. Quantitative Monitoring of Gene Expression Patterns with a Complementary DNA Microarray. *Science*, 270(5235), p.467 LP-470.
Schneider, D.S. et al., 2007. *Drosophila eiger* Mutants Are Sensitive to Extracellular Pathogens. *PLOS Pathogens*, 3(3), p.e41.
Schulte, L.N. et al., 2011. Analysis of the host microRNA response to *Salmonella* uncovers the control of major cytokines by the let-7 family.

The EMBO Journal, 30(10), pp.1977–1989.
Schultz, M., 2008. Theobald Smith. *Emerging Infectious Diseases*, 14(12), pp.1940–1942.
Schumacher, M. a et al., 2015. HipBA-promoter structures reveal the basis of heritable multidrug tolerance. *Nature*, 524(7563), pp.59–64.
Scott, C.C., Botelho, R.J. & Grinstein, S., 2003. Phagosome Maturation: A Few Bugs in the System. *The Journal of Membrane Biology*, 193(3), pp.137–152.
Shah, D. et al., 2006. Persisters: a distinct physiological state of *E. coli*. *BMC Microbiology*, 6(1), p.53-62.
Shan, Y. et al., 2017. ATP-Dependent Persister Formation in *Escherichia coli*. *mBio* , 8(1).
Shan, Y. et al., 2015. Genetic Basis of Persister Tolerance to Aminoglycosides in *Escherichia coli*. *mBio*, 6(2), pp.e00078-15.
Sharma, C.M. et al., 2010. The primary transcriptome of the major human pathogen *Helicobacter pylori*. *Nature*, 464(7286), pp.250–255.
Shinzawa, N. et al., 2009. p38 MAPK-Dependent Phagocytic Encapsulation Confers Infection Tolerance in Drosophila. *Cell Host & Microbe*, 6(3), pp.244–252.
Shukla, V.K. et al., 2000. Carcinoma of the Gallbladder—Is It a Sequel of Typhoid? *Digestive Diseases and Sciences*, 45(5), pp.900–903.
Slater, S. et al., 1995. *E. coli* SeqA protein binds oriC in two different methyl-modulated reactions appropriate to its roles in DNA replication initiation and origin sequestration. *Cell*, 82(6), pp.927–936.
Song, J. et al., 2010. A mouse model for the human pathogen *Salmonella* Typhi. *Cell Host & Microbe*, 8(4), pp.369–376.
Spanò, S., Ugalde, J.E. & Galán, J.E., 2008. Delivery of a *Salmonella* Typhi Exotoxin from a Host Intracellular Compartment. *Cell Host & Microbe*, 3(1), pp.30–38.
Spoering, A.L. & Lewis, K., 2001. Biofilms and planktonic cells of Pseudomonas aeruginosa have similar resistance to killing by antimicrobials. *J Bacteriol*, 183, pp.6746–6751.
Stewart, P.S., 2002. Mechanisms of antibiotic resistance in bacterial biofilms. *Int J Med Microbiol*, 292, pp.107–113.
Sullivan, N.L., Marquis, K.A. & Rudner, D.Z., 2009. Recruitment of SMC to the origin by ParB-parS organizes the origin and promotes efficient chromosome segregation. *Cell*, 137(4), pp.697–707.
Sultan, M. et al., 2014. Influence of RNA extraction methods and library selection schemes on RNA-seq data. *BMC Genomics*, 15(1), p.675.
Sun, Q., Yu, X.-C. & Margolin, W., 1998. Assembly of the FtsZ ring at the central division site in the absence of the chromosome. *Molecular Microbiology*, 29(2), pp.491–503.
Theodore, A., Lewis, K. & Vulić, M., 2013. Tolerance of *Escherichia coli* to Fluoroquinolone Antibiotics Depends on Specific Components of the SOS Response Pathway. *Genetics*, 195(4), pp.1265–1276.
Toledo-Arana, A. et al., 2009. The *Listeria* transcriptional landscape from saprophytism to virulence. *Nature*, 459(7249), pp.950–956.
Valdez, Y., Ferreira, R.B.R. & Finlay, B.B., 2009. Molecular Mechanisms of *Salmonella* Virulence and Host Resistance. *Molecular Mechanisms of Bacterial Infection via the Gut*. ed. C. Sasakawa. Berlin, Heidelberg:

Springer, pp. 93–127.
Velculescu, V.E. et al., 1995. Serial Analysis of Gene Expression. *Science*, 270(5235), p.484-487.
Verstraeten, N. et al., 2015. Obg and Membrane Depolarization Are Part of a Microbial Bet-Hedging Strategy that Leads to Antibiotic Tolerance. *Molecular Cell*, 59(1), pp.9–21.
Völzing, K.G. & Brynildsen, M.P., 2015. Stationary-Phase Persisters to Ofloxacin Sustain DNA Damage and Require Repair Systems Only during Recovery. *mBio* , 6(5), pp.731-745.
Wang, J.D. & Levin, P.A., 2009. Metabolism, cell growth and the bacterial cell cycle. *Nat Rev Micro*, 7(11), pp.822–827.
Wang, J.D., Sanders, G.M. & Grossman, A.D., 2007. Nutritional Control of Elongation of DNA Replication by (p)ppGpp. *Cell*, 128(5), pp.865–875.
Wang, X., Reyes-Lamothe, R. & Sherratt, D.J., 2008. Modulation of *Escherichia coli* sister chromosome cohesion by topoisomerase IV. *Genes & Development*, 22(17), pp.2426–2433.
Wang, Z., Gerstein, M. & Snyder, M., 2009. RNA-Seq: a revolutionary tool for transcriptomics. *Nat Rev Genet*, 10(1), pp.57–63.
Watson, K.G. & Holden, D.W., 2010. Dynamics of growth and dissemination of *Salmonella* in vivo. *Cellular Microbiology*, 12(10), pp.1389–1397.
Westermann, A.J. et al., 2016. Dual RNA-seq unveils noncoding RNA functions in host–pathogen interactions. *Nature*, 529(7587), pp.496–501.
Westermann, A.J., Gorski, S.A. & Vogel, J., 2012. Dual RNA-seq of pathogen and host. *Nat Rev Micro*, 10(9), pp.618–630.
Wilson, R.P. et al., 2008. The Vi-capsule prevents Toll-like receptor 4 recognition of *Salmonella*. *Cellular Microbiology*, 10(4), pp.876–890.
Windgassen, T.A. et al., 2017. Mechanisms of bacterial DNA replication restart. *Nucleic Acids Research*, 46(2) p.1203-1203.
Winther, K. et al., 2016. VapCs of *Mycobacterium tuberculosis* cleave RNAs essential for translation. *Nucleic Acids Research*, 44(20), pp.9860-9871.
Winther, K.S. & Gerdes, K., 2011. Enteric virulence associated protein VapC inhibits translation by cleavage of initiator tRNA. *Proceedings of the National Academy of Sciences*, 108(18), pp.7403–7407.
Wong, M.H.Y. et al., 2014. Emergence of Clinical *Salmonella* enterica Serovar Typhimurium Isolates with Concurrent Resistance to Ciprofloxacin, Ceftriaxone, and Azithromycin. *Antimicrobial Agents and Chemotherapy*, 58(7), pp.3752–3756.
World Health Organisation, 2017. Global priority list of antibiotic-resistant bacteria to guide research, discovery, and development of new antibiotics.
Wotherspoon, A.C. et al., 1991. Helicobacter pylori-associated gastritis and primary B-cell gastric lymphoma. *The Lancet*, 338(8776), pp.1175–1176.
Yamaguchi, Y. & Inouye, M., 2011. Regulation of growth and death in *Escherichia coli* by toxin–antitoxin systems. *Nat Rev Micro*, 9(11), pp.779–790.
Yoder-Himes, D.R. et al., 2009. Mapping the *Burkholderia cenocepacia* niche response via high-throughput sequencing. *Proceedings of the National Academy of Sciences* , 106(10), pp.3976–3981.
Yuan, J., Yamaichi, Y. & Waldor, M.K., 2011. The Three *Vibrio cholerae* Chromosome II-Encoded ParE Toxins Degrade Chromosome I following

Loss of Chromosome II . *Journal of Bacteriology* , 193(3), pp.611–619.
Zhang, S. et al., 2003. Molecular Pathogenesis of *Salmonella enterica* Serotype Typhimurium-Induced Diarrhea. *Infection and Immunity*, 71(1), pp.1–12.
Zyskind, J.W. & Smith, D.W., 1986. The bacterial origin of replication, oriC. *Cell*, 46(4), pp.489–490.

Appendix

Appendix table 1: Read statistics for preliminary dual RNA-Seq run

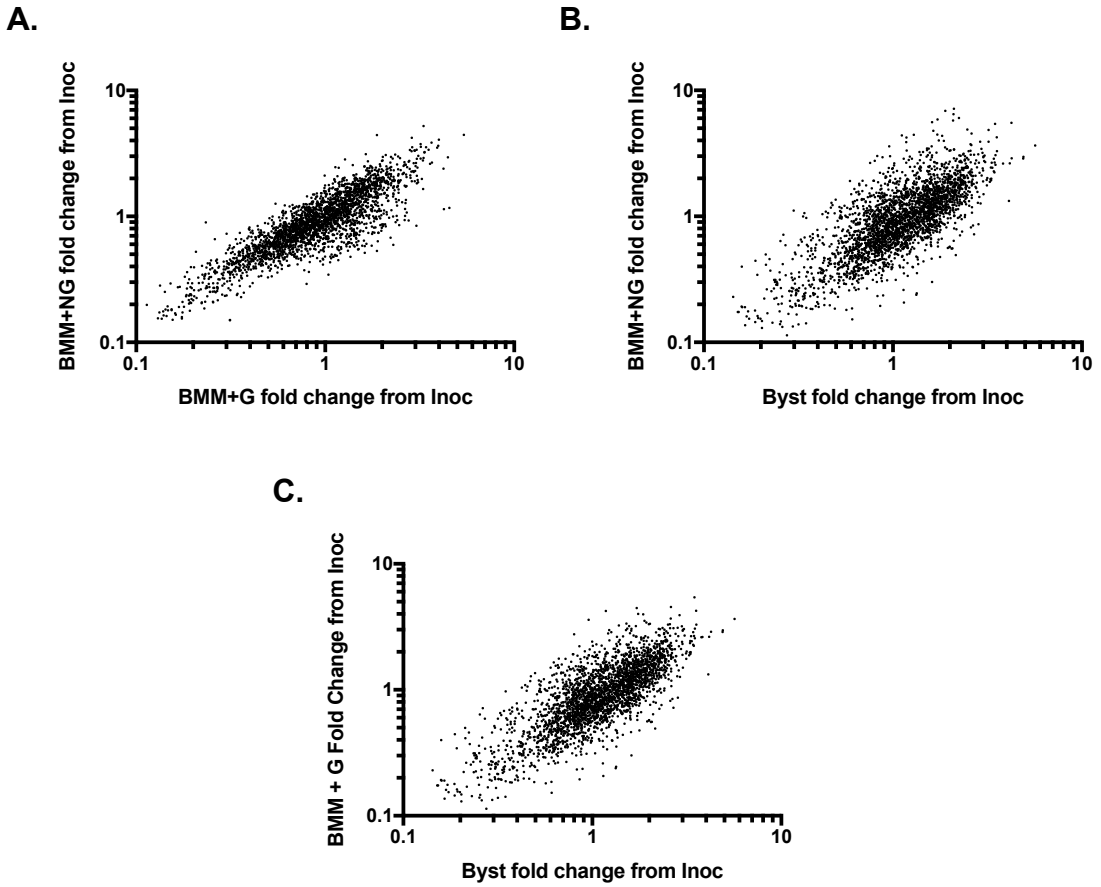
Libraries	Bact. Ctrl	Degraded	uninfected	persisters	replicators	mock
No. of input reads	188,169,396	183,053,712	237,029,686	228,100,734	188,720,036	207,340,034
No. of reads - PolyA detected and removed	96,005,856	74,954,390	101,515,500	99,348,684	77,357,404	77,208,482
No. of reads - Single 3' A removed	13,979,304	16,674,730	22,018,032	19,315,800	16,471,128	19,993,384
No. of reads - Unmodified	78,184,236	91,424,592	113,496,154	109,436,250	94,891,504	110,138,168
No. of reads - Removed as too short	22,203,242	5,609,742	11,299,398	9,879,688	16,595,700	8,156,852
No. of reads - Long enough and used for alignment	165,966,154	177,443,970	225,730,288	218,221,046	172,124,336	199,183,182
Total no. of aligned reads	144,092,034	154,930,042	199,043,986	176,444,122	138,935,424	170,651,850
Total no. of unaligned reads	21,874,120	22,513,928	26,686,302	41,776,924	33,188,912	28,531,332
Total no. of uniquely aligned reads	100,909,018	119,001,310	159,701,966	129,309,782	95,626,438	125,396,252
Total no. of alignments	338,417,888	342,621,330	404,574,650	396,032,264	335,439,416	361,158,828
Total no. of split alignments	1,860,860	2,496,330	3,332,774	3,120,130	2,504,384	2,997,710
Percentage of aligned reads (compared to total input reads)	77	85	84	77	74	82
Percentage of uniquely aligned reads (in relation to all aligned reads)	70	77	80	73	69	73
total mouse reads	111,268,485	148,908,744	191,684,761	171,406,642	120,935,024	161,317,245
% total mouse reads	81.43	99.46	99.89	98.85	88.88	99.92
Sum of Salmonella reads	26754871	838912	228238	2022921	15454160	134905
Salmonella %	18.57	0.54	0.11	1.15	11.12	0.08

Appendix table 2: Read statistics for repeated dual RNA-Seq runs

Libraries	Bystanders_no_1	Bystanders_no_2	Bystanders_no_3	Degradated_no_1	Degradated_no_2	Degradated_no_3	Inoculum_no_1	Inoculum_no_2	Inoculum_no_3
No. of input reads	23573381	25806865	20238983	19274892	21667435	19669797	13762251	16310433	17667208
No. of reads - PolyA detected and removed	2920280	2539212	2286819	1898201	2860604	1470613	1857165	1041503	1241193
No. of reads - Single 3' A removed	3447316	3899173	3286491	2247515	3571062	2729963	2147260	2376813	1826636
No. of reads - Unmodified	17205785	19368480	14665673	15129176	15235769	15469221	9757826	12892117	14599379
No. of reads - Removed as too short	8055680	4587260	3839344	5137952	7993820	544505	4496473	791090	3005268
No. of reads - Long enough and used for alignment	15517701	21219605	16399639	14136940	13673615	19125292	9265778	15519343	14661940
Total no. of aligned reads	12442887	20214277	14956907	11749003	11401920	18512293	7492466	14601304	12503627
Total no. of unaligned reads	3062024	995484	1430543	2370428	2238369	593835	1700691	847439	2078883
Total no. of uniquely aligned reads	9289056	16405812	12820627	7114331	8751139	15051824	6038468	11753849	8934137
Total no. of alignments	31332689	39124699	25763669	43177303	24245724	35451045	11930708	22876842	21316623
Total no. of split alignments	1225222	2504645	1655638	1272191	1299475	2009522	401436	626296	493783
Percentage of aligned reads (compared to no. of input reads)	52.78	78.33	73.9	60.95	52.62	94.12	54.44	89.52	70.77
Percentage of aligned reads (compared to no. of long enough reads)	80.19	95.26	91.2	83.11	83.39	96.79	80.86	94.08	85.28
Percentage of uniquely aligned reads (in relation to all aligned reads)	74.65	81.16	85.72	60.55	76.75	81.31	80.59	80.5	71.45
salmonella reads [% of total aligned reads]	0.523937893	0.230000806	0.43780442	1.39998262	1.298026999	0.505842253	87.01667782	98.16779378	96.37625147
mouse reads [%]	99.476062111	99.769999199	99.562195558	98.600017338	98.701973	99.494157775	12.98332218	1.832206219	3.623748533
Libraries	Non-replicating_no_1	Non-replicating_no_2	Non-replicating_no_3	Replicating_no_1	Replicating_no_2	Replicating_no_3	Uninfected_no_1	Uninfected_no_2	Uninfected_no_3
No. of input reads	15397021	18513849	21682462	17218186	13855543	9605290	16947594	64481791	19592486
No. of reads - PolyA detected and removed	1336382	1450548	2359084	1483067	1163456	928965	1314587	5616815	1218152
No. of reads - Single 3' A removed	2400806	2864361	3253053	2712564	2155037	1344559	2599506	9565602	2548302
No. of reads - Unmodified	11659833	14198940	16070325	13022555	10537050	7331766	13033501	49299374	15826032
No. of reads - Removed as too short	1027722	847267	2709138	1418297	1321559	1261496	1038065	9597252	658406
No. of reads - Long enough and used for alignment	14369299	17666582	18973324	15799889	12533984	8343794	15909529	54884539	18934080
Total no. of aligned reads	13750422	17012223	17934051	14998186	11832166	7788744	15259038	51778360	18339754
Total no. of unaligned reads	610115	644599	1021316	788999	686103	546750	637441	3067888	590659
Total no. of uniquely aligned reads	11541596	14291762	15320906	12411153	9548257	6616659	11971181	40853609	14582771
Total no. of alignments	24143887	30950908	30676069	27383117	23338348	14669791	33068526	106397968	39521783
Total no. of split alignments	1629812	2004938	2007651	1688227	1209021	688563	1381076	5505566	1802123
Percentage of aligned reads (compared to no. of input reads)	89.31	91.89	82.71	87.11	85.4	81.09	90.04	80.3	93.61
Percentage of aligned reads (compared to no. of long enough reads)	95.69	96.3	94.52	94.93	94.4	93.35	95.91	94.34	96.86
Percentage of uniquely aligned reads (in relation to all aligned reads)	83.94	84.01	85.43	82.75	80.7	84.95	78.45	78.9	79.51
salmonella reads [% of total aligned reads]	0.408809271	0.915541725	0.631474729	2.753379642	6.48618351	2.792889328	1.043244011	0.268108144	0.091064471
mouse reads [%]	99.591190737	99.084458277	99.368525277	97.246620336	93.513816449	97.207110677	98.95675599	99.73189186	99.90893553

Appendix table 3: Genes differentially upregulated in growing v NG *Salmonella* comparison (preliminary run)

Up in Gs			Up in NGs		
Gene	**Function**	**Fold change**	**Gene**	**Function**	**Fold change**
asr	putative secreted stress response protein	3.49	umuD	DNA repair protein	0.112595964
SL1344_P1_0044	hypothetical protein	3.11	SL1344_1210	putative inner membrane protein	0.123609925
finO	thr operon leader peptide	3.04	pspB	bacteriophage shock protein B	0.138356372
slyB	outer membrane lipoprotein SlyB	2.99	SL1344_1722	hypothetical protein	0.157659881
SL1344_4339	hypothetical protein	2.51	SL1344_tRNA0053	-	0.177315843
csrA	carbon storage regulator	2.48	mobA	molybdopterin-guanine dinucleotide biosynthesis protein MobA	0.189843281
SL1344_1768	hypothetical protein	2.31	SL1344_tRNA0064	-	0.191707284
SL1344_1767	hypothetical protein	2.28	SL1344_tRNA0003	-	0.192269083
pagK	bacteriophage encoded pagK %28phoPQ-activated protein%29	2.24	SL1344_0845	putative tetR family transcriptional regulator	0.194704026
rpsO	30S ribosomal protein S15	2.21	slyD	FKBP-type peptidyl-prolyl cis-trans isomerase	0.195506348
rpsM	30S ribosomal protein S13	2.19	SL1344_tRNA0004	-	0.199155851
traS	hypothetical protein	2.15	SL1344_tRNA0068	-	0.20131399
lppA	major outer membrane lipoprotein	2.08	SL1344_1098	hypothetical protein	0.203298268
lexA	LexA repressor	2.08	SL1344_3354	hypothetical protein	0.20910679
rplL	50S ribosomal protein L7%2FL12	2.01	priB	primosomal replication protein N	0.210040303
-	-		SL1344_1425	hypothetical protein	0.220052402
-	-		pspA	bacteriophage shock protein A	0.220714185
-	-		pspC	bacteriophage shock protein C	0.221097335
-	-		SL1344_tRNA0055	-	0.22630605
-	-		trbE	DnaJ protein	0.228501556



Appendix figure 1: Comparisons of BMM transcriptomic profiles during infection with *Salmonella* (Preliminary test). Scatter plot showing the expression of genes in macrophage subpopulations (A) BMM+G and BMM+NG, (B) BMM+NG and bystanders, (C) BMM+G and bystanders at 18 h.p.i. with *Salmonella* shown as fold changes from uninfected mock infection macrophage transcript levels. n=1.

Appendix table 4: Genes differentially upregulated in BMM+G v BMM+NG comparison (preliminary run)

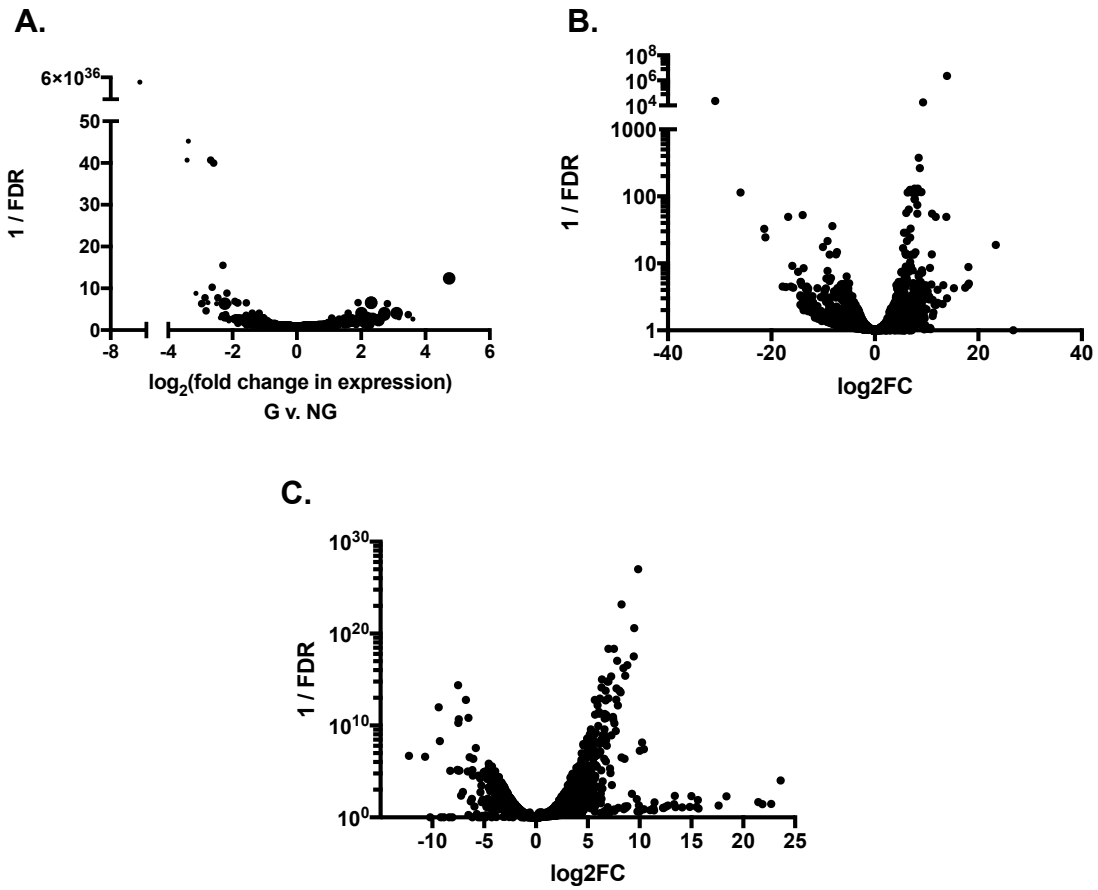
up in BMM+Gs			Up in BMM+NGs		
Gene	**Function**	**Fold change**	**Gene**	**Function**	**Fold change**
Mir328	microRNA 328	0.40	Nisch	nischarin	3.84
mmu-let-7j	mmu-let-7j	0.40	Gadd45g	growth arrest and DNA-damage-inducible 45 gamma	2.53
Mir1249	microRNA 1249	0.40	Gm14328	predicted gene 14328	2.53
Mir350	microRNA 350	0.40	Mt1	metallothionein 1	2.42
Gm24148	Unknown function	0.40	Snora69	small nucleolar RNA, H/ACA box 69	2.35
Gm24016	Unknown function	0.40	Gm15432	predicted gene 15432	2.31
Mir148b	Unknown function	0.39	Scarna6	small Cajal body-specific RNA 6	2.23
Gm25744	Unknown function	0.39	Snora75	small nucleolar RNA, H/ACA box 75	2.17
Gm25789	Unknown function	0.39	HOTAIRM1_5	HOX antisense intergenic RNA myeloid 1 conserved region 5	2.13
Mir151	microRNA 151	0.39	Dusp2	dual specificity phosphatase 2	2.11
mt-Td	mitochondrially encoded tRNA aspartic acid	0.38	Odc1	ornithine decarboxylase, structural 1	2.10
Gm22455	Unknown function	0.38	Gm23297	predicted gene, 23297	2.06
n-R5s195	nuclear encoded rRNA 5S 195	0.38	Map1lc3b	microtubule-associated protein 1 light chain 3 beta	2.05
Snord23	small nucleolar RNA, C/D box 23	0.37	Spp1	secreted phosphoprotein 1	2.03
Mir1981	microRNA 1981	0.37	Ecm1	extracellular matrix protein 1	2.02
Mir146b	microRNA 146b	0.37	-	-	-
Gm25122	Unknown function	0.37	-	-	-
Gm24463	Unknown function	0.36	-	-	-
Gm24105	Unknown function	0.36	-	-	-
Snord35a	small nucleolar RNA, C/D box	0.36	-	-	-

Appendix table 5: Genes differentially upregulated in BMM+NG v bystanders comparison (preliminary run)

Up in Byst			Up in NGs		
Gene	**Function**	**Fold change**	**Gene**	**Function**	**Fold change**
Mir350	microRNA 350	0.36	mt-Ts1	mitochondrially encoded tRNA serine 1	2.73
Metazoa_SRP	Metazoan signal recognition particle RNA	0.36	Gm13339	unknown function	2.62
Gm26461	unknown function	0.36	mt-Nd1	mitochondrially encoded NADH dehydrogenase 1	2.39
Metazoa_SRP	Metazoan signal recognition particle RNA	0.36	mt-Nd4	mitochondrially encoded NADH dehydrogenase 4	2.32
Zfp949	zinc finger protein 949	0.35	Snord88a	small nucleolar RNA, C/D box 88A	2.20
Mir128-2	microRNA 128-2	0.35	mt-Nd5	mitochondrially encoded NADH dehydrogenase 5	2.14
Mir132	microRNA 132	0.35	Tnfaip2	tumor necrosis factor, alpha-induced protein 2	2.13
Mir30b	microRNA 30b	0.35	mt-Atp6	mitochondrially encoded ATP synthase 6	2.13
n-R5s195	nuclear encoded rRNA 5S 195	0.35	mt-Tq	mitochondrially encoded tRNA glutamine	2.11
Gm23037	unknown function	0.35	mt-Nd4l	mitochondrially encoded NADH dehydrogenase 4L	2.10
Mir126	microRNA 126	0.35	Gm10222	unknown function	2.10
Zfp791	zinc finger protein 791	0.35	Gm25395	unknown function	2.10
Gm15662	unknown function	0.34	mt-Co2	mitochondrially encoded cytochrome c oxidase II	2.08
Fabp5	fatty acid binding protein 5, epidermal	0.34	Zmynd15	zinc finger, MYND-type containing 15	2.07
Gm6166	unknown function	0.34	mt-Atp8	mitochondrially encoded ATP synthase 8	2.07
Gm23374	unknown function	0.34	mt-Th	mitochondrially encoded tRNA histidine	2.02
Mir1249	microRNA 1249	0.34	-	-	
Mir484	microRNA 484	0.33	-	-	
Gm12791	unknown function	0.32	-	-	
Mir5100	microRNA 5100	0.32	-	-	

Appendix table 6: Genes differentially upregulated in BMM+G v bystanders comparison (preliminary run)

Up in Byst			Up in G		
Gene	**Function**	**Fold change**	**Gene**	**Function**	**Fold change**
Gm6166	unknown function	0.18	mt-Ts1	mitochondrially encoded tRNA serine 1	3.75
Gm14328	unknown function	0.18	mt-Th	mitochondrially encoded tRNA histidine	3.58
Fabp5	fatty acid binding protein 5, epidermal	0.18	mt-Td	mitochondrially encoded tRNA aspartic acid	3.45
Mt1	metallothionein 1	0.19	Ikbke	inhibitor of kappaB kinase epsilon	2.79
Spp1	secreted phosphoprotein 1	0.23	Emr1	EGF-like module containing, mucin-like, hormone receptor-like sequence 1	2.72
Mir126	microRNA 126	0.23	Lmo4	LIM domain only 4	2.71
Gadd45g	growth arrest and DNA-damage-inducible 45 gamma	0.23	Cybb	cytochrome b-245, beta polypeptide	2.71
Cdkn2d	cyclin-dependent kinase inhibitor 2D	0.25	Prkcd	protein kinase C, delta	2.66
Odc1	ornithine decarboxylase, structural 1	0.26	mt-Ti	mitochondrially encoded tRNA isoleucine	2.63
Rhov	ras homolog gene family, member V	0.26	Csf1r	colony stimulating factor 1 receptor	2.60
Fcgr3	Fc receptor, IgG, low affinity III	0.27	Gm24016	unknown function	2.59
Pf4	platelet factor 4	0.27	Clec4e	C-type lectin domain family 4, member e	2.51
Gm26461	unknown function	0.27	Ctsc	cathepsin C	2.51
Zfp949	zinc finger protein 949	0.27	Zmynd15	zinc finger, MYND-type containing 15	2.50
Tubb6	tubulin, beta 6 class V	0.27	Snord42a	small nucleolar RNA, C/D box 42A	2.50
Nisch	nischarin	0.28	Ccdc88b	coiled-coil domain containing 88B	2.47
Metazoa_SRP	Metazoan signal recognition particle RNA	0.29	Gm25744	unknown function	2.46
Metazoa_SRP	Metazoan signal recognition particle RNA	0.29	Gm25789	unknown function	2.44
Mir100	microRNA 100	0.29	Xylt2	xylosyltransferase II	2.43
Gm23419	unknown function	0.29	Gm24428	unknown function	2.43



Appendix figure 2: Direct comparisons of *Salmonella* transcriptomic profiles during BMM infection (repeated experiment). Volcano plots showing the fold change in expression of genes in (A) growing v NG, (B) growing v inoculum and (C) NG v inoculum *Salmonella* comparisons to NG at 18 h infection of BMMs as log_2(fold change in expression). Plots representative of three independent experiments.

Appendix table 7: Genes differentially upregulated in growing v NG *Salmonella* comparison (repeated experiment)

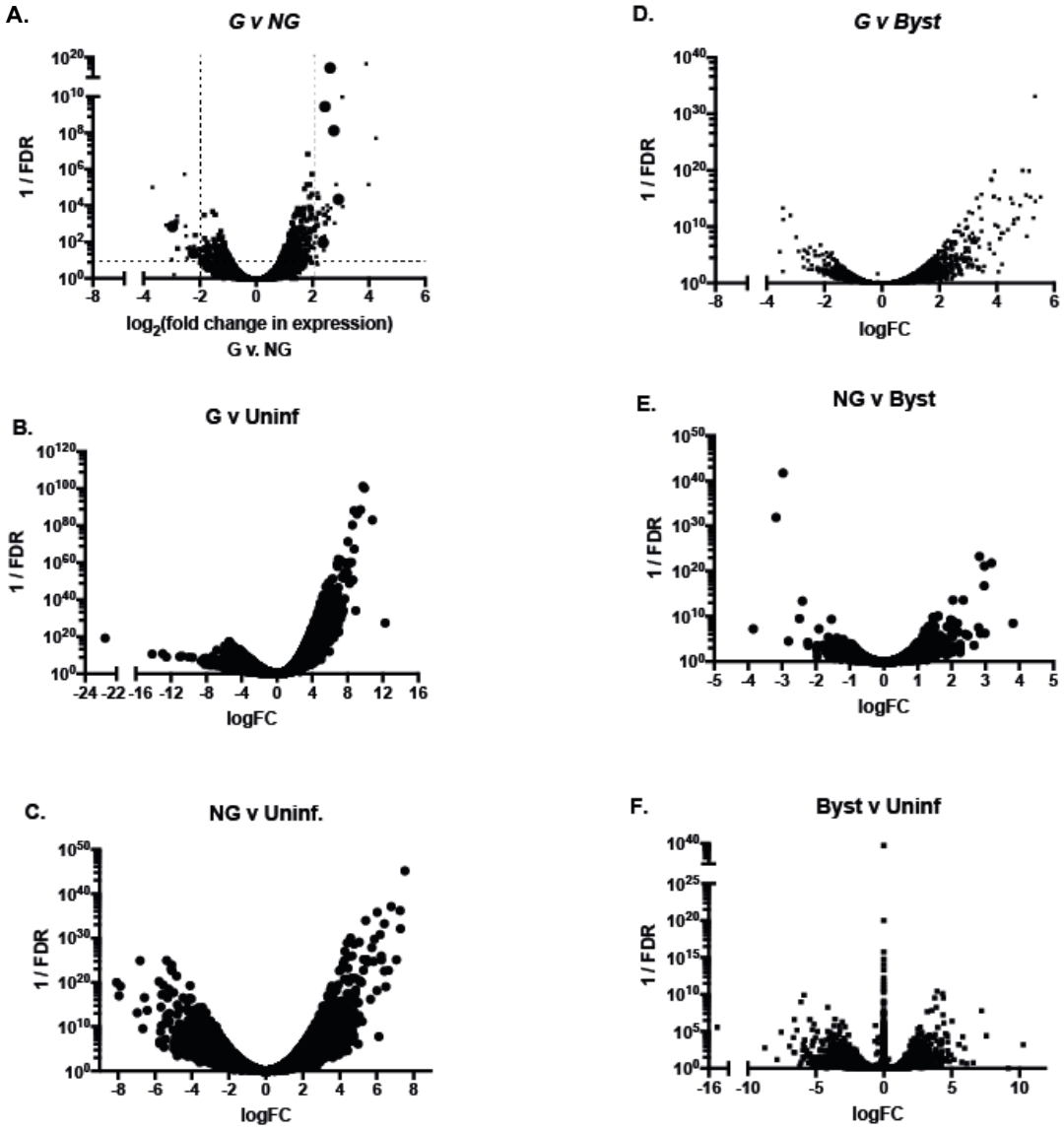
Up in NGs			Up in Gs		
Gene	**Function**	**log2FC**	**Gene**	**Function**	**log2FC**
shdA	host colonisation factor	6.36	iagB	cell invasion protein	-4.74
abc	putative ABC transporter ATP-binding protein	3.41	uraA	uracil permease	-3.61
sciO	hypothetical protein	3.37	fruK	1-phosphofructokinase	-3.46
trpB	tryptophan synthase beta chain	3.14	SL1344_4420	putative ATP-dependent Lon protease	-3.18
SL1344_3979	hypothetical protein	2.96	marB	multiple antibiotic resistance protein MarB	-3.10
SL1344_3107	hydrolase	2.91	birA	biotin operon repressor	-2.81
sseE	pathogenicity island protein	2.85	trpR	trp operon repressor	-2.73
sirA	invasion response-regulator	2.82	SL1344_3023	hypothetical protein	-2.71
SL1344_3540	hypothetical protein	2.76	SL1344_3744	putative DNA-binding protein	-2.54
trpD	anthranilate phosphoribosyltransferase	2.68	ybfA	hypothetical protein	-2.41
SL1344_0083	secreted protein	2.64	SL1344_2579	putative antitermination protein	-2.36
sseD	pathogenicity island effector protein	2.58	sicP	chaperone	-2.31
misL	autotransported protein	2.50	tehB	tellurite resistance protein	-2.31
hisI	histidine biosynthesis	2.46	lolA	lipoprotein carrier protein	-2.22
sseF	pathogenicity island effector protein	2.38	rfaQ	lipopolysaccharide core biosynthesis protein	-2.19
alr	alanine racemase	2.36	SL1344_3575	hypothetical protein	-2.18
SL1344_1301	hypothetical protein	2.30	SL1344_P1_0036	putative transglycosylase	-2.09
SL1344_0831	putative electron transfer flavoprotein	2.30	recF	recF protein	-2.01
rph	RNase PH	2.26	dedA	DedA protein %28dsg-1 protein%29	-2.00
pagM	virulence factor	2.24	yifK	amino acid permease	-1.94
SL1344_1593	hypothetical protein	2.21	flrD	anaerobic nitric oxide reductase flavorubredoxin	-1.93
SgrS		2.21	SL1344_3867	hypothetical protein	-1.90
fruR	fructose repressor	2.18	traN	conjugative transfer aggregate stability protein	-1.90
fis	Fis DNA-binding protein	2.18	SL1344_2781	putative transcriptional regulator	-1.89
StyR-88		2.18	treF	cytoplasmic trehalase	-1.88
trpE	anthranilate synthase component I	2.17	SL1344_1662	hypothetical protein	-1.85
RUF_247c		2.11	rfbX	putative O-antigen transporter	-1.81
SL1344_2302	putative transporter	2.11	sinR	LysR family regulator	-1.78
SL1344_1780	hypothetical protein	2.11	tehA	tellurite resistance protein	-1.72
SL1344_3198	membrane transport protein	2.10	spoU	tRNA guanosine-2-O-methyltransferase	-1.72
SL1344_2969	N-acetylmuramoyl-L-alanine amidase	2.05	SL1344_2315	hypothetical protein	-1.71

Appendix table 8: Genes differentially upregulated in growing v inoculum *Salmonella* comparison (repeated experiment)

Up in Gs			Up in Inoc		
Gene	**Function**	**log2FC**	**Gene**	**Function**	**log2FC**
tus	DNA replication terminus site-binding protein	23.61	STnc1285	sRNA	-12.25
ttdB	tartrate dehydratase	22.70	flgH	flagellar L-ring protein	-10.69
entD	enterobactin synthetase component D	21.84	fliL	flagella biosynthesis protein	-10.20
RUF_107c.23	-	21.46	fliA	RNA polymerase sigma transcription factor for flagellar operon	-9.39
SL1344_1422	putative ABC transporter membrane protein	18.38	flgD	flagellar hook formation protein FlgD	-9.27
StyR-24c	-	17.63	flgB	putative flagellar basal-body rod protein	-9.19
StyR-215f	-	15.70	SL1344_1504	hypothetical protein	-8.90
SL1344_2890	membrane transport protein	15.62	flgC	putative flagellar basal-body rod protein	-8.37
SL1344_1375	hypothetical protein	15.49	fliI	flagellum-specific ATP synthase	-8.28
SL1344_4187	hypothetical protein	15.01	fliE	flagellar hook-basal body complex protein FliE	-8.07
SL1344_1867	putative lipoprotein	14.85	fliG	flagellar motor switch protein FliG	-7.58
SL1344_1124	putative inner membrane lipoprotein	14.10	fliC	flagellin	-7.52
pyrB	aspartate carbamoyltransferase catalytic subunit	13.46	fliD	flagellar hook associated protein %28FliD%29	-7.49
dgkA	diacylglycerol kinase	13.40	flgI	flagellar P-ring protein	-7.48
SL1344_2134	putative lipoprotein	13.32	cheY	chemotaxis protein CheY	-7.45
StyR-262	-	12.72	fliF	flagellar basal-body M-ring protein	-7.38
miaE	tRNA hydroxylase	12.54	SL1344_3322	hypothetical protein	-7.22
flgE	flagellar hook protein FlgE	12.30	flgG	flagellar basal-body rod protein	-7.05
SL1344_0916	putative lipoprotein	12.27	ompD	outer membrane protein	-6.75
SL1344_1728	hypothetical protein	11.43	flhB	flagellar biosynthetic protein FlhB	-6.59
StyR-24f	-	11.39	fliT	flagellar protein FliT	-6.52
cspH	cold shock protein	11.33	fruB	pts system%2C fructose-specific IIA%2FFPR component	-6.52
iroE	hypothetical protein	11.03	fruK	1-phosphofructokinase	-6.40
rfaY	lipopolysaccharide core biosynthesis	10.43	SL1344_2619	hypothetical protein	-6.30

Appendix table 9: Genes differentially upregulated in NGs v inoculum *Salmonella* comparison (repeated experiment)

Up in NGs			Up in inoc		
Gene	**Function**	**log2FC**	**Gene**	**Function**	**log2FC**
SL1344_0994	bacteriophage protein %28pseudogene%29	26.75	StyR-215f	-	-30.85
pocR	pdu%2Fcob regulatory protein PocR	23.40	StyR-354	-	-25.98
SL1344_0327	putative hydrolase or acyltransferase	18.16	SL1344_2881	pathogenicity island 1 protein	-21.36
yjcC	hypothetical protein	18.08	entD	enterobactin synthetase component D	-21.16
SL1344_1772	putative membrane transport protein	17.98	fliB	lysine-N-methylase	-17.82
SL1344_0348	putative cation transport atpase	17.45	fliT	flagellar protein FliT	-17.21
yhgE	hypothetical protein	15.30	SL1344_1726	hypothetical protein	-16.75
shdA	host colonisation factor %28ShdA%29	13.95	STnc240	sRNA	-16.20
SL1344_3552	putative HlyD family secretion protein	13.94	SL1344_0956	bacteriophage protein	-15.96
ramA	transcriptional activator RamA	13.80	SL1344_0985	putative bacteriophage minor tail protein	-15.79
gabD	succinate-semialdehyde dehydrogenase	13.23	SL1344_0244	hypothetical protein	-14.85
sfbC	ABC transporter	13.11	flgH	flagellar L-ring protein	-14.41
SL1344_3631	putative electron-transport protein	12.16	Ig2335	-	-14.40
hutI	imidazolonepropionase	12.11	SL1344_4511	hypothetical protein	-14.38
cbpA	curved DNA-binding protein	11.82	SL1344_3280	hypothetical protein	-14.34
RUF_107c.53		11.78	livF	high-affinity branched-chain amino acid transport ATP-binding protein	-14.31
SL1344_3827	hypothetical protein	11.55	dnaQ	DNA polymerase III subunit epsilon	-14.11
SL1344_3000	amino acid transport protein	11.31	SL1344_1972	putative bacteriophage protein	-14.08
nrfB	penta-heme cytochrome c %2C subunit of nitrite reductase complex	11.20	SL1344_1031	hypothetical protein	-14.08
SL1344_1284	putative ligase%2Fsynthetase	11.19	SL1344_2379	hypothetical protein	-13.98
sseF	putative pathogenicity island effector protein	11.07	cheB	Chemotaxis response regulator protein-glutamate methylesterase	-13.97
SL1344_1596	hypothetical protein	11.03	fliL	flagella biosynthesis protein	-13.79
basS	two-component sensor kinase	10.94	hslJ	heat shock protein %28hslJ%29	-13.78
SL1344_2568	bacteriophage protein	10.77	SL1344_2946	hypothetical protein	-13.75
SL1344_3599	putative lacI family transcriptional regulator	10.72	flgE	flagellar hook protein FlgE	-13.58



Appendix figure 3: Direct comparisons of BMM transcriptomic profiles during infection with *Salmonella* (repeated **experiment).** Volcano plots showing the fold change in expression of genes in (A) BMM+G v BMM+NG (B) BMM+G v uninfected BMM (C) BMM+NG v uninfected BMM (D) BMM+G v bystander (E) BMM+NG v bystander and (F) bystander v uninfected BMM comparisons at 18 h infection with *Salmonella* as $\log_2$(fold change in expression). Plots representative of three independent experiments.

Appendix table 10: Genes differentially upregulated in BMM+NG v BMM+G comparison (repeated experiment)

Up in BMM+NG			Up in BMM+G		
Gene	**Function**	**log2FC**	**Gene**	**Function**	**log2FC**
Iqca	protein_coding	3.68	Xlr5a	protein_coding	-5.30
Zpld1	protein_coding	3.20	Tshz2	protein_coding	-4.61
RP24-231P10.4	TEC	3.00	Kctd17	protein_coding	-4.25
Gpr55	protein_coding	2.96	Cish	protein_coding	-3.98
Cux2	protein_coding	2.91	Ank2	protein_coding	-3.91
Fam213a	protein_coding	2.82	Rnf165	protein_coding	-3.07
Gm17782	unprocessed_pseudogene	2.80	Fam19a1	protein_coding	-3.05
Tdgf1-ps1	processed_pseudogene	2.78	Steap4	protein_coding	-2.92
Ctnna3	protein_coding	2.54	Enpp2	protein_coding	-2.84
Atp5d	protein_coding	2.50	Ccdc92	protein_coding	-2.79
Defb42	protein_coding	2.49	Tnfsf14	protein_coding	-2.76
Tgfbr3	protein_coding	2.45	Rasip1	protein_coding	-2.66
Fam196a	protein_coding	2.45	Timp1	protein_coding	-2.63
Gm14780	processed_pseudogene	2.36	Ocstamp	protein_coding	-2.56
Dynlt1b	protein_coding	2.34	Entpd3	protein_coding	-2.54
Gm18953	unprocessed_pseudogene	2.23	Wdr63	protein_coding	-2.52
Ntrk2	protein_coding	2.19	Gm16194	lincRNA	-2.45
Dnah12	protein_coding	2.16	Mt2	protein_coding	-2.44
Iqck	protein_coding	2.14	Ier5l	protein_coding	-2.44
Rnf170-ps	processed_pseudogene	2.04	Socs2	protein_coding	-2.43
Gm2904	processed_pseudogene	2.00	Marveld1	protein_coding	-2.41
Nudt14	protein_coding	1.99	Il1f5	protein_coding	-2.38
4930405A21Rik	processed_transcript	1.97	Mir511	miRNA	-2.38
Xlr4b	protein_coding	1.93	Acvr1c	protein_coding	-2.34
Tmem40	protein_coding	1.86	Cd28	protein_coding	-2.29
Cyp2b13	protein_coding	1.85	Pgf	protein_coding	-2.22
Gm23623	snRNA	1.85	Selp	protein_coding	-2.19
Zfp964	protein_coding	1.84	Nrcam	protein_coding	-2.19
BC048502	protein_coding	1.84	Gm28258	lincRNA	-2.18
Lad1	protein_coding	1.84	Hbegf	protein_coding	-2.16
Gm24830	snRNA	1.83	RP24-315D19.10	lincRNA	-2.14
RP23-430D14.1	processed_pseudogene	1.83	St8sia1	protein_coding	-2.14
Tpt1-ps6	processed_pseudogene	1.82	Pxdc1	protein_coding	-2.13
Tbc1d16	protein_coding	1.82	Gabbr2	protein_coding	-2.13
Gm25632	snoRNA	1.81	Pced1b	protein_coding	-2.12
4930469K13Rik	processed_transcript	1.78	Slc26a4	protein_coding	-2.09
Six5	protein_coding	1.78	Grik5	protein_coding	-2.08
Nipa1	protein_coding	1.77	Akap2	protein_coding	-2.08
Syt6	protein_coding	1.76	Saa4	protein_coding	-2.07
mmu-mir-191	miRNA	1.75	Gpr171	protein_coding	-2.06

Appendix table 11: Genes differentially upregulated in BMM+G v uninfected BMMs comparison (repeated experiment)

Up in BMM+G			Up in Uninf.		
Gene	**Function**	**log2FC**	**Gene**	**Function**	**log2FC**
Gm9888	antisense	12.26	Pcgf2	protein_coding	-6.12
RP23-336O18.3	TEC	10.80	Gm16861	lincRNA	-6.15
Lipg	protein_coding	9.90	Pbk	protein_coding	-6.16
Ccl7	protein_coding	9.74	Gm28308	protein_coding	-6.18
Nos2	protein_coding	9.46	Cd101	protein_coding	-6.19
Timp1	protein_coding	9.08	Hist1h3f	protein_coding	-6.21
Opcml	protein_coding	8.91	Prox2	protein_coding	-6.23
Ccl8	protein_coding	8.75	Gpr68	protein_coding	-6.37
Slfn4	protein_coding	8.74	Ckap2	protein_coding	-6.45
Arg1	protein_coding	8.60	Cd207	protein_coding	-6.49
Il1rn	protein_coding	8.54	Cyp2s1	protein_coding	-6.55
Saa3	protein_coding	8.44	Plekhg5	protein_coding	-6.57
Il33	protein_coding	8.21	Tmc8	protein_coding	-6.59
Upp1	protein_coding	8.19	Ccdc159	protein_coding	-6.74
Cxcl9	protein_coding	8.05	Slc25a27	protein_coding	-6.80
Ccl12	protein_coding	8.05	Ephx1	protein_coding	-6.81
Serpinb2	protein_coding	8.01	Fam64a	protein_coding	-7.08
Ccl2	protein_coding	7.97	Gm29642	lincRNA	-7.17
Ptgs2	protein_coding	7.87	Frat2	protein_coding	-7.19
AA467197	protein_coding	7.83	Hist1h3e	protein_coding	-7.25
Steap4	protein_coding	7.68	Tns4	protein_coding	-7.33
G530011O06Rik	processed_transcript	7.63	Sparc	protein_coding	-7.52
Ltb4r1	protein_coding	7.55	Ccdc120	protein_coding	-7.60
Gm38070	TEC	7.51	Nr1i3	protein_coding	-7.63
Saa1	protein_coding	7.39	Angptl4	protein_coding	-7.92
Scimp	protein_coding	7.37	D930048N14Rik	protein_coding	-8.11
2010005H15Rik	protein_coding	7.35	Kifc2	protein_coding	-8.13
Il19	protein_coding	7.22	Asrgl1	protein_coding	-8.16
Lcn2	protein_coding	7.19	Gm4980	protein_coding	-8.17
Sphk1	protein_coding	7.15	Mboat1	protein_coding	-8.21
Gipr	protein_coding	7.06	Nek2	protein_coding	-8.29
Socs3	protein_coding	7.02	Kcnk12	protein_coding	-8.56
Gm14085	protein_coding	6.99	Nup210	protein_coding	-9.56
Adora3	protein_coding	6.95	Aurkb	protein_coding	-9.98
Tshz2	protein_coding	6.94	Hist1h2bh	protein_coding	-10.75
Il1f5	protein_coding	6.94	Gm15523	antisense	-10.99
U90926	protein_coding	6.92	Gm23116	snRNA	-12.51
Xlr3c	protein_coding	6.90	Gm1673	protein_coding	-12.93
Il6	protein_coding	6.88	Ncs1	protein_coding	-14.11
Glipr2	protein_coding	6.87	Chil3	protein_coding	-22.71

Appendix table 12: Genes differentially upregulated in BMM+NG v uninfected BMMs comparison (repeated experiment)

Up in BMM+G			Up in Uninf.		
Gene	**Function**	**log2FC**	**Gene**	**Function**	**log2FC**
Nos2	protein_coding	7.53	Cenpm	protein_coding	-4.87
U90926	protein_coding	7.28	Ska1	protein_coding	-4.88
RP23-336O18.3	TEC	7.27	Gm9949	protein_coding	-4.89
Gm38070	TEC	7.06	Fam83d	protein_coding	-4.90
Ccl8	protein_coding	6.78	Gm9920	protein_coding	-4.91
Ms4a8a	protein_coding	6.63	Sapcd2	protein_coding	-4.98
Ccl7	protein_coding	6.50	Pianp	protein_coding	-4.98
Serpinb2	protein_coding	6.42	Abcd2	protein_coding	-4.98
Il1f9	protein_coding	6.41	Aspm	protein_coding	-5.01
Slfn4	protein_coding	6.25	Gpr183	protein_coding	-5.08
Gipr	protein_coding	6.24	Sort1	protein_coding	-5.09
Nrg1	protein_coding	6.19	Arap3	protein_coding	-5.13
Cgref1	protein_coding	6.11	Hist1h3h	protein_coding	-5.21
Il1rn	protein_coding	6.02	Ldhb	protein_coding	-5.21
Ifit1bl1	protein_coding	6.02	Fgf13	protein_coding	-5.26
Il1r1	protein_coding	5.88	Slco2b1	protein_coding	-5.32
Lipg	protein_coding	5.84	Plekhh2	protein_coding	-5.32
AA467197	protein_coding	5.73	Nat8l	protein_coding	-5.33
Gbp4	protein_coding	5.66	Zfyve28	protein_coding	-5.36
Upp1	protein_coding	5.48	Hist1h2ad	protein_coding	-5.38
Rhou	protein_coding	5.45	Kif7	protein_coding	-5.39
Ptgs2	protein_coding	5.40	Myh15	protein_coding	-5.43
Pdpn	protein_coding	5.29	Gm12856	processed_pseudogene	-5.50
Lhx2	protein_coding	5.28	Cxcr4	protein_coding	-5.54
Gm13415	processed_transcript	5.22	Hist1h1b	protein_coding	-5.62
Saa3	protein_coding	5.17	Frat2	protein_coding	-5.64
Il2ra	protein_coding	5.09	Sox4	protein_coding	-5.67
Ltb4r1	protein_coding	5.09	Gm20619	lincRNA	-5.69
Mmp13	protein_coding	5.06	Gm15612	antisense	-5.74
RP23-240E15.3	TEC	5.04	Gm15537	antisense	-5.75
Il6	protein_coding	5.03	Hist1h1d	protein_coding	-5.78
Mir147	miRNA	5.00	Lhfp	protein_coding	-6.42
Sema5a	protein_coding	5.00	Cmah	protein_coding	-6.57
Gm3810	processed_pseudogene	4.93	Ltc4s	protein_coding	-6.66
Il33	protein_coding	4.91	Gpr34	protein_coding	-6.80
2600014E21Rik	antisense	4.91	Cd34	protein_coding	-6.95
Gpr35	protein_coding	4.87	Rasgrp3	protein_coding	-7.87
Il23r	protein_coding	4.86	Nanos1	protein_coding	-7.95
Ccl12	protein_coding	4.83	Hpgd	protein_coding	-8.07

Appendix table 13: Genes differentially upregulated in BMM+G v bystanders comparison (repeated experiment)

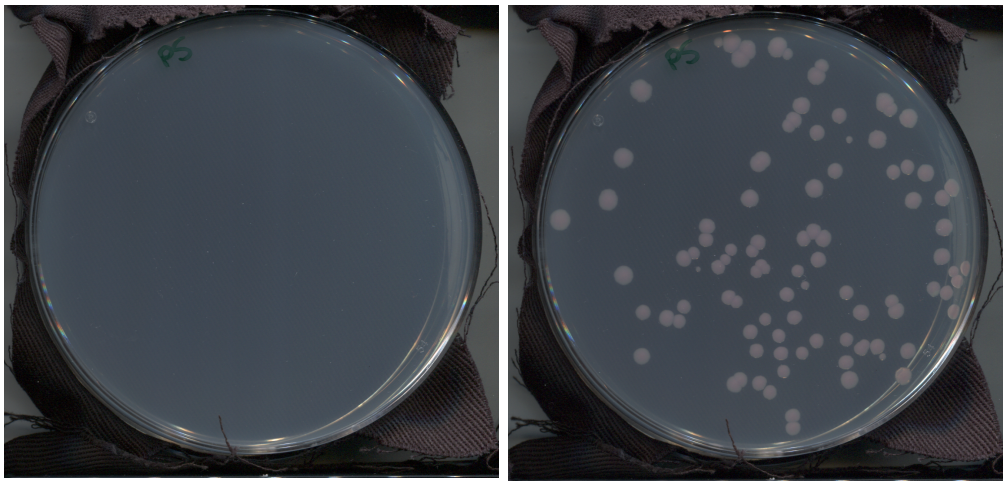
Up in BMM+G			Up in bystanders		
Gene	**Function**	**log2FC**	**Gene**	**Function**	**log2FC**
Bglap	protein_coding	6.96	Kcnn1	protein_coding	-3.55
Cxcl3	protein_coding	6.43	Sgip1	protein_coding	-3.45
Gm11771	unprocessed_pseudogene	5.53	Klri1	protein_coding	-3.44
Ppbp	protein_coding	5.35	Cux2	protein_coding	-3.43
Mrc1	protein_coding	5.33	Lrp1b	protein_coding	-3.17
Gm15880	antisense	5.28	Nrg3	protein_coding	-2.97
Steap4	protein_coding	5.17	Ctnna3	protein_coding	-2.89
Rgcc	protein_coding	5.13	Abcd2	protein_coding	-2.75
Il19	protein_coding	5.04	Amn	protein_coding	-2.72
Ndrg1	protein_coding	5.02	Ptpn21	protein_coding	-2.70
Ltb4r1	protein_coding	4.90	Ltbp1	protein_coding	-2.61
Il33	protein_coding	4.82	Gm18953	unprocessed_pseudogene	-2.57
Sphk1	protein_coding	4.74	Ly6c2	protein_coding	-2.56
Tnfsf14	protein_coding	4.59	Gpr55	protein_coding	-2.55
S100a8	protein_coding	4.59	Gpr132	protein_coding	-2.49
A4galt	protein_coding	4.56	Grin2b	protein_coding	-2.43
Fam198b	protein_coding	4.48	Cnbd1	protein_coding	-2.43
Nrg1	protein_coding	4.39	Wnk2	protein_coding	-2.33
Gja1	protein_coding	4.22	Gm12693	processed_pseudogene	-2.32
E230016K23Rik	processed_transcript	4.18	Rps3a2	processed_pseudogene	-2.26
Arhgap8	protein_coding	4.16	Gm15869	sense_intronic	-2.24
Entpd3	protein_coding	4.11	Tdgf1-ps1	processed_pseudogene	-2.22
Cacna1b	protein_coding	4.08	Nuak1	protein_coding	-2.18
Tfap2a	protein_coding	4.05	Gm26778	lincRNA	-2.18
RP23-336O18.3	TEC	4.04	RP24-314I8.2	unprocessed_pseudogene	-2.14
Ankrd55	protein_coding	3.95	Pstpip2	protein_coding	-2.14
Chst11	protein_coding	3.92	Gm17160	antisense	-2.12
Adarb1	protein_coding	3.91	Layn	protein_coding	-2.06
Tgm1	protein_coding	3.90	Ip6k3	protein_coding	-2.05
Tspan13	protein_coding	3.88	Fam196a	protein_coding	-2.04
Eps8	protein_coding	3.83	Hist1h2ad	protein_coding	-2.01
RP24-299A7.2	TEC	3.81	Gm3448	protein_coding	-2.01
Csf3	protein_coding	3.76	Gm13814	lincRNA	-2.00
Tm4sf1	protein_coding	3.75	Gm22701	misc_RNA	-2.00
Ocstamp	protein_coding	3.56	Arl5c	protein_coding	-1.98
Ptprn	protein_coding	3.51	Map2	protein_coding	-1.92
Il1r1	protein_coding	3.47	Rasgrp1	protein_coding	-1.92
Mt2	protein_coding	3.47	Gm15056	protein_coding	-1.91
Cxcl2	protein_coding	3.47	Mtl5	protein_coding	-1.89
Cxcl1	protein_coding	3.40	Gpr141	protein_coding	-1.89

Appendix table 14: Genes differentially upregulated in BMM+NG v bystanders comparison (repeated experiment)

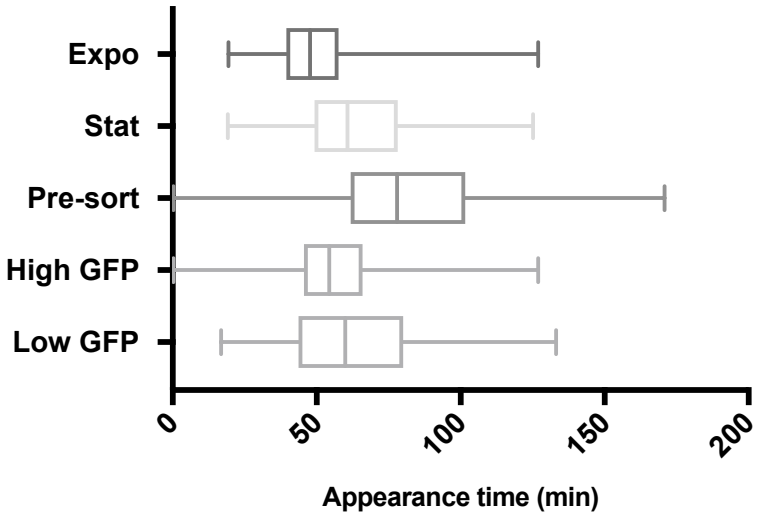
Up in BMM+NG			Up in bystanders		
Gene	**Function**	**log2FC**	**Gene**	**Function**	**log2FC**
Opcml	protein_coding	3.81	Cdh13	protein_coding	-3.85
Zfp759	protein_coding	3.18	Ptpn21	protein_coding	-3.18
Gm15880	antisense	2.99	Lrp1b	protein_coding	-2.97
Ltb4r1	protein_coding	2.97	Amn	protein_coding	-2.81
Mrc1	protein_coding	2.96	Lhfp	protein_coding	-2.49
Tm4sf1	protein_coding	2.85	Klri1	protein_coding	-2.40
RP23-336O18.3	TEC	2.83	Dlc1	protein_coding	-2.24
Il33	protein_coding	2.80	Gm1661	protein_coding	-2.23
Nrg1	protein_coding	2.67	Mfng	protein_coding	-1.98
Ppbp	protein_coding	2.48	Cd55	protein_coding	-1.97
Ndrg1	protein_coding	2.41	Chrnb1	protein_coding	-1.96
Tgm1	protein_coding	2.35	Pou2f3	protein_coding	-1.96
Acvr1c	protein_coding	2.26	Ccdc57	protein_coding	-1.91
A4galt	protein_coding	2.25	Erbb4	protein_coding	-1.78
Jag2	protein_coding	2.25	Sox6	protein_coding	-1.72
Gm11771	unprocessed_pseudogene	2.25	C530008M17Rik	protein_coding	-1.67
Rgcc	protein_coding	2.20	RP23-209N19.1	TEC	-1.67
Chst11	protein_coding	2.17	Srpx	protein_coding	-1.65
Cxcl3	protein_coding	2.12	Gm13832	lincRNA	-1.63
Amz1	protein_coding	2.06	Cacna1c	protein_coding	-1.63
Slc39a8	protein_coding	2.05	Gm25018	rRNA	-1.62
Eps8	protein_coding	2.04	Adgrf5	protein_coding	-1.62
Nxpe5	protein_coding	2.03	Gabrd	protein_coding	-1.62
Gm11263	processed_pseudogene	2.03	Hist1h2ad	protein_coding	-1.60
Enpp1	protein_coding	2.03	mmu-mir-191	miRNA	-1.59
Kif1a	protein_coding	2.01	Cct6b	protein_coding	-1.57
Parp16	protein_coding	2.00	Rpl15-ps2	processed_pseudogene	-1.56
Prune2	protein_coding	2.00	Mirlet7i	miRNA	-1.55
Tyms	protein_coding	1.98	Mir21a	miRNA	-1.54
Fam198b	protein_coding	1.97	Gm8885	processed_pseudogene	-1.53
Adarb1	protein_coding	1.93	Ltbp1	protein_coding	-1.52
Btg3	protein_coding	1.92	Ror1	protein_coding	-1.49
Il19	protein_coding	1.89	Suv39h2	protein_coding	-1.48
Gm13502	processed_pseudogene	1.87	5830416P10Rik	lincRNA	-1.47
Prokr1	protein_coding	1.87	mt-Ti	Mt_tRNA	-1.46
Ankrd55	protein_coding	1.87	Slc6a3	protein_coding	-1.44
Atp5d	protein_coding	1.84	Mir99b	miRNA	-1.44
Mir8107	miRNA	1.83	Hist1h2ac	protein_coding	-1.43
Il1r1	protein_coding	1.83	Tle2	protein_coding	-1.42
Gm12915	processed_transcript	1.80	Gpc6	protein_coding	-1.42

Appendix table 15: Genes differentially upregulated in bystanders v uninfected BMMs comparison (repeated experiment)

Up in bystanders			Up in Uninf.		
Gene	**Function**	**log2FC**	**Gene**	**Function**	**log2FC**
Mpz	protein_coding	10.26	Nanos1	protein_coding	-15.14
S100a9	protein_coding	9.18	Hpgd	protein_coding	-8.75
Chil3	protein_coding	7.56	Cd34	protein_coding	-7.88
Ccdc57	protein_coding	7.20	Gm15537	antisense	-7.55
Ngp	protein_coding	6.60	Apc2	protein_coding	-6.93
C1qtnf6	protein_coding	6.11	Plekhh2	protein_coding	-6.64
Col1a2	protein_coding	5.97	Hist1h1d	protein_coding	-6.61
U90926	protein_coding	5.81	Cxcr4	protein_coding	-6.59
Rad9a	protein_coding	5.75	Slco2b1	protein_coding	-6.56
Cdh13	protein_coding	5.53	Cmah	protein_coding	-6.38
Gpr158	protein_coding	5.16	Sox4	protein_coding	-6.17
Serpinb2	protein_coding	5.03	Tmem144	protein_coding	-6.09
Ms4a3	protein_coding	4.92	F13a1	protein_coding	-6.08
Rundc3a	protein_coding	4.81	1700122E12Rik	processed_transcript	-5.97
Gm17782	unprocessed_pseudogene	4.76	Ankle1	protein_coding	-5.95
Il6	protein_coding	4.70	Zfyve28	protein_coding	-5.91
Gm4613	processed_pseudogene	4.70	Nptx1	protein_coding	-5.90
Saa4	protein_coding	4.68	Ptgs1	protein_coding	-5.87
Gm11824	processed_pseudogene	4.67	Hist1h3h	protein_coding	-5.84
Serpinb1b	protein_coding	4.59	Kazald1	protein_coding	-5.82
Ptgs2	protein_coding	4.54	Hist1h2an	protein_coding	-5.68
Gm23805	snRNA	4.49	Bmyc	protein_coding	-5.65
Sema7a	protein_coding	4.46	Ier5l	protein_coding	-5.56
Shisa3	protein_coding	4.41	Frat2	protein_coding	-5.53
Lingo2	protein_coding	4.40	Cyp27a1	protein_coding	-5.45
Itga7	protein_coding	4.38	Ldhb	protein_coding	-5.45
Il1a	protein_coding	4.35	Cd207	protein_coding	-5.36
Mmp13	protein_coding	4.35	Cep72	protein_coding	-5.35
Nos2	protein_coding	4.29	Shisa9	protein_coding	-5.33
Pgf	protein_coding	4.28	Lrrc39	protein_coding	-5.33
Liph	protein_coding	4.27	Parpbp	protein_coding	-5.26
Pgam1-ps1	processed_pseudogene	4.27	Cux2	protein_coding	-5.25
Gm15998	antisense	4.25	Usp2	protein_coding	-5.25
Dao	protein_coding	4.24	Gm29397	processed_pseudogene	-5.23
Ocstamp	protein_coding	4.23	Rasgrp3	protein_coding	-5.21
Acy1	protein_coding	4.23	Tnnt3	protein_coding	-5.20
Il1f9	protein_coding	4.22	Pcyt1b	protein_coding	-5.18
Gm38146	TEC	4.20	Gm9920	protein_coding	-5.16
Il12b	protein_coding	4.10	Sort1	protein_coding	-5.14
Serpina3f	protein_coding	4.10	Cenpm	protein_coding	-5.07



Appendix figure 4: Example plate from ScanLag experiment. Images of the same plate at the start (left) and at the end (right) of incubation for ScanLag. Smaller colonies are late-appearing and represent bacteria in the original sample with a longer lag time after plating.



Appendix figure 5: Growth rates of colonies detected by ScanLag are highly variable. *E. coli* carrying pFCcGi was grown to stationary phase, GFP expression was induced with arabinose and the bacteria were sorted based on GFP fluorescence and plated for ScanLag analysis. Box and whisker plots of colony growth rates for exponential phase, stationary phase (24 h), pre-sort (post-induction) *E. coli*, and sorted 'high-GFP' and 'low-GFP' cells are displayed. Data was pooled for three independent experiments and samples of 728 colonies were randomly selected for each condition.